School of Civil Engineering
Structural Department
Institute for Structural Analysis & Anti-Seismic Research

Novel mathematical programming procedures for the force-based inelastic analysis of three-dimensional framed structures

Thesis submitted for the degree of

Doctor of Philosophy in Engineering

at the National Technical University of Athens

by

Theodoros N. Patsios
Dipl. Civil Engineer (NTUA), M.Sc. ADS

Supervisor: Dr. Konstantinos V. Spiliopoulos, Professor

March 2019

«Δῶς μοι πᾶ στῶ καὶ τὰν γᾶν κινάσω» (Αρχιμήδης)
“Give me a place to stand and I shall move the earth” (Archimedes)

Hermes running while holding his caduceus with his left hand, as usual.
[Attican Lecythus, approx. 480–470 B.C.][*]

[*] Image Source: https://commons.wikimedia.org/wiki/File:Lekythos_of_Hermes.jpg (Wikipedia)

TABLE OF CONTENTS

1 Introduction

1.1 Summary

In this work, a method for the inelastic analysis of planar (2D) and spatial (3D) statically indeterminate structural frames is developed. Plasticity is modeled following the concentrated/lumped approach (*plastic hinges*). A novel, fully automated formulation that uses Lagrange multipliers to model discontinuities in a simple and efficient way is proposed. The redundant (*indeterminate*) forces serve as the primary unknowns (*also referred to as "independent" variables*). Material hardening, internal discontinuities (*e.g. articulations*), nodal eccentricities (*also referred to as "rigid" elements*), are all taken into account. A formulation including geometric non-linearity (*also referred to as "P-Δ" and "P-Δ-δ" effects*) is also investigated within the context of this work.

A mixed-code computer program was written in FORTRAN 2003/2008 and ANSI C/C++, that is able to follow the exact event-to-event plasticization and the development of post-elastic deformations of a structural frame according to a predefined loading pattern and under the assumption of non-holonomic plastic behaviour, until the point of plastic collapse is efficiently determined.

The proposed method, which is a step-by-step method, is formulated within the frameworks of graph algorithms, non-holonomic plasticity, and mathematical programming.

1.2 Motivation for this Work

The force method has a smaller number of unknowns than the displacement method. Also, mathematical programming provides a framework in order to implement a natural formalism that describes material non-holonomic behavior. Furthermore, there are many graph and optimization algorithms available in order to implement the necessary automation and solution techniques.

1.2.1 Choosing the Approach with the Smaller Number of Unknowns

When referring to structural engineering applications, matrix-based structural analysis is a necessity for efficient design and bearing capacity evaluation. Traditionally, this work is carried out using the Finite Element Method (FEM), by following the direct stiffness methodical approach.

When following the direct stiffness (*kinematic*) approach to perform structural analysis with the FEM, a beam element in the 3D space has six (6) (*kinematic*) Degrees of Freedom (DoF) at each of its' nodes. Despite the fact that the boundary (*fixed*) DoFs are known and thus reduce algebraically the size of the problem, a significant number of unknowns is still required. However, when following the flexibility (*static*) approach, a much smaller number of unknowns is expected; these unknowns are the redundant quantities, and they are related to the 1st Betti number of the abstract planar graph that may be used as a concept to topologically model the connectivity of a structure. A brief proof follows below, for the case of externally statically indeterminate structural frames.

Let "N" be the number of nodes, "M" the number of members, and "N_{BN}" the number of boundary nodes of a spatial (3D) structural frame, where "N_{BN}" is by definition smaller than or equal to "N". Furthermore, at each of the end nodes of a finite beam/column element, the sum of the number of discontinuities "N_d" and the number of continuities "N_c" is always equal to 6; with reference to the whole structure, the following equality holds for the boundary nodes:

$$\sum_{i=1}^{N_{BN}} N_{c,i} + \sum_{i=1}^{N_{BN}} N_{d,i} = 6 \cdot N_{BN} \quad (1)$$

Wherein (1), it is assumed that only one element is connected to each boundary node (*which is a fairly reasonable assumption, considering that the soil-structure interaction is usually modelled using*

rotational and longitudinal springs attached to the respective boundary nodes of a structural frame — see Figure 1 below).

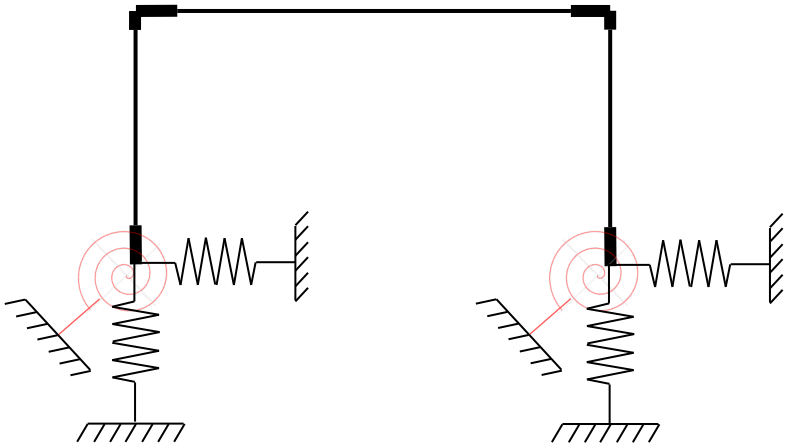

Figure 1: A simple example of a portal structural frame, where soil-structure interaction is simulated with longitudinal and rotational springs (*the latter have been denoted with Archimedean spirals*).

According to the aforementioned definitions, the number of unknowns of the corresponding direct stiffness-based problem is:

$$n_s = 6 \cdot N - \sum_{i=1}^{N_{BN}} N_{c,i} \tag{2}$$

Wherein (2) only the non-zero kinematic degrees of freedom are taken into account regarding the linear system that need be solved.

By assuming that all boundary nodes of the same structure are connected to a common virtual (*ground*) node (*see Figure 2*), so that a complete set of closed loops (*topological cycles*) may be formed, then, for the flexibility-based problem, the number of unknowns is (*according to Betti's 1st number*):

$$n_f = 6 \cdot [(M + N_{BN}) - (N + 1) + 1] - \sum_{i=1}^{N_{BN}} N_{d,i} \tag{3}$$

Where in (3) it is assumed that the structural frame is simulated as a planar graph or at least as a synthesis of planar graphs, so that the referenced topological constant is valid.

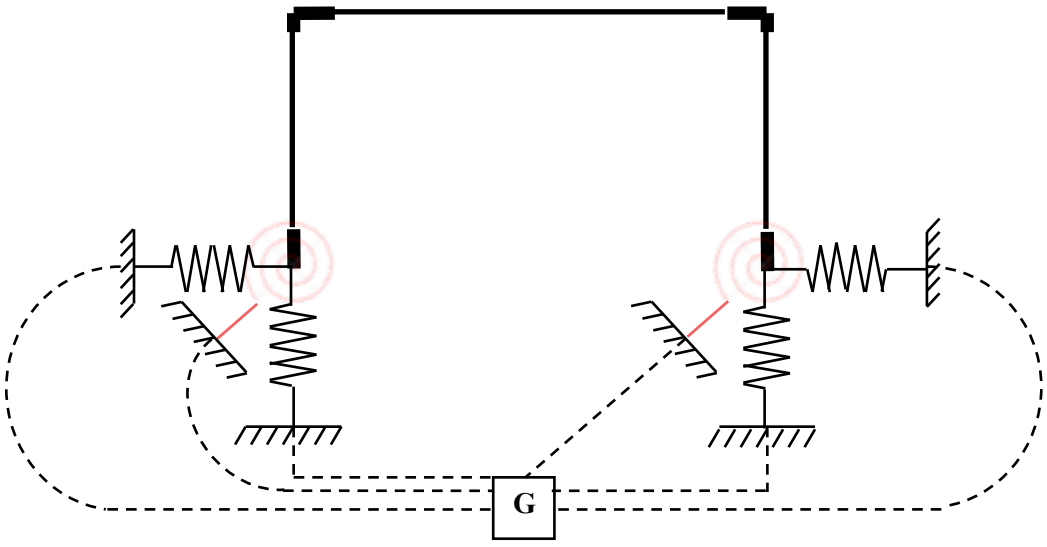

Figure 2: Graph representation of a planar structural frame, where the "ground" (*datum*) node is denoted with the letter "G".

By subtracting (3) from (2), and with the help of (1), a comparison between the basic unknowns of the stiffness and the flexural approaches can be made:

$$n_s - n_f = 6 \cdot \left[(N - M) + (N - \frac{\sum_{i=1}^{N_{BN}} N_{c,i}}{3}) \right] \quad (4)$$

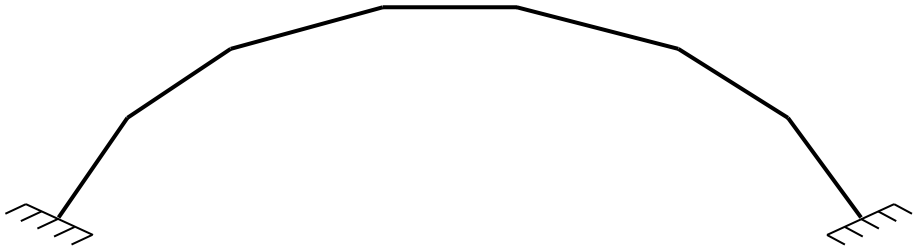

Figure 3: The case of a continuous arch that has been simulated as a finite set of seven (7) linear segments (*beam finite elements*); as it may be easily observed, the number of nodes, including the boundary ones, is equal to the number of members, plus one.

Since the number of nodes of a structure will always be greater than the number of members by at least a value of one (*see Figure 3 above*), the first of the two terms in the right-hand side of (4) will always be a positive number. By further assuming that the second term corresponds to a fully continuous structure, the maximum expected value for the one third of the number of continuities of all of the structure's boundary conditions cannot be greater than twice the number of boundary nodes of the structure; thus the difference between the two numbers of unknowns will in most cases be positive, with the exception of structures whose boundary nodes are more than half of their total number of nodes (*e.g. small-sized grillages — see Figure 4 below*). Therefore, it may be deduced that, for the majority of externally statically indeterminate structures, the force-based matrix method of analysis will always have a smaller number of unknowns than the direct stiffness method.

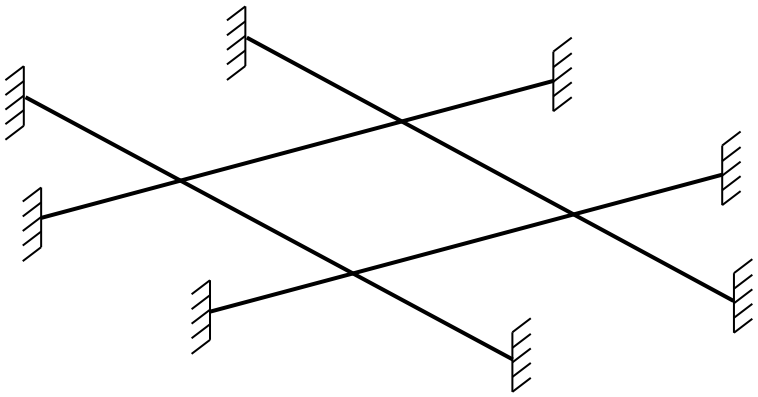

Figure 4: Example of a small grillage with twelve (12) nodes in total, out of which eight (8) –which are more than half of the number of nodes of the structure in total– are boundary nodes; in the sense of non-zero valued degrees of freedom, the direct-stiffness based problem for this structure has twenty-four (24) unknowns, while the force-based problem has forty-eight (48) unknowns.

It may be easily shown that, for internally statically indeterminate structures, the difference described by Equation (4) is a generally positive quantity as well.

1.2.2 Available Algorithms for implementing Automation and Solution Techniques

An additional motivation for this research work was one regarding the task of generating the equilibrium matrices automatically: There is a large variety of algorithms that are able to determine

shortest (*minimal or at least near-minimal*) paths among distant and/or consequent nodes of planar graphs, a feature that is crucial in order to evaluate equilibrium conditions due to external loads and internal stress redistribution due to static indeterminacy. Moreover, past research has proposed the usage of Lagrange multipliers in order to model the internal/external discontinuities of a structure for automated structural analysis, a feature that is useful when performing both limit and incremental, generally non-linear analyses (*modelling and solution of the inverse problem*), because only continuities need be assumed when evaluating the equations of the equilibrium matrices of the flexural approach. Therefore, the task of the automatic generation of the equilibrium matrices was only a technical problem.

Finally, non-holonomic plasticity that is mathematically defined with the help of a linear complementarity condition between plastic potential and Lagrange multipliers can be easily computed with the help of optimization algorithms (*e.g. Quadratic Programming, Sequential Quadratic Programming, and Interior Point Methods*); Lagrange multipliers may also be used to yield a satisfactory compatibility of deformations in the case of elastic discontinuities. Particularly in the latter case, there is practically no latency in CPU time as compared to completely continuous structures: the number of constraints due to discontinuities is always twice the number of the respective discontinuities, which, in general is a smaller number than the number of constraints that describe the yield loci of continuities; the latter holds especially for 3D structures, wherein the minimum possible number of interacting stress components is two (*e.g. biaxial bending*), which, for the case of a yield function with only one equation will yield a total of four constraints.

Thus, a unified and simple to implement theoretical framework in order to build a fully automated flexural approach was at hand, and we chose to investigate its' potential.

2 Literature Review

In the following context, a chronological literature review in the fields of the force method and applications of mathematical programming in engineering plasticity, are presented; a short bibliographic reference to the respective optimization algorithms that were used and tested within the current work as well as on some unconventional methods in plasticity is also made.

2.1 Force Method of Analysis

Before the time of automated structural analysis, engineers were working primarily on the flexural approach: The theory of bending of a beam due to a combined action of a lateral distributed load and an axial compression or tension has been officially documented by J. Perry since 1892 [1], and, since 1919, A. Berry had solved the problem of geometric non-linearity due to bending moment-axial force interaction on beams, based on the three-moment equation [2]; fully deployed tables of the Berry functions may be found in [3]. Things changed radically later on with the appearance of digital computers, which also gave the actual boost to the development of the Finite Element Method (FEM), whose principles were already known at least since 1943 [4]. To the author's knowledge, K.J. Dallison was the first to present a force method for the stress analysis of circular frames in 1953 [5]. The first papers on the generalized finite element method were published a year later by J.H. Argyris and S. Kelsey [6]. During the same time period, two more papers from the same authors were published, that signalled the development of the automation of the force method for structural analysis ([7],[8]). W.R. Spillers [9] was the first to mention that, in matrix-based structural analysis, the force method has a smaller number of unknowns than the displacement method. In 1965, a complete theory for 3D elastic structural frames that follows a force-based approach in order to derive the governing equations was published by Ath. Roussopoulos [10]: in this work, the concept of ''mutualities", which is a generalization of the Betti-Maxwell theorem of reciprocity, is also derived. A fully automated force-based formulation including geometric non-linearity and a holonomic plasticity approach based on a Ramberg-Osgood constitutive law appeared first in 1966, by J.T. Oden and A. Neighbors in [11]. A paper that proposes the usage of algebraic topological constants in the structural analysis of frames appeared in 1969, by J. C. de C. Henderson and E. A. W. Maunder [12]. Formulations for plastic analysis and minimal weight design first appear by S.J. Fenves and A. Gonzalez-Caro in 1971 [13]. The integrated force method was introduced by S.N. Patnaik in 1973 [14]. Techniques for automatically selecting a cycle basis appeared in the literature by A.C. Cassel, J.C. de C. Henderson, and A. Kaveh, in 1974 ([15],[16]). An improvement in cycle basis search technique was presented by A. Kaveh in 1978 [17]. A force method that treats the problem of geometric non-linearity by introducing a set of fictitious deformable members around the nodes of the structure so as to create a geometric flexibility matrix that complements the classic flexibility matrix due to linear elasticity was proposed in 1978 by C. Polizzotto [18]; in essence, this approach is an algebraic method. The integrated force method was applied to frequency analysis by S.N. Patnaik and S. Yadagiri in 1978 [19]. A combinatorial optimization process that used matroid theory and the greedy algorithm in order to produce optimal (*minimal*) cycle bases on skeletal structures was introduced by A. Kaveh in 1979 [20]. In 1982, some improvements in the algebraic procedures regarding the computation of the equilibrium matrices were discussed by I. Kaneko, M. Lawo, and G. Thierauf in [21]. Various techniques for obtaining minimal (*or near minimal*) cycle and statical bases have been also presented by A. Kaveh ([22],[23],[24]). A. Jennings and T.K.H. Tam first presented an automated force-based approach for the optimal plastic design of frames in 1986 [25]; in the same year, S.N. Patnaik and K.T. Joseph presented two schemes for generating the compatibility matrix in the integrated force method [26].

A first attempt to follow a force-based approach within the framework of mathematical programming was first made by N.Z. Pereira, L.A. Borges, and M.B. Hecke in 1988 [27]; both static and kinematic approaches were formulated and solved using the dual algorithm of Lemke. During the same year, A. Kaveh presented some methods for studying the topological properties of skeletal structures whose application rendered some new methods for determining the degree of statical indeterminacy [28]. In 1991, A. Kaveh proposed a relative stiffness criterion for the cycle basis selection process that contributes to the optimal conditioning of flexibility matrices [29]. A direct flexibility method that is designed to work in interconnection with the direct stiffness method was proposed by C.A. Felippa and K.C. Park, in 1997 [30]; in the context of automated optimal plastic design, a novel automation technique was proposed by K.V. Spiliopoulos [31], while an automated collapse load analysis approach was introduced by K.V. Spiliopoulos and P.G. Souliotis in the same year [32]. A recursive technique for the incremental reduction of the structural indeterminacy has been presented by V.K. Koumousis in 1998 in [33]. Recent advances of the integrated force method were discussed by S.N. Patnaik, R.M. Coroneos, D.A. Hopkins during the same year in [34]. An extension of the integrated force method to cater for non-linear structures was presented by N.R.B. Krishnam Raju and J. Nagabhushanam in [35]. Design of frames using genetic algorithms was first presented by A. Kaveh and V. Kalatjari in 2002 [36] and 2004 [37], and A. Kaveh and A.Abdietehrani in 2004 [38]. A set of benchmark case studies in structural optimization using SQP algorithms and an integrated method was presented by R. Sedaghati in 2005 [39]. A geometrically non-linear force method for tensegrity structures (*and generally infinitesimal mechanisms*) was presented the same year be Y. Luo and J. Lu in [40]. The incorporation of semi-rigid joints by Kaveh and Moez was introduced in 2005 [41]. Genetic algorithms for structural optimization were applied by A. Kaveh and H. Rahami in 2006 ([42],[43]) and H. Rahami, A. Kaveh, and Y. Gholipour in 2008 [44]. Heuristic algorithms were applied in the plastic limit analysis of frames by A.Kaveh and M. Jahanshani in the same year [45]. A somewhat incremental progress in analysis with semi-rigid joints was presented by A. Kaveh and H. Moez during the same year [46]. In 2009, an existing limit analysis procedure was extended to cater for uniaxially tied framed structures [47]. In 2010, A. Kaveh and S. Malakouti Rad introduced a technique for simultaneous analysis and design of structures using genetic algorithms and particle swarm optimization [48]; in the same year, an efficient mathematical programming method was presented in [49] for structural frames of elastic-perfectly plastic material. In 2011, meta-heuristic algorithms were applied for optimal structural design by Kaveh and Talatahari [50]. Novel techniques for reducing the computational cost in the analysis of near-regular structures were introduced by Kaveh et al. in 2012 [51]. A numerical, force-based study of the elastoplastic response of planar frames with non-holonomic plastic hinges and bending moment and axial force interaction undergoing pseudo-static cyclic loading scenarios was presented in [52]. An extension of an existing force-based approach on limit analysis of 2D skeletal frames in order for it to work for 3D structures was proposed by K.V. Spiliopoulos and N.G. Dais in 2013 [53]. A non-linear optimization program for the 2nd order incremental elastoplastic analysis of planar frames was presented in [54]. An isotropic material hardening rule using non-holonomic plastic hinges for 1st order step−by−step analysis by the force method was first presented in [55]. In 2016, an existing step−by−step force method was further extended to the analysis of inelastic 3D structural frames [56]; a linear transformation for projecting the stress components to the local axes of each member is introduced, that requires fewer computer operations as the equivalent one that was proposed in [53]; linearized convex yield functions are formulated in an automated pattern. A purely force-based approach to the elastoplastic analysis of frames with hardening plastic hinges is presented in [57], which, in essence, is a

unification of the up-to-day findings of the related research work of the authors of [52],[54],[55], and [56].

2.2 Mathematical Programming

Mathematical Programming (MP) is a special branch of numerical analysis that treats the problem of finding stationary points of continuous (*but also discrete*) functions that are either bounded by a set of (*equality and/or inequality*) constraints, or unbounded. In this short section, a brief literature review on the aforementioned field of applied mathematics and computer science follows, since, from the engineering point of view, one is interested only in applying those numerical techniques.

The technique for solving the bounded stationary point problem is based on the idea of creating a linear combination of the function and its' constraints, and was first proposed in 1811 by J.L. Lagrange [58]; this technique is particularly useful for multivariable functions under equality constraints. In a memoire to the French Academy of Sciences [59], J.-B.J. Fourier poses a series of questions regarding the determination of the optimal solution to problems where the unknown variables are bound by constraints whose number is equal to or even larger than the number of the variables; furthermore, he assumes that these constraints may be inequality functions of the unknowns. He demonstrates the expected complexity via a few simple examples of geometrical stability. In 1823, Fourier became the first person to express the need for the development of optimization algorithms, something that emerged about a century later. Primary work on MP was first devised and applied by L.V. Kantorovich in 1939 [60]; in this work, which in essence is a primary foundation of Linear Programming (LP), the practical problem of optimizing the production of a plywood facility is addressed. In the same year, the necessary and sufficient conditions for a bounded stationary point were first proven by W. Karush in his M.Sc. Dissertation [61]; later on, the development of digital computers gave rise to this new branch of numerical analysis which is commonly referred to as "Mathematical Programming" (MP).

In the following context, a brief reference to the respective bibliographic resources that were used in this doctoral work is presented; an in-depth approach on the subject was not made part of the present work, because, from the engineering point of view, the main interest was to investigate the performance of these algorithms in the problem of incremental non-linear structural analysis.

The first optimization algorithms ever developed belong to the family of the Simplex method, which was introduced in 1951 by Dantzig [62]. These algorithms find an optimal solution (*minimization/maximization*) of a linear function that is subject to a set of linear constraints (*equalities/inequalities*), and, from a historical perspective, they were initially developed for military purposes (*operation research*). The dual method of Lemke [63] is also a historical algorithm that has several computational advantages in various applications (*e.g. in operations research and structural plasticity with material softening*). An analytical presentation of Linear Programming (LP) may be found in [64]; another detailed resource for the respective bibliography may be found in [65].

In the following years, use of the Simplex method found applications in various sectors of the economy, including the design of transportation systems, portfolio management, optimal plastic (*minimum weight*) design and collapse (*limit*) load analysis of framed structures; these applications gave the spark for the rise of a novel branch of numerical analysis, the development of optimization algorithms for non-linear problems. Since the early 1980's, the novel approaches of Quadratic Programming (QP), Sequential/Successive Quadratic Programming (SQP) and Interior Point Methods (IPM) have been developed; detailed presentations of their underlying principles and implementation may be found in the literature (e.g. [66],[67]).

Bounded stationary points of a whole class of generally non-linear functions under generally non-linear constraints can nowadays be easily numerically evaluated, using a large variety of available solvers, some of them being also suitable for sparse matrices (e.g. [68] – [73]). The main characteristics of these algorithms include good convergence properties, yet only a linear/super-linear rate of convergence.

2.3 Engineering Plasticity by Mathematical Programming

Mathematical Programming (MP) is known to provide the most natural formalism to incorporate plasticity in a variety of engineering problems with the usage of Lagrange multipliers via a linear complementarity condition. In the following context, the existing literature regarding the applications of mathematical programming in non-linear structural analysis methods that mainly follow the plastic hinge approach, will be presented.

To the author's knowledge, the earliest work relating engineering plasticity and MP was presented in 1951 by A.C. Charnes and H.J. Greenberg in the form of a preliminary report during a meeting of the American Mathematical Society (AMS) in Minnesota [74]; the problem addressed was that of determining the limit load of a structure. In 1957, W.S. Dorn and H.J. Greenberg proposed three basic types of linear programs for the problem of limit analysis that had smaller memory requirements and developed and tested various efficient procedures in trusses [75]. In 1959, A. Charnes, C.E. Lemke and O.C. Zienkiewicz solved the problem of representing the static and kinematic plastic collapse principles of frames in the form of dual linear programming problems [76].

A book on the theory of structures as seen through the prism of mathematical programming was authored in 1965 by W. Prager [77]; it was also interesting to find the cooperation of G. Maier and D.C. Drucker [78]. The first paper dealing with the theoretical problem of material plastic softening [79] was authored by G. Maier, as well as the correlation between structural analysis and Quadratic Programming (QP) ([80],[81]).

The QP approach concept was followed for formulating incremental elastoplastic analysis problems for elastic-work-hardening continua by G. Maier and M. Capurso [82]; particular focus is given to the elastic-perfectly plastic material constitutive law; this work is in essence the MP version of the incremental principles of plasticity introduced by W. Prager, D. Hodge, and H.J. Greenberg. In [83], G. Maier formulated a set of piecewise linear constitutive laws with associated plastic flow rules in matrix notation for the elastoplastic analysis of structures including kinematic and isotropic hardening; both incremental/step-by-step and shakedown analyses are addressed. In [84], G. Maier investigated the problem of incremental analysis under the assumptions for large displacements and the respective physical destabilizing effects, within the context of rate-dependent plasticity; a detailed presentation including analytical formulations and proofs of the respective theorems is followed throughout this paper. O. De Donato and G. Maier [85] proposed three procedures for the inelastic analysis of concrete beams under the assumption of material hardening behaviour with limited rotation capacity; the proposed methodologies also allow for the estimation of the distribution of the plastic deformations along the beams. L. Corrandi and G. Maier [86] formulated the necessary and sufficient conditions for the case where the dynamic response of frames and continuous systems under cyclic excitations does not lead to shakedown. G. Maier G., A. Zavelani Rossi and J.C. Dotreppe [87] studied the problem of equilibrium branching (*bifurcation*) due to material softening; in this work, bifurcation is acknowledged as a phenomenon that can occur even in the absence of geometric effects. S.B. Abdel-Baset, D.E. Grierson and N.C. Lind [88] studied the 2nd order collapse load of frames by following a LP approach; the effects

of the axial forces on the bending moment plastic capacities and on the elastic flexibility due to bending are both taken into account. O. de Donato and G. Maier [89] formed the problem of incremental elastoplastic analysis of frames under hardening plastic hinges as a Parametric Linear Complementarity Problem (PLCP). In [90], G. Maier applied a linearization of yield criteria, and, later, I. Kaneko [91] devised a reformulation of ([85],[89]) and applied it also in reinforced concrete frames. G. Maier, D.E. Grierson, and M.J. Best [92] showed that a series of Linear Programming (LP), Restricted Basis Linear Programming (RBLP), and Quadratic Programming (QP) problems may be formulated for evaluating the post elastic response of structures using a finite element approach under assumptions for elastic-perfectly plastic as well as hardening plastic material; in particular, for elastic-perfectly plastic material behaviour, the QP algorithms were found to yield the best performance. D.L. Smith [93] devised a solution schema to the Parametric Linear Complementarity Problem (PLCP) using the Wolfe-Markowitz algorithm and by enforcing complementarity at each pivotal step of the Simplex method; the latter functions as a restriction of the variables that enter the basis. Slight modifications of the algorithm were sufficient to convert it to work for non-holonomic plasticity as well; extension to piecewise proportional loading is also demonstrated. Maier et. al. ([94],[95]) applied elastic and elastoplastic analysis on pipelines resting on the sea bottom for various seabed profiles and soil types, and discussed in detail the parameter tuning of their devised numerical technique, which was found to yield satisfactory convergence properties and quality of results; geometric non-linearities are also accounted for, while the proposed approaches can serve as a basis for the respective optimal design problem (*cost minimization*). I. Kaneko [96] proposed an altered LCP formulation for material hardening that requires less computational times and storage. A restricted basis linear programming technique [97] was applied by G. Maier, S. Giacomini, and F. Paterlini in elastoplastic and limit analysis. G. Maier and T. Hueckel [98] published a study on incremental elastoplastic constitutive laws that are primarily suitable for geotechnical and rocky materials, but also fit for concrete; in this study, the dependence of the elastic moduli on plastic deformations is identified, as well as material instability phenomena within the range of material plastic hardening. An edited book containing a variety of articles on plasticity by mathematical programming including detailed texts containing fundamental work done and presented by some of the founding fathers of plasticity may be found in reference [99].

I. Kaneko [100] worked directly on incremental quantities and was able to incorporate non-holonomic plasticity with no particular remedies such as the ones required in ([92],[93]). A. Franchi and M.Z. Cohn [101] provide a general purpose computer programs' approach by creating their own PLCP algorithm, which is perceived as rather involved by some researchers. L. Faravelli and P. Zanon [102] demonstrated the significance of taking into account the effect of shear force in the evaluation of the limit load of frames; a formulation for limit analysis was devised, wherein the shear force effect is incorporated in the form of a parameter that affects the bending moment vs. axial force interaction surface; the DIN-18880 {M,V,N} interaction surface for steel objects is also used as a comparative reference. G. Maier, F. Giannessi, and A. Nappi [103] proposed a holonomic approach to the inverse problem of tracing the elastoplastic response of elastic-perfectly plastic and/or elastic-plastic hardening structures via series of Quadratic Programming (QP) formulations which are solved by devising various numerical procedures that take into advantage the features of each formulation; these techniques have computational advantages as compared to other, generic 'direct search' optimization techniques. F. Giannessi, L. Jurina, and G. Maier [104] proposed a quadratic optimization problem formulation for computing a minimum cost design for a pipeline resting on a rough sea bottom using the limits of the bending moments' curvature as constraints; several examples are presented. A state-of-the-art literature review paper on the applications

of MP in engineering plasticity (*up to the year 1982*) was presented by G. Maier and J. Munro in [105]: In this work, subjects of plastic constitutive laws, plastic limit analysis, shakedown analysis, bounding methods, elastoplastic analysis, large displacement and instability analysis, contact problems and locking systems as well as dynamic plasticity are presented; computational and theoretical aspects are also discussed. An interesting paper that proposes a mathematical programming formulation for the boundary element method with reference to the numerical step-by-step analysis of elastoplastic systems has been authored by G. Maier and G. Novati [106]; the paper covers both elastic-perfectly plastic and elastic-hardening plastic systems. J.A.T. De Freitas and D.L. Smith ([107],[108]) proposed a general methodology/unified approach to the non-linear analysis problem using both statics and kinematics in their Lagrangian-based formulation, being able to also cater for large displacements and the post-buckling behaviour of domes and 3D arches. G. Maier and A. Nappi authored a book chapter in [109] that analytically presents the physical interpretation of constrained optimization and linear complementarity theory used in engineering plasticity by mathematical programming; with reference to these relations, a series of plasticity problems can be formulated and efficiently solved, including fracture. P.D. Panagiotopoulos, C.C. Baniotopoulos, and A.B. Avdelas, proposed a method [110] for linearizing QP problems, which shares the advantages of optimization algorithms and of linear system solvers. P.D. Panagiotopoulos authored an analytical textbook [111] that focuses on problems in mechanics that are formulated as functions of variables representing incremental changes which are also subject to inequality constraints: The author attempts (*among others*) to provide a mathematical background for finding bounded stationary points of generally non-convex problems, by considering them as superpositions of a convex and a concave part; applications in plasticity are also included, for both static and dynamic problems. In a review paper dedicated to the memory of Prof. J. Munro, G. Maier and D.L. Smith [112] summarize the recent contributions in the field of mathematical programming applications to engineering plastic analysis up to the year 1986. Although the Interior Point Method (IPM) had already made its' debut at the time, it was too early to have an impact on the aforementioned field, as commented by the authors. Furthermore, the authors stress out the potential of mathematical programming applications in mechanics, and that it has not yet achieved a full impact in engineering practice. In essence, this paper is an update to a previous literature review paper by G. Maier and J. Munro ([105]). W.X.Zhong and R.L. Zhang authored a paper [113] wherein the parametric variational principles of minimum potential energy and minimum complementarity energy are used to formulate and solve incremental problems in plasticity that may also include material softening; solution is acquired with the help of quadratic programming. An application in geomechanics is also presented. G. Maier and A. Nappi generalized a backward-difference integration scheme for solving rate-dependent, dynamic problems in elastoplasticity, by adding generalized yield functions and plastic hardening [114]. In this procedure, the plastic multipliers correspond to plastic strain rates; the essence of this method coincides with the rate-independent step-wise holonomic QP problems in elastoplasticity with piecewise linear material with plastic hardening. F. Tin-Loi and M.B. Wong [115] presented a mathematical programming-based approach to the elastoplastic analysis of frames; although this procedure requires a large number of constraints –primarily due to the linearization of the non-linear convex yield surfaces used therein– it can efficiently trace phenomena of local unloading and the respective non-unique displacement fields.

G. Maier and G. Novati [116] used the same variational principles as in [113], and by assuming that each yield function is expressed as the sum of two parts (*one function that is defined using the limits of the local stress components, and one function that is defined using the yield limit constants with reference to the constitutive law of the material*) devised a basis for formulating and solving non-linear optimization

problems; the yield limits can be a generally non-linear functional of the internal variables/parameters that describe the material`s constitutive law. The presented paper provides a unified framework for a variety of problems, including, but not limited to, elastic-perfectly plastic and linear plastic hardening. F. Tin-Loi [117] studied the optimal plastic design of frames under combined bending moment and axial force; only 1st order criteria are used, and the formulated LP optimization solution schema works on a two-phase, purely flexibility-based process that assumes a rigid plastic behaviour for predicting the collapse mechanism that yields the minimum weight design withstanding the desired monotonic loading. The same author proposed in [118] a heuristic linearization procedure for the yield surface that helps getting a better estimate of the limit load by locally increasing the interpolation points of the generally non-linear convex yield function at the point of intersection with the stress vector of the section in reference; rigid plastic behaviour is also assumed herein. R.R. Wakefield and F. Tin-Loi [119], based on the work of Kaneko [100], investigated the problem of non-uniqueness in the displacements computed in incremental non-holonomic elastoplastic analysis, and demonstrated how such diverse results may be acquired below the state of collapse. The same authors addressed the problem of computing large-scale non-holonomic elastoplastic analysis [120]; in particular, with reference to the LCP, remedies regarding the reduction of memory storage and propagation of round-off errors were proposed. Some aspects of optimization under complementarity constraints are discussed by G. Giannessi and G. Maier in [121]; primarily, the common mathematical properties of structural optimization and inelastic response as well as of contact problems, are presented. A. Nappi [122] devised a formulation for the incremental elastoplastic analysis of frames that is primarily based on a free energy and a dissipation function; the proven extremum properties of the respective formulation lead to solving unconstrained optimization problems; limit and shakedown analysis are also discussed within the context of the presented formalism; the internal variables used may either correspond to internal structural element forces, external load or displacement or displacement rate increments (*which, in the case of shakedown, may also be functions of time*). The proposed numerical procedures are based on the Newton-Raphson algorithm, thus exhibited good convergence properties and quality of results for the stepwise holonomic approach. Z. Cen and G. Maier [123] adopted a cohesive crack model for simulating fracture in structures made of concrete-like material, and studied bifurcation and instability phenomena due to material softening. It was found that the craze tip advancement –which is a monotonously increasing quantity–, should be used as a governor variable for the incremental procedure, and that boundary integral equations' approaches are of good use for this type of problems, since no re-meshing is required; once more, it is stressed out that non-holonomic behaviour plays an important role in the analysis results in the presence of local unloading. The effects of material softening in the dynamic response of structures were studied by G. Maier and and U. Perego in [124]. F. Tin-Loi proposed a first order optimal plastic design procedure for arches, under the assumption of rigid-plastic material behaviour and a suitable linearization of the yield criteria applied [125]; the procedure is based on a flexural approach and the static theorem of limit analysis. F. Tin-Loi and J.S. Pang [126] proposed a method for the incremental analysis of plastic hardening structures that is cast on the basis of a Non-Linear Complementarity Problem (NLCP); the method was tested for cyclic loading scenarios and yielded good results. A. Corigliano studied elastoplastic structural systems in quasi-static problems under assumptions for small strains [127]; both rate-dependent and rate-independent plasticity formulations are derived. G. Bolzon, G. Maier, and G. Novati [128] discussed some aspects of incremental analysis under assumptions for quasi-brittle material within the context of linear complementarity formalism. A piecewise linear constitutive law for the cohesive crack model that describes the traction vs. the opening displacement of the crack is adopted (*G.I. Barrenblatt's model*).

Both holonomic and non-holonomic material behaviour approaches are followed and two mathematical formalisms are devised to model crack propagation using a finite element method incremental problem approach: a Linear Complementarity Problem (LCP) and a Quadratic Programming Problem (QPP). Geometric non-linearity effects are also accounted for in the form of a stepwise linearization; criteria for overall instability are also adopted (*negative second order work*), and the criteria for the occurrence of bifurcations are formulated from the LCP in terms of rates of the respective quantities (*e.g. work, boundary conditions, displacements, external loads, yield functions*). W.Q. Shen [129] proposed a novel technique for the limit analysis of plane frames by Linear Programming (LP); it was tested in planar frames under vertical and wind loads. A comparative study of mathematical programming approaches on quasi-brittle structures was published by G. Bolzon, G. Maier, and F. Tin-Loi [130]; primarily "branch-and-bound" (*exhaustive exploration of a binary tree*), and Newton-type algorithms were used in this work. M. Mroz and G. Giambanco [131] presented an interface model that is suitable for the analysis of discontinuities under monotonic and cyclic loading; the presented work is particularly suitable for modelling the response of granular materials. F. Tin-Loi and V. Vimonsatit [132] presented a 2nd order formulation for the elastoplastic analysis of planar frames with material hardening; the solution schema is based on an iterative application of the Wolfe-Markowitz algorithm that is also able to trace the equilibrium path beyond the point of instability; however, it is acknowledged that the procedure lacks robustness in the sense that, as the number of active plastic hinges increases, the number of basic solutions that need be identified also increases. A predictor-corrector computational schema that also uses an arc-length technique to model the 2nd order inelastic response of planar frames as a Non-Linear Complementarity Problem (NLCP) is presented by F. Tin-Loi and J.S. Misa in [133]. C. Comi and A. Corigliano [134] devised a variational formulation for evaluating the dynamic elastoplastic response of solids with isotropic softening; a mixed variational formulation is derived, wherein the equations describe a softening gradient-dependent material and time discretization is done using a generalized mid-point integration rule. Sufficient conditions for solution uniqueness and an upper bound on the integration time step are also presented, as well as numerical examples. G.Bolzon, D. Ghilotti, and G. Maier [135] addressed the inverse problem of parameter identification for the cohesive crack model with reference to concrete structures that are simulated within the framework of LCPs; the evolution of displacements during the experiments that were carried out was measured using laser interferometers, and computations were carried out using a least-squares data fitting approach which is expressed as the minimization of a quadratic function that measures the diversion between the experimental and the theoretically predicted displacements The Sequential Quadratic Programming (SQP) method and a direct-search Genetic Algorithm (GA) were used to determine the parameters; the SQP method was found to perform better when dealing with real experimental data. However, in every case, a relaxation of the complementarity condition was required in order to achieve convergence easily. G. Bolzon, G. Maier, and F. Tin-Loi [136] discuss the issue of multiplicity of solutions in the analysis under assumptions for quasi-brittle fracture of the material; both rate-dependent and rate-independent plasticity approaches are followed: The efficient solution schemas for the formulated LCPs, the respective mathematical programming algorithms that yield good results, the potentials and limitations, are all discussed. The proposed methodology is able to efficiently identify the multiplicity, even the lack of solution(s). Y.H. Liu, V. Carvelli, and G. Maier [137] investigated the integrity of defective pressurized pipelines using limit analysis and shakedown; they were found to be more economical (*in terms of CPU time*) and more reliable than their alternate, direct stiffness-based step-by-step procedures. G. Bolzon and G. Cocchetti [138] investigated crack propagation (*kinking and branching*) in brittle solids, phenomena that also affect the equilibrium path`s bifurcation;

various numerical techniques are presented and compared. It is specified that crack kinking occurs in the case of "mode I" (*in plane tension*) cracking, and that sharp crack branching occurs in the case of "mode II" (*in plane shear*) cracking; however, crack branching is also augmented by higher loading rates as well as from the lack of homogeneity in the material. The analyses procedures were applied on the classical three-point bending experiments on beams; it was found that an isotropic state of stress is typical around the crack propagation zone; furthermore, it was found that symmetric or unsymmetrical crack propagation is equally possible after a state of equi-biaxial stress is reached, which implies difficulties in tackling the non-uniqueness of the problem's solution, a fact that will definitely play a role in the analysis of more complicated structures. G. Bolzon and F. Tin-Loi [139] studied the problem of physical instability and 2nd order effects in structural frames under the assumptions of lumped plasticity and an elastic-softening plastic bending vs. rotation constitutive law: Applications on simple planar frames demonstrate bifurcation and limit points, as well as snap-through and snap-back phenomena; although the proposed methodology may be easily extended to large scale, 3D structures, it is acknowledged by the authors that, in such a case, the determination of such points (*and multiplicity of solutions or proof of non-existence of any solution*) would not be an easy task, because of the combinatorial nature of the problem. F. Giambanco [140] proposed an asymtptotic pivoting computational schema for solving the LCP problem of step-by-step elastoplastic analysis of framed structures; the main idea is to solve a sequence of LCPs, for which the constraints' matrix consists only of the main diagonal elements of the constraints' matrix of the original LCP. A proof of convergence, as well as a Fortran 77 subroutine, is also provided. The method yields good convergence properties.

In the beginning of the year 2000, a special issue on direct methods was published by G. Maier, V. Carvelli, and G. Cocchetti [141]. S.M. Karakostas and E.S. Mystakidis [142] proposed a non-convex QP formulation for steels structures of holonomic material with smooth plastic softening properties that yielded good convergence properties. G. Maier, G. Bolzon. And F. Tin-Loi [143] discussed a series of open problems that require interdisciplinary considerations, since they address both the fields of engineering mechanics and mathematical programming. Such problems are the kinematic approach for evaluating the strength of ductile materials with periodic heterogeneity, the problem of bounding post-shakedown analysis quantities using an optimization formulation approach, incremental collapse and alternating plasticity phenomena observable in poro-plasticity (*e.g. periodical loadings on two-phase saturated materials*), the simulation of fracture of structures made of quasi brittle materials (*e.g. concrete*), and the identification of cracking parameters for the latter systems. The open issues discussed are primarily of concern to experts in mathematical programming algorithms. F. Giambanco [144] presented an iterative method that is generally suitable for solving LCPs, the "Asymptotic Pivoting Method (APM)"; it is implemented in a formulation that is able to solve the incremental problem of elastoplastic analysis, but it can also consider dynamic degrees of freedom. The basis of the APM is a recursive solution of a sequence of LCPs in which the constraints matrix is diagonal and contains only the main-diagonal elements of the LCP matrix; the proposed computational schema is proved to have good convergence properties and requires little storage space. Furthermore, it was found to require short CPU time; the source code of the APM subroutine is also provided in Fortran 77 at the Appendix of the paper. M. Papadrakakis, N.D. Lagaros, Y. Tsompanakis, and V. Plevris investigated the efficiency of various optimization methods that are based either on MP and/or Genetic Algorithms (GA) for solving structural optimization problems [145]; modified procedures that are based on both types of algorithms are also investigated and were found particularly promising. The main subject addressed is the optimal (*minimum weight*) design of a structure using a series of reference artificial accelerograms that are suitably scaled to

match the reference seismic code requirements. A neural network is used to predict the necessary data for the structural analysis phase of the tests; advanced decomposition techniques for parallel computing are also implemented in this work. The results demonstrate the efficiency and the respective computational advantages of the proposed mixed procedures as compared to the QP/SQP and GA based procedures; also, the proposed procedures were found particularly suitable for parallel processing. F. Tin-Loi and N.S. Que presented a work on parameter identification of quasi-brittle materials ([146],[147]); this work, which is an inverse problem, is formulated as a Mathematical Program with Equilibrium Constraints (MPEC) which is then converted into a standard NLP by a smoothening (*relaxation*) of the complementarity condition and the constraints. The smoothening problem is approximated via a solution of series of NLP problems, with good results. G. Cocchetti and X. Shen [148] applied the cohesive crack model in various piecewise linear constitutive laws (*both wrt. yield functions and interface models adopted*), in order to provide a unified set of simple mathematical tools (LCP) for the inelastic analysis of quasi-brittle material, such as concrete dams. The procedure traces efficiently both the multiplicity and the non-existence of solutions that may arise from material softening. H. Zhang and X. Zhang [149] developed a new algorithm for the dynamic analysis of structures from elastic-hardening/softening plastic material; the method is a Parametric Quadratic Programming (PQP) algorithm combined with direct time-integration of the dynamic equations (*via a precise integration and/or via the Newmark method*), which is solved as a standard linear complementarity problem. Numerical examples of a dynamically loaded truss, a cantilever under dynamic tension, and of a double-notched specimen under impact loading demonstrate the efficiency of the proposed method. G. Cocchetti and G. Maier [150] provide a unified methodology for the inelastic analysis of skeletal structures with reference to the recent research findings on complementarity theory of MP. A classical plastic hinge approach is followed that obeys piece-wise linear (PWL) material constitutive laws that also include plastic hardening and plastic softening; both holonomic and non-holonomic approaches are discussed within the context of LCP-based formulations, for both rate-dependent and rate-independent plasticity that also predict non-unique solutions (*e.g. bifurcations*). A simple test case is used to demonstrate the sensitivity of the solution, wrt. the changes in the constitutive law of the reference structure's plastic hinges for material softening. H.Zhang, X. Zhang, and J.S. Chen [151] applied a newly developed algorithm (*that was first presented in* [149]) for the dynamic elastoplastic analysis of structures with hardening/softening plasticity in various new test cases. H.W. Zhang, W.X. Zhong, C.H. Wu, and A.H. Liao [152] presented their recent advances in the Parametric Quadratic Programming (PQP) method for studying elastoplastic contact problems with friction; within the context of this work, the PQP problem is converted to a standard LCP via a linearization of the constitutive law that models friction, and a general-purpose, 3D FEM program was also developed, which was applied on special test cases that demonstrate its' efficiency. S. Tangaramvong and F. Tin-Loi ([153],[154]) extended the PLCP approach to cater for structural frames with material softening behaviour. K. Krabbenhøft, A.V. Lyamin and S.W. Sloan [155] formulated a series of plasticity problems as conic programming problems, which is a formulation suitable for efficient use with interior point algorithms (*although some issues/problems were also detected, as pointed out by the authors*). S. Tangaramvong and F. Tin-Loi also devised a method that determines in a single step the ultimate collapse load and deformation distribution of strain softening frames under combined stresses [156]; it is formulated as a Mathematical Program with Equilibrium Constraints (MPEC). R. Ardito, G. Cocchetti, and G. Maier [157] provided a method for the safety assessment of structures that considers holonomic material softening; although bifurcation phenomena due to linear complementarity are not treated, applications using generalized finite elements are included in this very interesting work. F. Pastor, E.

Loute, and J. Pastor [158] proposed a novel decomposition approach to limit analysis using the upper-bound theorem; in practice, the solution schema begins from a coarse discretization of the mesh, which is incrementally refined after each solution in order to achieve the desired solution accuracy. An Interior Point Method (IPM) solver for convex problems is used, that exhibits good convergence properties and improved quality of results even in relatively large-scale problems wrt. the available computational resources. S. Tangaramvong and F.Tin-Loi [159] extended the classical problem of the 1st order limit analysis of frames, in order to include geometric non-linearity; material behaviour is assumed elastic−perfectly plastic. The problem is formulated as a MPEC; despite the fact that the proposed approach is a direct method, it is able to predict −in a single step− both the maximum load and the actual maximum corresponding deformations of the structure without the need to follow the plasticization sequence, as would be the case with any step-by-step method. A detailed book chapter on limit analysis methods that may serve as a useful basis for teaching purposes was authored by F. Tin-Loi [160]. The proposed formalism follows the flexural approach; a detailed formulation and presentation of several examples with step-by-step instructions and computer code are a good introduction for the unfamiliar. S. Tarangamvong and F. Tin-Loi [161] applied a MPEC approach to the limit analysis of frames considering 2nd order effects and material softening; the proposed approach is efficient for the majority of structures in engineering practice, but has limitations in the seldom case where local buckling phenomena are prominent to lead to bifurcations.

In [162], S. Tarangamvong and F. Tin-Loi considered a holonomic approach to the same problem examined in [161], with good results; in the case where non-holonomic phenomena may occur within the same step, special correction remedies are applied to the next step of the procedure. M.A.A. Skordeli and Ch. Bisbos [163] studied three-dimensional (3D) frames by performing step-by-step and shakedown analyses under considerations for ellipsoidal yield surfaces (*e.g. according to Orbisson*). M.R. Mahini, H. Moharrami, and G.Cocchetti [164] formulated a MP that solves the step-by-step analysis of frames with plastic hinges of elastic-perfectly plastic material by requesting the maximization of the dissipation energy; the proposed method uses the revised Simplex method, it is easy to code, has rapid convergence properties and potential for including material softening as well. D.Wu, W. Gao, S. Tangaramvong, and F. Tin-Loi [165] followed a deterministic approach to the uncertainty quantification problem of the determination of the collapse load and mechanism of frames. The uncertain quantities are the material, the geometry of the cross-section, and the loading conditions, and are modelled using upper and lower bound intervals. The outcome of the procedure provides an upper and lower bound value of the collapse load as well as the values of the respective uncertain quantities that trigger these bounds. The results are compared to those following a classical Monte-Carlo approach, and were found to be in good accordance; however, for buckling analysis of structures whose eigenvalues are of similar or identical value, further research is required. S. Tarangamvong and F. Tin-Loi [166] investigated the optimal topological plastic design of truss structures considering material softening properties; an MPEC approach is followed, and the optimization problem is solved in a two-step pattern, where in the first phase the lower bounds of the basic structure's parameters are updated and a solution using an NLP solver is acquired; in the second phase, the solution from the first phase is used as a basis; any cross-sections whose stress configurations are at their lower bounds are discarded, and a new optimal direction is sought by solving yet another NLP problem. Although no theoretical proof can be provided for a truly optimal solution, comparisons of the proposed method's results with step-by-step elastoplastic analyses demonstrates the good quality of the method in practical terms. M.M.S. Manola and V. Koumousis [167] proposed a reduced complementarity approach for the incremental analysis of structural frames; in this work, an efficient technique that

significantly reduces the constraints of the problem is presented, under the assumption that, within the same step of analysis, the axial force of the member does not significantly increase in order to cause a jump from one hyperplane of the constraints manifold to a consecutive one, something which is usually the case for most civil engineering structures. H. Moharrami, M.R. Mahini, and G. Cocchetti [168] presented an extension of the restricted basis linear programming technique for plane stress/strain structures using generalized finite elements. Y. Kanno [169] proposed a fast-converging approach for the 1st order analysis of elastoplastic skeletal structures using interior point algorithms; the proposed schema is an unconstrained non-smooth convex problem that has good convergence properties and can be extended to parallel computing. A design optimization technique of planar frames by setting the maximum stability as a criterion was authored by M. Cacho-Pérez [170].

For further reading on other applications of mathematical programming in structural engineering and plasticity, including, but not limited to shakedown analysis, generalized FEM modelling and soil and fracture mechanics, the reader should have a look in an excellent literature review paper by G. Bolzon [171].

2.4 Unconventional Engineering Plasticity Methods

Although not belonging to the class of MP methods, the following methods caught the author's eye while searching for bibliographic references; a short review follows below.

The work of G. Royer-Carfangi and G. Buratti [172] is worth mentioning, for they have presented various constitutive models for accurate modelling of material plastic softening in beams which were found to be consistent with experimental data. The Linear Matching Method (LMM) is also worth mentioning, for it is known for its ability to yield the collapse load using only a continuous change on (*linear*) elasticity modules [173]; recently, O. Barrera, A.C.F. Cocks and A.R.S. Ponter improved its' convergence properties [174].

3 Flexibility-based Beam/Column Finite Elements

In this chapter, the 1st order constitutive elasticity relations that correlate deformations (*axial elongation, torsion and bending rotations*) and generalized forces (*axial force, torsion and bending moments*) at the ends of each finite beam-column element of a skeletal structure are briefly presented.

3.1 Definitions

From a vector's notation point of view, every finite beam/column element in the 3D space may be seen as a directed line segment (*vector*) that is defined by a local, right-hand-ruled Cartesian coordinate system with basis {1,2,3}, where axis "1" is identical to the line segment that connects the start "*i*" and finish "*j*" nodes of the element; the start and finish nodes are the centres of gravity points of the respective cross-section(s). For the end of the beam, the positive directions for the local force and moment components are defined according to the local coordinate system {1,2,3}, and for the start of the beam in a complementary way (*see Figure 5 below*).

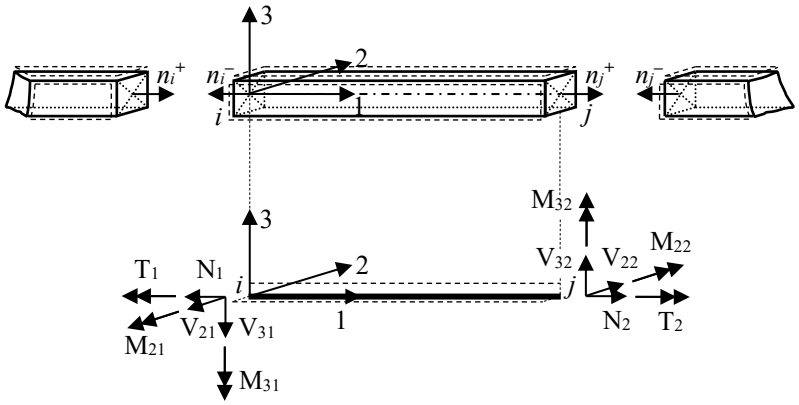

Figure 5: Finite beam/column element with end nodes, local axes, and local force/moment components.

For every such beam/column element, a set of independent, local, elastic deformations may be defined (*see Figure* 6*, Figure* 7*, and Figure* 8 *below*). These deformations are linked to their corresponding stress components via the material's property of flexibility.

3.2 Axial Component

For axial forces, the unassembled flexibility coefficient is described by Equation (5), with reference to Figure 6 below:

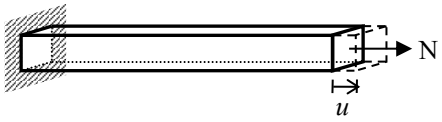

Figure 6: Axial force (N) and elongation (u)

$$\sigma = E \cdot \varepsilon \Rightarrow \frac{\mathrm{N}}{A} = E \cdot \frac{du}{dL} \Rightarrow \boxed{u = \frac{L}{E \cdot A} \cdot \mathrm{N}} \tag{5}$$

3.3 Torsion Component

For torsion, the unassembled flexibility coefficient is described by Equation (6), with reference to Figure 7 below, where warping deformations and their respective bi-moments are neglected (*1st order analysis*):

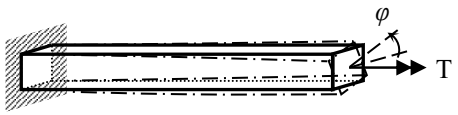

Figure 7: Torsion moment (T) and rotation (φ)

$$\tau = G \cdot \gamma \Rightarrow \frac{T}{I_T} = G \cdot \frac{d\varphi}{dL} \Rightarrow \boxed{\varphi = \frac{L}{G \cdot I_T} \cdot \mathrm{T}} \tag{6}$$

Wherein (6), the rate of change of the twisting angle is considered to be constant along the length of the finite beam/column element.

3.4 Bending Components

For bending moments, the 1st order unassembled flexibility coefficients may be derived by solving the respective differential equation of the planar (2D) problem; see Figure 8 below:

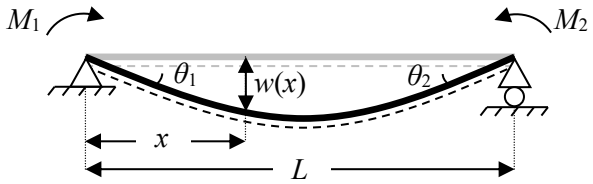

Figure 8: Deflection (w) due to end bending moments {M_1,M_2} for the planar (2D) problem.

The differential equation of the deflection is (*with reference to Figure 8*):

$$E \cdot I \cdot w''(x) = -\left[M_1 + \left(\frac{M_2 - M_1}{L} \right) \cdot x \right] \tag{7}$$

Where in (7) the assumption of sufficient rigidity in order for the deflections "$w(x)$" to be small has been made for the curvature "κ":

$$\kappa = \frac{w''(x)}{\sqrt{\left[1 + (w'(x))^2\right]^3}} \cong w''(x) \tag{8}$$

The solution of (7) is obtained via sequential integration:

$$E \cdot I \cdot w'(x) = \int_{y=0}^{y=x} \left[M_1 + \left(\frac{M_2 - M_1}{L} \right) \cdot y \right] \cdot dy + C_1 = M_1 \cdot x + \left(\frac{M_2 - M_1}{2 \cdot L} \right) \cdot x^2 + C_1 \tag{9}$$

$$E \cdot I \cdot w(x) = \int_{y=0}^{y=x} \left[M_1 \cdot x + \left(\frac{M_2 - M_1}{L} \right) \cdot x^2 + C_1 \right] \cdot dy + C_2 = \frac{M_1}{2} \cdot x^2 + \left(\frac{M_2 - M_1}{6 \cdot L} \right) \cdot x^3 + C_1 \cdot x + C_2 \tag{10}$$

Where, in (9), "w'(x)" stands for the slope of the deflection w(x), which is the rotation θ(x). By applying the boundary conditions "$w(0)=0$" and "$w(L)=0$" in (10), the values of "C_2" and "C_1" are acquired, respectively:

$$C_1 = -\left(\frac{2 \cdot M_1 + M_2}{6} \right) \cdot L \quad , \quad C_2 = 0 \tag{11}$$

By substituting (11) into (9), the end rotation values "$\theta(0)$" and "$\theta(L)$", are easily acquired:

$$\theta(0) = -\frac{L}{6 \cdot E \cdot I} \cdot \left(2 \cdot M_1 + M_2 \right) \quad , \quad \theta(L) = -\frac{L}{6 \cdot E \cdot I} \cdot \left(M_1 + 2 \cdot M_2 \right) \tag{12}$$

By setting "$\theta(0)=-\theta_1$" and "$\theta(L)=\theta_2$" in (12), the respective matrix of the unassembled, 1st order flexibility coefficients is obtained:

$$\begin{Bmatrix} \theta_1 \\ \theta_2 \end{Bmatrix} = \frac{L}{6 \cdot E \cdot I} \cdot \begin{bmatrix} 2 & 1 \\ 1 & 2 \end{bmatrix} \cdot \begin{Bmatrix} \mathrm{M}_1 \\ \mathrm{M}_2 \end{Bmatrix} \tag{13}$$

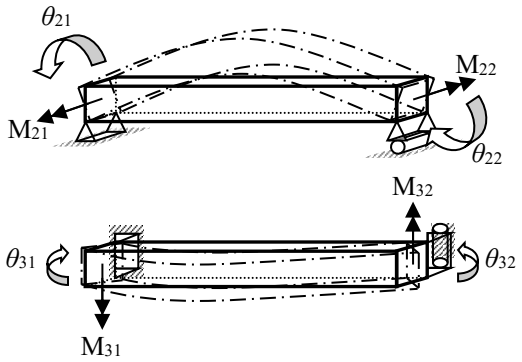

Figure 9: Bending moments (M) and rotations (θ) around axis 2 (top); around axis 3 (bottom).

A proper index may be added to (13), for the weak and strong bending axes, respectively (*with reference to Figure 9 above*):

$$\begin{Bmatrix} \theta_{j1} \\ \theta_{j2} \end{Bmatrix} = \frac{L}{6 \cdot E \cdot I_j} \cdot \begin{bmatrix} 2 & 1 \\ 1 & 2 \end{bmatrix} \cdot \begin{Bmatrix} \mathrm{M}_{j1} \\ \mathrm{M}_{j2} \end{Bmatrix} \quad , \quad j = \{2,3\} \tag{14}$$

4 Governing Equations

In this section, a listing of the governing equations for the herein developed force-based structural analysis method is presented. An incremental approach is followed, using the beam/column finite element definitions that were presented in Chapter 3.

The stress component increments of a structure may be represented by a vector "$\Delta\mathbf{Q_s}$" which is expressed as a sum of a vector "$\Delta\mathbf{Q}_0$" due to external loads, and a vector "$\Delta\mathbf{Q}_1$" due to internal redundant stresses; the latter applies to statically indeterminate structures:

$$\Delta\mathbf{Q_s} = \Delta\mathbf{Q}_0 + \Delta\mathbf{Q}_1 \tag{15}$$

Equation (15) may be further developed by expressing each of the two linearly independent vectors as the product of a matrix "$\mathbf{B}_i$" and a vector "$\Delta\mathbf{p}_i$", where $i=\{0,1\}$. These matrices express the values of the stress component increments of the structure due to unit valued external load increments "$\Delta\mathbf{p}_0$" and unit valued internal redundant stress increments "$\Delta\mathbf{p}_1$", respectively:

$$\Delta\mathbf{Q_s} = \mathbf{B}_0 \cdot \Delta\mathbf{p}_0 + \mathbf{B}_1 \cdot \Delta\mathbf{p}_1 \tag{16}$$

Where, with reference to Figure 6, Figure 7, and Figure 9, by grouping the corresponding stress components for the whole structure, we have:

$$\Delta\mathbf{Q_s}^T = \left\{\Delta\mathbf{N}^T \quad \Delta\mathbf{T}^T \quad \Delta\mathbf{M}_2^T \quad \Delta\mathbf{M}_3^T\right\} \tag{17}$$

The redundant stress vector increments "$\Delta\mathbf{p}_1$" in Equation (16) are computed with the help of the compatibility condition, as was first proposed by James Clerk−Maxwell:

$$\mathbf{B}_1^T \cdot \Delta\mathbf{q_s} = \mathbf{0} \tag{18}$$

Where in (18), vector "$\Delta\mathbf{q_s}$" denotes the generalized, local deformation increments of the structure at its points of reference (*critical sections*), which may be expressed as the summation of their elastic "$\Delta\mathbf{q_{el}}$" and plastic "$\Delta\mathbf{q_{pl}}$" components:

$$\Delta\mathbf{q_s} = \Delta\mathbf{q_{el}} + \Delta\mathbf{q_{pl}} \tag{19}$$

Where, with reference to Figure 6, Figure 7, and Figure 9, by grouping the corresponding deformation components for the whole structure, we have:

$$\Delta\mathbf{q_s}^T = \left\{\Delta\mathbf{u}^T \quad \Delta\boldsymbol{\varphi}^T \quad \Delta\boldsymbol{\theta}_2^T \quad \Delta\boldsymbol{\theta}_3^T\right\}_{\mathbf{s}} \tag{20}$$

The elastic components in (19) are computed with the help of the unassembled flexibility matrix "$\mathbf{F}$":

$$\Delta\mathbf{q_{el}} = \mathbf{F} \cdot \Delta\mathbf{Q_s} \tag{21}$$

Where in (21), "$\mathbf{F}$" is defined for the whole structure with reference to equations (5),(6) and (14), and the ordering of the elastic components in "$\Delta\mathbf{q_{el}}$" is according to (20):

$$\mathbf{F} = \begin{bmatrix} \mathbf{F_N} & \mathbf{0} & \mathbf{0} & \mathbf{0} \\ & \mathbf{F_T} & \mathbf{0} & \mathbf{0} \\ & & \mathbf{F_{M_2}} & \mathbf{0} \\ & & & \mathbf{F_{M_3}} \end{bmatrix} \tag{22}$$

For an elastic-ideally plastic material, the plastic components in (19) may be computed with the help of the axiom of maximization of plastic work (*from a physics point of view, it may be seen as an equivalent to that of the maximization of entropy*), using the stress derivative of an adequately defined yield function "g(**Q**)":

$$\Delta\mathbf{q}_{\mathbf{pl}} = \Delta\lambda \cdot \frac{\partial g(\mathbf{Q})}{\partial \mathbf{Q}} \tag{23}$$

Where in (23) "$\Delta\lambda$" denotes a Lagrange multiplier. This multiplier may be explicitly computed within the framework of mathematical programming, using a linear complementarity condition:

$$\mathbf{Y}_*^T \cdot \Delta\boldsymbol{\lambda} = 0 \quad , \quad \mathbf{Y}_* \geq 0 \quad , \quad \Delta\boldsymbol{\lambda} \geq 0 \tag{24}$$

Where in (24), "$\mathbf{Y}_*$" is the vector of plastic potentials for the whole structure; the plastic potential is defined as a scalar, nonnegative, dimensionless quantity, and it expresses the numerical difference between the maximum and the actual value of a yield function. Schematically, the concept of the plastic potential "Y_*" and its corresponding Lagrange multiplier may be depicted in Figure 10 below, for the case of two interacting components {Q_1,Q_2}:

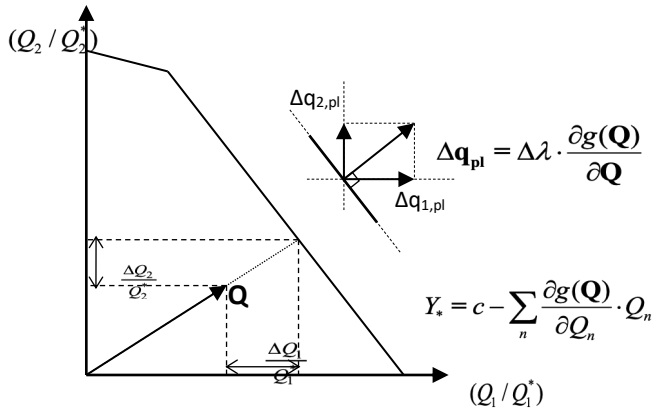

Figure 10: Plastic potential and corresponding Lagrange multiplier.

For a linearly hardening plastic material, the plastic deformation increments are associated with their respective stress increments:

$$\Delta\mathbf{q}_{\mathbf{pl},S} = \mathbf{F}_S \cdot \Delta\mathbf{Q}_\mathbf{s} \tag{25}$$

Where in (25), "$\mathbf{F}_S$" is a diagonal matrix whose non-zero entries depend on the interacting stress components of the yield functions that have been adopted for the respective members of the structure.

The displacement increments along the direction of the external loads may be computed with the help of the Static−Kinematic Duality (SKD):

$$\Delta\mathbf{u}_\mathbf{s} = \mathbf{B}_0^T \cdot \Delta\mathbf{q}_\mathbf{s} \tag{26}$$

5 Equilibrium Matrices

This chapter contains the required equations for describing and calculating equilibrium in the 3D space, as well as the respective automation techniques. For reasons of brevity, only the novel parts of the automation processes are presented; nevertheless, all required references to related previous works have been included.

5.1 Equilibrium Conditions in the Three-Dimensional Space

Considering the outer (*cross*) product in matrix form for a Cartesian space, the reacting moments "**M**" at a particular point "*f*" due to a force vector "**F**" applied at another point "*s*" may be described by the following equation:

$$\mathbf{M} = -\mathbf{d}_R \cdot \mathbf{F} \Leftrightarrow \begin{Bmatrix} M_x \\ M_y \\ M_z \end{Bmatrix} = -\left[\begin{array}{c|c|c} 0 & +\Delta z & -\Delta y \\ \hline -\Delta z & 0 & +\Delta x \\ \hline +\Delta y & -\Delta x & 0 \end{array}\right] \cdot \begin{Bmatrix} F_x \\ F_y \\ F_z \end{Bmatrix} \tag{27}$$

Where

$$\Delta x = x_f - x_s \quad , \quad \Delta y = y_f - y_s \quad , \quad \Delta z = z_f - z_s \tag{28}$$

The equilibrium condition in global coordinates between the two points "*f*" and "*s*" may then be written in matrix form, as follows:

$$\begin{Bmatrix} \mathbf{F} \\ \mathbf{M} \end{Bmatrix}_f = -\begin{bmatrix} \mathbf{I}_{3x3} & \mathbf{0}_{3x3} \\ \mathbf{d}_R & \mathbf{I}_{3x3} \end{bmatrix} \cdot \begin{Bmatrix} \mathbf{F} \\ \mathbf{M} \end{Bmatrix}_s \tag{29}$$

5.2 Linear Projections from Global to Local Three-Dimensional Cartesian Coordinates

A simple to implement, yet efficient linear transformation from global to local coordinates, is the following:

$$\mathbf{v}_L = \mathbf{T}_R \cdot \mathbf{v}_G \tag{30}$$

Where $\mathbf{v}_G = \{v_x \quad v_y \quad v_z\}^T$ is a vector whose components are defined with respect to a global Cartesian coordinate system with basis {x,y,z}, and $\mathbf{v}_L = \{v_1 \quad v_2 \quad v_3\}^T$ is the same vector with respect to a local Cartesian coordinate system with basis {1,2,3}. All coordinate systems are assumed to be right-hand ruled (*see also Figure 11 below*).

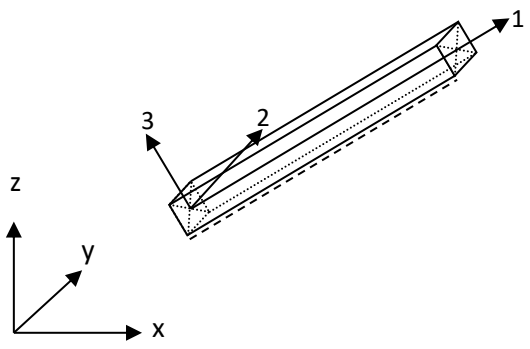

Figure 11: Global and local coordinate systems (*right-hand ruled*).

For the general case, the transformation matrix " $\mathbf{T}_R$"may be then expressed as follows:

$$\mathbf{T}_R = \left[\begin{array}{c|c|c} +\frac{v_x}{L} & +\frac{v_y}{L} & +\frac{v_z}{L} \\ \hline -\frac{v_x}{L}\cdot\frac{v_z}{L_{xy}}\cdot\cos\alpha + \frac{v_y}{L}\cdot\sin\alpha & -\frac{v_y}{L}\cdot\frac{v_z}{L_{xy}}\cdot\cos\alpha - \frac{v_x}{L}\cdot\sin\alpha & +\frac{L_{xy}}{L}\cdot\cos\alpha \\ \hline +\frac{v_x}{L}\cdot\frac{v_z}{L_{xy}}\cdot\sin\alpha + \frac{v_y}{L}\cdot\cos\alpha & +\frac{v_y}{L}\cdot\frac{v_z}{L_{xy}}\cdot\sin\alpha - \frac{v_x}{L}\cdot\cos\alpha & -\frac{L_{xy}}{L}\cdot\sin\alpha \end{array}\right] \tag{31}$$

Where $L = \sqrt{{v_x}^2 + {v_y}^2 + {v_z}^2}$ and $L_{xy} = \sqrt{{v_x}^2 + {v_y}^2}$ and "α" is a rotation angle around the axis of the vector " $\mathbf{v}_G$" or " $\mathbf{v}_L$".

For each of the special cases where the global vector " $\mathbf{v}_G$" is perpendicular to a Cartesian plane {x,y} or {y,z} or {z,x}, the elements of the transformation matrix " $\mathbf{T}_R$" are defined by the group of equations (32):

$$\begin{aligned} &\vec{v}_L \perp \left(\vec{v}_x \times \vec{v}_y\right): \quad \mathbf{T}_R = \left[\begin{array}{c|c|c} 0 & 0 & p \\ \hline |p| & 0 & 0 \\ \hline 0 & p & 0 \end{array}\right], \quad p = sign\left(v_1 \cdot v_z\right) \\ &\vec{v}_L \perp \left(\vec{v}_y \times \vec{v}_z\right): \quad \mathbf{T}_R = \left[\begin{array}{c|c|c} p & 0 & 0 \\ \hline 0 & |p| & 0 \\ \hline 0 & 0 & p \end{array}\right], \quad p = sign\left(v_1 \cdot v_x\right) \\ &\vec{v}_L \perp \left(\vec{v}_z \times \vec{v}_x\right): \quad \mathbf{T}_R = \left[\begin{array}{c|c|c} 0 & p & 0 \\ \hline 0 & 0 & |p| \\ \hline p & 0 & 0 \end{array}\right], \quad p = sign\left(v_1 \cdot v_y\right) \end{aligned} \tag{32}$$

Where in (32), the absolute value of "*p*" helps to maintain a right-hand ruled coordinate system. The rotation of angle "α" around the longitudinal axis is then applied separately, with the help of the corresponding tensor "**R**":

$$\mathbf{R} = \left[\begin{array}{c|c|c} +1 & 0 & 0 \\ \hline 0 & +\cos\alpha & +\sin\alpha \\ \hline 0 & -\sin\alpha & +\cos\alpha \end{array}\right] \tag{33}$$

An equivalent practice for setting the direction of the local axes of a member in the 3D space is by setting an auxiliary point, that, together with the longitudinal axis (#1), defines the hemi-plane on which the vector of the weak axis (#2) lies. A suitable linear transformation that is based on the auxiliary point definition may be found in [53].

5.3 Evaluation Formulae for {$\mathbf{B_0}$,$\mathbf{B_1}$}

From a computational implementation perspective, it is convenient to define the equilibrium matrices "$\mathbf{B_0}$" and "$\mathbf{B_1}$" using a set of mathematical formulae that simultaneously express equilibrium in 3D space as well as transformation of the stress components from the global coordinate system to the local of each member of the structure. By combining equations (27) − (31) or (27) − (30) and (32) − (33), depending on the member's direction, we have a similar form of the equations that were first presented in [10]:

$$\mathbf{B}_i = -Sign\{m\} \cdot \left[\begin{array}{c|c} \mathbf{T}_R & \mathbf{0}_{3x3} \\ \hline \mathbf{T}_R \cdot \mathbf{d}_R & \mathbf{T}_R \end{array} \right] \quad , \quad i = \{0,1\} \tag{34}$$

Herein, the newly introduced multiplier "$Sign\{m\}$" applies an additional (±) sign to each row of (34), according to whether the direction of the local axes of the member/element "m" coincide with the direction of the shortest path ($\mathbf{B_0}$) / mesh ($\mathbf{B_1}$), or not.

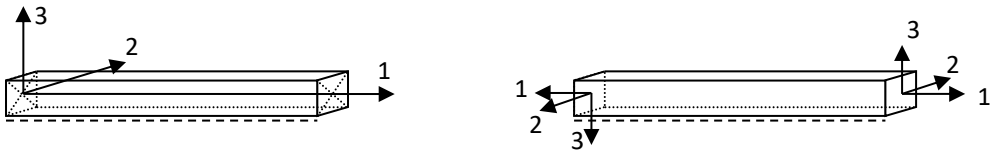

Figure 12: Element's directional axes (*left*); section axes for the local force and moment components (*right*).

For a given set of external load and redundant stress component increments, and with the help of equations (16) and (34), the stress component increments of each structural member may be easily evaluated.

5.4 Procedures for the Determination of Statical Bases

The computation of the equilibrium matrices (*see Equation (34)*) depends on the automated selection of a statical basis that carries the external loads (*matrix* "$\mathbf{B_0}$") and of a statical basis that defines the redundant stresses (*matrix* "$\mathbf{B_1}$"); these automation techniques are based on graph theory and algorithms.

For the external loads, equilibrium is satisfied along cantilevers which mark the quickest path from the load application points to the boundary nodes of the structure. For the redundant stresses, equilibrium is satisfied along the independent closed loop-form cantilevers which are defined by the topological cycles of the graph of the structure. In the following section, a brief presentation of the respective algorithms is presented, that is based on the publications [31],[47],[49], and [53]. For the shortest path finding problem, Nicholson's method was used in all cases.

5.4.1 External Loads

In this section, the determination of a statical basis for the external loads of the structure (*matrix* $\mathbf{B_0}$) is presented.

The main idea is to create a set of independent cantilevers that transfer the potentially applied external loads from each free node of the structure to the ground (*boundary nodes*). The process is quite simple in principle; for each node "k" of the structure, where $k \rightarrow \{1,2,...,N_{nodes}\}$:

0. Store all boundary nodes of the structure in a list.
1. Find the shortest paths that lead from node *k* to the each of the boundary nodes of the structure, and store the sequence of nodes that form each path in a list, as well as its' respective length.
2. Among the determined shortest paths, select the one with the minimum length as valid.

5.4.2 Redundant Components

In this section, the determination of a statical (*cycle*) basis for the redundant components of the structure (*matrix* $\mathbf{B_1}$) is presented.

The main idea is to create a set of independent closed loops (*topological cycles*) that represent the concept of self-equilibrating systems that exist within the structure and define the stress redistribution due to structural indeterminacy.

5.4.2.1 Basic Process

1. Let "N" be the number of nodes of the structure. Create an additional datum (*ground*) node with index number "N+1", and connect all boundary nodes to this node (*see step 2 for evaluating the distance matrix*).
2. Form the distance matrix "d(i,j)" that simulates the structure as a graph: For all connected node couples (i,j), where {i,j}→{1,2,...,N+1} and "N+1" is the number of nodes of the graph, input the value "1" into the respective memory position "d(i,j)"; for all node couples that are not connected, input a theoretically infinite value in "d(i,j)" (*e.g. "N_{total}+1", where "N_{total}" is the number of nodes of the whole graph*).
3. Sort all nodes of the graph according to their valency (*i.e. the number of elements that are connected to them*) and store their numbers in a list. Also, form a list with the index numbers of the members that are adjacent (*connected*) to each node of the graph.
4. Set a counter index: k=1.
5. Select the k^{th} node of the list created in step #3, and find the shortest path between the two ends of the 1st member adjacent to this node; in order to avoid the trivial solution, mind to input a theoretically infinite value for the distance between the start and end nodes of the reference member before performing the search.
6. Given that the inequality "$L_{SP}<2\cdot(N_{nodes}-1)$" or "$L_{SP}<2\cdot N_{nodes}$" holds, where "$L_{SP}$" is the sum of the lengths of the members and "N_{nodes}" is the number of nodes that form the shortest path that was found in step #5 respectively, assign the value "2" in the respective entries of the distance matrix "d(i,j)" that correspond to the lengths of the members that form the cycle. (*Note: The aforementioned type of inequalities is referred to as "cycle admissibility rule". According to* [53]*, the second inequality quoted above is a preferable cycle admissibility rule for 3D structures*).
7. Continue by searching for the next topological cycle from the next member of the k^{th} node, until all the members adjacent to that node have been processed (*i.e. their length has received the value "2"*).
8. Set k→k+1 and repeat the search process (*steps #5 to #6*), until all nodes of the graph have been processed.

5.4.2.2 Amending the Problem of Embedded Cycles

In the case where the process that was described in Section 5.4.2.1 yields a number of topological cycles that is smaller than Betti's 1st number, then the following process need also be executed, in order to locate and remove nodes that cause cycle embedding:

0. Set a counting index k=1.
1. Start from the k^{th} node of the list of nodes sorted according to their valency; select an adjacent member whose length is equal to "2".

2. Find the shortest path between the ends of the selected member; in order to avoid the trivial solution, mind to set a theoretically infinite value for the member's length (*e.g. "N_{nodes}+1", where "N_{nodes}" is the number of nodes of the graph*) before starting the search for the shortest path.
3. After determining a topological cycle, check whether the cycle admissibility rule is valid, and assign the length value "2" in the respective entries of the distance matrix "d(i,j)" for all members that form the cycle.
4. Check in the distance matrix "d(i,j)" whether all members of the graph have a length value equal to "2"; if yes, then a complete set of independent topological cycles has been determined and therefore the process may move on to step #6; if no (*e.g. there are still members with a length value equal to "1"*), select a new member that is adjacent to the k^{th} node and repeat steps #1 to #4, until all adjacent members of the k^{th} node have been processed.
5. Set $k \rightarrow k+1$ and return to step #1, until all nodes of the graph have been processed.
6. Let "$N_{c,k}$" be the number of determined topological cycles: Check whether "$N_{c,k}$" is equal to Betti's 1st number; if yes, the process is successfully terminated; if no, move on to step #7.
7. Remove the k^{th} node in reference from the graph (*e.g. set a theoretically infinite length value to all members adjacent to the node*), and repeat steps #1 to #4: When all remaining members of the graph have a length value equal to "2", move on to step #8.
8. Replace the k^{th} node of the graph, as well as all its' adjacent members, and execute steps #2 and #3 for each of the adjacent to the node members. Let "$N'_{c,k}$" be the new total number of topological cycles that were determined.
9. If $N'_{c,k}=N_{c,k}+1$, then the k^{th} node in reference causes dependent (*embedded*) topological cycles, thus both the node and its' adjacent members must be removed from the graph; if not, choose another node (*e.g. set* $k \rightarrow k-1$), and go to to step #7.
10. Repeat steps #7 to #9 for as many times as the number of missing topological cycles in order to reach the 1st number of Betti; this way, a set of independent topological cycles that does not contain the nodes that cause dependencies (*embedded cycles*) will be determined.
11. Add the missing nodes to the graph, as well as their adjacent members, and execute steps #2 and #3 for all their adjacent members, in order to find a complete set of independent topological cycles.

It should be noted that the processes described in section 5.4.2 will not always yield a minimal, but a near-minimal cycle basis. This disadvantage leads to creating global flexibility matrices with a number of elements greater than the minimum possible one.

6. Element Eccentricities

In general terms, one could say that, the more detailed a structural model, the better the quality of analysis results. However, there are several limitations to this generic concept. As a mesh discretisation becomes denser, the analysis becomes more demanding in computational resources. However, computational resources are limited, and increasing the mesh density beyond a certain point results in severe latency in the numerical procedure's convergence time. Therefore, in order for the professional engineer to be efficient, a series of proper simplifying assumptions are required, so as for the calculations of the structural model of any structure to be carried out with as much precision and ease as possible, and within reasonable time.

In simulation of structural systems, a common practice is that of considering the joints between beams and columns (nodes) as non-deformable. When the prerequisites for such an assumption are satisfied, carrying out of the structural calculations becomes a much easier task, since all design and/or bearing capacity values at the ends of each element are acquired much faster. (*In general, it is important to perform a stress capacity check in the volume(s) of the node(s), according to the principles of limit analysis on which all modern structural codes are based on*).

A rigid part of an element is by definition non-deformable; thus, it does not store potential energy; from a mathematical point of view, it has zero flexibility (*or infinite stiffness, in the dual sense*). Therefore, element eccentricity is only of geometrical importance in the force method [9]: only the starting and ending points of the deformable part of a beam/column element need be defined so as to calculate its Euclidean length, which is required for the evaluation of the unassembled flexibility matrices (*see Equation (22)*), as well as for the equilibrium conditions at each end (*see Equation (34) with reference to (27) – (33)*). Note that the aforementioned groups of equations as well as their attached procedures remain unaffected by the inclusion of element eccentricities.

Let $\{x_i,y_i,z_i\}$ be the coordinates of the starting node "*i*" and $\{x_j,y_j,z_j\}$ the coordinates of the ending node "*j*" of a beam/column element of the structure, and let $\{\vec{e}_{x,i},\vec{e}_{y,i},\vec{e}_{z,i}\}$ be the eccentricities next to node "*i*", and $\{\vec{e}_{x,j},\vec{e}_{y,j},\vec{e}_{z,j}\}$ next to node "*j*", respectively; these quantities are defined as vector components that are parallel to the basis' components of the global coordinate system (*see Figure 13 below*). Then, the deformable length of the member as well as its projections on each global plane ($\{x,y\},\{y,z\},\{z,x\}$) are evaluated using the following modified coordinates:

$$\begin{matrix} x_i^{'} \to x_i + \vec{e}_{x,i} \\ y_i^{'} \to y_i + \vec{e}_{y,i} \\ z_i^{'} \to z_i + \vec{e}_{z,i} \end{matrix} \quad , \quad \begin{matrix} x_j^{'} \to x_j + \vec{e}_{x,j} \\ y_j^{'} \to y_j + \vec{e}_{y,j} \\ z_j^{'} \to z_j + \vec{e}_{z,j} \end{matrix} \tag{35}$$

Where, in the above group of Equations (35), eccentricity components are defined as directed quantities (*positive or negative*), depending on whether their direction is in accordance with the basis' components of the global coordinate system, or not.

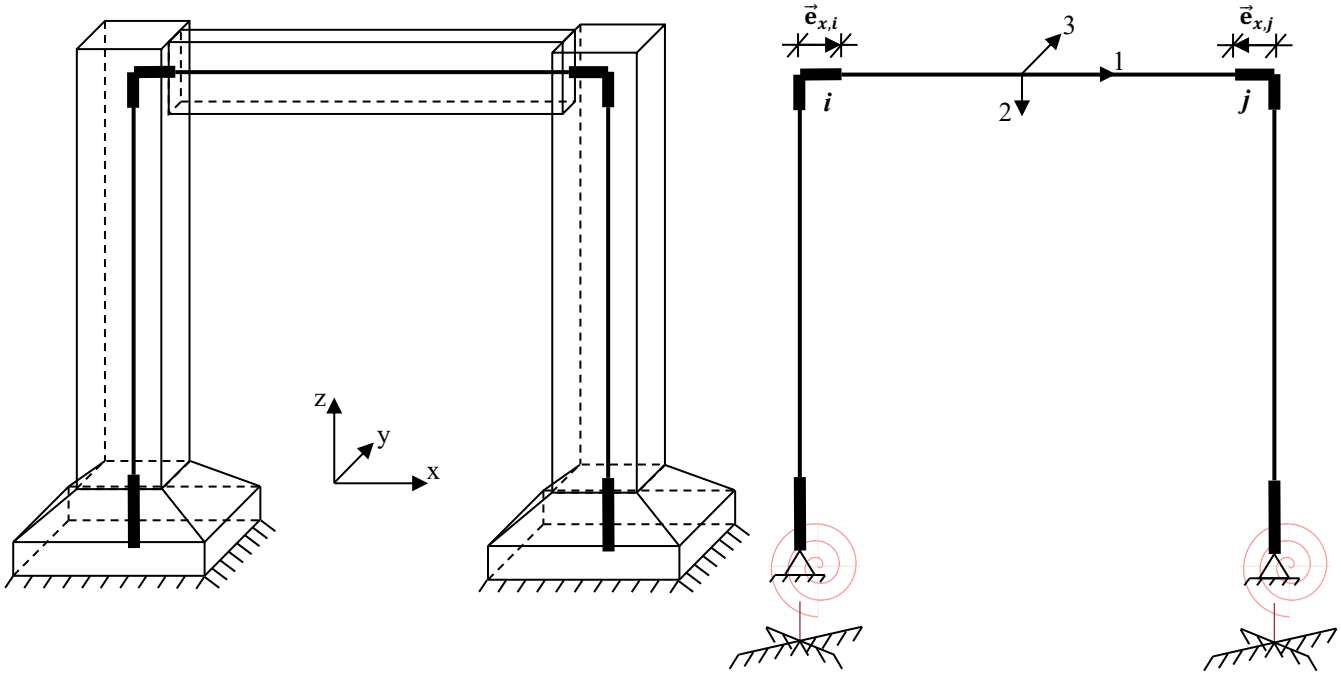

Figure 13: A simple example of a structural frame with element eccentricities due to the beam-column and column-foundation joints; soil-structure interaction is simulated with rotational springs (*denoted with an Archimedean Spiral*).

7 Yield Functions

In this chapter, a special set of functions that constitute the limits between elastic and plastic material conditions are defined. The form of these functions requires the deformation and stress distribution simplification assumptions regarding the bending problem (*pure or combined with other actions*), in order to correspond to the assumptions regarding the zero-length plastic hinges of the Euler-Bernoulli beam/column finite elements that are used in this work.

Furthermore, it is shown that the same type of functions may be used to set zero-valued limits on any of the local stress components at the ends of a beam/column finite element, in order to describe all forms of internal discontinuities.

7.1 Linearized Yield Functions

For an analysis of a structural frame that takes into account material post−elastic behaviour, a plastic hinge approach is traditionally followed. From the strength of materials' point of view, the conventional limits between elastic and plastic deformations may be defined using a closed, convex shell; in the case of the proposed method, this shell is further approximated by a convex polyhedron, whose hyper-planes are defined with the help of a linearized yield function (*see also Figure 10 and Figure 14*):

$$g_i(\mathbf{Q}) = \sum_{n=1}^{N_{isc}(i)} s_n \cdot \frac{Q_n}{Q_n^{*(\pm)}} - c_i \le 0 \quad , \quad i = \left\{1,2,...,N_{eq}\right\} \tag{36}$$

Wherein (36), "N_{eq}" is the number of equations that constitute the yield function, "$N_{isc}(i)$" is the number of interacting stress components of the i^{th} equation of the yield function "$g_i(\mathbf{Q})$", "$\mathbf{Q}$" is a vector that contains only the interacting out of the potentially six in total stress components (*see Figure 5*), and "c" is a dimensionless constant (e.g. c=1).

Due to the 3D nature of the problem, a series of stress interaction criteria may be defined, e.g. {N,M_2,M_3} or {T,M_2,M_3} or {T,V_2,V_3} or {N,V_2,M_3} or {N,V_3,M_2} or {N,V_2,V_3,M_2,M_3}, etc; applied implementations of such criteria may be found in structural codes.

For example, the AISC−LRFD [175] proposes a criterion which is a bi-segmented yield function for bending moment and axial force interaction; schematically, it is presented in Figure 14 below:

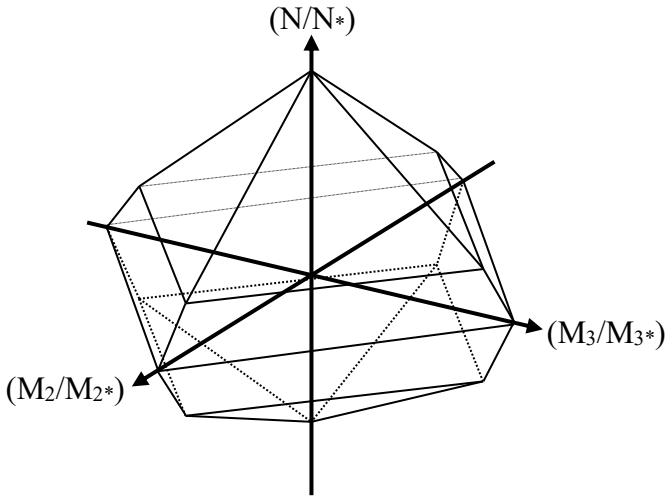

Figure 14: 3D illustration of the adopted form of the AISC-LRFD bilinear yield function.

Another example from engineering practice is the failure criterion according to DIN−18880, which is a multi−segmented yield function for bending moment, shear, and axial force interaction. A definition of this function for planar frames is analytically presented in [176]; herein, the corresponding coefficients for implementing this function according to Equation (36) are summarized in Table 1 below:

S_i	N	Q	M
Eq. 1	−	−	1.00
Eq. 2	1.00	−	1.00/1.10
Eq. 3	−	0.45/1.15	1.00/1.15
Eq. 4	1.10/1.25	0.45/1.25	1.00/1.25
Eq. 5	−	1.00/0.90	−

Table 1: Coefficients "S_i" for the yield functions according to DIN-18800.

In order to model the positive or negative plastic capacity for every stress component a set of (±) signs have been introduced in (36), which are used to define the sector of the hyperspace wherein each one of the polyhedron's stress interaction hyper planes is located; this may be easily implemented with the help of the basic principle of enumeration.

For the case of two interacting stress components, the distinct sequence of combinations shown in Figure 15 below is formed:

{+,+},{+,−},{−,+},{−,−}

Figure 15: Sequence for the signs of a yield function with two interacting components.

For the case of three interacting components, the distinct sequence of combinations shown in Figure 16 below is formed:

{+,+,+},{+,+,−},{+,−,+},{+,−,−}
{−,+,+},{−,+,−},{−,−,+},{−,−,−}

Figure 16: Sequence for the signs of a yield function with three interacting components.

For the case of five interacting components, the distinct sequence of combinations shown in Figure 17 below is formed:

{+,+,+,+,+},{+,+,+,+,−},{+,+,+,−,+},{+,+,+,−,−}
{+,+,−,+,+},{+,+,−,+,−},{+,+,−,−,+},{+,+,−,−,−}

{+,−,+,+,+},{+,−,+,+,−},{+,−,+,−,+},{+,−,+,−,−}
{+,−,−,+,+},{+,−,−,+,−},{+,−,−,−,+},{+,−,−,−,−}

{−,+,+,+,+},{−,+,+,+,−},{−,+,+,−,+},{−,+,+,−,−}
{−,+,−,+,+},{−,+,−,+,−},{−,+,−,−,+},{−,+,−,−,−}

{−,−,+,+,+},{−,−,+,+,−},{−,−,+,−,+},{−,−,+,−,−}
{−,−,−,+,+},{−,−,−,+,−},{−,−,−,−,+},{−,−,−,−,−}

Figure 17: Sequence for the signs of a yield function with five interacting components.

By using the aforementioned principle, any form of polyhedron that corresponds to any type of linearized yield function may be formed in an automated pattern.

7.2 Implementation of Discontinuities

For the case of members that have internal releases (*e.g. articulations*), a disjunction of the interacting components of the corresponding plastic hinge may be imposed; this allows plasticization only for the remaining continuous stress component(s).

For example, consider an articulated beam element with plastic hinges according to AISC−LRFD [175], defined for $\{N,M_2,M_3\}$ interaction. Since the element has articulations at both its ends, the $\{M_2\}$ and $\{M_3\}$ components will be always zero, for both positive and negative rotations; this leaves only the $\{N\}$ component as an active candidate for plasticization. In practice, this means that a separate static admissibility condition for each stress component must be defined: ergo, a yield function consisting of three separate parts (*one for each component*), with the formulae for $\{M_2\}$ and $\{M_3\}$ being degenerate in order to describe that the corresponding bearing capacity is zero. This disjunct yield function is presented in Equation (37) below:

$$\begin{aligned} g_1(\mathbf{Q}) &= \left\{1/N^{*(\pm)} \quad 0 \quad 0\right\}\cdot\mathbf{Q}-1\le 0 \\ g_2(\mathbf{Q}) &= \left\{0 \quad 1/M_2^{*(\pm)} \quad 0\right\}\cdot\mathbf{Q}\le 0 \\ g_3(\mathbf{Q}) &= \left\{0 \quad 0 \quad 1/M_3^{*(\pm)}\right\}\cdot\mathbf{Q}\le 0 \end{aligned} \tag{37}$$

Where $\mathbf{Q}=\{N \quad M_2 \quad M_3\}^T$ is the vector of the interacting stress components of the corresponding critical section, and the (±) sign is used to denote upper and lower bounds.

The proposed disjunction technique presented in (37) may be used to define all sorts of internal releases; the corresponding Lagrange multiplier due to the complementarity condition of the inequality constraint (*see Equation (24)*) is added to the corresponding elastic generalized displacement (*see Equation (19) with reference to (23)*) in order to yield the actual elastic generalized displacement of the corresponding internal release.

It should be noted that, although the implementation of internal releases using equalities instead of inequalities would perhaps seem like a more appropriate choice in the first place, it was not the right one: testing of various examples by following this approach showed that the Lagrange multiplier of an equality constraint always occurs as a negative quantity, regardless of the expected direction of the (*local*) elastic generalized deformation to which it corresponds to.

8 Material Plastic Hardening

In this chapter, a summary of the governing equations used in hardening structural plasticity as well as a complete mathematical formalism for their implementation in non-holonomic incremental analysis, are presented.

8.1 Piece−Wise Linear Constitutive Laws

In the plastic hinge approach, non−linear behaviour is approximated by a piecewise linear constitutive law. Schematically, the concept is presented in the following Figure 18, wherein a typical diagram of bending moment vs. rotation according to the ATC−40 [177], is presented:

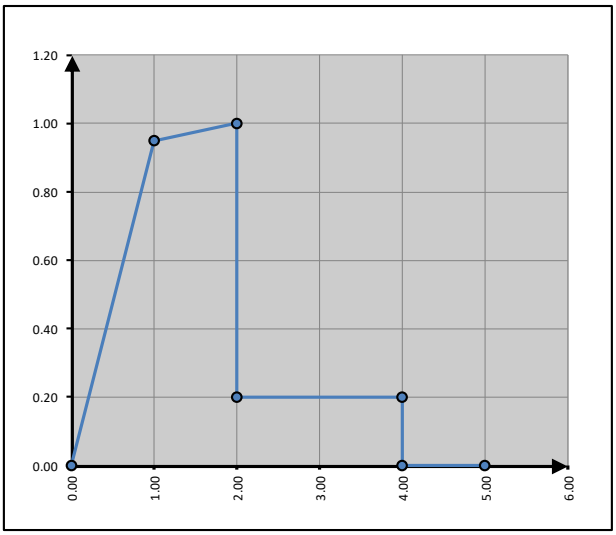

Figure 18: ATC-40 capacity curve of a reinforced concrete cross-section under bending moment.

The numerical values that define the above illustrated piece-wise linear curve are presented in Table 2 below, wherein moment and rotation values have been normalized with the ultimate bending moment capacity and the yield rotation, respectively:

i	M	θ
0	0.000E+00	0.000E+00
1	9.500E-01	1.000E+00
2	1.000E+00	2.000E+00
3	2.000E-01	2.000E+00
4	2.000E-01	4.000E+00
5	0.000E+00	4.000E+00
6	0.000E+00	+∞

Table 2: Dimensionless coordinates of the ATC-40 bearing capacity curve.

As it is specifically noted in [177], from point 2 and onwards (*see Table 2*), “significant strength degradation begins; beyond this deformation, continued resistance to reversed cyclic lateral forces can no longer be guaranteed”. Thus, the proposed analysis method will be developed in order to be able to terminate at the point beyond which the material’s degradation begins, which corresponds to limited plastic hardening.

8.2 Unassembled Flexibility Coefficients for Material Hardening

In order to be able to formulate the governing equations of the force method for hardening plasticity, the principle of disjunction must first be applied in order to separate elastic from plastic deformation components. Schematically, this process is illustrated in Figure 19 below for an arbitrary stress-strain diagram with limited plastic hardening:

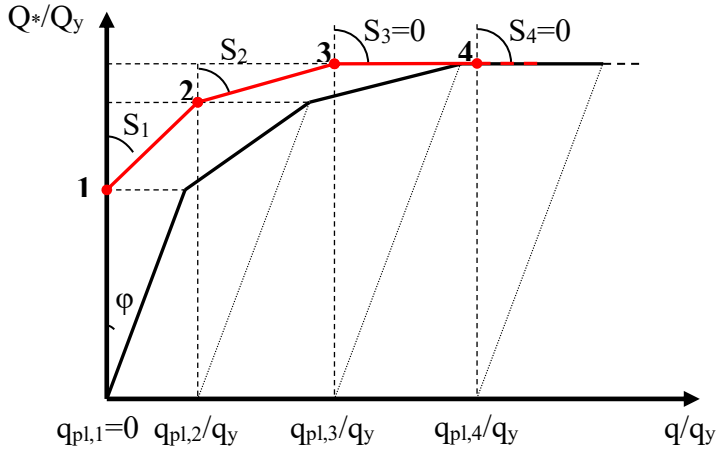

Figure 19: Normalized capacity curve (stresses vs. plastic deformations).

Where in Figure 19 above, "Q_*" is an abstract, arbitrary stress component (*e.g. bending moment*), "Q_y" is its corresponding (*conventional*) yield value, and "q_y" is the yield deformation corresponding to "Q_y". The formula for the evaluation of the above curve is given below:

$$\left(\frac{q_{pl,i}}{q_y}\right)=\left(\frac{q_{total,i}}{q_y}\right)-\left(\frac{Q_{*,i}}{Q_y}\right)\cdot\tan\varphi \tag{38}$$

Where in (38), $i=\{1,2,3,4\}$, tanφ=1 is the elastic flexibility, and $q_{pl,4}\to+\infty$. The normalized flexibility coefficients "S_i" that correspond to plastic hardening may then be easily computed using the following formula:

$$S_i=\begin{cases}\left(\dfrac{q_{pl,i+1}-q_{pl,i}}{Q_{*,i+1}-Q_{*,i}}\right)\cdot\left(\dfrac{Q_y}{q_y}\right) & ,\ if\quad Q_{*,i+1}-Q_{*,i}\neq 0\\ 0 & ,\ if\quad Q_{*,i+1}-Q_{*,i}=0\end{cases} \tag{39}$$

Where in (39), $i=\{1,2,3,4\}$; note that these coefficients are zero only in the case of perfectly plastic material, because then non-holonomic behaviour is served by the linear complementarity condition (*see Equation (24)*).

The physical flexibility coefficients of the structure's unassembled hardening matrices may be evaluated using the formula below, with reference to Equation (39):

$$F_{S,i}=S_i\cdot\left(\frac{q_y}{Q_y}\right) \tag{40}$$

Where in (40) above, "q_y" is the corresponding yield generalized displacement, and $i=\{1,2,3,4\}$ (*see Figure 19*). This class of formulae is valid for any constitutive law, regardless of the number of

peaks/branches the latter may contain; in the case of experimental data processing, the only prerequisite is an appropriate linearization of the physically measured curve.

In order to be able to compare with other commercial software, an adaptation of the above formulae is required; for reasons of comparison with SAP2000 [178], the following values were adopted:

$$F_{S,N} = S \cdot \left(\frac{L}{E \cdot A} \right) \quad , \quad F_{S,M_2} = S \cdot \left(\frac{L}{6 \cdot E \cdot I_2} \right) \quad , \quad F_{S,M_3} = S \cdot \left(\frac{L}{6 \cdot E \cdot I_3} \right) \tag{41}$$

Where in (41) above, "S" is a universal hardening coefficient, according to (39). Using (40) or (41), the unassembled flexibility matrix "$\mathbf{F}_S$" for material hardening may be evaluated (*see Equation (25)*).

8.3 Mathematical Implementation of Material Hardening

The simplest material hardening rule is the one according to D.C. Drucker [179]. For the plastic hinge approach, it is considered that each point of the piece−wise linear curve represents a uniformly distributed (*isotropic*) change in the volume of the corresponding convex yield locus.

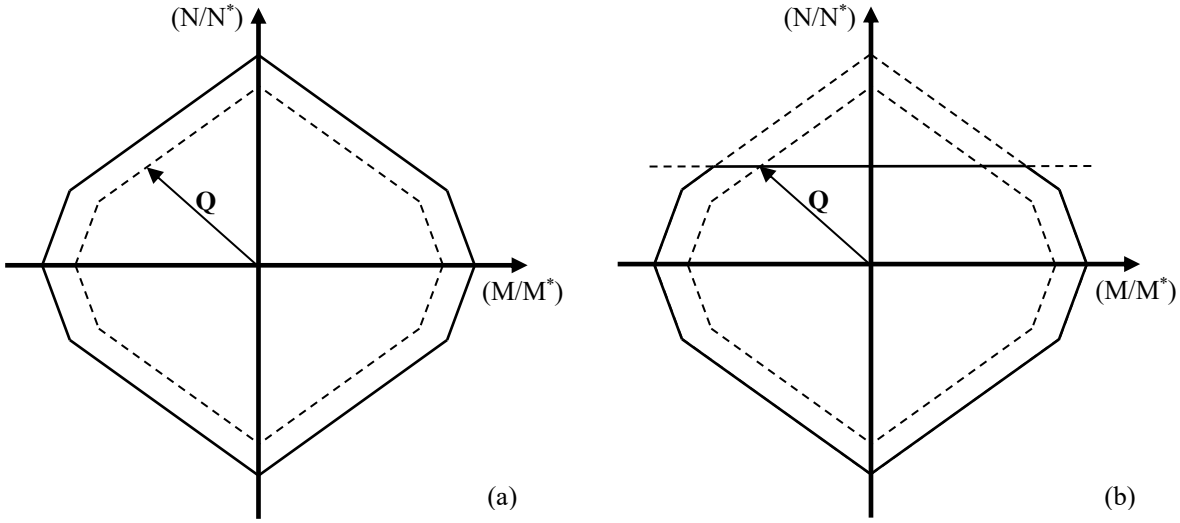

Figure 20: (a) Isotropic hardening; (b) Isotropic hardening assuming a perfectly plastic axial component.

Where in Figure 20(a) and Figure 20(b) above, the locus that defines the yield limit is shown in dotted line format, and the locus that defines the end of the hardening branch of the piece-wise linear constitutive law of the material is denoted with a continuous line format.

Another simple material hardening rule that is also suitable for studying cyclic loading scenarios, is the one according to E. Melan [180] and W. Prager [181]. This type of hardening is linear; thus, it is the simplest form of kinematic hardening. During this kinematic hardening, the volume of the yield locus remains constant, while it moves along a specified direction defined as perpendicular to the activated yield plane.

Schematically, this translocation is presented in Figure 21 below for a 2D problem, for two cases; one where the axial forces participate in the hardening phase of the material (*see Figure 21(a)*), and one where a perfectly plastic axial component is assumed (*see Figure 21(b)*):

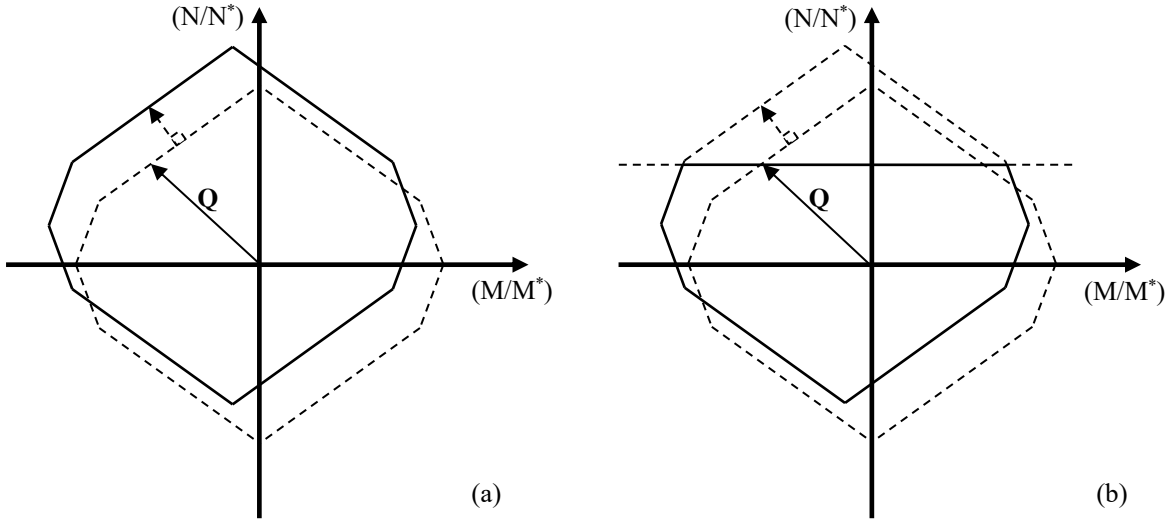

Figure 21: (a) Prager's kinematic hardening; (b) Prager's hardening assuming a perfectly plastic axial component.

The kinematic hardening rule best suitable for studying cyclic loading scenarios is the one according to H. Ziegler [182]; this is the most natural form of material hardening because it yields the most accurate stress configuration of a structure, particularly in the case where the axial forces are not constant during a cyclic loading.

According to Ziegler's hardening rule, the displacement vector of the yield locus of a section is parallel to the direction of the stress vector of the section as it is evaluated on the analysis step in which it first touches the surface of the yield function. Schematically, this is presented in Figure 22(a) below, for the first hardening branch of a piece-wise linear material constitutive law; for two successive hardening branches of a piece-wise linear material constitutive law, the function of the process is illustrated in Figure 22(b) below:

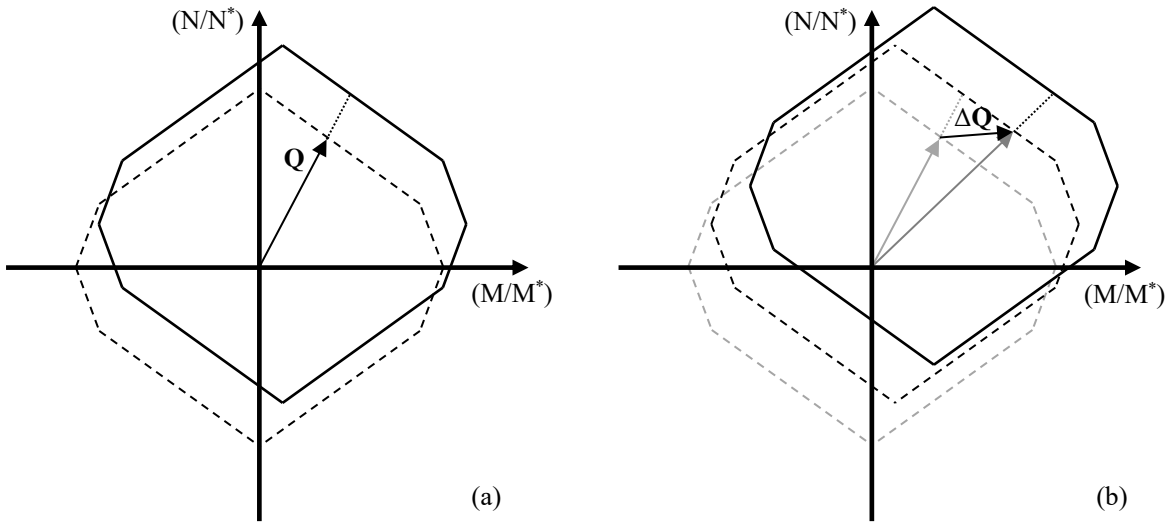

Figure 22: (a) Ziegler's kinematic hardening; (b) Ziegler's hardening for two successive hardening branches.

From a mathematical and computational point of view, a set of pre-solved formulae are required in order to be able to apply the transformation or translocation of the manifold due to isotropic or kinematic hardening, respectively. These equations are derived within the context of analytical geometry and vector algebra.

The yield locus' transformation due to Drucker's isotropic hardening means that a uniform dilation is applied to the manifold. Thus, we need only update the constants that describe the bounds of the yield function (*with reference to Equation (36)*):

$$c_i^{'} = c_i + \delta_{PWL} \tag{42}$$

Where "δ_{PWL}" is depicted in Figure 23 below on an abstract normal stress vs. normal strain linearized diagram, wherein the coordinates have been normalized with their respective yield values:

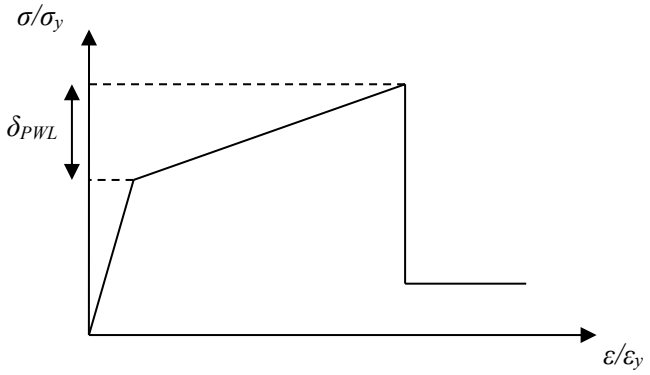

Figure 23: Stress scaling factor "δ_{PWL}" due to material hardening.

The yield locus' translocations due to the kinematic hardening rules of Melan−Prager and Ziegler are analytically described next.

Let $\vec{\mathbf{n}}$ be a unit vector that points towards the direction of the yield locus's translocation due to material hardening, and let $g_i(\vec{\mathbf{Q}})$ be the set of yield equations that describe the polyhedron of constraints, where $i = \{1, 2, 3..., N_{eq}\}$ and $\vec{\mathbf{Q}}$ be a vector containing the interacting stress components. If, by using the nabla, we symbolize the gradient of the yield function with respect to the stresses as "$\vec{\nabla} g_i$", this set of equations may be expressed with the help of the inner (*dot*) product (*with reference to Equation (36)*):

$$g_i(\vec{\mathbf{Q}}) = \left(\vec{\nabla} g_i \bullet \vec{\mathbf{Q}}\right) - c_{i,(k)} \le 0 \tag{43}$$

Where in (43), subscript "*k*" denotes the step of the incremental analysis in which the translocation takes place. Using the above notation, the equations of the displaced yield locus due to material hardening may be written as:

$$g_i^{'}(\vec{\mathbf{Q}}) = g_i(\vec{\mathbf{Q}}) - \delta_{PWL} \cdot \left(\vec{\nabla} g_i \bullet \vec{\mathbf{n}}\right) \tag{44}$$

For the case of Melan's−Prager's hardening, the translocation's directional vector "$\vec{\mathbf{n}}$" is parallel to the gradient of the activated yield function's equation "$\vec{\nabla} g_a$" (*where the subscript "α" denotes the activated hyperplane*), while for the case of Ziegler's hardening, it is parallel to a stress vector "$\vec{\mathbf{Q}}_h$" that touches the yield locus at the time point where the new hardening plastic flow is about to begin. In essence, "$\vec{\mathbf{n}}$" is defined for each hardening rule via a normalization of a reference "hardening" vector; thus, Equation (44) may be rewritten as:

$$g_i^{'}(\vec{\mathbf{Q}}) = \begin{cases} g_i(\vec{\mathbf{Q}}) - \dfrac{\delta_{PWL}}{\left\|\vec{\nabla} g_a\right\|} \cdot \left(\vec{\nabla} g_i \bullet \vec{\nabla} g_a\right) & \text{(Melan}-\text{Prager)} \\ g_i(\vec{\mathbf{Q}}) - \dfrac{\delta_{PWL}}{\left\|\vec{\mathbf{Q}}_h\right\|} \cdot \left(\vec{\nabla} g_i \bullet \vec{\mathbf{Q}}_h\right) & \text{(Ziegler)} \end{cases} \tag{45}$$

Since the dot product is a scalar quantity, it is practical to apply the translocation directly to the constants "$c_{i,(k)}$" of the inequalities; thus, by combining (42) and (45) in order to have a complete set of expressions for all forms of hardening, we have:

$$c_{i,(k)}^{'} = \begin{cases} c_{i,(k)} + \delta_{PWL} & \text{(Drucker)} \\ c_{i,(k)} + \dfrac{\delta_{PWL}}{\left\|\vec{\nabla} g_a\right\|} \cdot \left(\vec{\nabla} g_i \bullet \vec{\nabla} g_a\right) & \text{(Melan}-\text{Prager)} \\ c_{i,(k)} + \dfrac{\delta_{PWL}}{\left\|\vec{\mathbf{Q}}_h\right\|} \cdot \left(\vec{\nabla} g_i \bullet \vec{\mathbf{Q}}_h\right) & \text{(Ziegler)} \end{cases} \tag{46}$$

The above process is applied to all hyper-planes $j=\{1,2,...,2^{Nisc(i)}\}$ of each equation "i" of the yield function.

8.4 A Physically Consistent Implementation of Material Hardening

Drucker's postulate ensures the irreversibility of plastic processes ([183],[184],[185]); it has the following mathematical form, in terms of generalized stress and plastic strain increments:

$$\Delta W_{pl} \propto \Delta\sigma \cdot \Delta\varepsilon_{pl} \geq 0 \tag{47}$$

For the case of concentrated plasticity (*plastic hinges*), Equation (47) may be re-defined in terms of generalized force/moment and plastic displacement/rotation increments.

In order to re-write the postulate by using only generalized force quantities, the axiom of maximization of plastic work is utilized; furthermore, an important constraint is to establish a numerically efficient formula that is able to yield the required results within the framework of rate independent plasticity:

$$\underbrace{\vec{\nabla} g_a(\mathbf{Q})}_{Stress} \bullet \underbrace{\left\{ S \cdot \Delta\vec{\mathbf{Q}} \right\}}_{Strain} \geq 0 \tag{48}$$

Where "$\nabla g_a(\mathbf{Q})$" is the gradient of the hyper-plane of the yield locus that has triggered the hardening plastic flow and is computed with reference to Equation (36), and "S" is computed with reference to Equation (39); since the yield function`s gradient points towards the direction of evolution of the local plastic strain/deformation increments, and since the hardening plastic flow defines that the associated local plastic strain/deformation increments need be proportional to their corresponding local stress increments, then all internal sub-products must be positive, in order to be in accordance with the active hyper-plane of the yield locus.

Schematically, the meaning of Equation (48) is presented in Figure 24 below, for the simple case of two interacting stress components $\{Q_1,Q_2\}$ under kinematic hardening:

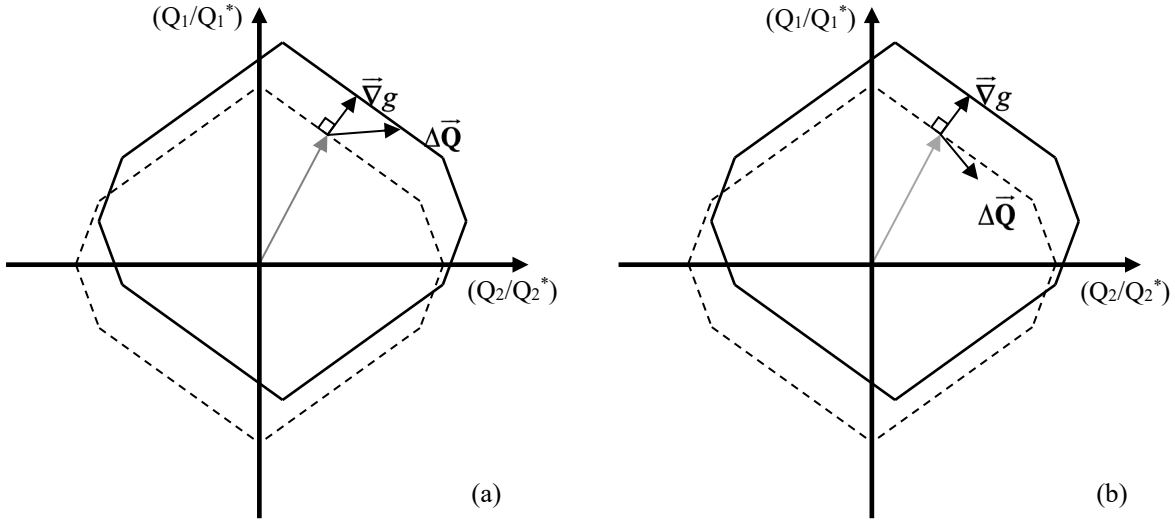

Figure 24: Drucker's postulate: (a) satisfied; (b) violated.

8.5 Mathematical Implementation of Local Unloading in Hardening Plastic Flow

The phenomenon of local unloading during a hardening plastic flow state is related to the violation of Drucker's postulate – see Equations (47) and (48). In such a case, a retraction of the yield locus is required, so that the interruption of the hardening plastic flow is described; this is done by setting new proper bounds for the static admissibility condition. To this extend, a variant of Equations (46) is used for all forms of hardening, respectively:

$$c'_{i,(k)} = \begin{cases} \delta_{UNL} & \text{(Drucker)} \\ c_{i,(k)} - \dfrac{\delta_{UNL}}{\left\|\vec{\nabla} g_a\right\|} \cdot \left(\vec{\nabla} g_i \bullet \vec{\nabla} g_a\right) & \text{(Melan}-\text{Prager)} \\ c_{i,(k)} - \dfrac{\delta_{UNL}}{\left\|\vec{\mathbf{Q}}_h\right\|} \cdot \left(\vec{\nabla} g_i \bullet \vec{\mathbf{Q}}_h\right) & \text{(Ziegler)} \end{cases} \tag{49}$$

Where:

$$\delta_{UNL} = \begin{cases} \left(\vec{\nabla} g_\alpha \bullet \vec{\mathbf{Q}}_{(k-1)}\right) & \text{(Drucker)} \\ \dfrac{c_{\alpha,(k)} - \left(\vec{\nabla} g_\alpha \bullet \vec{\mathbf{Q}}_{(k-1)}\right)}{\dfrac{1}{\left\|\vec{\nabla} g_a\right\|} \cdot \left(\vec{\nabla} g_\alpha \bullet \vec{\nabla} g_a\right)} & \text{(Melan}-\text{Prager)} \\ \dfrac{c_{\alpha,(k)} - \left(\vec{\nabla} g_\alpha \bullet \vec{\mathbf{Q}}_{(k-1)}\right)}{\dfrac{1}{\left\|\vec{\mathbf{Q}}_h\right\|} \cdot \left(\vec{\nabla} g_\alpha \bullet \vec{\mathbf{Q}}_h\right)} & \text{(Ziegler)} \end{cases} \tag{50}$$

Wherein Equations (49) and (50), the subscript "α" denotes the reference hyper-plane of the equation of the yield locus that has triggered the hardening plastic flow, which is now violating Drucker's postulate and must be deactivated.

9 Static-Kinematic Duality

In this section, the fundamental principles of physics / mechanics that correlate the work and displacement of the external forces applied on a deformable continuous structure with the work and deformations of the internally developed stresses, will be briefly presented.

9.1 The Principle of Leverage

From a historical point of view [186], the first formulation of the principle of virtual works was done by Archimedes of Syracuse for the elementary mechanical system of a momentum Libra, widely known as "the principle of leverage" (*see also* Figure 25 *below*).

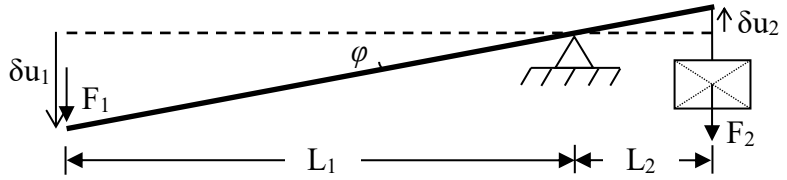

Figure 25: The principle of leverage.

The work required to move the mass "F_2" upwards by an incremental displacement "δu_2", is equal to the work required to move the lever on the other side of the Libra downwards. By taking into account that the forces $\{F_1,F_2\}$ are applied at a infinitesimally small and constant rate through time "t", and that the occurring incremental displacements $\{\delta u_1,\delta u_2\}$ are so small that for any infinitesimally small time increment "δt" the system is at equilibrium, then, the axiom of energy conservation yields the required force "F_1":

$$\Delta W_1=\Delta W_2 \rightarrow F_1\cdot\delta u_1=F_2\cdot\delta u_2 \rightarrow F_1=F_2\cdot(\delta u_2/\delta u_1) \tag{51}$$

Where (51) is valid when $(\delta F_1/\delta t)=0$, $(\delta F_2/\delta t)=0$, $(\delta u_1/\delta t)\rightarrow 0$, and $(\delta u_2/\delta t)\rightarrow 0$ hold. Considering the lever as rigid, the two displacements $\{\delta u_1,\delta u_2\}$ are correlated via the tangent of angle "φ" (*see Figure 25*):

$$\tan\varphi=(\delta u_1/L_1)=(\delta u_2/L_2)\rightarrow(\delta u_2/\delta u_1)=(L_2/L_1) \tag{52}$$

By combining Equations (51) and (52), it may be easily found that the required lifting force "F_1" is proportional to the ratio of the two levers $\{L_1,L_2\}$:

$$F_1=F_2\cdot(L_2/L_1) \tag{53}$$

9.2 Principle of Virtual Works

A constitutive relation between forces and displacements, with similar physical meaning as the one presented in the previous section, can be established also for deformable structures. The work of the externally applied loads on a structural system is equal to the potential energy that is stored within the system's mass in the form of strain energy; with reference to the governing equations of Chapter 4, the aforementioned energy equilibrium is expressed in symbolic form as follows:

$$\Delta W_{external} = \Delta W_{internal} \Rightarrow \Delta \mathbf{p}_0^T \cdot \Delta \mathbf{u_s} = \tfrac{1}{2} \cdot \Delta \mathbf{Q_S}^T \cdot \Delta \mathbf{q_s} \tag{54}$$

Equation (54) may be further developed with the help of Equations (16), (19) and (21), where in (19) the components of the plastic deformations' increments have been omitted due to the assumption for structures of purely elastic material:

$$\Delta\mathbf{p}_0^T \cdot \Delta\mathbf{u}_\mathbf{s} = \frac{1}{2} \cdot \Delta\mathbf{p}_0^T \cdot \left[\mathbf{B}_0^T \cdot \mathbf{F} \cdot \mathbf{B}_0\right] \cdot \Delta\mathbf{p}_0 + \Delta\mathbf{p}_0^T \cdot \left[\mathbf{B}_0^T \cdot \mathbf{F} \cdot \mathbf{B}_1\right] \cdot \Delta\mathbf{p}_1 + \frac{1}{2} \cdot \Delta\mathbf{p}_1^T \cdot \left[\mathbf{B}_1^T \cdot \mathbf{F} \cdot \mathbf{B}_1\right] \cdot \Delta\mathbf{p}_1 \quad (55)$$

By considering that the applied external load increments "$\Delta\mathbf{p_0}$" are constant and near-zero through time, the derivative of the above equation with respect to the load increments yields the solution for the minimum potential energy:

$$\Delta\mathbf{u}_\mathbf{s} = \left[\mathbf{B}_0^T \cdot \mathbf{F} \cdot \mathbf{B}_0\right] \cdot \Delta\mathbf{p}_0 + \left[\mathbf{B}_0^T \cdot \mathbf{F} \cdot \mathbf{B}_1\right] \cdot \Delta\mathbf{p}_1 \quad (56)$$

With the help of (16), (19) and (21), the above equation receives its' compacted form, which is Equation (26).

The above was first formulated for elastic planar trusses by James Clerk–Maxwell, in the form of the compatibility condition (*see Equation (18)*); in this incremental form, it may be shown that these equations are valid for any type of structure and material, elastic or plastic.

10 Load & Displacement Control

In this section, a brief presentation of the load and displacement control techniques that are necessary for the herein developed numerical method is given.

10.1 Prediction of Critical Load-Scaling Factors

By abstractly supposing that a feasible direction for the solution of the incremental analysis problem is at hand, a proper scaling of the solution's vector would be required in order to accurately satisfy at least one new constraint as equality at every step of the procedure.

Using the gradient of (36), the static admissibility condition may be re-formulated on a section level in the form of an internal (*dot*) product:

$$\vec{\nabla} g_i \bullet \left(\vec{\mathbf{Q}}_{(k-1)} + \Delta \vec{\mathbf{Q}}_{(k)} \right) - c_{i,(k)} \le 0 \Rightarrow \vec{\nabla} g_i \bullet \left(\vec{\mathbf{Q}}_{(k-1)} + \Delta\gamma \cdot \Delta \vec{\mathbf{Q}}_{(k)} \right) = c_{i,(k)} \tag{57}$$

Where in (57) "*i*" represents the yield function's equation index (see Equation (36)), "*k*" represents the current step of the incremental analysis, and "$\Delta\gamma$" is a scaling factor.

Out of (57), the critical load scale factor for every critical section's yield locus may be defined as the minimum positive scalar quantity by which the current step`s stress increments "$\Delta \vec{\mathbf{Q}}_{(k)}$" need to be multiplied in order to satisfy (57) in the form of an equality. Symbolically, this may be expressed as:

$$\Delta\gamma_{\min} = \min\left\{\Delta\gamma_i\right\} \quad , \quad i = \{1, 2, ..., N_{eq}\} \tag{58}$$

Where:

$$\Delta\gamma_i = \min\left\{ \Delta\gamma_j = \frac{c_{j(i),(k)} - \left(\vec{\nabla} g_{j(i)} \bullet \vec{\mathbf{Q}}_{(k-1)} \right)}{\left(\vec{\nabla} g_{j(i)} \bullet \Delta \vec{\mathbf{Q}}_{(k)} \right)} : \Delta\gamma_j > 0 \right\} \quad , \quad j = \{1, ..., 2^{Nisc(i)}\} \tag{59}$$

Wherein (59), all quantities are defined with reference to the definition of a generic yield function according to Equation (36).

Since Equations (58) and (59) hold for one critical section, the globally minimum scale factor for the whole structure occurs as the minimum value among all critical sections' minimum scalar values.

For numerical efficiency purposes (*e.g. avoiding null steps in an incremental loading procedure*), the inequality mask contained in (59) may be replaced with a relaxed condition, e.g. "$\Delta\gamma_i > \rho$", where "ρ" is a positive, but small number (*e.g.* $\rho = 0.001$).

10.2 Displacement Control

A maximum threshold for a reference displacement of the structure is often required (*e.g. target displacement in pushover analysis*); to this extend the aforementioned scale factor in Equations (58) and (59) may be further adjusted:

$$\Delta\gamma_{\min} \le \frac{u_{\max} - u_{(k-1)}}{\Delta u_{(k)}} \tag{60}$$

Wherein (60), with the letter "*u*", the displacement of a reference node of the structure is denoted, "*k*" represents the current step of the incremental analysis, and "$\Delta u_{(k)}$" is computed from the SKD (*see* Equation (26)), with the help of (16),(19),(21),(23), and (25).

11 A Force-based Method for 1st Order Analysis

11.1 Problem's Formulation

In order to be able to efficiently trace all the plasticization events along any given loading/displacement path, an incremental procedure need be formulated. Thus, the mathematical program's formulation will be derived for a typical step "*k*", where $k \in \{1,2,3...\}$.

According to the definition of the yield function, a stress distribution is admissible only if it satisfies (36) at every step of analysis. Thus, we may rewrite the respective part of (24) as:

$$\mathbf{Y}_* = \mathbf{c}_{(k)} - \nabla g^T \cdot \mathbf{Q}_{(k)} = \mathbf{c}_{(k)} - \nabla g^T \cdot (\mathbf{Q}_{(k-1)} + \Delta\mathbf{Q}_{(k)}) = \mathbf{c}_{(k)} - \nabla g^T \cdot \mathbf{Q}_{(k-1)} - \nabla g^T \cdot \Delta\mathbf{Q}_{(k)} \geq \mathbf{0} \tag{61}$$

By combining Equations (16), (36), and substituting into (61), the plastic potential "$\mathbf{Y}_*$" may be explicitly expressed as a function of the external loads and the redundant stresses. If the coefficients of this composite function are packed into an incidence matrix "$\overline{\mathbf{N}}$" [49], a linear constraint inequality may be established:

$$\mathbf{Y}_* = \mathbf{c}_{(k)} - \overline{\mathbf{N}}^T \cdot \mathbf{Q}_{(k-1)} - \left(\overline{\mathbf{N}}^T \cdot \mathbf{B}_0\right) \cdot \Delta\mathbf{p}_{0,(k)} - \left(\overline{\mathbf{N}}^T \cdot \mathbf{B}_1\right) \cdot \Delta\mathbf{p}_{1,(k)} \geq \mathbf{0} \tag{62}$$

By substituting Equation (16) into (21), then evaluating (23) with the help of (36), and (25) with the help of (16), then substituting all three into (19) and then into (18), we have:

$$\left[\mathbf{B}_1^T \cdot \left(\mathbf{F} + \mathbf{F}_S\right) \cdot \mathbf{B}_0\right] \cdot \Delta\mathbf{p}_{0,(k)} + \left[\mathbf{B}_1^T \cdot \left(\mathbf{F} + \mathbf{F}_S\right) \cdot \mathbf{B}_1\right] \cdot \Delta\mathbf{p}_{1,(k)} + \left(\mathbf{B}_1^T \cdot \overline{\mathbf{N}}\right) \cdot \Delta\boldsymbol{\lambda}_{(k)} = \mathbf{0} \tag{63}$$

Wherein (63), "**F**" is evaluated according to (22), and "$\mathbf{F}_S$" according to (40) or (41) (*with reference to (39)*), respectively.

Within the framework of the current work, all step-by-step analysis types that were implemented (*predefined loading scenarios, pushover analysis, cyclic loading*) were defined as load-controlled numerical procedures. Therefore, the vector of external load increments "$\Delta\mathbf{p}_0$" in Equations (62) and (63) is a known parameter; as such, it may be substituted by the corresponding defining constant vector "$\mathbf{r}_p$", which is abstractly presented in Figure 26 below for a single loading path branch ($\mathbf{p}_{0,A} \rightarrow \mathbf{p}_{0,B}$):

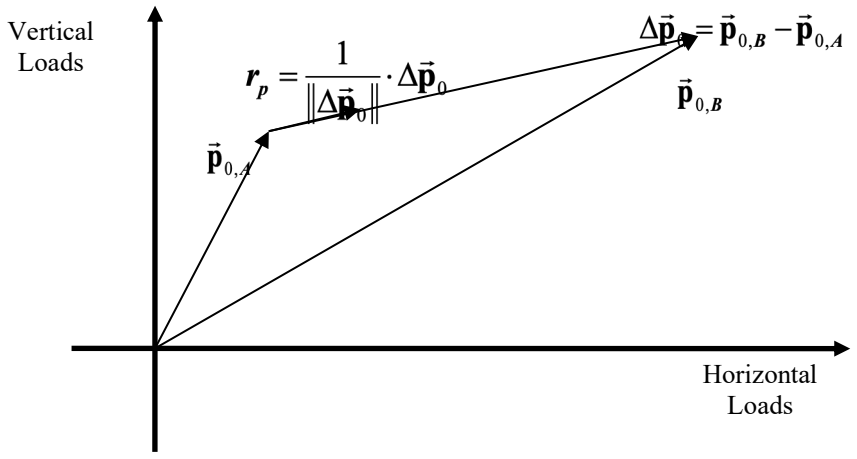

Figure 26: Predefined loading paths.

Equations (63), (62), and (24), may be seen as the Karush−Kuhn−Tucker (KKT) conditions of an optimization problem whose primary variables are the redundant forces/moments. Specifically, Equation

(63) is the gradient of a Lagrange function. The last of the three additive terms in (63) is the gradient of an inequality constraints' function which is defined by Equation (62). Equation (24) is the linear complementarity condition. Thus, the following formulation may be written (*with reference to Figure 26*):

Minimize:

$$f(\Delta\mathbf{p}_1) = \frac{1}{2}\cdot\Delta\mathbf{p}_{1,(k)}^{T}\cdot\left[\mathbf{B}_1^{T}\cdot\left(\mathbf{F}+\mathbf{F}_S\right)\cdot\mathbf{B}_1\right]\cdot\Delta\mathbf{p}_{1,(k)} + \mathbf{r}_p{}^{T}\cdot\left[\mathbf{B}_0^{T}\cdot\left(\mathbf{F}+\mathbf{F}_S\right)\cdot\mathbf{B}_1\right]\cdot\Delta\mathbf{p}_{1,(k)} \tag{64}$$

Subject to:

$$\left(\overline{\mathbf{N}}^{T}\cdot\mathbf{B}_1\right)\cdot\Delta\mathbf{p}_{1,(k)} \le \mathbf{c}_{(k)} - \overline{\mathbf{N}}^{T}\cdot\mathbf{Q}_{(k-1)} - \overline{\mathbf{N}}^{T}\cdot\mathbf{r}_p$$

Since the above Quadratic Programme (QP) is strictly convex, its solution is not only existent, but also unique. The problem (64) is solved in an incremental, iterative form; a detailed description of the devised numerical strategy follows in the next section.

11.2 Numerical Strategy

Within the context of the present work, a simple load-controlled numerical strategy was devised and implemented for solving (64). The main idea is to scale down the load change "$\mathbf{r}_p$" vector in order to determine a feasible direction for the solution [49]; this is achieved by multiplying with a positive, but small number "ρ" (*e.g.* $\rho=10^{-3}$). A detailed presentation is given below; it caters for non-holonomic, perfectly- and hardening-plastic materials.

0. Read and pre-process input data.
1. Form a minimal statical basis due to external loads and a (*near*) minimal statical basis due to redundancy and evaluate the problem`s equilibrium matrices $\mathbf{B}_i$, where $i=\{0,1\}$, respectively; see Section 2.5.
2. Set the predefined load path vectors, "$\mathbf{r}_p$"; see Figure 26.
3. Initialize the predefined load/displacement path's branch counter $n=1$.
4. For the current path branch "n", evaluate all corresponding flexibility matrices ($\mathbf{B}_i^{\mathrm{T}}\cdot\mathbf{F}\cdot\mathbf{B}_j$), where $\{i,j\}=\{0,1\},\{1,1\}$; the updating process of the flexibility matrices is done using Equation (22) and the rows of Equation (34) that correspond to the components of (17), with reference to (27) − (31) or (27) − (30) and (31) − (32), depending on the member's direction.
5. Initialize incremental step counter $k=1$.
6. Check for newly activated or violated associated plastic flows. An associated plastic flow is considered about to be activated when the tip of a critical section's stress vector touches a hyper-plane of the yield locus (*e.g. Figure 27(a) and Figure 27(e)*); thus, the corresponding component of the plastic potentials' vector becomes zero (*e.g.* $Y\le10^{-8}$). The checking process for violated associated plastic flows (*see Figure 27(c)*) is done using Equation (48), with reference to (16), the gradient of (36), and (39); also, in (16), the following replacement is needed: $\Delta\mathbf{p}_0\rightarrow\rho\cdot\mathbf{r}_p$:
   a. If no new events were triggered (*e.g. beginning of analysis or continuing holonomic behaviour – Figure 27(b) and/or Figure 27(f)*), go to step 8.
   b. If a new set of events was detected (*e.g.: activation of new associated plastic flows – see Figure 27(a) and/or Figure 27(e); and/or signal of plastic unstressing – see Figure 27(c)*), execute steps

7 to 10, then return to step (6.b) and re-check; if no new events were detected after the re-check (*e.g. Figure 27(b) and/or Figure 27(d) and/ or Figure 27(f)*), go to step 11.

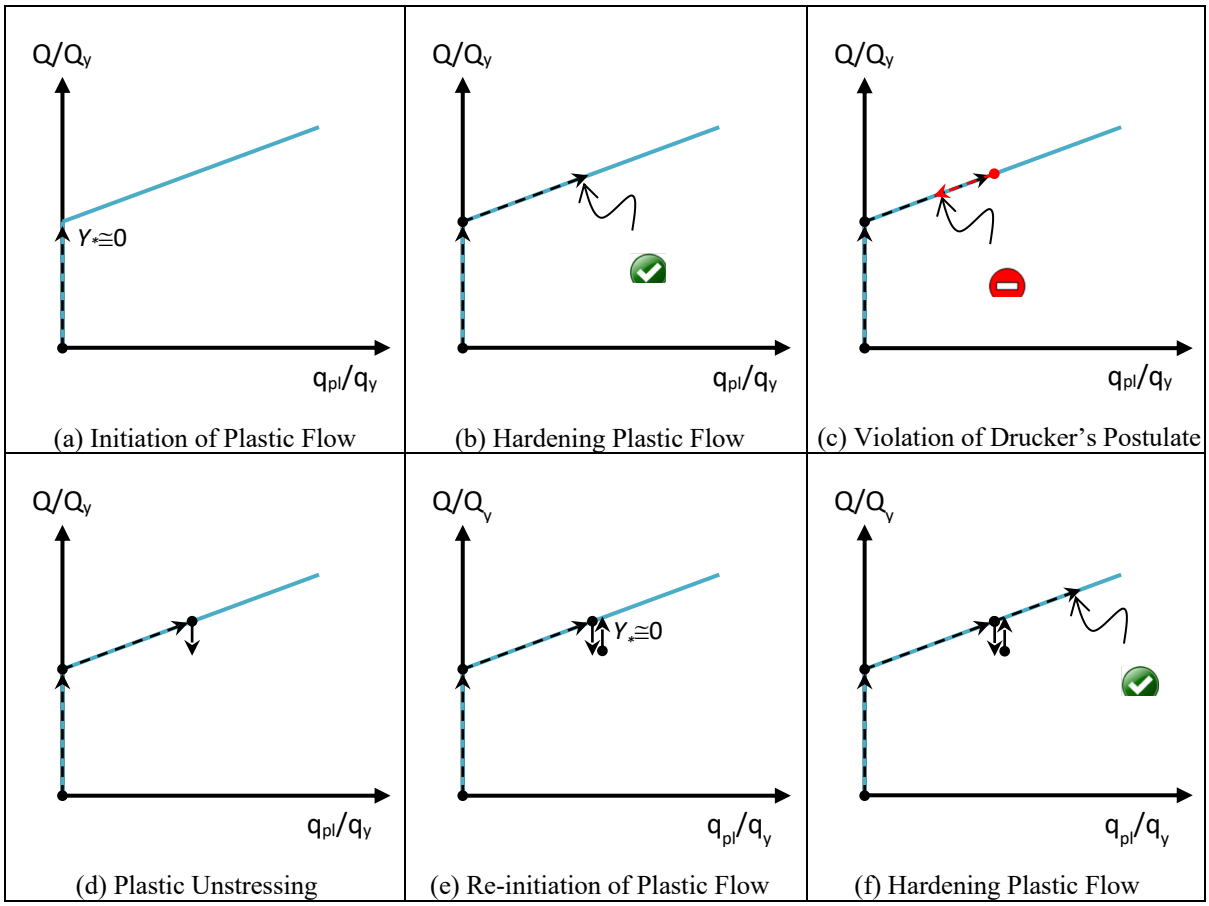

Figure 27: Hardening Plastic Flow and Non-Holonomic Material Behaviour.

7. Evaluate the part of the matrices ($\mathbf{B}_i^T \cdot \mathbf{F}_S \cdot \mathbf{B}_j$) due to plastic hardening, where $\{i,j\}=\{0,1\},\{1,1\}$. The updating process of the hardening matrices is done using the rows of Equation (34) that correspond to each critical section's set of interacting stress components which contribute to material hardening (*in accordance to the selected yield function – see Equation (36)*), and Equations (40) or (41) (*with reference to Equation (39)*). In the case where Drucker's postulate is violated, the respective components of the hardening matrices are set to zero.
8. Evaluate the right-hand side of the problem's constraints (*see Equation (64)*). The updating process of the constraints' constants "$\mathbf{c}_{(k)}$" is done using Equation (46), depending on the hardening rule adopted. In the case of plastic unstressing, the yield locus is moved backwards along the hardening vector's direction, so that the active yield plane touches the tip of the critical section's stress vector that was determined at the end of the previously completed step ($k-1$): Equations (49) and (50) are used.
9. Since the components of the load change vector "$\mathbf{r}_p$" may be large enough to cause a violation of the static admissibility condition, a proper scaling is required in order to maintain complementarity: Scale "$\mathbf{r}_p$" using a small factor "ρ". (*In the examples presented within the context of this work, values of* $\rho \in [10^{-6},1]$ *were generally found to be sufficient, with a value of* $\rho=10^{-3}$ *being an optimal compromise between computational speed and accuracy*).

10. Solve the problem described by Equation (64) using any efficient algorithm (*e.g.* [68],[69],[70]) and obtain a set of primal and dual variables. If the algorithm fails to converge, go to step 20, because a state of collapse was reached.
11. Divide the components of the acquired solution vectors $\{\Delta\mathbf{p}_1,\Delta\boldsymbol{\lambda}\}$ with "ρ".
12. Evaluate "$\Delta\mathbf{Q}_{(k)}$". Use Equations (16) and (34); the shear force increments may also be easily evaluated from the local equilibrium conditions along each element.
13. Evaluate "$\Delta\mathbf{q}_{\mathrm{el},(k)}$"; use Equation (21).
14. Evaluate "$\Delta\mathbf{q}_{\mathrm{pl},(k)}$". For perfectly plastic material, use Equation (23); for hardening plastic material, use Equation (25), wherein the flexibility coefficients may be computed from Equation (40) or (41), with reference to (39).
15. Find the minimal solution scale factor "$\Delta\gamma_k$" that activates a new plastic hinge, ensuring that the computed value does not exceed the current branch of the examined loading path: Determine the minimum load scale factor using Equations (58) and (59); then, if required, re-scale according to the maximum desired reference displacement with the aid of (60).
16. Scale corresponding stress and strain increments using the above computed scale factor:

$$\Delta\mathbf{Q}_{(k)} \rightarrow \Delta\gamma_k \cdot \Delta\mathbf{Q}_{(k)} \quad , \quad \Delta\mathbf{q}_{\mathrm{el},(k)} \rightarrow \Delta\gamma_k \cdot \Delta\mathbf{q}_{\mathrm{el},(k)} \quad , \quad \Delta\mathbf{q}_{\mathrm{pl},(k)} \rightarrow \Delta\gamma_k \cdot \Delta\mathbf{q}_{\mathrm{pl},(k)}$$

17. Add up the computed stress and strain increments of the new step (k) to the respective values of the previously completed step ($k-1$):

$$\mathbf{Q}_{(k)}=\mathbf{Q}_{(k-1)}+\Delta\mathbf{Q}_{(k)} \quad , \quad \mathbf{q}_{\mathrm{el},(k)}=\mathbf{q}_{\mathrm{el},(k-1)}+\Delta\mathbf{q}_{\mathrm{el},(k)} \quad , \quad \mathbf{q}_{\mathrm{pl},(k)}=\mathbf{q}_{\mathrm{pl},(k-1)}+\Delta\mathbf{q}_{\mathrm{pl},(k)}$$

18. Evaluate "$\Delta\mathbf{u}_{\mathbf{s},(k)}$" using Equation (26). Then, add them up to the displacement values of the previously completed step ($k-1$):

$$\mathbf{u}_{\mathbf{s},(k)}=\mathbf{u}_{\mathbf{s},(k-1)}+\Delta\mathbf{u}_{\mathbf{s},(k)}$$

19. If the end of the current loading branch was reached (*i.e. if* $\left|\left\|\Delta\mathbf{p}_0\right\|-\sum_{i=1}^{i=k}\Delta\gamma_i\right|\le\rho$ *holds – see Figure 26*), go to step 4 and repeat the process for $n\rightarrow n+1$; if the end of the whole loading path or the maximum reference displacement was reached, go to step 20; else, return to step 6 and repeat the process for $k\rightarrow k+1$.
20. Print output data, and terminate.

12 Investigating the Extension to 2nd Order Analysis

In this section, the governing equations and matrices for the herein developed 1st order force method are extended so that the effect of axial forces on bending deformations is taken into account; the proposed methodology includes both "*P–Δ*" and "*P–Δ–δ*" effects.

12.1 Flexibility Coefficients for Bending Components

For bending moments, the 2nd order unassembled flexibility coefficients may be derived by solving the differential equation of the planar bending problem in the deformed state, where the contribution of the axial force components in the development of additional bending rotations due to the lateral deflection is taken into account; see Figure 28 below, illustrating the planar (2D) problem:

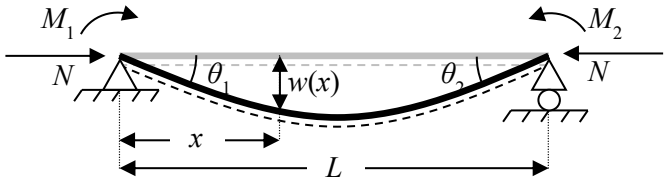

Figure 28: Increased bending deflection (w) due to axial forces (N) for the planar (2D) bending problem.

The differential equation of the deflection is (*with reference to Figure 28 above*):

$$w''(x)+\mu^2\cdot w(x)=-\left[M_1\cdot\left(1-\frac{x}{L}\right)+M_2\cdot\frac{x}{L}\right] \tag{65}$$

Where, in the above Equation (65), the ratio of the axial force vs. per unit of length bending rigidity of the cross-section has been denoted with:

$$\mu^2=\frac{N}{E\cdot I} \tag{66}$$

In the above Equation (66) it is assumed that, for compression (N<0), "μ^2>0" holds, and for tension (N>0), "μ^2<0" holds. With reference to (66), the solution of (65) is:

$$\begin{aligned}
&\mu^2>0: \quad w(x)=A_1\cdot\sin(\mu\cdot x)+A_2\cdot\cos(\mu\cdot x)-\frac{1}{\mu^2}\cdot\left[M_1\cdot\left(1-\frac{x}{L}\right)+M_2\cdot\frac{x}{L}\right]\\
&\mu^2<0: \quad w(x)=A_1\cdot e^{\mu\cdot x}+A_2\cdot e^{-\mu\cdot x}-\frac{1}{\mu^2}\cdot\left[M_1\cdot\left(1-\frac{x}{L}\right)+M_2\cdot\frac{x}{L}\right]
\end{aligned} \tag{67}$$

By applying the boundary conditions "$w(0)$=0" and "$w(L)$=0" in (67), the values of "A_1" and "A_2" are acquired, respectively:

$$\begin{aligned}
&\mu^2>0: \quad A_1=-\frac{1}{\mu^2}\cdot\left[\frac{M_1}{\tan(\mu\cdot L)}-\frac{M_2}{\sin(\mu\cdot L)}\right] \quad , \quad A_2=\frac{M_1}{\mu^2}\\
&\mu^2<0: \quad A_1=\frac{-e^{-\mu\cdot L}\cdot M_1+M_2}{\mu^2\cdot\left(e^{\mu\cdot L}-e^{-\mu\cdot L}\right)} \quad , \quad A_2=\frac{e^{\mu\cdot L}\cdot M_1-M_2}{\mu^2\cdot\left(e^{\mu\cdot L}-e^{-\mu\cdot L}\right)}
\end{aligned} \tag{68}$$

By substituting (68) into (67), then differentiating with respect to "x", the respective function of the bending rotation "θ" is acquired:

$$\begin{aligned} \mu^2 > 0: \quad & \theta(x) = \frac{M_1}{\mu \cdot L} \cdot \left[\frac{1}{\mu} - \frac{L \cdot \cos(\mu \cdot x)}{\tan(\mu \cdot L)} \right] + \frac{M_2}{\mu \cdot L} \cdot \left[\frac{L}{\sin(\mu \cdot L)} - \frac{\sin(\mu \cdot x)}{\mu} - \frac{1}{\mu} \right] \\ \mu^2 < 0: \quad & \theta(x) = \frac{-e^{-\mu \cdot L} \cdot M_1 + M_2}{\mu \cdot \left(e^{\mu \cdot L} - e^{-\mu \cdot L} \right)} \cdot e^{\mu \cdot x} - \frac{e^{\mu \cdot L} \cdot M_1 - M_2}{\mu \cdot \left(e^{\mu \cdot L} - e^{-\mu \cdot L} \right)} \cdot e^{-\mu \cdot x} + \frac{M_1 - M_2}{\mu^2 \cdot L} \end{aligned} \tag{69}$$

By setting "$\theta(0)=\theta_1$" and "$\theta(L)=-\theta_2$" in (69), the respective matrix of the unassembled flexibility coefficients is obtained:

$$\begin{Bmatrix} \theta_1 \\ \theta_2 \end{Bmatrix} = \frac{L}{6 \cdot E \cdot I} \cdot \begin{bmatrix} 2 \cdot F_{11} & F_{12} \\ F_{21} & 2 \cdot F_{22} \end{bmatrix} \cdot \begin{Bmatrix} \mathrm{M}_1 \\ \mathrm{M}_2 \end{Bmatrix} \tag{70}$$

Where, for compressive axial forces, it holds:

$$F_{11} = F_{22} = +\frac{3}{\mu \cdot L} \cdot \left[\frac{1}{\mu \cdot L} - \frac{1}{\tan(\mu \cdot L)} \right] \quad \& \quad F_{12} = F_{21} = -\frac{6}{\mu \cdot L} \cdot \left[\frac{1}{\mu \cdot L} - \frac{1}{\sin(\mu \cdot L)} \right] \tag{71}$$

And, for tensile axial forces, it holds:

$$F_{11} = F_{22} = -\frac{3}{\mu \cdot L} \cdot \left[\frac{1}{\mu \cdot L} - \frac{1}{\tanh(\mu \cdot L)} \right] \quad \& \quad F_{12} = F_{21} = +\frac{6}{\mu \cdot L} \cdot \left[\frac{1}{\mu \cdot L} - \frac{1}{\sinh(\mu \cdot L)} \right] \tag{72}$$

The above Equations (65) − (72) were derived from the solution that was first presented by A. Berry in [2].

As it has been already made evident, different formulae are required for the calculation of the bending rotations due to axial tension and compression, respectively. However, in terms of classical functional programming, this raises difficulties in the automation of the calculations; in order to tackle this problem, the first two terms of a Maclaurin series expansion of the formulae of (71) and (72) are used instead, since their forms are common for both tension and compression. Thus, Equation (70) becomes:

$$\begin{Bmatrix} \theta_{j1} \\ \theta_{j2} \end{Bmatrix} = \left(\frac{L}{6 \cdot E \cdot I_j} \cdot \begin{bmatrix} 2 & 1 \\ 1 & 2 \end{bmatrix} + \frac{L^3}{360 \cdot \left(E \cdot I_j \right)^2} \cdot diag \begin{Bmatrix} \mathrm{N}_1 \\ \mathrm{N}_2 \end{Bmatrix} \cdot \begin{bmatrix} 8 & 7 \\ 7 & 8 \end{bmatrix} \right) \cdot \begin{Bmatrix} \mathrm{M}_{j1} \\ \mathrm{M}_{j2} \end{Bmatrix} \quad , \quad j = \{2,3\} \tag{73}$$

The above choice comes with a "heavy" computational toll; in order to efficiently approximate the values of the non-linear functions in (70), every beam/column element must be subdivided into smaller ones. In this way, the omitted skew-symmetrical terms of the Maclaurin series in Equation (73) cause a minimal cost in computational accuracy.

12.2 Unassembled Flexibility Matrices

The part of the unassembled flexibility matrix that corresponds to bending moments is a function of the axial components "$\Delta\mathbf{N_s}$" of the stress increments "$\Delta\mathbf{Q_s}$":

$$\mathbf{F} \to \mathbf{F} + diag\begin{Bmatrix} \mathbf{0} \\ \mathbf{0} \\ \mathbf{0} \\ \mathbf{0} \\ \hline \Delta\mathbf{N_s} \\ \Delta\mathbf{N_s} \end{Bmatrix} \cdot \mathbf{F}_g = \begin{bmatrix} \mathbf{F_N} & \mathbf{0} & \mathbf{0} & \mathbf{0} & \mathbf{0} & \mathbf{0} \\ & \mathbf{F_{Q_2}} & \mathbf{0} & \mathbf{0} & \mathbf{0} & \mathbf{0} \\ & & \mathbf{F_{Q_3}} & \mathbf{0} & \mathbf{0} & \mathbf{0} \\ & & & \mathbf{F_T} & \mathbf{0} & \mathbf{0} \\ & & & & \mathbf{F_{M_2}} & \mathbf{0} \\ & & & & & \mathbf{F_{M_3}} \end{bmatrix} + diag\begin{Bmatrix} \mathbf{0} \\ \mathbf{0} \\ \mathbf{0} \\ \mathbf{0} \\ \hline \Delta\mathbf{N_s} \\ \Delta\mathbf{N_s} \end{Bmatrix} \cdot \begin{bmatrix} \mathbf{0} & \mathbf{0} & \mathbf{0} & \mathbf{0} & \mathbf{0} & \mathbf{0} \\ & \mathbf{0} & \mathbf{0} & \mathbf{0} & \mathbf{0} & \mathbf{0} \\ & & \mathbf{0} & \mathbf{0} & \mathbf{0} & \mathbf{0} \\ & & & \mathbf{0} & \mathbf{0} & \mathbf{0} \\ & & & & \mathbf{F^g_{M_2}} & \mathbf{0} \\ & & & & & \mathbf{F^g_{M_3}} \end{bmatrix} \quad (74)$$

Where in (74), "$\mathbf{F_{M_j}}$" and "$\mathbf{F^g_{M_j}}$", j={2,3}, are the 1st and 2nd order flexibility terms of Equation (73), respectively. The rest of the governing equations are the same as in 1st order analysis.

12.3 Procedures for the Equilibrium Matrices

The inclusion of geometric non-linearity (*also referred to as "P−Δ" and "P−Δ−δ" effects*) requires evaluating equilibrium in the deformed state. Thus, the corresponding matrices {$\mathbf{B_0}$, $\mathbf{B_1}$} need be redefined. The proposed methodology is an extension of what was first presented in [54] for 2D structures.

12.3.1 Matrix "$\mathbf{B_0}$"

The computation steps required for the evaluation of matrix "$\mathbf{B_0}$" due to external loads in the deformed state, are provided below:

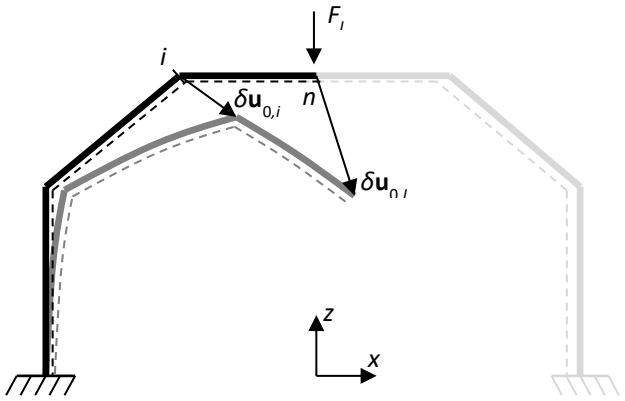

Figure 29: The shortest path of node "*n*" and its' deformed shape due to the "L^{th}" load component (F_z).

1. Compute equilibrium matrix "$\mathbf{B_0}$" according to Equation (34), for all shortest paths of the structure and the respective critical sections that are affected by all possible load components of the starting node of each shortest path; use the respective statical basis that was generated with a suitable algorithm (*e.g.* [47],[49]).
2. For all nodes of the structure n={*1,2,...,N*}, execute sub-steps (2.a) – (2.e):
   a. Select the column "$\mathbf{b_{0,L}}$" of matrix "$\mathbf{B_0}$" that contains the stress components of the whole structure corresponding to the *L-th* external, unit-valued load of node "*n*", where "*L*" is a column index

corresponding only to force loads $\delta p_{\mathbf{0},L} \triangleq \{F_x, F_y, F_z\}$; for reasons of consistency in the nomenclature adopted throughout this work, we denote a purely symbolic pointer to it, with reference to Equations (15) and (16):

$$\delta \mathbf{Q}_{\mathbf{0},L} \to \delta p_{\mathbf{0},L} \cdot \mathbf{b}_{\mathbf{0},L} \tag{75}$$

b. Compute the generalized local elastic deformations "$\delta \mathbf{q}_{0,L}$" that are due to the external force load component of the *L-th* column of matrix "$\mathbf{B_0}$", using Equation (21). If the Berry functions are taken into account (*"P−Δ−δ" effects – see Equation (73)*), use both the 1st and 2nd order terms of (73) in (21); if only the "P−Δ" effects are taken into account, use only the 1st order terms of (73) in (21):

$$\delta \mathbf{q}_{\mathbf{0},L} = \mathbf{F} \cdot \delta \mathbf{Q}_{\mathbf{0},L} \tag{76}$$

Where vector "$\delta \mathbf{Q}_{\mathbf{0},L}$" was defined in sub-step (2.a).

c. Compute the global elastic displacements of the node on which the unit-valued dummy generalized force that corresponds to the *L-th* column of matrix "$\mathbf{B_0}$" is applied, using Equation (26):

$$\delta u_{0,j} = \mathbf{b}_{\mathbf{0},j}^T \cdot \delta \mathbf{q}_{\mathbf{0},L} \tag{77}$$

Where $j \triangleq \{F_x, F_y, F_z\}$, thus:

$$\delta \mathbf{u}_{0,L}^T = \begin{Bmatrix} \delta u_{0,x} & \delta u_{0,y} & \delta u_{0,z} \end{Bmatrix} = \begin{Bmatrix} \Delta x_L & \Delta y_L & \Delta z_L \end{Bmatrix} \tag{78}$$

The vector of displacements in (78) is abstractly depicted in Figure 29 above.

d. Move along the shortest path that corresponds to the *L-th* column of matrix "$\mathbf{B_0}$", and, for each critical section "*i*", execute sub-steps (2.d.i) – (2.d.iv):

i. Select the column "$\mathbf{b}_{\mathbf{0},k}$" of matrix "$\mathbf{B_0}$" corresponding to the *k-th*, unit-valued degree of freedom, where $k \triangleq (u_x, u_y, u_z, \varphi_x, \varphi_y, \varphi_z)$, and compute the elastic generalized displacements "$\delta u_{0,k}$" of the current critical section which are due to the unit-valued dummy generalized force that corresponds to the *L-th* column of matrix "$\mathbf{B_0}$"; use Equation (26):

$$\delta u_{0,k} = \mathbf{b}_{\mathbf{0},k}^T \cdot \delta \mathbf{q}_{\mathbf{0},L} \tag{79}$$

Where $k \triangleq \{F_x, F_y, F_z, M_x, M_y, M_z\}$, thus:

$$\delta \mathbf{u}_{0,i}^T = \begin{Bmatrix} \Delta x_i & \Delta y_i & \Delta z_i \end{Bmatrix} \vdots \begin{Bmatrix} \Delta \varphi_{x,i} & \Delta \varphi_{y,i} & \Delta \varphi_{z,i} \end{Bmatrix} \tag{80}$$

The displacements' part of the vector in (80) is abstractly depicted in Figure 29 above.

ii. Evaluate the increment "$\delta \mathbf{d}_R$" of matrix "$\mathbf{d}_R$" (*"P−Δ" effects*) according to Equation (27), where $\{\Delta x, \Delta y, \Delta z\}$ are computed below, following sub-steps (2.c) and (2.d.i):

$$\begin{aligned} \Delta x &= \Delta x_i - \Delta x_L \\ \Delta y &= \Delta y_i - \Delta y_L \\ \Delta z &= \Delta z_i - \Delta z_L \end{aligned} \tag{81}$$

iii. For the case where the Berry functions are additionally taken into account (*"P−Δ−δ" effects*), compute the change "$\delta\mathbf{T}_R$" in the transformation matrix "$\mathbf{T}_R$" according to the following formula, where use of the quantities that were computed during sub-step (2.d.i) is being made; else, skip sub-step (2.d.iii):

$$\delta\mathbf{T}_R = (\mathbf{R}_x \cdot \mathbf{R}_y \cdot \mathbf{R}_z) \cdot \mathbf{T}_R \tag{82}$$

Where in (82), "$\mathbf{R}_x$", "$\mathbf{R}_y$", "$\mathbf{R}_z$" are the rotation tensors around the respective axes of the global coordinate system $\{x,y,z\}$; their components are computed using the respective angle increments from Equation (80).

iv. Evaluate and store the increment "$\delta\mathbf{B}_0$" of equilibrium matrix "$\mathbf{B}_0$" according to Equation (34):

$$\delta\mathbf{B}_0 = -Sign\{m\} \cdot \left[\begin{array}{c|c} \delta\mathbf{T}_R & \mathbf{0}_{3x3} \\ \hline \delta\mathbf{T}_R \cdot \delta\mathbf{d}_R & \delta\mathbf{T}_R \end{array}\right] \tag{83}$$

Note that the transformation matrix is considered to be unaffected by the deformed status of the beam/column elements of the statically determinate basis when the Berry functions (*"P−Δ−δ" effects*) are not taken into account ($\delta\mathbf{T}_R = \mathbf{T}_R$).

e. Return to sub-step (2.a) and repeat for all force load components of node "*n*"; then, set $n \to n+1$ and move on to the next node.

12.3.2 Matrix "$\mathbf{B}_1$"

The following computation steps are required for the evaluation of matrix "$\mathbf{B}_1$" due to redundant components in the deformed state:

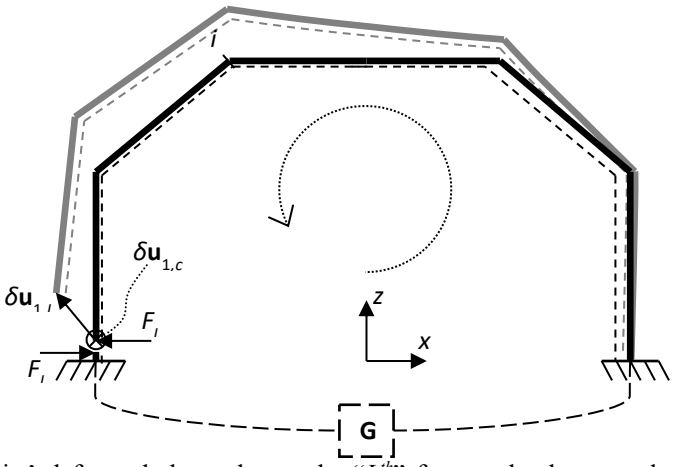

Figure 30: The "n^{th}" mesh and its' deformed shape due to the "L^{th}" force redundant coupled component (F_x); a "ground" virtual node that helps to create the closed loops at the supports of the structure is denoted with "G".

1. Compute equilibrium matrix "$\mathbf{B}_1$" according to Equation (34), for all meshes of the structure and the respective critical sections that are affected by the redundant stress quantities of each mesh; use the respective statical basis that was determined with a suitable algorithm (e.g. [53]).

2. For all meshes of the structure $n=\{1,2,...,N\}$, execute sub-steps (2.a) – (2.g):
   a. Select the column "$\mathbf{b}_{1,L}$" of matrix "$\mathbf{B}_1$" that contains the stress components of the whole structure corresponding to the *L-th* internal, unit-valued redundant quantity of mesh "*n*", where "*L*" is a column index corresponding only to force redundant components $\delta p_{1,L} \triangleq \{F_x, F_y, F_z\}$; for reasons of consistency in the nomenclature adopted throughout this work, we denote a purely symbolic pointer to it, with reference to equations (15) and (16):

$$\delta\mathbf{Q}_{1,L} \rightarrow \delta p_{1,L} \cdot \mathbf{b}_{1,L} \tag{84}$$

   b. Compute the generalized local elastic deformations "$\delta\mathbf{q}_{1,L}$" that are due to the unit-valued, couple of redundant force components of the *L-th* column of matrix "$\mathbf{B}_1$", using Equation (21). If the Berry functions are taken into account (*"P−Δ−δ" effects − see Equation (73)*), use both the 1st and 2nd order terms of (73) in (18); if only the "P−Δ" effects are taken into account, use only the 1st order terms of (73) in (18):

$$\delta\mathbf{q}_{1,L} = \mathbf{F} \cdot \delta\mathbf{Q}_{1,L} \tag{85}$$

   Where vector "$\delta\mathbf{Q}_{1,L}$" was defined in sub-step (2.a).
   c. Compute the relative displacements of the bi-sections of the imposed cut on the current mesh "*n*", which are due to the unit-valued, couple of redundant force components that corresponds to the *L-th* column of matrix "$\mathbf{B}_1$", using Equation (26):

$$\delta u_{1,j} = \mathbf{b}_{1,j}^T \cdot \delta\mathbf{q}_{1,L} \tag{86}$$

   Where $j \triangleq \{F_x, F_y, F_z\}$, thus:

$$\delta\mathbf{u}_{1,L}^T = \{\delta u_{1,x} \quad \delta u_{1,y} \quad \delta u_{1,z}\} = \{\Delta x_L \quad \Delta y_L \quad \Delta z_L\} \tag{87}$$

   The vector of displacements in (87) is abstractly depicted in Figure 30 above.
   d. Evaluate the increments "$\delta\mathbf{d}_R$" of the external product levers for the 2nd order moments that occur due to the relative displacement of the internal cut that has been imposed to the current mesh (*"P−Δ" effects*) according to Equation (27), where $\{\Delta x, \Delta y, \Delta z\} \rightarrow \{\Delta x_L \quad \Delta y_L \quad \Delta z_L\}$ are the relative displacements that were computed in the previous sub-step (2.c).
   e. For the case where the Berry functions are taken into account (*"P−Δ−δ" effects*), select the column "$\mathbf{b}_{1,k}$" of matrix "$\mathbf{B}_1$" corresponding to the *k-th*, unit-valued, couple of redundant moment components, where $k \triangleq (\varphi_x, \varphi_y, \varphi_z)$, and compute the rotations "$\delta u_{1,k}$" of the critical section "c" of the imposed cut considered, which are due to the unit-valued, couple of redundant forces that correspond to the *L-th* column of matrix "$\mathbf{B}_1$"; use Equation (26):

$$\delta u_{1,k} = \mathbf{b}_{1,k}^T \cdot \delta\mathbf{q}_{1,L} \tag{88}$$

   Where $k \triangleq \{M_x, M_y, M_z\}$, thus:

$$\delta\mathbf{u}_{1,c}^T = \{\Delta\varphi_{x,k} \quad \Delta\varphi_{y,k} \quad \Delta\varphi_{z,k}\} \tag{89}$$

The rotation's vector in (89) is abstractly depicted in Figure 30 above.

f. Move along the mesh that corresponds to the *L-th* column of matrix "$\mathbf{B_1}$", and, for each critical section "*i*", execute sub-steps (2.f.i) – (2.f.ii):

   i. For the case where the Berry functions are taken into account (*"P−Δ−δ" effects*), compute the change "$\delta\mathbf{T}_R$" in the transformation matrix "$\mathbf{T}_R$" of each critical section of the mesh according to the following formula, where use of the quantities that were evaluated during sub-step (2.e) is being made; else, skip sub-step (2.f.i):

$$\delta\mathbf{T}_R = (\mathbf{R}_x \cdot \mathbf{R}_y \cdot \mathbf{R}_z) \cdot \mathbf{T}_R \tag{90}$$

   Where in (90), "$\mathbf{R}_x$", "$\mathbf{R}_y$", "$\mathbf{R}_z$" are the rotation tensors around the respective axes of the global coordinate system $\{x,y,z\}$; their components are computed using the respective angle increments from Equation (89).

   ii. Evaluate and store the increment "$\delta\mathbf{B_1}$" of equilibrium matrix "$\mathbf{B_1}$" according to Equation (34):

$$\delta\mathbf{B_1} = -Sign\{m\} \cdot \left[\begin{array}{c|c} \mathbf{0}_{3x3} & \mathbf{0}_{3x3} \\ \hline \delta\mathbf{T}_R \cdot \delta\mathbf{d}_R & \mathbf{0}_{3x3} \end{array}\right] \tag{91}$$

   Where "$\delta\mathbf{d}_R$" is the matrix of external product levers that was computed in sub-step (2.d). Note that, due to the relative nature of the displacements of the ends of the cut imposed to the mesh, the main block-diagonal terms of the above equilibrium matrix are equal to zero.

   Note that the transformation matrix is considered to be unaffected by the relative deformed status of the beam/column elements of the cycle basis when the Berry functions (*"P−Δ−δ" effects*) are not taken into account ($\delta\mathbf{T}_R = \mathbf{T}_R$).

g. Return to sub-step (2.a) and repeat for all force redundant components of mesh "*n*"; then, set $n \to n+1$ and move on to the next mesh.

Once both of the procedures described in sub-sections 12.3.1 and 12.3.2 have been completed, the respective components of the equilibrium matrices may be updated according to the following formula:

$$\mathbf{B}_i \to \mathbf{B}_i + \delta\mathbf{B}_i(\Delta\mathbf{p}_i) \quad , \quad i = \{0,1\} \tag{92}$$

Where in Equation (92), "$\mathbf{B}_i$" is now a function of the external load force increments "$\Delta\mathbf{p_0}$" or of the redundant quantities' force increments "$\Delta\mathbf{p_1}$", respectively.

12.4 Stress Component Increments

As it was shown in the previous section (12.3), geometric non-linearity means that the equilibrium conditions are evaluated in the deformed state; the superposition formula is thus modified as follows:

$$\Delta\mathbf{Q_s} = \mathbf{B}_0(\Delta\mathbf{p}_0) \cdot \Delta\mathbf{p}_0 + \mathbf{B}_1(\Delta\mathbf{p}_1) \cdot \Delta\mathbf{p}_1 \tag{93}$$

Where in (93) the equilibrium matrices $\{\mathbf{B_0}, \mathbf{B_1}\}$ are functions of the external loads "$\Delta\mathbf{p_0}$" and the redundant components "$\Delta\mathbf{p_1}$", respectively.

12.5 Problem Formulation

According to the definition of the yield function, a stress distribution is admissible only if it satisfies (36) at every step of analysis. Thus, we may rewrite the corresponding part of (24) as:

$$\mathbf{Y}_* = \mathbf{c}_{(k)} - \nabla g^T \cdot \mathbf{Q}_{(k)} = \mathbf{c}_{(k)} - \nabla g^T \cdot (\mathbf{Q}_{(k-1)} + \Delta\mathbf{Q}_{(k)}) = \mathbf{c}_{(k)} - \nabla g^T \cdot \mathbf{Q}_{(k-1)} - \nabla g^T \cdot \Delta\mathbf{Q}_{(k)} \geq \mathbf{0} \tag{94}$$

By combining Equations (16), (36), and substituting into (61), the plastic potential "$\mathbf{Y}_*$" may be explicitly expressed as a function of the external loads and the redundant stresses. If the coefficients of this composite function are packed into an incidence matrix "$\overline{\mathbf{N}}$" [49], a constraints' inequality may be established:

$$\mathbf{Y}_* = \mathbf{c}_{(k)} - \overline{\mathbf{N}}^T \cdot \mathbf{Q}_{(k-1)} - \left(\overline{\mathbf{N}}^T \cdot \mathbf{B}_0\right) \cdot \Delta\mathbf{p}_{0,(k)} - \left(\overline{\mathbf{N}}^T \cdot \mathbf{B}_1\right) \cdot \Delta\mathbf{p}_{1,(k)} \geq \mathbf{0} \tag{95}$$

By substituting Equation (93) into (21), then evaluating (23) with the help of (36), and (25) with the help of (93), then substituting all three into (19) and then into (18), we have:

$$\left[\mathbf{B}_1^T \cdot \left(\mathbf{F} + \mathbf{F}_S\right) \cdot \mathbf{B}_0\right] \cdot \Delta\mathbf{p}_{0,(k)} + \left[\mathbf{B}_1^T \cdot \left(\mathbf{F} + \mathbf{F}_S\right) \cdot \mathbf{B}_1\right] \cdot \Delta\mathbf{p}_{1,(k)} + \left(\mathbf{B}_1^T \cdot \overline{\mathbf{N}}\right) \cdot \Delta\boldsymbol{\lambda}_{(k)} = \mathbf{0} \tag{96}$$

By substituting equation (93) into (21), then evaluating (23) with the help of (36), and (25) with the help of (93), then substituting all three into (19) and then into (26), we have:

$$\left[\mathbf{B}_0^T \cdot \left(\mathbf{F} + \mathbf{F}_S\right) \cdot \mathbf{B}_0\right] \cdot \Delta\mathbf{p}_{0,(k)} + \left[\mathbf{B}_0^T \cdot \left(\mathbf{F} + \mathbf{F}_S\right) \cdot \mathbf{B}_1\right] \cdot \Delta\mathbf{p}_{1,(k)} + \left(\mathbf{B}_0^T \cdot \overline{\mathbf{N}}\right) \cdot \Delta\boldsymbol{\lambda}_{(k)} = \Delta\mathbf{u}_{\mathbf{s},(k)} \tag{97}$$

With the help of (96) and (97), and by packing "$\Delta\mathbf{p}_0$" and "$\Delta\mathbf{p}_1$" into a single vector, we have:

$$\left[\begin{array}{c|c} \left[\mathbf{B}_0^T \cdot \left(\mathbf{F} + \mathbf{F}_S\right) \cdot \mathbf{B}_0\right] & \left[\mathbf{B}_0^T \cdot \left(\mathbf{F} + \mathbf{F}_S\right) \cdot \mathbf{B}_1\right] \\ \hline \left[\mathbf{B}_1^T \cdot \left(\mathbf{F} + \mathbf{F}_S\right) \cdot \mathbf{B}_0\right] & \left[\mathbf{B}_1^T \cdot \left(\mathbf{F} + \mathbf{F}_S\right) \cdot \mathbf{B}_1\right] \end{array}\right] \cdot \left\{\begin{array}{c} \Delta\mathbf{p}_0 \\ \hline \Delta\mathbf{p}_1 \end{array}\right\}_{(k)} + \left(\left[\begin{array}{c} \mathbf{B}_0^T \\ \hline \mathbf{B}_1^T \end{array}\right] \cdot \overline{\mathbf{N}}\right) \cdot \Delta\boldsymbol{\lambda}_{(k)} = \left\{\begin{array}{c} \Delta\mathbf{u}_{\mathbf{s}} \\ \hline \mathbf{0} \end{array}\right\}_{(k)} \tag{98}$$

The inclusion of geometric non-linearity in the flexibility matrix "**F**" (*see Equation (74) with reference to (5), (6), and (73)*) as well as in the equilibrium matrices {$\mathbf{B_0}$,$\mathbf{B_1}$} (*see Equation (92) and the respective processes in Sections 12.3.1 and 12.3.2*) affects the form of Equations (95) and (98), due to the fact that the axial force increments "*diag*{$\Delta\mathbf{N_s}$}" exist in (74) and the respective force components "$\Delta\mathbf{p}_i$" exist in (92), where i={0.1}; specifically, the Hessian matrix in (98) becomes a function of the primary unknowns "$\Delta\mathbf{p}_0$" and "$\Delta\mathbf{p}_1$", and the constraints of the problem become non-linear (*see Equation (95) containing the vector of plastic potentials, "*$\mathbf{Y}_*$*"*). On the other hand, matrix "$\mathbf{F}_S$" is still evaluated according to (40) or (41), respectively (*with reference to Equation (39)*).

Equation (98), together with (95) and (24), may be seen as the Karush−Kuhn−Tucker (KKT) conditions of the following –generally non-linear– optimization problem:

Minimize:

$$f\left(\left\{\begin{array}{c} \Delta\mathbf{p}_0 \\ \hline \Delta\mathbf{p}_1 \end{array}\right\}\right) = \int\left[\left\{\Delta\mathbf{p}_0^T \;\vdots\; \Delta\mathbf{p}_1^T\right\}_{(k)} \cdot \left[\begin{array}{c|c} \mathbf{B}_0^T \cdot \left(\mathbf{F} + \mathbf{F}_S\right) \cdot \mathbf{B}_0 & \mathbf{B}_0^T \cdot \left(\mathbf{F} + \mathbf{F}_S\right) \cdot \mathbf{B}_1 \\ \hline \mathbf{B}_1^T \cdot \left(\mathbf{F} + \mathbf{F}_S\right) \cdot \mathbf{B}_0 & \mathbf{B}_1^T \cdot \left(\mathbf{F} + \mathbf{F}_S\right) \cdot \mathbf{B}_1 \end{array}\right]_{(k)} - \left\{\Delta\mathbf{u}_{\mathbf{s}(k)}^T \;\vdots\; \mathbf{0}\right\}\right] \cdot \mathbf{d}\left(\left\{\begin{array}{c} \Delta\mathbf{p}_0 \\ \hline \Delta\mathbf{p}_1 \end{array}\right\}_{(k)}\right) \tag{99}$$

Subject to:

$$\int\left(\overline{\mathbf{N}}^{T}\cdot\left[\mathbf{B}_{0}\ \vdots\ \mathbf{B}_{1}\right]\right)\cdot\mathbf{d}\left(\left\{\begin{array}{c}\Delta\mathbf{p}_{0}\\ \hdashline \Delta\mathbf{p}_{1}\end{array}\right\}_{(k)}\right)\leq\mathbf{c}_{(k)}-\overline{\mathbf{N}}^{T}\cdot\mathbf{Q}_{(k-1)}$$

The objective function in (99) is of cubic (*or higher*) order polynomial form, depending on the approximation followed for the equilibrium matrices (*see Equation (92)*); thus, the optimization problem is a NLP. In particular, if specific values are set for "$\Delta\mathbf{p}_i$" in Equation (92), where i={0,1}, then the inverse problem of force-based, 2nd order structural analysis is approximated by evaluating the bounded stationary point of a polynomial objective function of cubic order under linear constraints; from the numerical implementation point of view, this means that the equilibrium matrices are then treated as constants.

The vector of unknowns in Equation (99) may be reduced for the case of an analysis where a predefined loading path is examined; since, in the case of loading path scenarios, the external loads' increments "$\Delta\mathbf{p}_0$" are well-defined, they may be substituted into the formulation by their corresponding defining constant vector "$\mathbf{r}_p$" (*see Figure 26*).

Thus, a condensed formulation may be written down, where the displacements' increments "$\Delta\mathbf{u}_{\mathbf{s}(k)}$" have been removed, since they can now be computed via Equation (26) as derived quantities which are a function of the redundant stress component increments "$\Delta\mathbf{p}_{\mathbf{1}}$,(k)" and of the Lagrange multiplier increments "$\Delta\boldsymbol{\lambda}_{(k)}$":

Minimize:

$$f(\Delta\mathbf{p}_1)=\int\Delta\mathbf{p}_{1,(k)}^{T}\cdot\left[\mathbf{B}_1^{T}\cdot\left(\mathbf{F}+\mathbf{F}_S\right)\cdot\mathbf{B}_1\right]\cdot\mathbf{d}\left(\Delta\mathbf{p}_{1,(k)}\right)+\mathbf{r}_p{}^{T}\cdot\left[\mathbf{B}_0^{T}\cdot\left(\mathbf{F}+\mathbf{F}_S\right)\cdot\mathbf{B}_1\right]\cdot\Delta\mathbf{p}_{1,(k)}$$

Subject to: (100)

$$\int\left(\overline{\mathbf{N}}^{T}\cdot\left[\mathbf{B}_1\right]\right)\cdot\mathbf{d}\left(\Delta\mathbf{p}_{1,(k)}\right)\leq\mathbf{c}_{(k)}-\overline{\mathbf{N}}^{T}\cdot\mathbf{Q}_{(k-1)}-\overline{\mathbf{N}}^{T}\cdot\mathbf{r}_p$$

The above problem is not convex; for its solution according to the existing optimization algorithmic technology, a diagonal perturbation of the non-linear Hessian may be required.

Each problem (*see Equations (99) and (100)*) may be solved in an iterative form; a displacement- and a load-controlled numerical strategy are required, respectively; detailed descriptions follow below.

12.6 A Load-Controlled Numerical Strategy

A numerical strategy based on an optimization algorithm (*e.g. QP, SQP, IPM*) will seek for an optimal solution under a strict satisfaction of the constraint bounds. With reference to the physical problem examined herein, no return to the yield surface will be required during the execution of the process, as it would be the case when working with a direct stiffness methodical approach; however, this computational advantage has a disadvantage as well: The "optimal" solution determined assumes that a full plasticization of the structure will take place prior to the occurrence of any local or global instability phenomena.

From a more specific point of view, optimization algorithms require a strictly convex problem as input in order to yield a solution that corresponds to a global minimum; in other words, a positive-definite Hessian matrix need be supplied as input. Should a problem be quasi-convex or non-convex, a diagonal perturbation is always applied to its' Hessian matrix by the optimization algorithm itself; in physical terms with regard to the herein examined problem, this means that structural stability is assumed and enforced. Therefore, if an optimization algorithm-based incremental procedure were to approach a point

where the Hessian matrix of the problem would become positive semi-definite or positive indefinite, it would fail determining the critical load of the examined structure.

From a practical point of view, and with respect to the above presented limitations, a load-controlled numerical strategy for solving the 2nd order problem described by Equation (100) is possible to derive. Such a numerical strategy would (*for example*) be able to efficiently simulate the post-elastic response of steel frames up to ten (10) storeys that have been designed and constructed with cross-sections of category 1 (*in some cases of category 2 as well*) according to the Eurocode 3 (E.C.3).

The numerical strategy presented below caters for both non-holonomic elastic-perfectly plastic, as well as hardening-plastic materials under geometric non-linearity considerations. In essence, it is a variant of the one presented in Section 11.2, with the main difference being the recursive evaluation of the equilibrium matrices:

0. Read and pre-process input data.

1. Form a minimal statical basis due to external loads and a (*near*) minimal statical basis due to redundancy and evaluate the problem`s equilibrium matrices $\mathbf{B}_i$, where i={0,1}, respectively; see the processes referenced and described in Section 5.4 and 12.3.

2. Set the predefined load path, "$\mathbf{r}_p$"; see *Figure 26*.

3. Initialize the predefined load path's branch counter n=1.

4. For the current path branch "n", evaluate all corresponding flexibility matrices ($\mathbf{B}_i^T \cdot \mathbf{F} \cdot \mathbf{B}_j$), where {$i$,$j$}={0,0},{0,1}{1,0},{1,1}. The updating process of the "**F**" due to elasticity is done using Equations (5), (6), and (14) or (73), for 1st and 2nd order analysis, respectively. For the equilibrium matrices "$\mathbf{B}_i$" , where i={0,1}, Equation (34) (*with reference to (27) – (33)*) is used for 1st order analysis, and Equation (92) (*with reference to (83) and (91) as well as their attached processes*) is for 2nd order analysis; herein, the starting order of the polynomial approximation was reduced to cubic and the constraints were degenerated to linear, by assuming that the "$\delta\mathbf{B}_i$" sub-matrices in Equation (92) are functions of their respective "$\Delta\mathbf{p}_i$" unit-valued increments, where i={0,1}.

5. Initialize incremental step counter k=1.

6. Check for newly activated or violated associated plastic flows. An associated plastic flow is considered about to be activated when a critical section's stress vector touches a hyperplane of the yield locus; thus, the corresponding component of the plastic potentials' vector becomes zero (*see Equation (95)*). The checking process for violated associated plastic flows is done using Equation (48), with reference to the gradient of (36) with respect to the stresses, (39), and (93):

   a. If no new events were triggered (*e.g. beginning of analysis or continuing holonomic behaviour*), go to step 8.

   b. If a new set of events was detected (*e.g. activation of new associated plastic flows and/or plastic unstressing*), execute steps 7 to 9, then return to step (6.b) and re-check; if no new events were detected after the re-check, go to step 10.

7. Evaluate the matrices ($\mathbf{B}_i^T \cdot \mathbf{F}_S \cdot \mathbf{B}_j$) due to plastic hardening, where {i,j}={0,0},{0,1}{1,0},{1,1}; the updating process of the flexibility matrices due to plastic hardening is done using Equation (40) or the group of Equations (41) (*with reference to Equation (39), and a suitable set of yield deformations, e.g. the elastic variant (S=1) of Equation (40) or of the group of Equations (41)*).

8. Evaluate the problem's constraints. The updating process of the constraints' constants "$\mathbf{c}_{(k)}$" is done using Equation (46), depending on the hardening rule adopted. In the case of plastic unstressing, the yield locus is moved backwards along the hardening vector's direction, so that the active yield plane

touches the tip of the critical section's stress vector that was determined at the end of the previously completed step (*k−1*): Equations (49) and (50) are used.

9. Since the components of the load change vector "$\mathbf{r}_p$" may be large enough to cause a violation of the static admissibility condition, a proper scaling is required in order to maintain complementarity; scale the load change vector of the formulation using a minimal fictitious factor $\rho\epsilon(0,1]$. (*In the herein presented examples, values of* $\rho \epsilon [10^{-6},10^{-2}]$ *were generally found to be sufficient, with* $\rho=10^{-3}$ *being an optimal compromise between computational speed and accuracy*).

10. Solve the problem (100) using any efficient algorithm (*e.g.* [68] *for 1st order analysis or* [70] *for 2nd order analysis, or the respective variant of* [194] *for each case*) and obtain a set of primal and dual variables. If the algorithm fails to converge, go to step 17, because a state of collapse was reached. Note that, in load-controlled analysis of large-scale problems, when the state of collapse is approached, the solver may yield minor incremental increases in the loads while the reference displacement(s) have already gained large values. This is considered to be due to the computer's round-off error; a simple criterion to avoid redundant steps is to compare the relative change of the base shear between successive steps, e.g.:

$$\text{If } \left| \frac{\left\| \bar{\mathbf{V}}_{b,(k)} \right\| - \left\| \bar{\mathbf{V}}_{b,(k-1)} \right\|}{\left\| \bar{\mathbf{V}}_{b,(k-1)} \right\|} \right| \cdot 100\% < 1\% \text{ Terminate}$$

11. Divide the components of the acquired solution vectors $\{\Delta\mathbf{p}_1,\Delta\boldsymbol{\lambda}\}$ with "ρ".

12. Evaluate "$\Delta\mathbf{Q}_{(k)}$". Use Equations (16) and (34); the shear force increments may also be easily evaluated from the local equilibrium conditions along each element.

13. Evaluate "$\Delta\mathbf{q}_{\text{el},(k)}$". Use Equation (22) with reference to Equations (5), (6); and (14) or (73), for 1st and 2nd order analysis, respectively.

14. Evaluate "$\Delta\mathbf{q}_{\text{pl},(k)}$". For perfectly plastic material, use Equation (23); for hardening plastic material, use Equation (25), wherein the flexibility coefficients may be computed from Equation (40) or (41), with reference to (39).

15. Find the minimal solution scale factor "$\Delta\gamma_k$" that activates a new plastic hinge, ensuring that the computed value does not exceed the current branch of the examined loading path: Determine the minimum load scale factor using Equations (58) and (59); then, if required, re-scale according to the maximum desired reference displacement with the aid of (60).

16. Scale corresponding stress and strain increments using the above computed scale factor:

$$\Delta\mathbf{Q}_{(k)} \rightarrow \Delta\gamma_k \cdot \Delta\mathbf{Q}_{(k)} \quad , \quad \Delta\mathbf{q}_{\text{el},(k)} \rightarrow \Delta\gamma_k \cdot \Delta\mathbf{q}_{\text{el},(k)} \quad , \quad \Delta\mathbf{q}_{\text{pl},(k)} \rightarrow \Delta\gamma_k \cdot \Delta\mathbf{q}_{\text{pl},(k)}$$

17. Add up the computed stress and strain increments of the new step (k) to the respective values of the previously completed step (k−1):

$$\mathbf{Q}_{(k)}=\mathbf{Q}_{(k-1)}+\Delta\mathbf{Q}_{(k)} \quad , \quad \mathbf{q}_{\text{el},(k)}=\mathbf{q}_{\text{el},(k-1)}+\Delta\mathbf{q}_{\text{el},(k)} \quad , \quad \mathbf{q}_{\text{pl},(k)}=\mathbf{q}_{\text{pl},(k-1)}+\Delta\mathbf{q}_{\text{pl},(k)}$$

18. Evaluate "$\Delta\mathbf{u}_{\mathbf{s},(k)}$" using Equation (26). Then, add them up to the displacement values of the previously completed step (*k−1*):

$$\mathbf{u}_{\mathbf{s},(k)}=\mathbf{u}_{\mathbf{s},(k-1)}+\Delta\mathbf{u}_{\mathbf{s},(k)}$$

19. If the end of the current loading branch was reached (*i.e. if* $\left| \left\| \Delta\mathbf{p}_0 \right\| - \sum_{i=1}^{i=k} \Delta\gamma_i \right| \le \rho$ *holds – see Figure 26*), go to step 4 and repeat the process for $n \rightarrow n+1$; if the end of the whole loading path or the

maximum reference displacement was reached, go to step 20; else, return to step 6 and repeat the process for $k \rightarrow k+1$.

20. Print output data, and terminate.

As it was pointed out at the beginning of this section, although the above presented numerical strategy yields good convergence properties, its' main deficiency is the inability to trace the critical equilibrium point (*buckling load*) of a structure.

12.7 Some Thoughts for a Displacement-Controlled Numerical Strategy

In this section, a numerical strategy based on a variant of Newton's method is devised in order to investigate whether the formulation of Equation (98) is capable of efficiently tracing the buckling load of a structural frame; due to the nature of the already proposed automation approach for the equilibrium matrices $\{\mathbf{B_0},\mathbf{B_1}\}$, the following methodology is derived under pure structural continuity and material elasticity assumptions ($\mathbf{F}_S=0$), where no Lagrange multipliers are required ($\Delta\boldsymbol{\lambda}_{(k)}=0$).

In essence, the following numerical strategy makes use of the arc-length method, which is the work of G.A. Wempner [187], E. Riks [188], and M.A. Crisfield [189]. Since the original method in reference was developed with the direct stiffness-based structural analysis formulation in mind, it has been suitably adjusted herein for the force-based problem, which is presented below:

0. Read and pre-process input data.

1. Form a minimal statical basis due to external loads and a (*near*) minimal statical basis due to redundancy and evaluate the problem`s 1st order equilibrium matrices $\mathbf{B}_i$, where $i=\{0,1\}$, respectively (*see Equation (34)*).

2. Set the predefined load path vectors, "$\mathbf{r}_p$" (*see Figure 26*).

3. Initialize indices $k=0$, $n=0$.

4. Set the new predefined load/displacement path's branch counter $n \rightarrow n+1$.

5. Initialize by defining a statically feasible direction for the solution:

5.a. Define the load change vector "$\mathbf{r}_p$" according to the current branch "n" of the loading path.

5.b. Assume that stability holds, and acquire an initial direction for the solution using the compatibility condition:

$$\begin{Bmatrix} \Delta\mathbf{p}_0 \\ \Delta\mathbf{p}_1 \end{Bmatrix}_{(k)} = \rho \cdot \begin{bmatrix} \mathbf{I} \\ -(\mathbf{B}_1^T \cdot \mathbf{F} \cdot \mathbf{B}_1)^{-1} \cdot (\mathbf{B}_1^T \cdot \mathbf{F} \cdot \mathbf{B}_0) \end{bmatrix} \cdot \{\mathbf{r}_p\} \tag{101}$$

Where:

$$0<\rho<1$$

Note: If specific values are set for "$\Delta\mathbf{p}_i$" (*where i={0,1}*) in the formulae for evaluating "$\mathbf{B_0}$" and "$\mathbf{B_1}$" (*see Equation (92) with reference to (83) and (91) as well as their attached processes*) then the equilibrium matrices can be treated as constants during the initialization phase.

5.c. Evaluate 1st order terms of the Hessian (*in skyline form*):

$$\mathbf{H}_{(1st)} = \begin{bmatrix} (\mathbf{B}_0^T \cdot \mathbf{F} \cdot \mathbf{B}_0) & (\mathbf{B}_0^T \cdot \mathbf{F} \cdot \mathbf{B}_1) \\ (\mathbf{B}_1^T \cdot \mathbf{F} \cdot \mathbf{B}_0) & (\mathbf{B}_1^T \cdot \mathbf{F} \cdot \mathbf{B}_1) \end{bmatrix} \tag{102}$$

Comment: The particular storage schema saves only the respective part of each of the Hessian's columns that spans from the main diagonal and upwards, until the last non-zero element. It is the most suitable storage form when the Hessian's factorization is applied in a three-factor product, i.e. lower triangular by diagonal by upper triangular matrix, where the last factor is the transpose of the first factor. This factorization schema is called LDL^T.

Comment: The name "*skyline*" is due to the resemblance between the abstract polyline that encloses the nonzero element zones of the upper-triangular part of the (non-factorized) part of the Hessian and that of the abstract polyline being formed between the skyscrapers of the American big cities and the horizon.

5.d. Evaluate 2nd order terms of the Hessian (*in skyline form*) using the initial guess of the (*1st order*) solution from (101) in Equations (92):

$$\mathbf{H}_{(2nd)} = \begin{bmatrix} \left(\mathbf{B}_0^T \cdot \mathbf{F_{gnl}} \cdot \mathbf{B}_0\right) & \left(\mathbf{B}_0^T \cdot \mathbf{F_{gnl}} \cdot \mathbf{B}_1\right) \\ \left(\mathbf{B}_1^T \cdot \mathbf{F_{gnl}} \cdot \mathbf{B}_0\right) & \left(\mathbf{B}_1^T \cdot \mathbf{F_{gnl}} \cdot \mathbf{B}_1\right) \end{bmatrix}_{(k)} \tag{103}$$

Where, with reference to Equation (74):

$$\mathbf{F_{gnl}} = \mathrm{diag}\left\{\Delta\mathbf{N}_{(k)}\right\} \cdot \mathbf{F_g} = \mathrm{diag}\left\{ \begin{bmatrix} \mathbf{B}_{0,N} & \mathbf{B}_{1,N} \end{bmatrix} \cdot \begin{Bmatrix} \Delta\mathbf{p}_0 \\ \Delta\mathbf{p}_1 \end{Bmatrix}_{(k)} \right\} \cdot \mathbf{F_g} \tag{104}$$

Note: The two parts of the Hessian are stored in a common skyline data structure.

5.e. Apply an LDL^T factorization to the Hessian:

$$\mathbf{H}_{(1st)} + \mathbf{H}_{(2nd)} \rightarrow \left(\mathbf{L} \cdot \mathbf{D} \cdot \mathbf{L}^T\right)_{(k)} \tag{105}$$

5.f. Is the Hessian matrix positive definite?

(i) Yes: Estimate the reference displacement increment(s) using both the 1st and 2nd order terms for the equilibrium matrices (*see Equation (92)*) in the SKD/PVW (*see Equation (26)*):

$$\Delta\mathbf{u}_{s\,(k)} = \left[\left(\mathbf{B}_0^T \cdot (\mathbf{F} + \mathbf{F_{gnl}}) \cdot \mathbf{B}_0\right) \quad \left(\mathbf{B}_0^T \cdot (\mathbf{F} + \mathbf{F_{gnl}}) \cdot \mathbf{B}_1\right)\right] \cdot \begin{Bmatrix} \Delta\mathbf{p}_0 \\ \Delta\mathbf{p}_1 \end{Bmatrix}_{(k)} \tag{106}$$

Where, with reference to (74):

$$\mathbf{F_{gnl}} = \mathrm{diag}\left\{\boldsymbol{\Delta N}_{(k)}\right\} \cdot \mathbf{F_g} = \mathrm{diag}\left\{ \begin{bmatrix} \mathbf{B}_{0,N} & \mathbf{B}_{1,N} \end{bmatrix} \cdot \begin{Bmatrix} \Delta\mathbf{p}_0 \\ \Delta\mathbf{p}_1 \end{Bmatrix}_{(k)} \right\} \cdot \mathbf{F_g} \tag{107}$$

Then, check whether the external work is positive:

$$\Delta\mathbf{p}_0^T \cdot \Delta\mathbf{u}_{s\,(k)} \geq 0 \tag{108}$$

If (108) is not satisfied, a bifurcation point was determined; return to step **5.b** and scale down the guess for the initial solution (*e.g. select a smaller value for the arc-length "ρ"*). If (108) holds, solve the linearized system below based on the set of estimated reference displacement increment(s) from (106):

$$\left(\mathbf{L} \cdot \mathbf{D} \cdot \mathbf{L}^T\right)_{(k)} \cdot \begin{Bmatrix} \Delta\mathbf{p}_0 \\ \Delta\mathbf{p}_1 \end{Bmatrix}_{(k)} = \begin{Bmatrix} \Delta\mathbf{u}_s \\ \mathbf{0} \end{Bmatrix}_{(k)} \tag{109}$$

Note: At this point, the relative values between the two solutions are checked; no significant diversion is to be expected.

(ii) No: The structure is unstable; terminate.

6. Start a new incremental step *k*:

$$\text{Set } k \rightarrow k+1, \text{ then set } \begin{Bmatrix} \Delta\mathbf{p}_0 \\ \Delta\mathbf{p}_1 \end{Bmatrix}_{(k)} = \begin{Bmatrix} \Delta\mathbf{p}_0 \\ \Delta\mathbf{p}_1 \end{Bmatrix}_{(k-1)} \tag{110}$$

7. Evaluate 1st order terms of the Hessian – see Equation (102).

8. Evaluate 2nd order terms of the Hessian using the initial guess of the 1st order solution – see Equation (103), where:

$$\mathbf{F_{gnl}} = \text{diag}\left\{\sum_{i=0}^{k-1} \Delta\mathbf{N}_i + \Delta\mathbf{N}_{(k)}\right\} \cdot \mathbf{F_g} = \text{diag}\left\{\sum_{i=0}^{k-1} \Delta\mathbf{N}_i + [\mathbf{B}_{0,N} \quad \mathbf{B}_{1,N}] \cdot \begin{Bmatrix} \Delta\mathbf{p}_0 \\ \Delta\mathbf{p}_1 \end{Bmatrix}_{(k)}\right\} \cdot \mathbf{F_g} \tag{111}$$

Note: The two parts of the Hessian (*1st & 2nd order terms*) are stored in a common skyline data structure.

9. Apply an LDL^T factorization to the Hessian – see Equation (105).

10. Is the Hessian matrix positive definite?

(a) Yes: Estimate the reference displacement increment(s) using both the 1st and 2nd order terms in the SKD/PVW – use Equation (106) with the help of Equation (107).

(b) No: A critical point has been reached; provide a new feasible direction for the equilibrium path using the compatibility condition, but for a negative external load increment, in order to cater for the descending equilibrium path's branch:

$$\begin{Bmatrix} \Delta\mathbf{p}_0 \\ \Delta\mathbf{p}_1 \end{Bmatrix}_{(k)} = \rho \cdot \begin{bmatrix} \mathbf{I} \\ -(\mathbf{B}_1^T \cdot \mathbf{F} \cdot \mathbf{B}_1)^{-1} \cdot (\mathbf{B}_1^T \cdot \mathbf{F} \cdot \mathbf{B}_0) \end{bmatrix} \cdot \{-\mathbf{r}_p\} \tag{112}$$

Execute steps **7**, **8** and **9** for the same iteration index "*k*", then move on to step **11**.

11. Solve the updated Equation (109), according to the estimated reference displacement increment(s).

12. A new equilibrium path point was efficiently approximated. At this point, the two successive solution estimates must be compared for possible deviations; check the following condition(s):

$$-\rho \cdot \mathbf{r}_p \leq \Delta\mathbf{p}_{0(k)} \leq +\rho \cdot \mathbf{r}_p \quad \text{and} \quad \left| \left\|\Delta\mathbf{p}_{1(k)}\right\| - \left\|\Delta\mathbf{p}_{1(k-1)}\right\| \right| \leq \varepsilon \tag{113}$$

Or

$$\left| \left\| \begin{Bmatrix} \Delta\mathbf{p}_0 \\ \Delta\mathbf{p}_1 \end{Bmatrix}_{(k)} \right\| - \left\| \begin{Bmatrix} \Delta\mathbf{p}_0 \\ \Delta\mathbf{p}_1 \end{Bmatrix}_{(k-1)} \right\| \right| \leq \varepsilon \tag{114}$$

Where "ε" is the CPU's round-off error (*or some other suitably selected numerical tolerance*); if one/both of the above condition(s) is/are not satisfied, return to step **7** and repeat for the same iteration index "*k*"; else, move on to step **13**.

13. Update all static and kinematic variables (*elastic distributions*):

$$\mathbf{Q}_{\mathbf{s},(k)} = \mathbf{Q}_{\mathbf{s},(k-1)} + \Delta\mathbf{Q}_{\mathbf{s},(k)} \quad , \quad \mathbf{q}_{\text{el},(k)} = \mathbf{q}_{\text{el},(k-1)} + \Delta\mathbf{q}_{\text{el},(k)} \quad , \quad \mathbf{u}_{\mathbf{s},(k)} = \mathbf{u}_{\mathbf{s},(k-1)} + \Delta\mathbf{u}_{\mathbf{s},(k)}$$

14. If a maximum reference displacement was reached, go to step **15**; if the end of the current loading branch was reached, go to step **4** and define a new loading path branch "*n*"; else go to step **6** and start a new incremental step "*k*".

15. Print output data, and terminate.

The above presented numerical strategy may only be seen as a concept for a future research direction; no complete testing has been conducted yet, thus neither functionality nor efficiency are either assumed or proven within the context of this work.

13 Examples

In the following context, several indicative examples are presented in order to demonstrate the functionality of the proposed force−based formulation. Where possible, results are quantitatively compared with those of a widely accepted commercial program that uses the equivalent direct stiffness method; where not, with results according to methods found in the literature.

13.1 A Single-Storey, Single-Bay, Eccentric Braced Frame (3D)

The following frame (*see Figure 31*) is used as a first example. The frame's height is H=3m, and distances between columns are L_x=L_y=6m. All columns are placed so that their strong bending axis is parallel to the y-axis of the global coordinate system, and are fully fixed at the basis. Beams are placed so that they bend along their strong axis due to external forces applied along the z-axis, and are subdivided into smaller elements of length L=0.6m each. The braces are placed inside the openings which are parallel to the y-z plane, are assumed articulated at both of their ends, and are load-free.

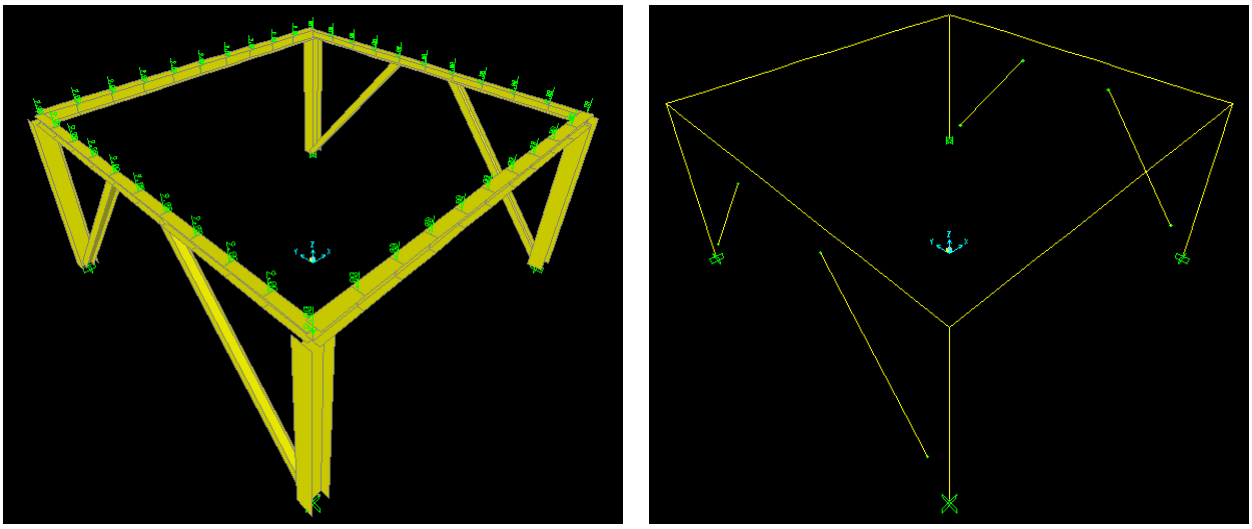

Figure 31: 3D illustrations of the 1−storey 1−bay, eccentric−braced frame (snapshots from SAP2000).

The frame's definitions (*nodal numbering & coordinates, member connectivity, section assignments and interacting stress components*) are summarized in Tables 3 and 4 below.

Node	x	y	z	Node	x	y	z
1	6.00	6.00	0.00	7	0.00	3.60	3.00
2	0.00	6.00	0.00	8	0.00	2.40	3.00
3	0.00	0.00	0.00	9	0.00	0.00	3.00
4	6.00	0.00	0.00	10	6.00	0.00	3.00
5	6.00	6.00	3.00	11	6.00	2.40	3.00
6	0.00	6.00	3.00	12	6.00	3.60	3.00

Table 3: Nodal coordinates of the 1−storey 1−bay, eccentric−braced frame.

Member	Node: Start → End	Section	Interacting Components	Member	Node: Start → End	Section	Interacting Components
1	1 → 5	HEM260	{N,M_2,M_3}	9	6 → 5	HEM180	{M_2,M_3}
2	2 → 6	HEM260	{N,M_2,M_3}	10	9 → 8	HEB140	{M_2,M_3}
3	3 → 9	HEM260	{N,M_2,M_3}	11	8 → 7	HEB140	{M_2,M_3}
4	4 → 10	HEM260	{N,M_2,M_3}	12	7 → 6	HEB140	{M_2,M_3}
5	1 → 12	HEB140	{N,M_2,M_3}	13	9 → 10	HEM180	{M_2,M_3}
6	2 → 7	HEB140	{N,M_2,M_3}	14	10 → 11	HEB140	{M_2,M_3}
7	3 → 8	HEB140	{N,M_2,M_3}	15	11 → 12	HEB140	{M_2,M_3}
8	4 → 11	HEB140	{N,M_2,M_3}	16	12 → 5	HEB140	{M_2,M_3}

Table 4: Connectivity, sections, and interacting components of the 1−storey 1−bay, eccentric−braced frame.

The material of the structure is S235, with a Young's Modulus E=2.0E+8kPa, a conventional yield stress of f_y=235MPa, and is considered to be elastic-perfectly plastic.

To simulate material non−linearity, the concentrated plasticity approach is followed. For the columns, the bilinear AISC−LRFD criterion is used [175], for {N,M_2,M_3} interaction. For the beams, the coupled bending moment {M_2,M_3} variant of the same criterion is applied, without the participation of the axial forces {N}; in order to be able to compare with SAP2000 [178], the effect of torsion {T} on beams was purposefully left out, since no torsion-bending interaction is supported by the available version of the program [178] (*however, for the specific external load definitions presented below, the participation of torsion in the developed stress configuration of the structure is very small*). A linear relation between {M_2} and {M_3} was adopted for both interaction criteria. Articulations at the ends of the braces were implemented according to Equation (37).

All beams are subject to a uniform load of 15kN/m. Each beam is divided into smaller elements of 0.6m length, and uniform loads are converted into a finite set of equally sized point loads of 9kN. Lateral loads are applied to the four top-corner nodes of the frame.

Two pushover analyses were run, one for each horizontal direction {x,y}. The base shear vs. roof displacement curves of the structure are presented in Figure 32 and Figure 33 below, where quantitative comparisons with SAP2000 are also included; for SAP2000, default analysis parameters were used.

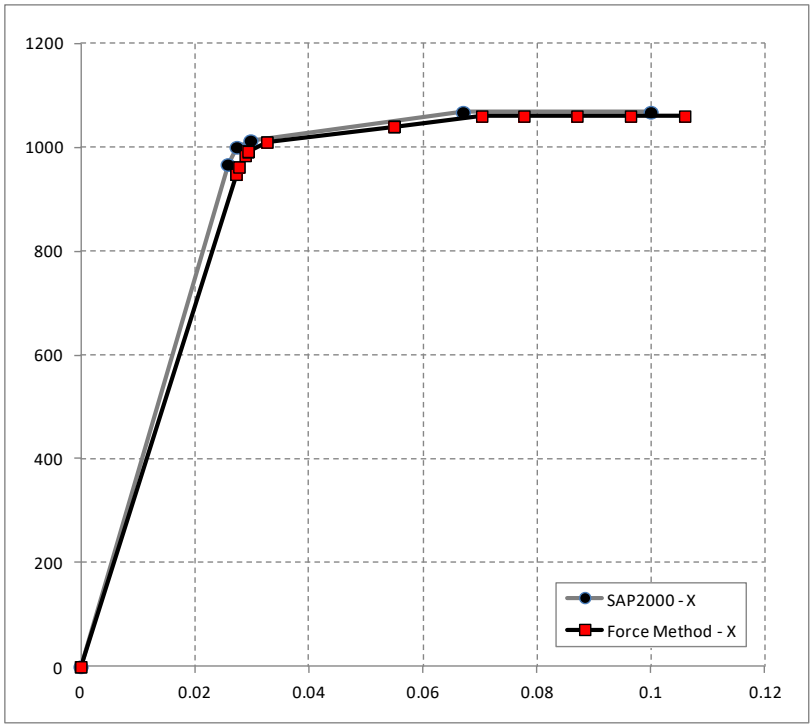

Figure 32: Pushover curve of the 1−storey, 1−bay, eccentric−braced frame; X−Direction; Units: {kN,m}.

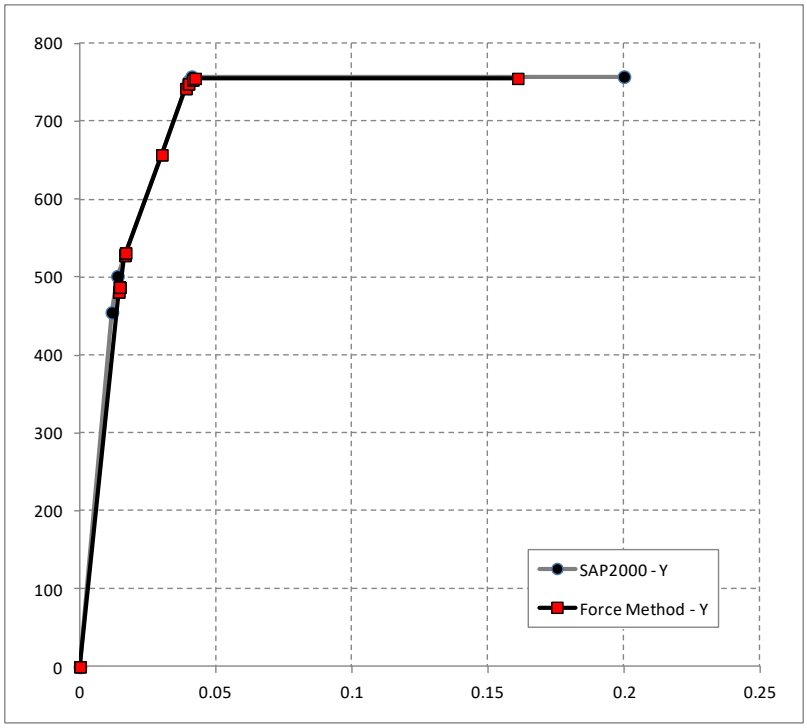

Figure 33: Pushover curve of the 1−storey, 1−bay, eccentric−braced frame; Y−Direction; Units: {kN,m}.

As it may be seen, results are in good accordance; the ultimate base shear is $V_{b,x}$~1067kN for the x-direction, and $V_{b,y}$~757kN for the y-direction.

13.2 Six-Storey, Single-Bay, Frame (3D)

A six-storey frame, with one-bay at each horizontal direction, is used as a second test example. Each storey has a height H=3.0m and each bay an opening L_x=L_y=6.0m. Beams are subdivided into smaller elements of length L=0.6m each; columns are placed so that their strong bending axis is parallel to the y-axis, and are fully fixed at the basis. The geometry of the frame is illustrated in Figure 34 below.

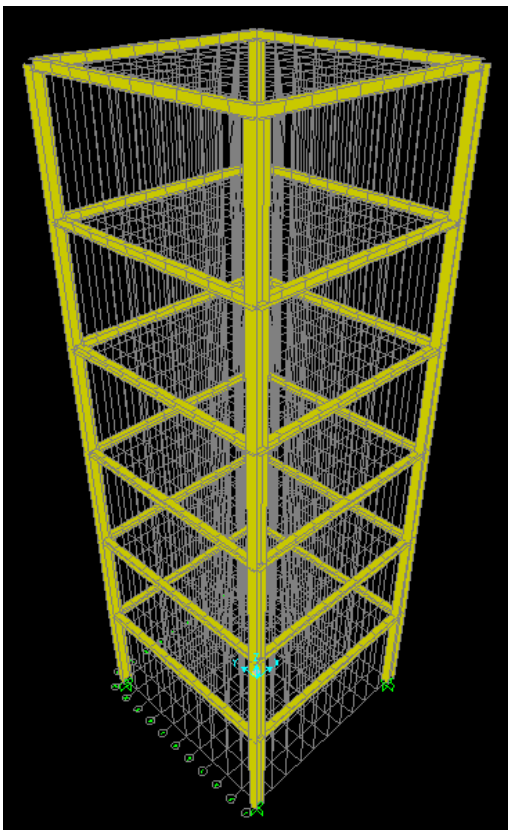

Figure 34: 3D illustration of the 6−storey frame (snapshot from SAP2000).

The sections of beams and columns were purposefully selected in order to form a strong column−weak beam sway mechanism, and are summarized in Table 5 below.

Members	Length	Section
Columns	3.0m	HEM300
Beams	6.0m	HEM180

Table 5: Section properties and member lengths of the six storey frame.

The material of the structure is S235, with a Young's Modulus E=2.0E+8kPa, a conventional yield stress of f_y=235MPa, and is considered to be elastic-perfectly plastic.

To simulate material non−linearity, the concentrated plasticity approach is followed, according to the exact assumptions that were made for the first example.

All beams are subject to a uniform vertical load of 15kN/m. Each beam is subdivided into ten smaller elements of length L=0.6m each, and the distributed loads are converted into a finite set of equally sized point loads of value 9kN each.

The beam−column junctions (*nodes*) are subject to a lateral lumped-load pattern which is defined as linearly varying with respect to the height of each storey according to the 1st eigenmode of the structure (*with a simplification assumption regarding the lack of participation of all higher order eigenmodes*).

Two pushover analyses were run, one for each horizontal direction (x,y). The base shear vs. roof displacement curves of the structure is presented in Figure 35 and Figure 36 below, where a quantitative comparisons with SAP2000 [178] are also included; for SAP2000, default analysis parameters were used.

As it may be seen, the results are in good accordance; the ultimate base shear along the x-direction is $V_{b,x}$~667kN, and along the y-direction is $V_{b,y}$~516kN.

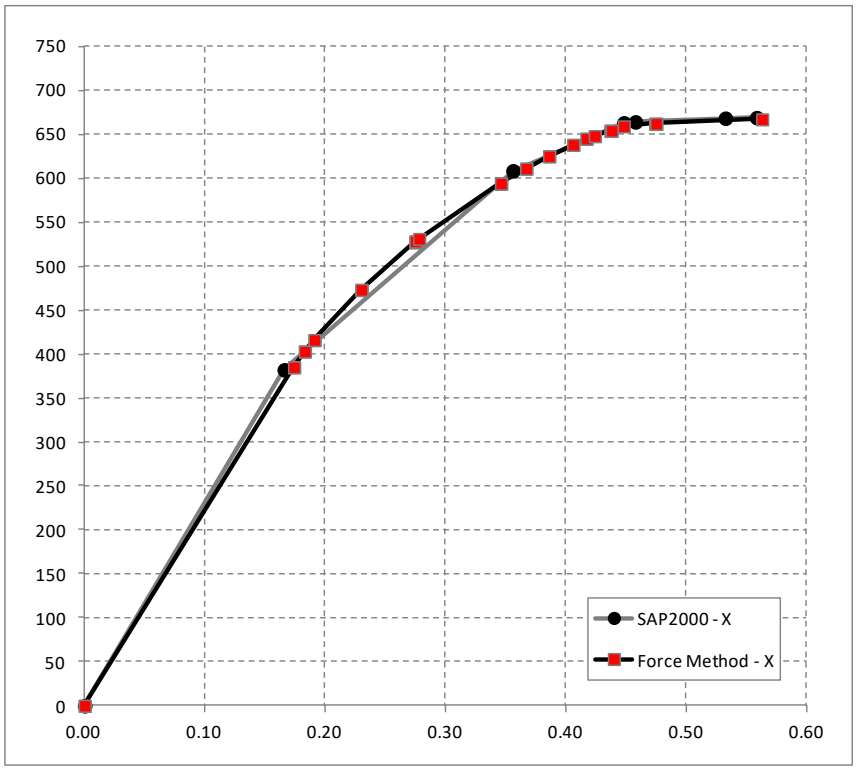

Figure 35: Pushover curves of the six−storey frame, x−direction; Units: {kN,m}.

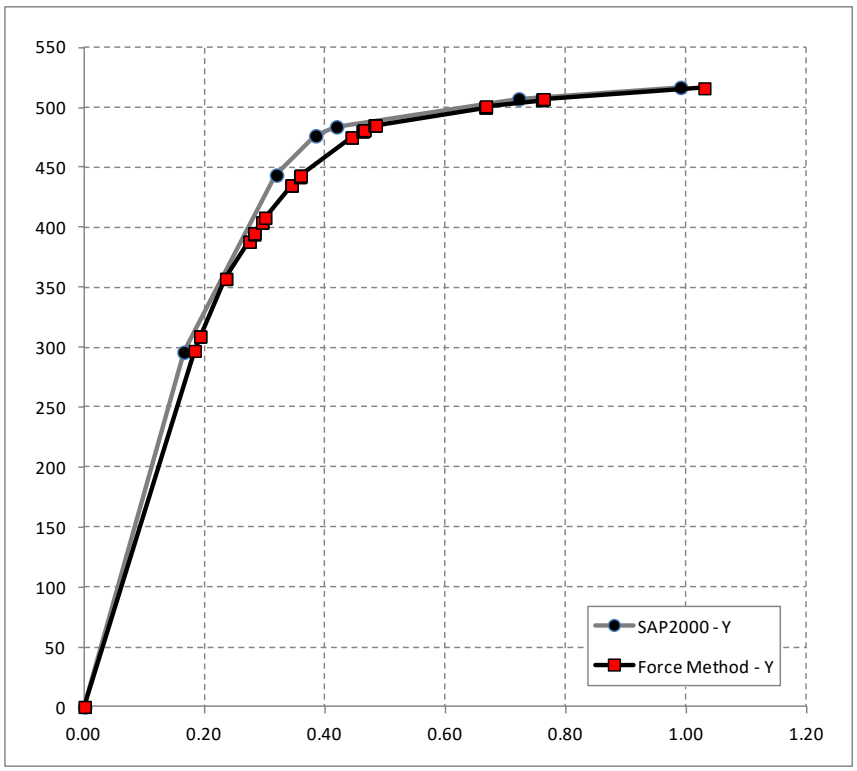

Figure 36: Pushover curves of the six−storey frame, y−direction; Units: {kN,m}.

13.3 Single-Storey, Single-Bay, Frame (2D)

This example is used to test the functionality of the herein implemented yield function according to DIN−18800, via a comparison with AISC−LRFD; to this extend, I-shaped sections are used.

The frame's height is H=3.0m and length L=6.0m. The beam's section is HEB160 and the columns' sections are HEM200. All structural elements are placed so as to bend around their strong axis. The beams are subdivided into smaller elements of length L=0.6m each. Columns are fully fixed at the basis. Schematically, the portal frame may be seen in Figure 37 below.

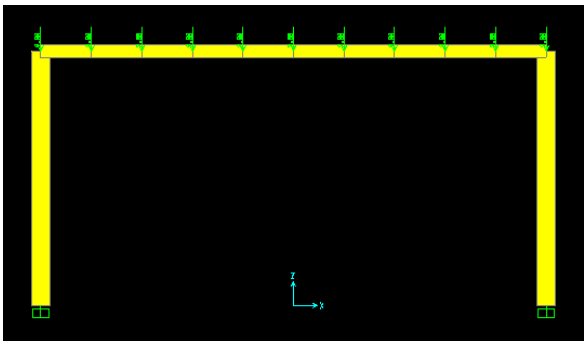

Figure 37: Geometry of the portal frame and vertical loads (snapshot from SAP2000).

The material of the structure is S235 with a Young's Modulus E=2.0E+8kPa, a conventional yield stress of f_y=235MPa, and is considered to be elastic-perfectly plastic.

A uniform vertical load of magnitude 15kN/m is applied to the beam, which is simulated by finite point loads of magnitude 9kN each, applied in equal distances of 0.6 m. A horizontal force is applied to the top left node.

Two pushover analyses were performed using the proposed formulation; one using the AISC−LRFD yield function and one using the DIN−18800. The results were compared to those of SAP2000 [178] and were found in good accordance. All base shear vs. roof displacement curves have been plotted in Figure 38 below.

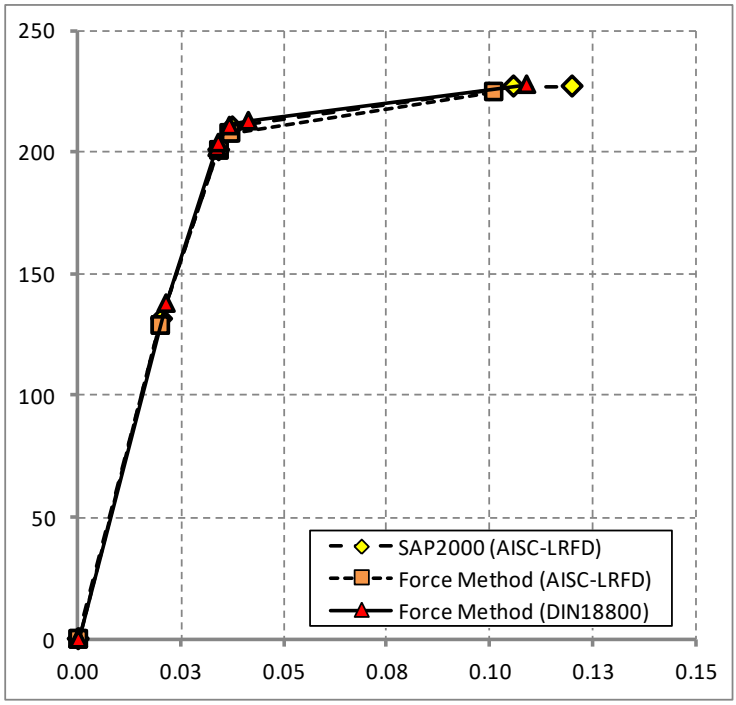

Figure 38: Pushover curves of the 2D portal frame; Units: {kN,m}.

13.4 A Simple Grillage (3D)

This simple example is used to demonstrate the functionality of the proposed formulation for structures where the contribution of torsion is important. Grillages are a typical case; a simple grillage found in [190] is used as reference. Schematically, it is presented in Figure 39 below.

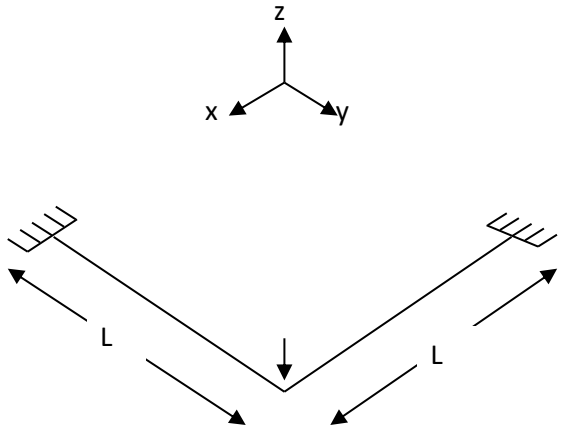

Figure 39: Geometry and loading of the grillage.

As it may be observed, the geometrical proportions and loading conditions are the same as in [190]; herein, elements have a length L=3m and a rectangular tube section with dimensions (bxh)=(160x160)mm and thickness t=10mm.

The material of the structure is S235 with a Young's Modulus E=2.0E+8kPa, a conventional yield stress of f_y=235MPa, and is considered to be elastic-perfectly plastic.

In addition to the assumptions above, the yield locus was linearized so as to be in accordance with the proposed formulation. An analytical derivation of the collapse load according to the linear yield function adopted follows below:

$$g(T,M_3)=\frac{T}{T_p}+\frac{M_3}{M_{3,p}}-1\le 0 \tag{115}$$

The partial derivatives of the yield function with respect to each stress component are:

$$\frac{\partial g}{\partial T}=\frac{1}{T_p} \quad , \quad \frac{\partial g}{\partial M_3}=\frac{1}{M_{3,p}} \tag{116}$$

Thus, with the help of (116), the ratio of bending (θ) to torsion (γ) plastic rotations will be:

$$\frac{\theta}{\gamma}=\left(\frac{T_p}{M_{3,p}}\right)\cdot\frac{M_3}{T} \tag{117}$$

As also stated in [190], a plastic bending rotation in the proximity of a support node of one beam will result in an equal rotation due to torsion in the other beam, in the proximity of the connection node between the two elements. Thus, from (117) we infer the following linear proportion:

$$\frac{M_3}{M_{3,p}}=\frac{T}{T_p} \tag{118}$$

According to [190], the equation that gives the collapse load is the following:

$$\frac{1}{2}\cdot P\cdot L = M_3 + T \tag{119}$$

By combining (118) and (119), and by assuming for simplicity that $M_{3p}=T_p$, we have:

$$P_C = \frac{2\cdot M_{3,p}}{L} \tag{120}$$

For the selected cross-section and material, $M_{3p}=79.4kNm$; thus, from (120), P_C=52.93kN.

An analysis using the proposed formulation of (64) was run, and the resulting load vs. corresponding displacement curve is presented in Figure 40 below:

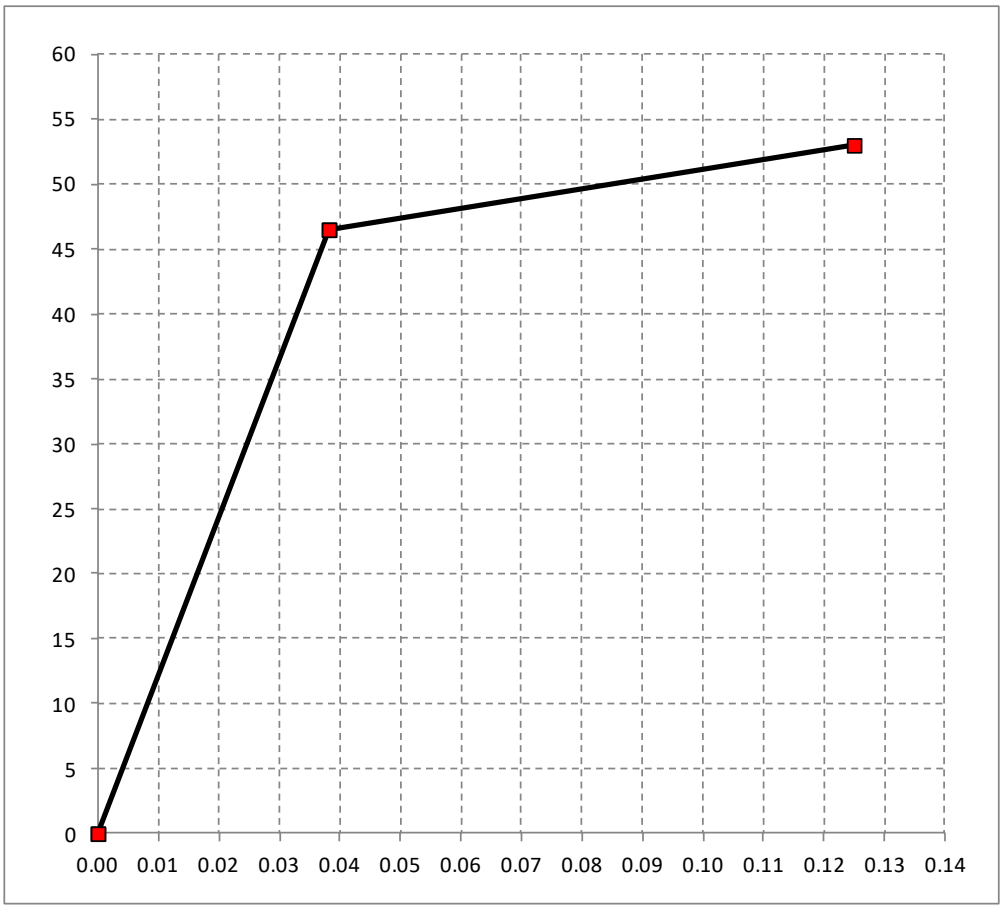

Figure 40: Load vs. corresponding displacement curve of the grillage; Units: {kN,m}.

As it may be seen, the results are in good accordance; the collapse load according to the proposed method is P_C~53kN.

13.5 Double-Span Steel Beam/Girder (2D)

This example is a planar (2D) 2-span steel beam that exhibits non-holonomic hardening plastic behaviour. The geometry and loading considerations, as well as the critical section numbering of the corresponding structural model may be seen in Figure 41 below:

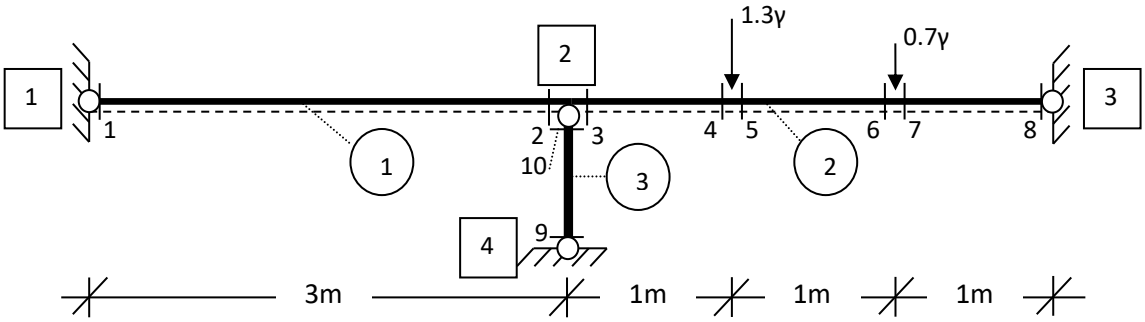

Figure 41: Frame's geometry and loading considerations, node, member, and critical section numbering.

The structure's material is S220 with a conventional yield stress f_y=220000 kPa and a Young's modulus E=2.0E+08 kPa. The beam section is HEB160 and is placed so that it bends around its strong axis (#3), while the mid-supporting articulated beam is considered as a rigid element with L=1.0 m and A=1.0E+08 m^2. Member #2 is sub-divided into three finite elements of equal length. The material hardening behaviour was assumed isotropic (*Drucker*) and was modelled according to Table 6 below. With reference to Table 6, the plastic hinge backbone curves were computed using Equations (38) and (39), and the yield rotations were evaluated using the elastic form (S=1) of the group of Equations (41).

Backbone Curve	
Strain	*Stress*
0.00	0.00
1.00	1.00
7.00	1.25
+∞	1.25

Table 6: Piecewise linear constitutive law (normalized wrt. to the yield strain and stress values, respectively).

The scale factor "γ" of the loads applied to the beam (*see Figure 41*) was proportionally increased, in order to determine the collapse load and mechanism. The plasticization and local unloading sequence until the point of collapse is presented in Table 7 below:

Steps	Critical Section #3	Critical Sections #4 & #5	Critical Section #6
1		●	
2		H.P.: ●	●
3	●	P.U.: ▬	H.P.: ●
4	H.P.: ●	P.U.: ▬	H.P.: ●
5	H.P.: ●	H.P.: ●	P.P.: ●
6	P.P.: ●	H.P.: ●	P.P.: ●

Table 7: Plasticization event history {H.P.=Hardening Plastic, P.P.=Perfectly Plastic, P.U.=Plastic Unstressing}.

A comparative analysis was run using SAP2000 [178], and the resulting load vs. corresponding displacement curves may be seen in Figure 42; the collapse load determined using the proposed method is ~4% less than the one using SAP2000.

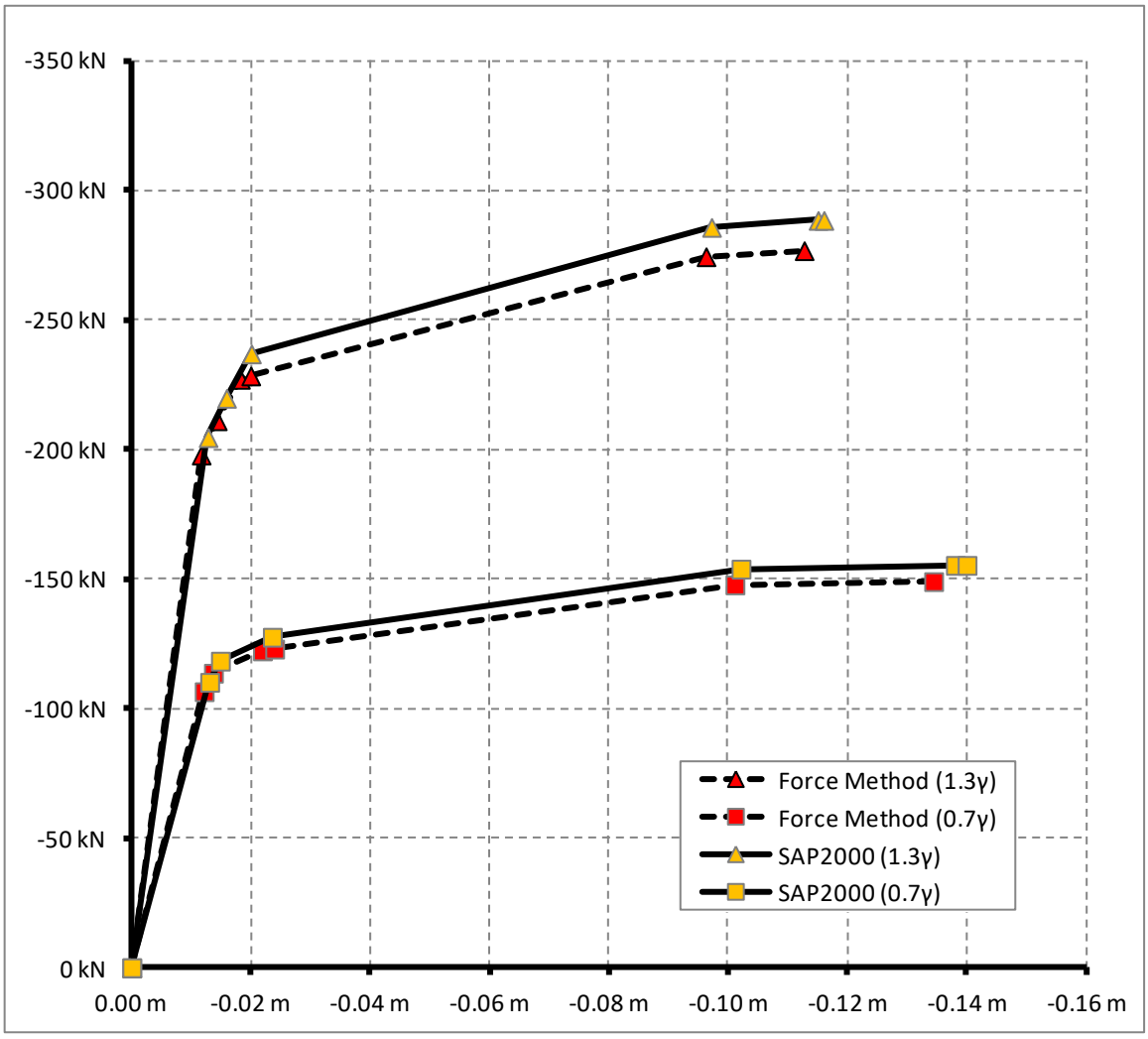

Figure 42: Load vs. corresponding displacement curves {Units: kN,m}.

The corresponding bending moment vs. plastic rotation comparative diagrams for critical sections 3, 4, and 6, may be seen in Figures 43–45, with reference to Figure 41 for the critical section numbering. Critical section 5 was omitted, because it has identical results to those of critical section 4. As it may be seen, a minor plastic unstressing occurs in section 4. Results are in good agreement.

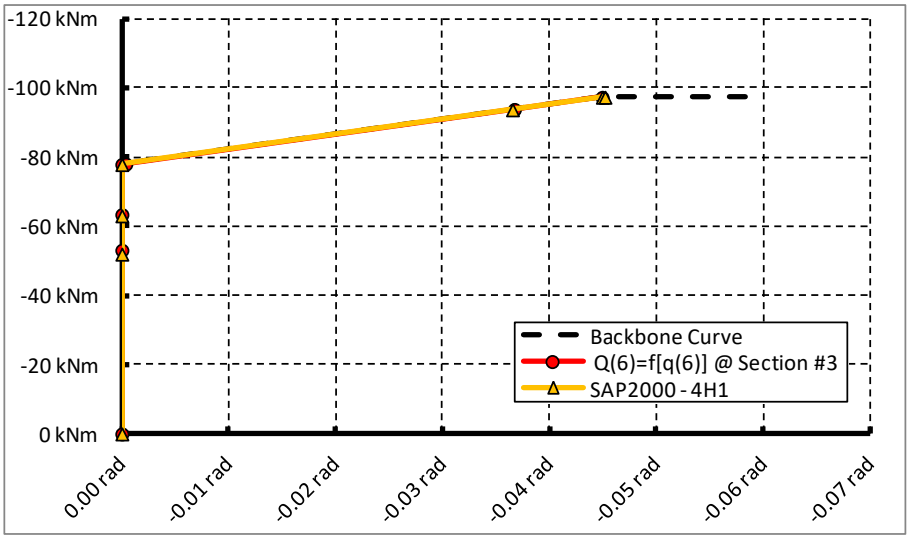

Figure 43: Bending moment vs. corresponding plastic rotation curves for critical section #3 {Units: kNm, rad}.

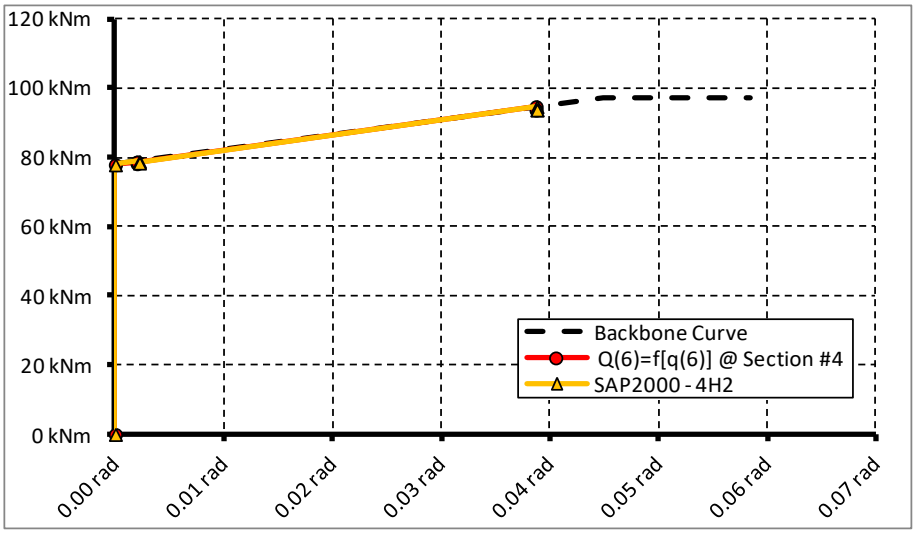

Figure 44: Bending moment vs. corresponding plastic rotation curves for critical section #4 {Units: kNm, rad}.

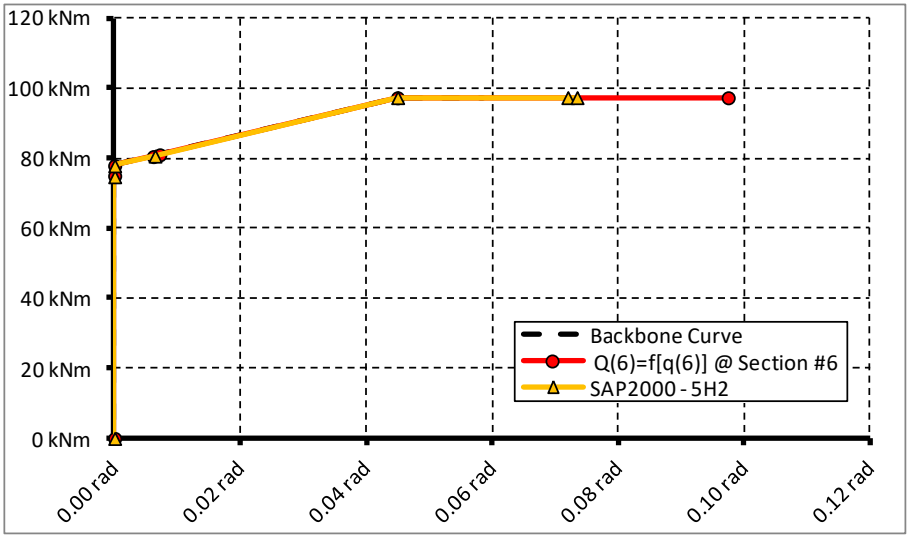

Figure 45: Bending moment vs. corresponding plastic rotation curves for critical section #6 {Units: kNm, rad}.

13.6 Single-Storey, Three-Bay Reinforced Concrete Frame (2D)

This example was selected in order to demonstrate the efficiency of the proposed method regarding nodal eccentricities as well as its' suitability for analysing reinforced concrete frames. It is a planar (2D) frame that has been also analysed by O. De Donato and G. Maier in [89]; all data have been converted to SI units {kN,m} herein, and gravity acceleration was set equal to 10m/s^2. The structure's geometry may be seen in Figure 46 below.

Every beam and column member has potentially one plastic hinge at each of its ends. Furthermore, each beam member (*members with numbers 5-10 in Figure 46 below*) is divided into two finite elements of equal length, in order to be in accordance with the structural model in [89]. As a consequence of the aforementioned finite element division, the uniformly distributed gravity "g" and mobile "p" loads defined in [89] have been converted to a finite set of point loads denoted herein with "G" and "P", respectively, which may be seen in Figure 46 below.

The frame is subjected to a predefined loading scenario where all loads are incrementally applied to the structure, in the following sequential order (*as defined in* [89]): First, only the dead loads (g) are applied to all beams with a value range from 0 up to 50kN/m; then, the horizontal load (W) is applied to node 5 with a value range from 0 up to 50kN, and, finally, the mobile loads (p) are applied to the left beam only, with a value range from 0 up to 13kN/m. The aforementioned distributed loads have been converted into equivalent point loads; their maximum values may be seen in Figure 46 below.

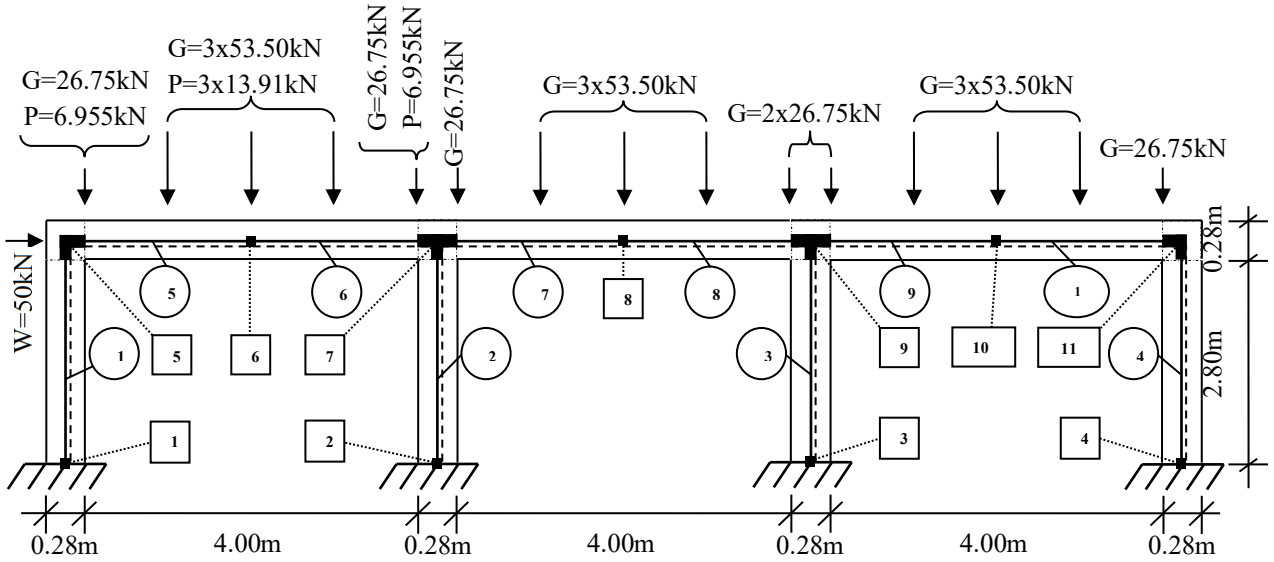

Figure 46: Frame's geometry, node and member numbering, nodal eccentricities, and loading considerations.

The material in the square areas of the joints between columns and beams is assumed to be rigid (*see Figure 46 above*).

In order to model the flexural behaviour of the deformable parts of the structure, an arbitrary value of E=25786967.4 kPa was adopted for the elasticity modulus and of ν=0.25 for Poisson's ratio. The effective cross-section with (bxh)=(0.30x0.28m) was assumed for all elements; thus, the value of A=0.7840E-01 m^2 was set for the cross-section`s area and the values of I_2=5.488E-04 m^4 and I_3=6.300E-04 m^4 for the bending moments of inertia around the weak and strong axes, respectively.

In Figures 47−49, one may see the backbone curves for the plastic hinges of the frame. Pure bending behaviour was assumed, according to [89]; the flexural rotations were computed using the elastic form

($S=I$) of the group of Equations (41) and with the help of the selected values for E and I_3; where "L" in Equations (41), the deformable length of each member was given as input.

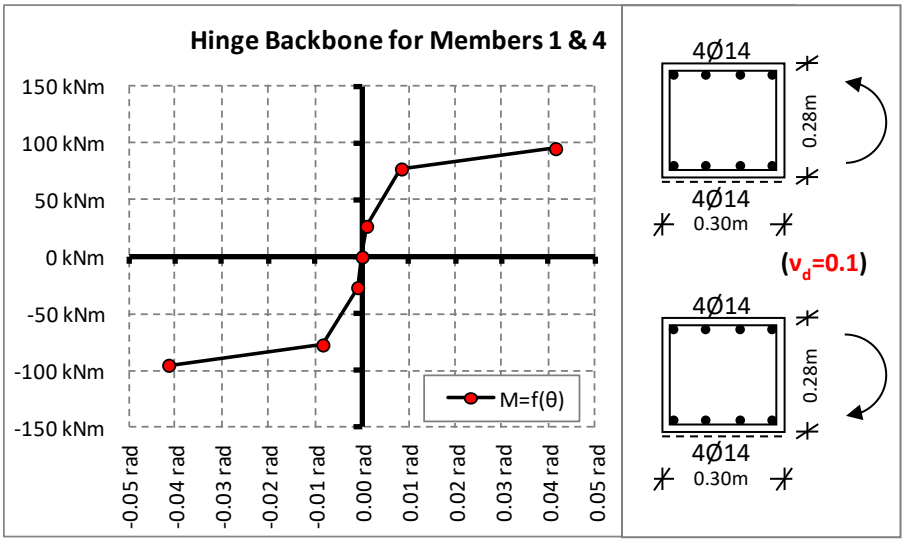

Figure 47: Plastic hinge backbone curve for the outer columns of the frame {units: kNm,rad}.

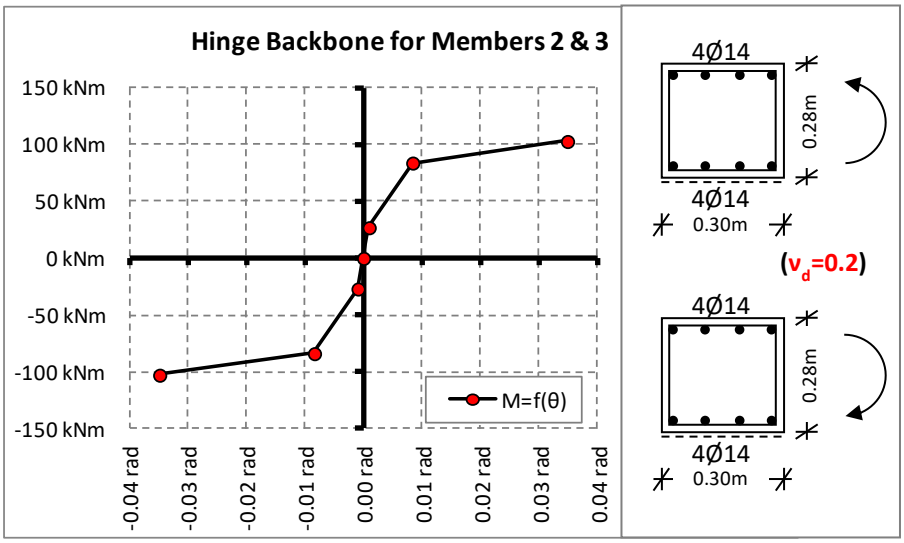

Figure 48: Plastic hinge backbone curve for the inner columns of the frame {units: kNm,rad}.

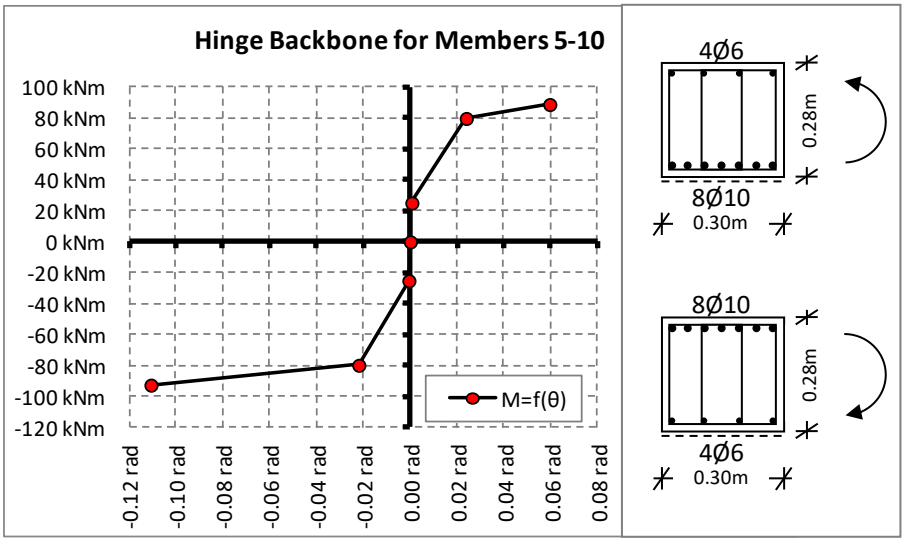

Figure 49: Plastic hinge backbone curve for the beams of the frame {units: kNm,rad}.

The loading scenario was run under the constraint that, should the limited rotation capacity due to plastic hardening of at least one of the structure's critical sections be reached during an incremental analysis step, the procedure would be terminated.

The resulting [M_3], [V_2], and [N] diagrams at the end of the analysis may be seen in Figure 50, Figure 51, and Figure 52, respectively.

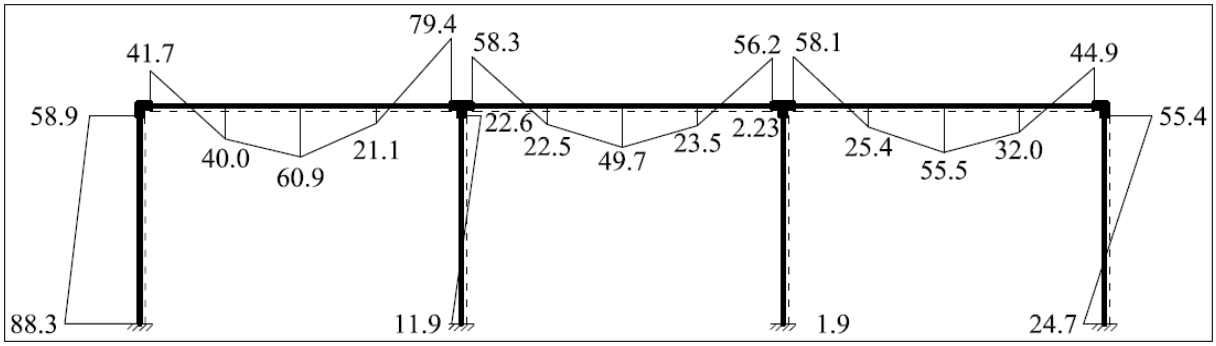

Figure 50: Bending moments' diagram at the end of the analysis {units: kNm}.

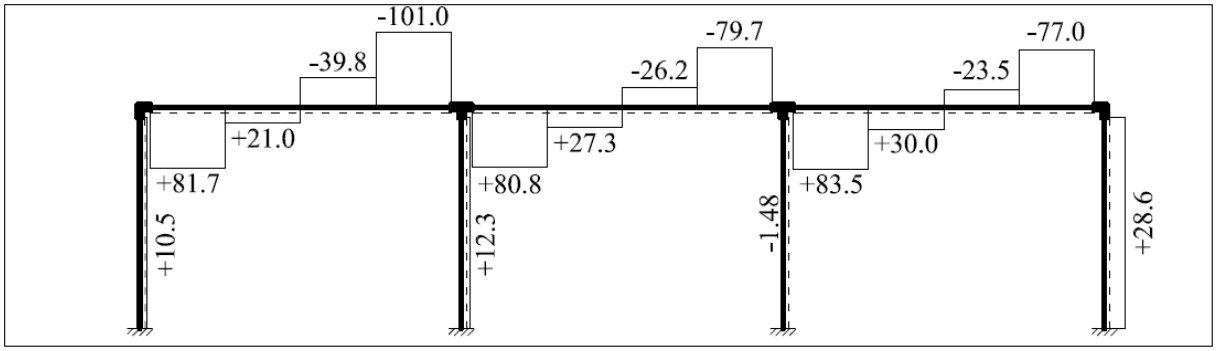

Figure 51: Shear forces' diagram at the end of the analysis {units: kN}.

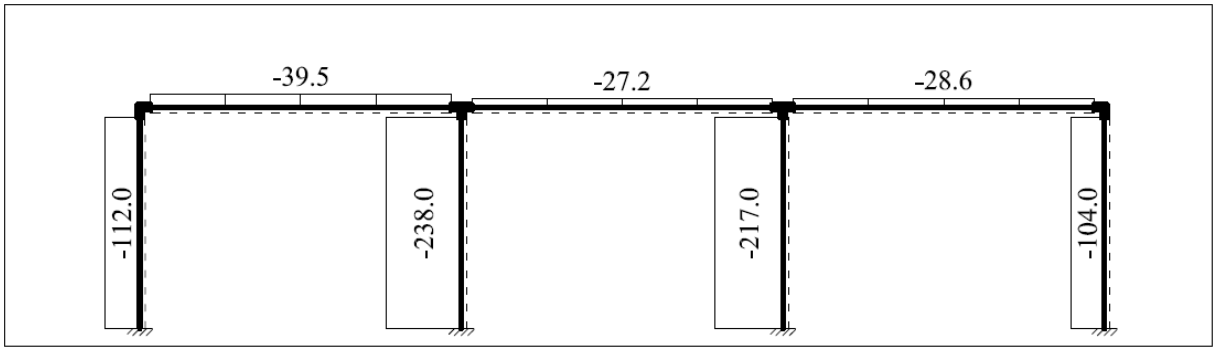

Figure 52: Axial forces' diagram at the end of the analysis {units: kN}.

The load values at the end of the analysis, together with the respective internal forces and moments at the beam-column joints of the structure, are shown in Figure 53; with the element eccentricities in mind, it may be easily verified that the nodal equilibrium conditions are satisfied.

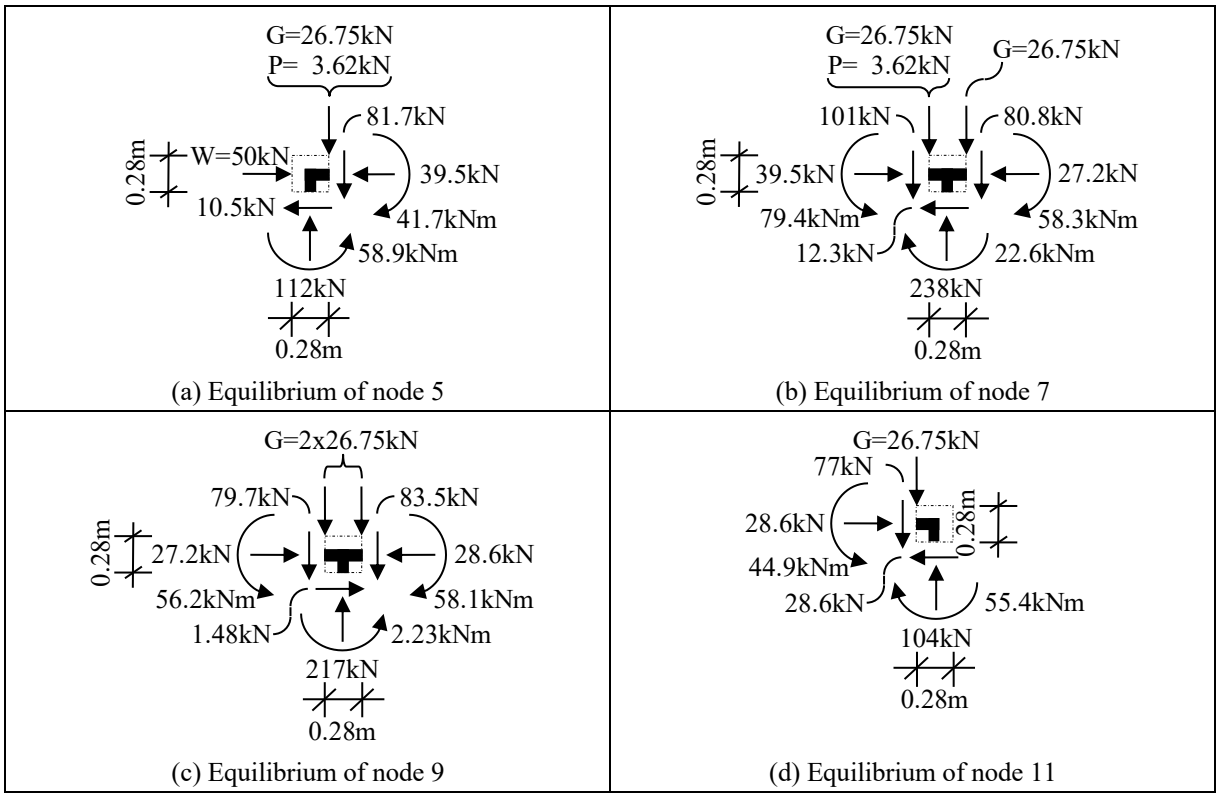

Figure 53: Equilibrium of beam-column joints of the structure at the end of the analysis {units: kN,m}.

The bending moment vs. plastic rotation diagrams of two indicative critical sections of the structure are shown in Figures 54 – 55; as it may be observed, critical section #1 reaches its plastic hardening limit (*see Figure 54*), and critical section #9 exhibits non-holonomic behaviour during its hardening plastic phase (*see Figure 55*).

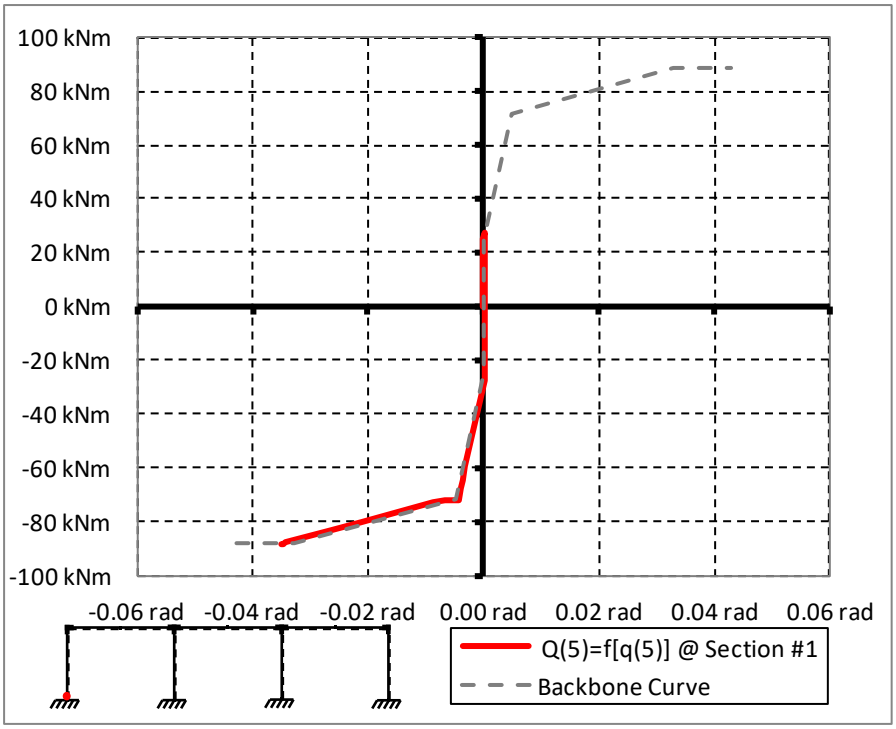

Figure 54: Bending moment vs. plastic rotation diagram of section 1 {units: kNm,rad}.

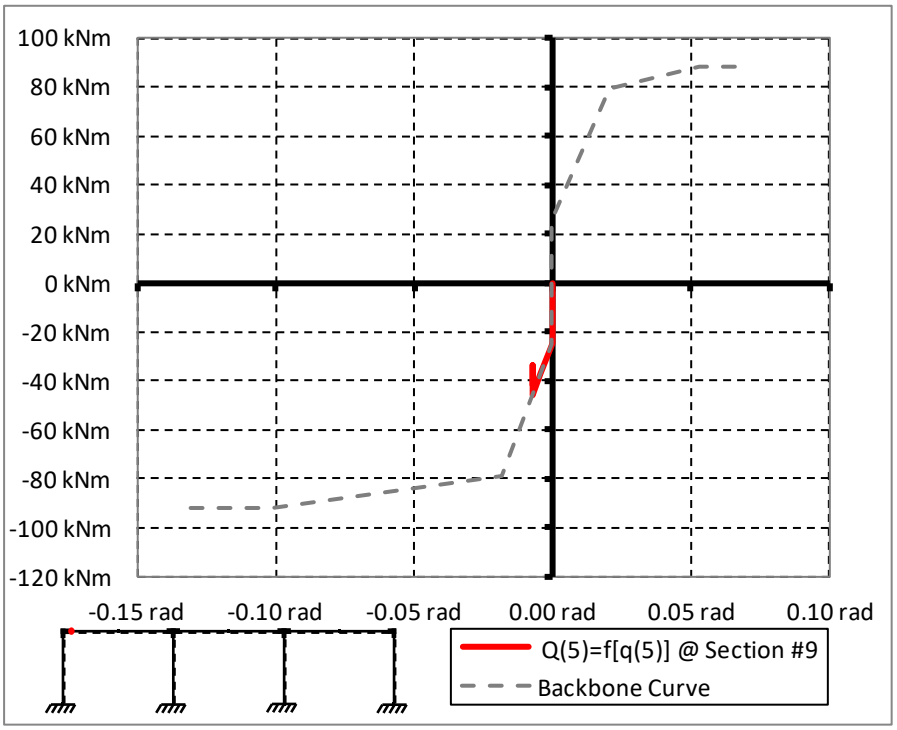

Figure 55: Bending moment vs. plastic rotation diagram of section 9 {units: kNm,rad}.

Finally, with reference to the load definitions in Figure 46, the horizontal load (W) vs. the corresponding horizontal displacement of node 5 may be seen in Figure 56, and the total vertical load (G+P) of node 6 vs. the corresponding vertical displacement in Figure 57.

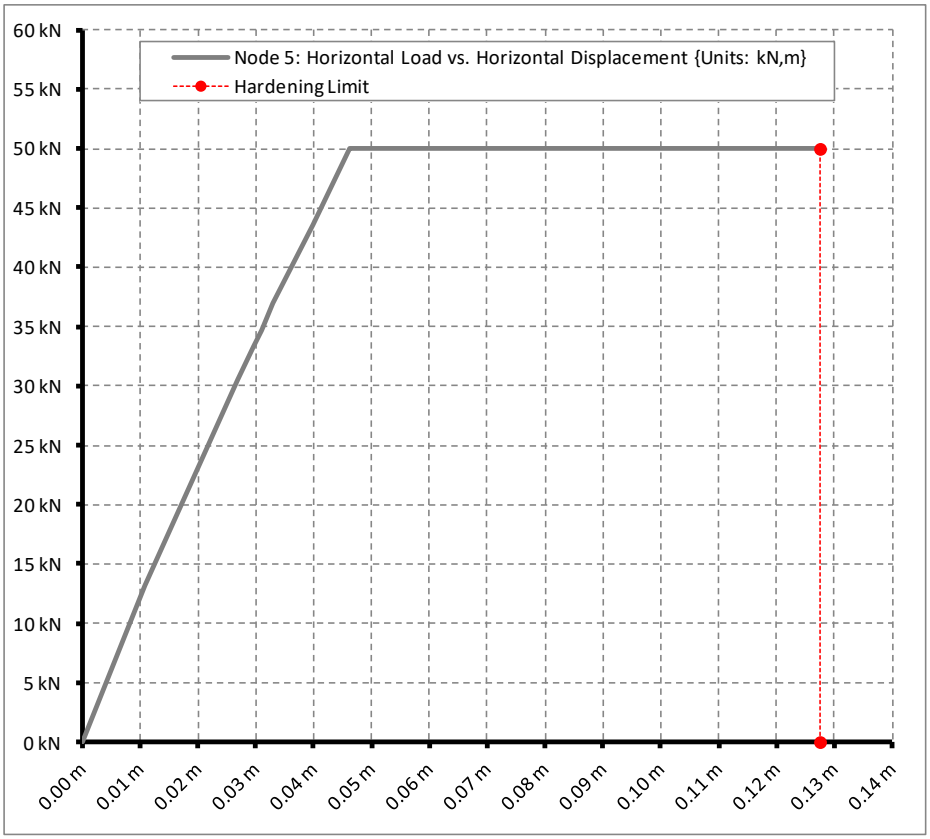

Figure 56: Horizontal load (W) vs. horizontal displacement of node 5 {units: kN,m}.

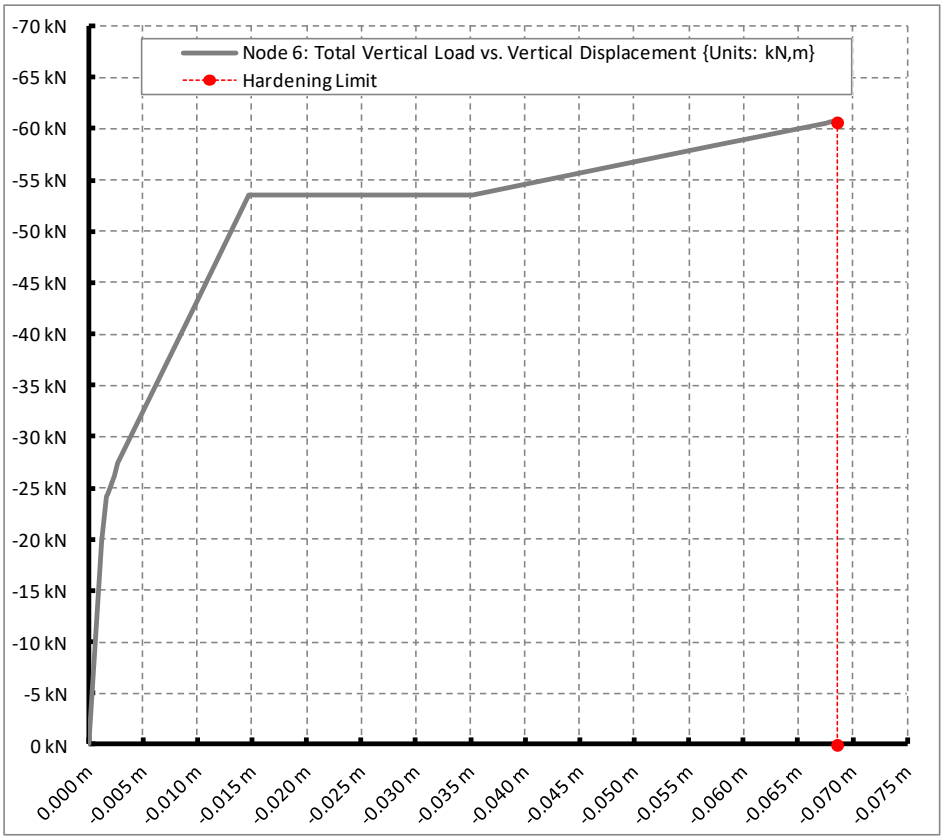

Figure 57: Sum of vertical loads (G+P) vs. vertical displacement of node 6 {units: kN,m}.

13.7 Offshore Jacket (2D)

This example is used to demonstrate the efficiency of the proposed method in computing cyclic loading scenarios. The structural frame's data were taken from [191]; geometry and loading considerations may be seen in Figure 58 below.

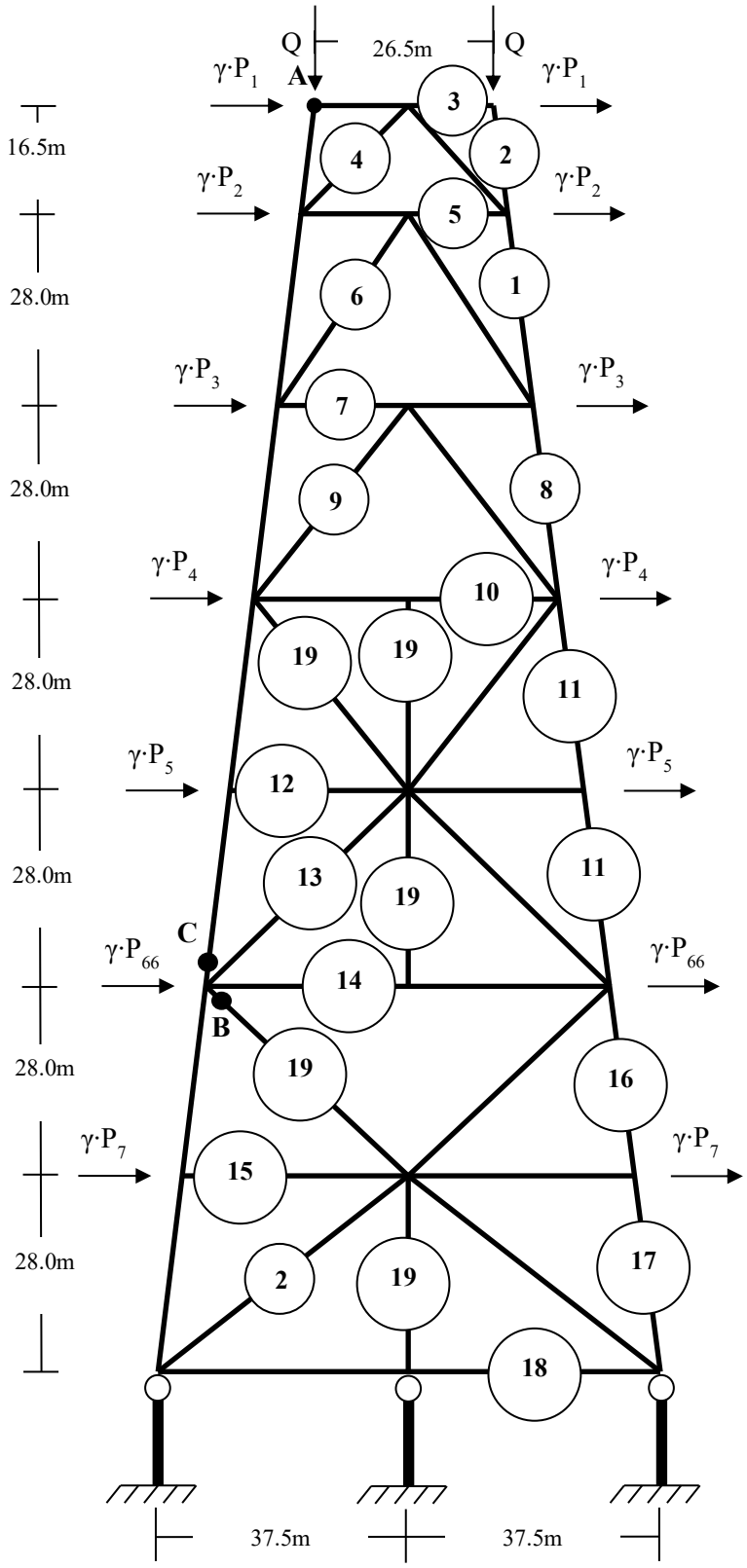

Figure 58: Structure's geometry, member cross-sections with reference to Table 8, loading considerations, reference node A (•) and critical sections B and C (•) {units: kN,m}.

The numbers in circles on each member of the structure in Figure 58 above correspond to the circular tube cross-sections that are listed in the following Table 8; note that the structure is symmetric.

Section	$R_{external}$	$R_{internal}$
1	1.0250 m	0.9750 m
2	0.6640 m	0.6360 m
3	0.3340 m	0.3180 m
4	0.3330 m	0.3170 m
5	0.4675 m	0.4325 m
6	0.6675 m	0.6325 m
7	0.5200 m	0.4800 m
8	1.0275 m	0.9725 m
9	0.6625 m	0.6375 m
10	0.4650 m	0.4350 m
11	1.5225 m	1.4775 m
12	0.4580 m	0.4420 m
13	0.6650 m	0.6350 m
14	0.4640 m	0.4360 m
15	0.4600 m	0.4400 m
16	3.0250 m	2.9750 m
17	3.0225 m	2.9775 m
18	0.5100 m	0.4900 m
19	0.6600 m	0.6400 m

Table 8: External and internal radii of the structure's tubular cross-sections.

The three supporting members in Figure 58 are considered as rigid, i.e. they are members with A=1.0E+08m^2 and I_{33}=1.0E+08m^4, and are assumed ideally elastic.

The structure's material is structural steel with Young's modulus E=2.1E+08kN/m^2, Poisson's Ratio ν=0.3, and yield stress f_y=350000kN/m^2.

The piece-wise linear constitutive law of Table 9 below was adopted, with limited kinematic hardening according to Ziegler's rule; the plastic hinge backbone curve was computed using Equations (38) and (39), and the yield rotations were evaluated using the elastic variant (*S=1*) of the group of Equations (41).

Although the above choice of material modelling is different than the custom hardening coefficients that were used in [191], it is a practically equivalent and easy to implement formulation that is consistent with the stress-coupled approach that is followed throughout this work; note that the strain value may be computed as the sum of the axial elongation normalized with the axial yield elongation and of the bending rotation normalized with the bending yield rotation.

Backbone Curve	
Strain	*Stress*
0.00	0.00
1.00	1.00
6.00	1.25
+∞	1.25

Table 9: Piecewise linear constitutive law (normalized wrt. to the yield strain and stress values, respectively).

All members of the structure are further divided into smaller beam/column finite elements of approximate length ~1.5m each; plasticization is allowed to occur at the ends of all beam/column elements that comprise each deformable member of the structure.

In order to approximate the theoretical parabolic yield function that was adopted in [191] as accurately as possible, a linearization consisting of four segments per quadrant was constructed; see Table 10 below, with reference to Equation (36):

	s_1 (N)	s_2 (M_3)
1	0.1600000000	1.0000000000
2	0.4683544304	0.9493670886
3	0.7464788732	0.8450704225
4	0.9203539823	0.7079646018
5	1.0000000000	0.5714285714

Table 10: Piecewise linear approximation of the theoretical yield function $g(N,M_3)= (N/N_*)^2+(M/M_{3*})-1\leq 0$.

The value of the two constant vertical loads is Q=34335kN, and the nominal values of the horizontal loads are P_1=742kN, P_2=6269kN, P_3=7294kN, P_4=6745kN, P_5=6781kN, P_6=6446kN, and P_7=7222kN (*see Figure 58*).

The scale factor "γ" of the horizontal loads applied to the structure (*see Figure 58*) is proportionally scaled up from value γ=0.0 to γ=+1.0, then down to γ=−0.8 and up to γ=+0.8, so that a cyclic loading scenario is created.

Satisfactory solutions of the problem were acquired using the QP and SQP algorithms implemented by M.J.D. Powell ([68],[70]).

The stress configurations of sections "B" and "C" (*see Figure 58*) for every step of the cyclic loading scenario, as well as the displacements of the respective yield loci due to material hardening, are shown in Figure 59 below.

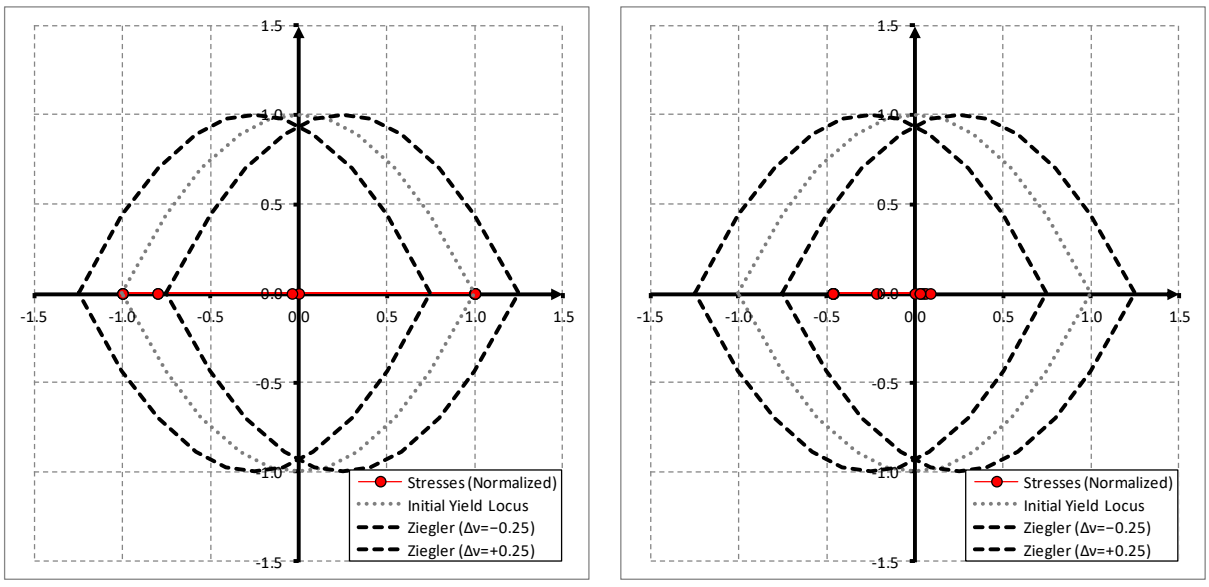

Figure 59: Stress history of section B (left) and of section C (right) {units: normalized values}.

The resulting base shear vs. the horizontal displacement of node "A" (*see Figure 58*) may be seen in Figure 60 below; the peak point's coordinates are $\{u_{max},V_b\}$={1.02m,8.22E+04kN}, which corresponds to the value of the sum of the nominal values of the horizontal loads multiplied with γ~0.99.

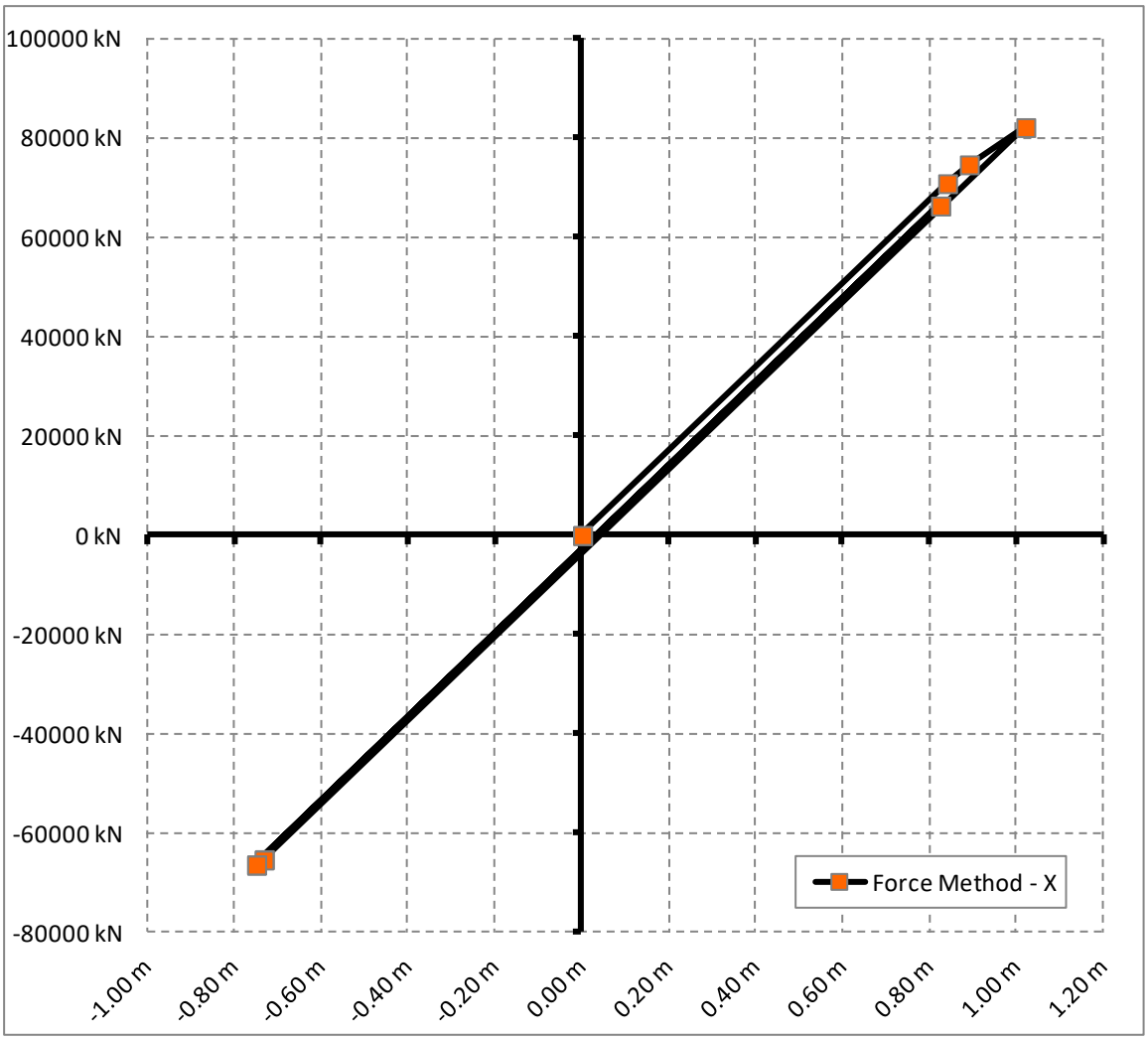

Figure 60: Base shear "Vb" vs. horizontal displacement "u" of the reference node A (•) {units: kN,m}.

Results are in good accordance with those reported in [191].

13.8 Yarimci's Single-Bay, Three-Storey Experimental Frame (2D)

This example is used to demonstrate the efficiency of the proposed method in computing cyclic loading scenarios. The selected structural frame is the specimen of an experiment that was performed by Yarimci and presented in [192]. The experimental data were taken from [193]; they were converted from Imperial to SI units, and then analyzed under the assumption for elastic-perfectly plastic material in [52]. Geometry and loading considerations may be seen in Figure 61 below.

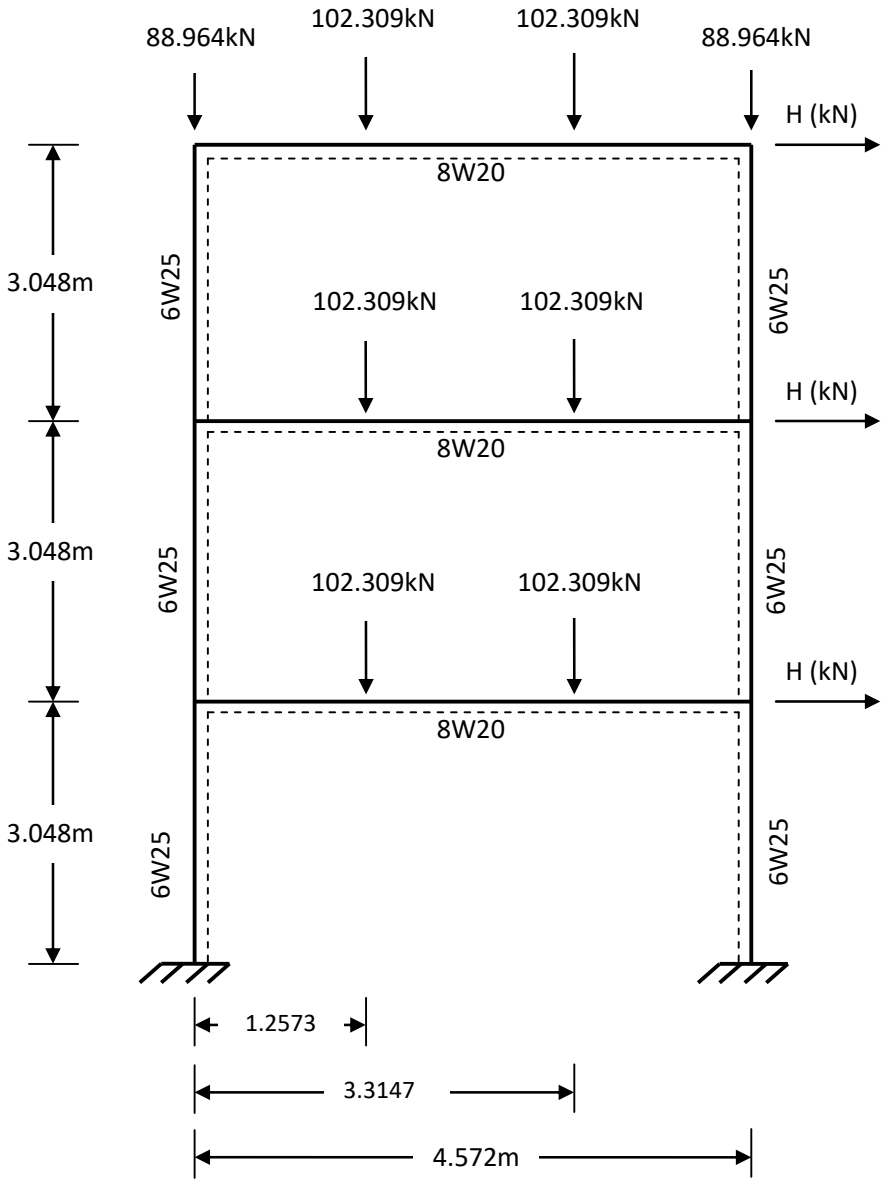

Figure 61: Yarimci's Frame; geometry and loading considerations {units: kN,m}.

Herein, a 1st order analysis was run, under the assumptions for a piece-wise linear constitutive stress-strain backbone curve described in Table 11 (*which corresponds to a limited plastic hardening with a 3% slope*) and a linearized yield function considering bending moment and axial force interaction (*see Table 10 with reference to Equation (36)*); these selections were made in order to achieve a relatively good data fitting. Material was assumed to be structural steel with E=199,947,961.5kPa, f_y=248,211.26kPa; Prager's kinematic hardening rule was adopted.

In order to simulate plasticity in a somewhat satisfactory way, each beam member was divided into three (3) beam finite elements. Material homogeneity and geometrical perfection was assumed for the whole model. Results are summarized in Figure 62.

Backbone Curve	
Strain	*Stress*
0.00	0.00
1.00	1.00
10.00	1.27
$+\infty$	1.27

Table 11: Piecewise linear constitutive law (normalized wrt. to the yield strain and stress values, respectively).

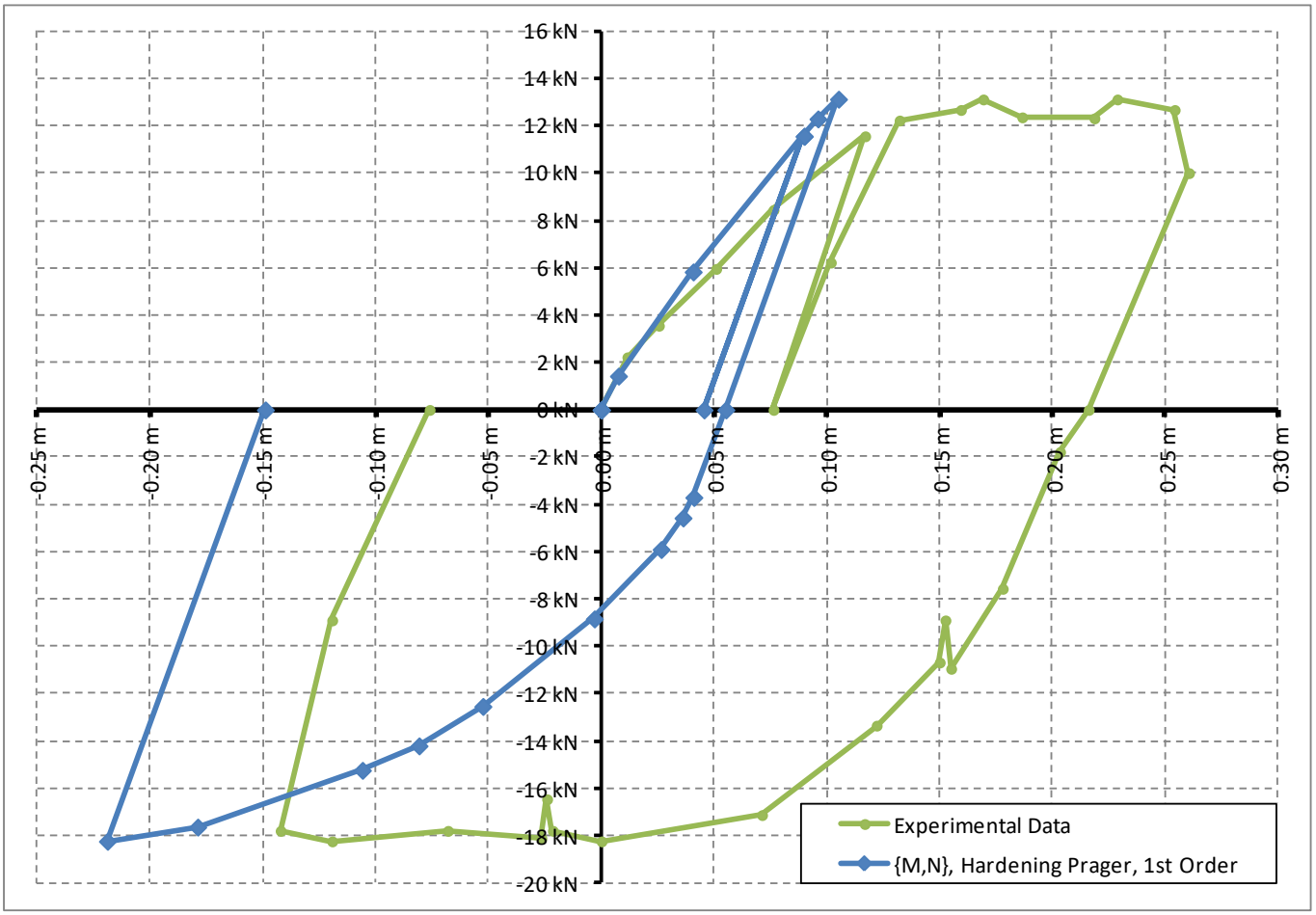

Figure 62: Horizontal load "H" vs. corresponding displacement "u" of the frame's top-right node {units: kN,m}.

The resulting solution provides a statically admissible load-displacement curve, where, despite the $\{N,M_3\}$ stress coupling, material non-holonomic behaviour is efficiently accommodated.

Since the herein implemented analysis method is load-controlled, it is difficult to acquire the displacements that a displacement-controlled experiment yields. A numerical investigation for each member of the modelled experimental structure regarding the actual variance of the material's mechanical properties (E, f_y) as well as of the backbone curve of each one of the plastic hinges, could lead to an improved computation of the displacements· however, this is beyond the scope of the present thesis.

13.9 Asymmetrically Loaded Steel Grillage (3D)

This example is a steel grillage that has also been analysed by R.R. Wakefield and F. Tin-Loi in [120]. The 3D view of the geometry and loading considerations of the structure may be seen in Figure 63 below:

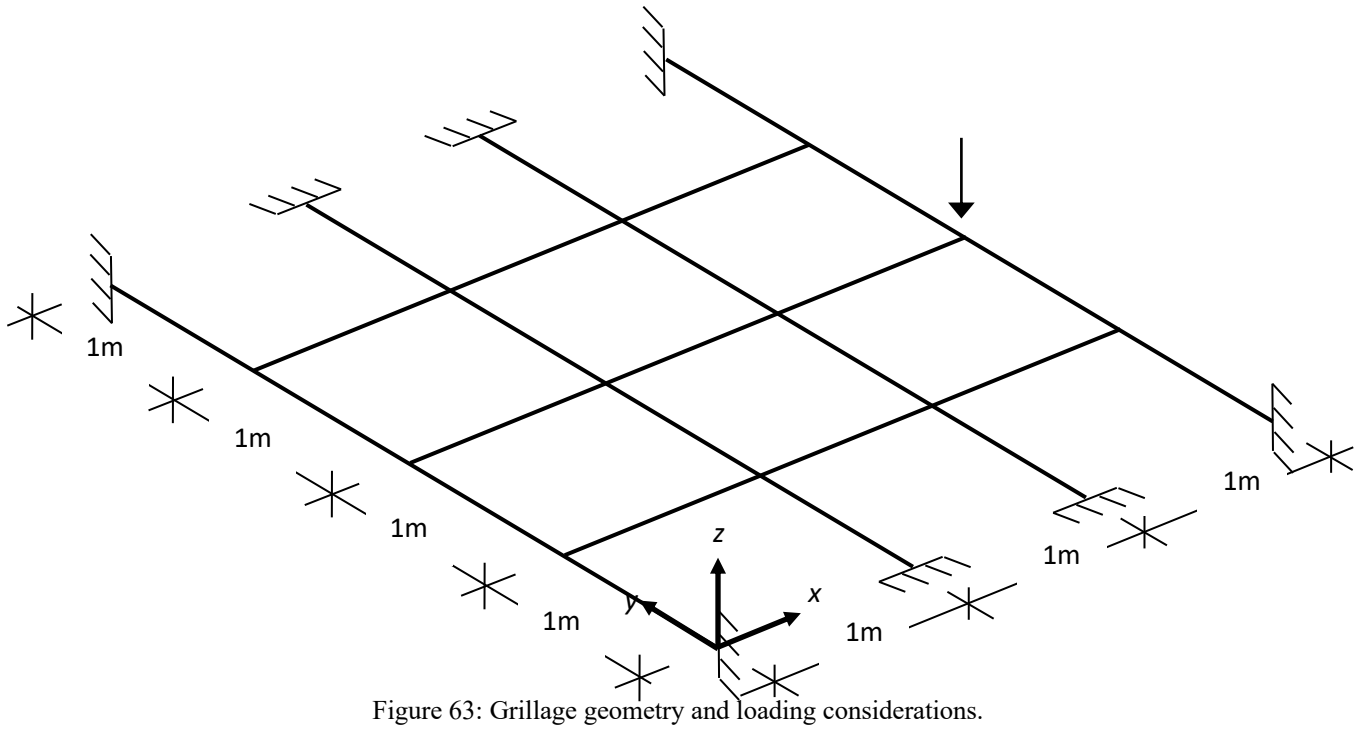

Figure 63: Grillage geometry and loading considerations.

The cross-section of all members is of type RHS {B=105mm, H=102mm, t_w=9.5mm}, and they have been set so that their strong bending axis (#3) is always located within the {x,y} plane. The material is S350 with an effective yield stress f_y=304347.8 kPa (*a safety factor γ_s=1.15 was adopted*), and is assumed to be elastic-perfectly plastic.

All members of the structure are assumed to yield under combined biaxial bending {M_2,M_3} and torsion {T}. The theoretical spherical yield surface is approximated by linear polyhedra. An approximation of 8 hyper-planes was made (*1 hyper-plane in each hyper-cube, as is also in* [120]); this linear polyhedron is triply symmetrical with reference to the {M_2,M_3}, {T,M_2} and {T,M_3} planes.

The single vertical concentrated load that is applied on the grillage is incrementally increased until the state of collapse is reached. The load vs. the corresponding displacement values are plotted in Figure 64 below:

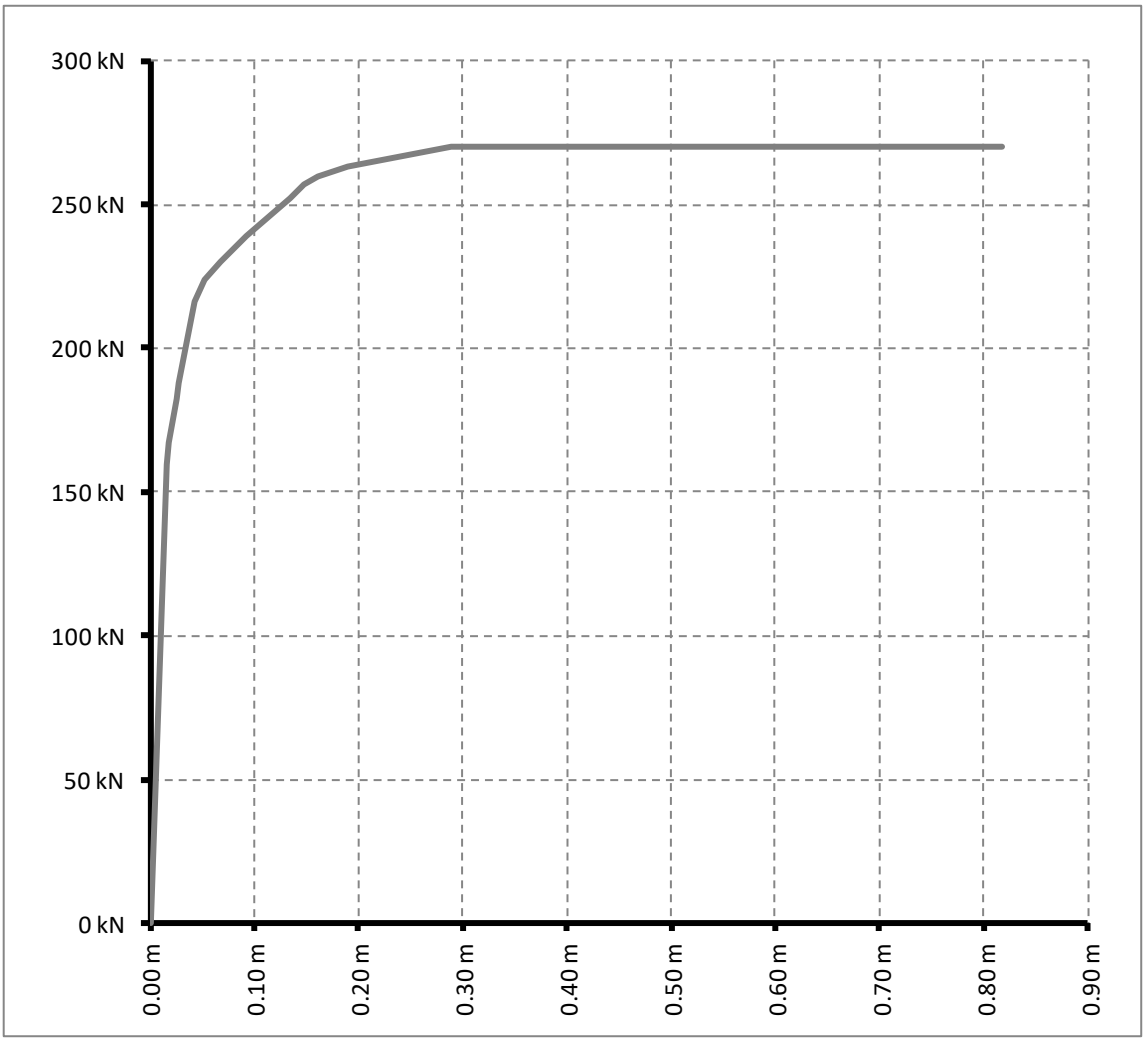

Figure 64: Load vs. corresponding displacement curve of the loaded node {units: kN,m}.

As it may easily be observed, the computed collapse load (~270kN) is close to the reference value (262.27kN) reported in [120]; the results are in agreement within a (~3%) accuracy.

13.10 Ten-Storey, Three-Bay, Steel Frame (3D)

This example is used to demonstrate the efficiency of the proposed method in analyzing structural frames of relatively large scale. The geometrical and loading considerations may be seen in Figure 65 below. Each span has a length/width of 6m, and each storey a height of 3m. Beam sections are HEM180 and column sections are HEM400. Each beam receives a uniformly distributed vertical load with direction ($-\vec{z}$) and a magnitude of 15kN/m; all beams have been placed so that they bear the vertical loads by bending around their strong axis (#3). The columns have been placed so that half of them bend around their strong axis and half of them around their weak axis. The lateral loading is applied along the direction ($+\vec{x}$) of the global coordinate system, where "γ" is the lateral load pattern's scale factor.

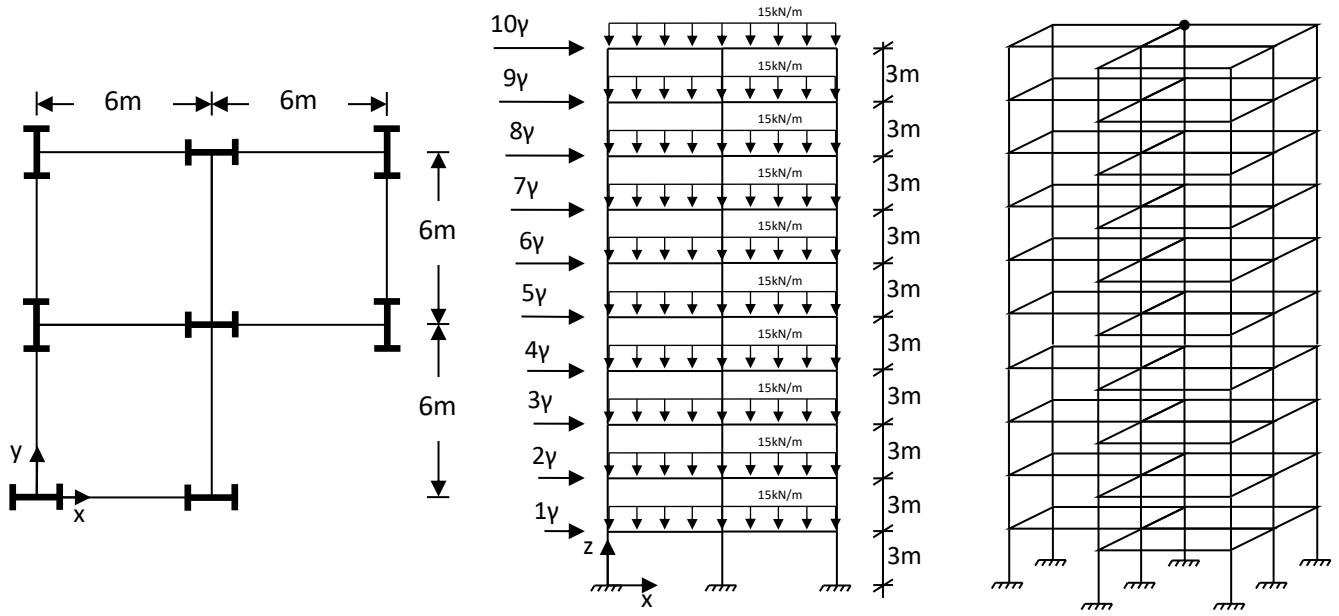

Figure 65: Structure's plan and side views, column sections' orientations, loading considerations, 3D wireframe schematic, and reference node (•) {units: kN,m}.

The material is S235 with a Young's modulus E=2.0E+08 kN/m^2, Poisson's ratio ν=0.3, and a conventional yield stress f_y=235000 kN/m^2; the symmetric backbone curve of Table 6 was defined for modelling the post-elastic behaviour.

A biaxial moment {M_2,M_3} linearized interaction surface was adopted for all beams, and the AISC-LRFD biaxial moment and axial force {N,M_2,M_3} interaction criterion for all columns. For computing the yield displacements/rotations, the elastic form (S=1) of the group of Equations (41) was used, wherein L=6m was set for the beams and L=3m for the columns. Drucker's hardening rule was adopted.

A series of pushover analyses were run using the force-based program written within the context of this work: a 1st order analysis was run using the QP [68] solver, and two 2nd order analyses were run using the SQP [70] and IPM [194] solvers, respectively. Two comparative analyses were also run; one using SAP2000 [178] for 1st order analysis, and one using the 900 node version 9.3 of ADINA for 2nd order analysis.

For 2nd order analysis, and in order to comply with the 900 node limit of ADINA, all columns of the structure and the beams that are parallel to the x-direction were divided into six finite elements, and the beams along the y-direction were divided into three elements; note that for 1st order analysis, no element subdivision was applied to the columns.

Furthermore, the moment-curvature piece-wise linear curves had to be supplied as input to the ADINA software due to the stress-decoupled implementation of the stress interaction feature of the program; these may be seen in Figure 66 and Figure 67 below for the strong and weak axes of a HEM180 section and in Figure 68 and Figure 69 for the strong and weak axes of a HEM400 section, respectively; the flexibility modulus for each moment-curvature diagram was computed using the elastic variant ($S=I$) of Equations (41), where in L=3m was set for all HEM400 and L=6m for all HEM180 sections, respectively. Note that the contribution of torsion was neglected by giving large yield values as input curves.

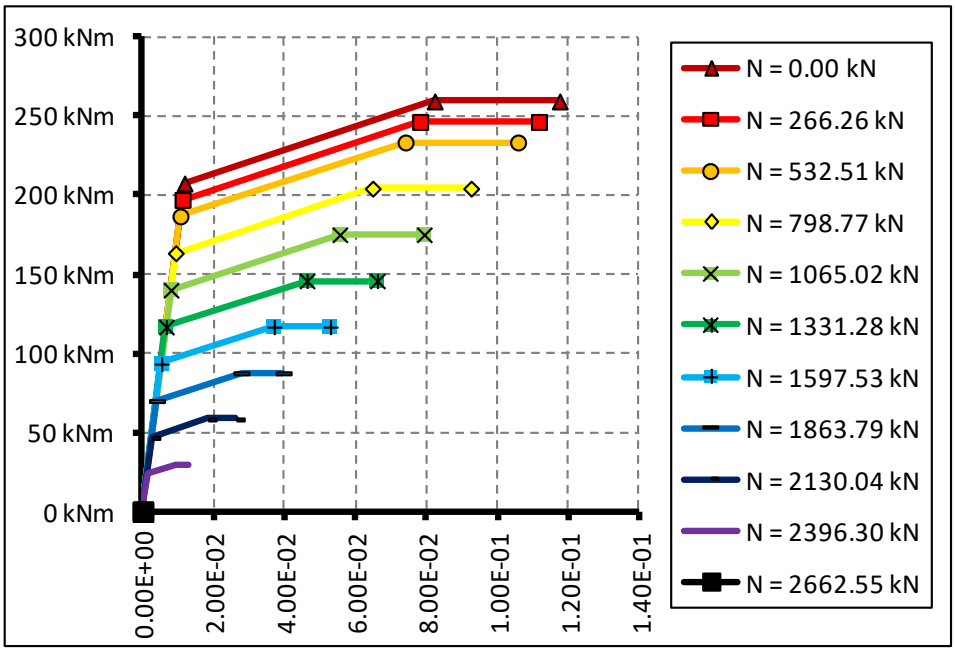

Figure 66: Moment-Curvature curves for HEM180 sections – strong axis {units: kN,m,rad}.

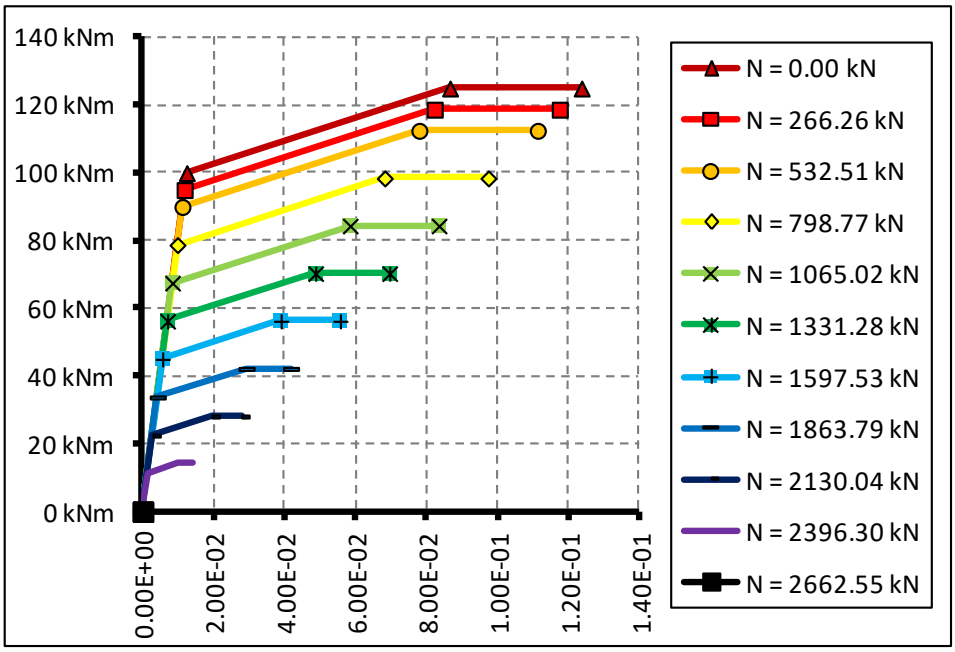

Figure 67: Moment-Curvature curves for HEM180 sections – weak axis {units: kN,m,rad}.

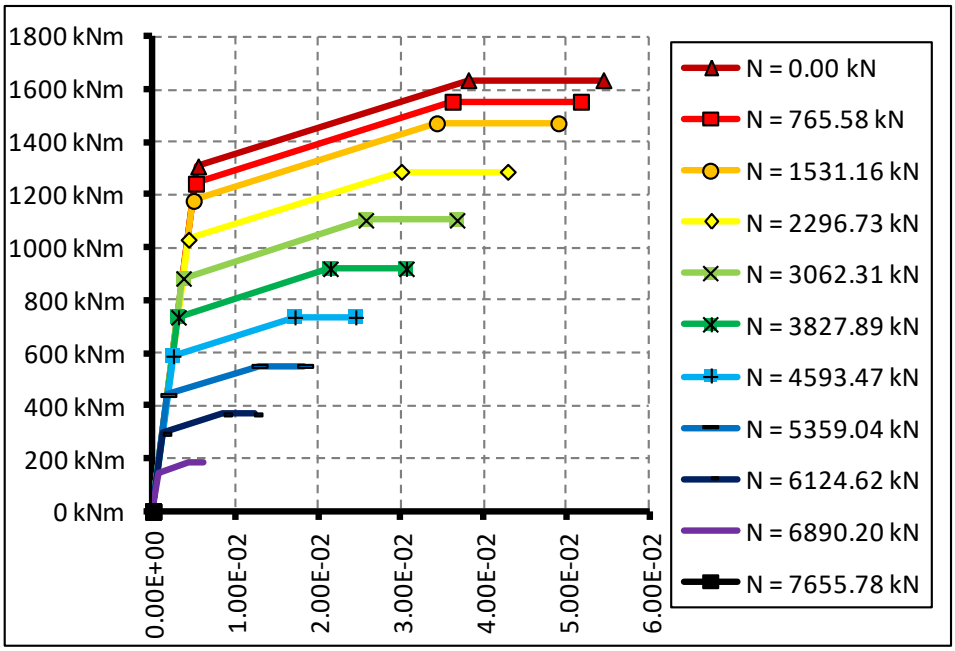

Figure 68: Moment-Curvature curves for HEM400 sections – strong axis {units: kN,m,rad}.

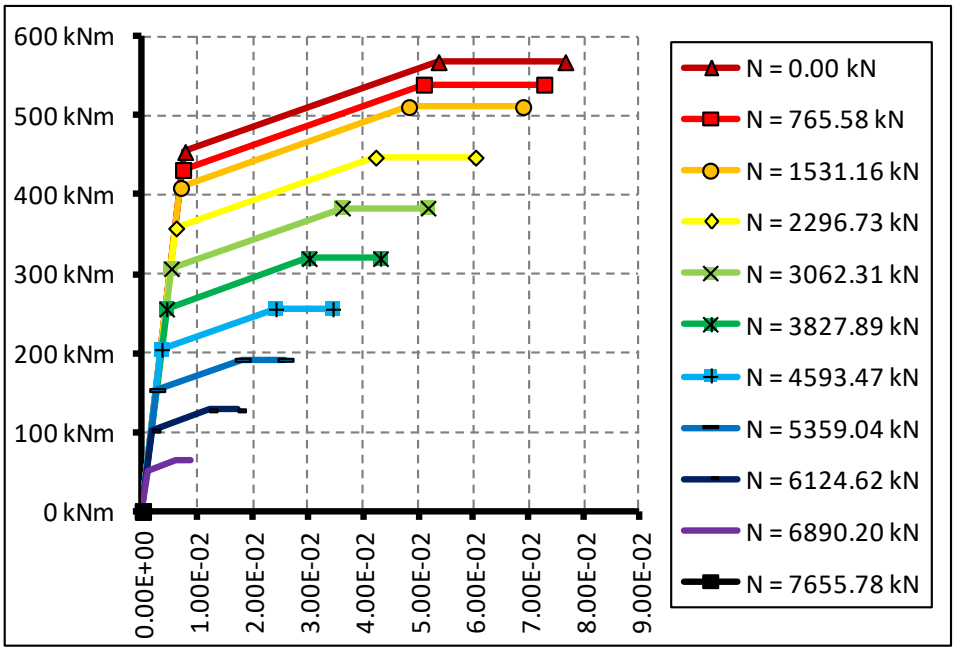

Figure 69: Moment-Curvature curves for HEM400 sections – weak axis {units: kN,m,rad}.

The resulting base shear vs. roof displacement curves may be seen in Figure 70 below. As it may be observed, results are in relatively good accordance.

For 1st order analysis, the proposed method yields a collapse load that is ~5% less than that reported by SAP2000; this difference is to be attributed to the coarser meshing of the structural model that was given to SAP2000 as input, as compared to the denser model that was computed using the herein proposed method.

For 2nd order analysis, the proposed method yields a collapse load that is ~1.5% less than that of ADINA; this difference is to be primarily attributed to the differing plastic hinge assumptions between the two programmes: ADINA works with stress decoupling, while the proposed method works with stress coupling.

The herein implemented stress coupling assumes that the value of the yield function represents the evolution of the normal stresses along the height of a critical section; although this plastic hinge approach is simple to implement and produces statically admissible stress configuration states, it is unable to produce acceptable diagrams of "M=*f*(θ)" (*bending moment vs. plastic rotation*) or "N=*f*(δ)" (*axial force vs. plastic elongation/compression*): In this example, moment redistribution between the two bending directions was observed as the lateral loads were proportionally increased; in particular, the least loaded bending direction would unload itself while simultaneously develop further plastic rotation. This phenomenon has no effect in the bearing capacity curve of the whole structure.

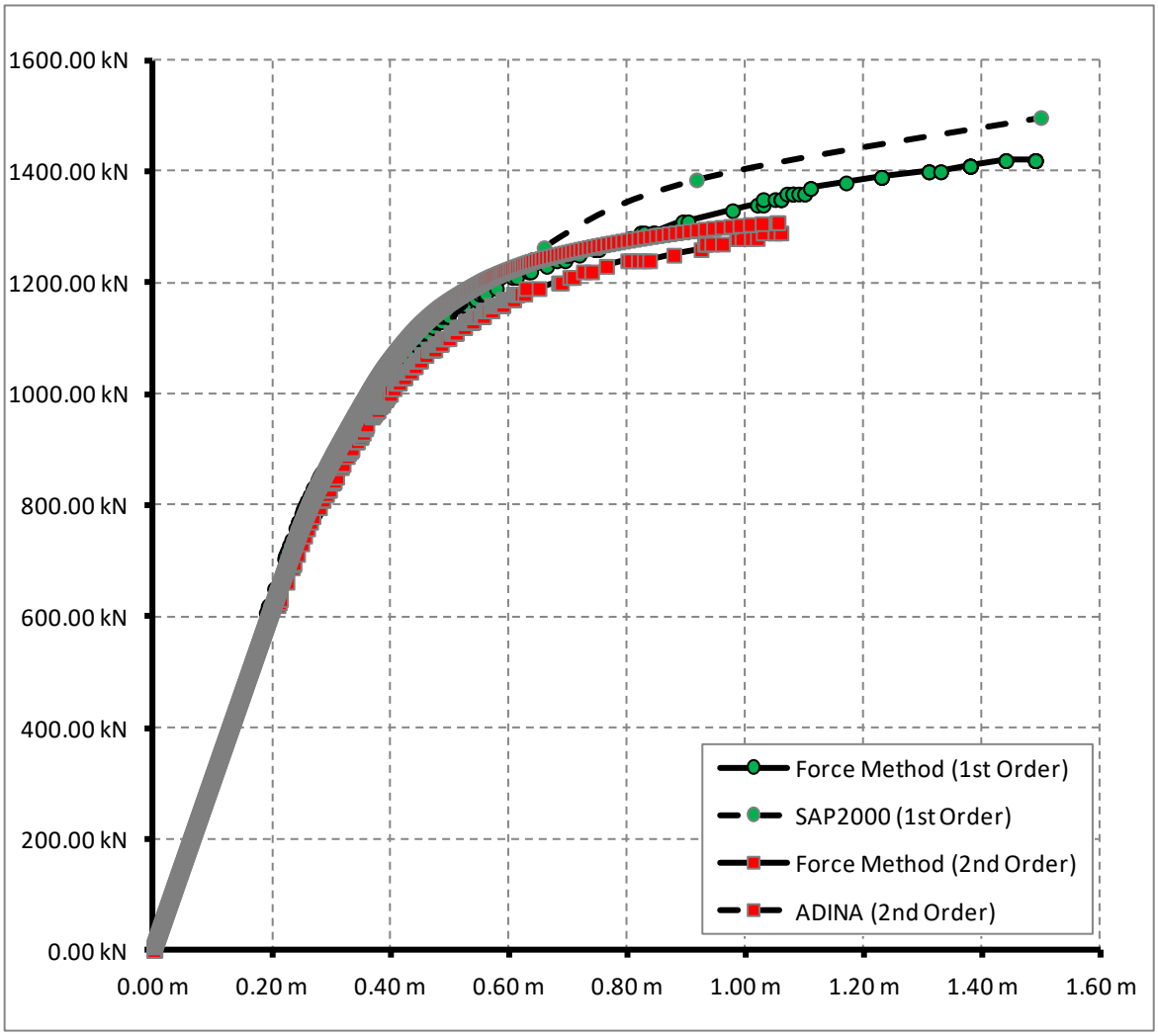

Figure 70: Base Shear vs. Roof Displacement of the reference node (•) {units: kN,m}.

The inclusion of a solver suitable for sparse matrices [194] resulted in an approximate 45% reduction of the CPU time as compared to the solver using full rank matrices [70]. However, it should be noted that, when running large scale examples, the super-linear convergence rate of the optimization algorithms is not competitive to the quadratic rate of the Newton-Raphson method.

Furthermore, the inclusion of non-holonomic hardening plastic behaviour in the force-based approach has an additional computational toll, since, for the satisfaction of Drucker`s Postulate at every step, a maximum of two solver calls may often be required, especially in large-scale examples.

14 Concluding Remarks

A simple to implement, fully automated, purely force-based approach to the step-by-step analysis of 2D/3D inelastic structural steel and reinforced concrete frames with non-holonomic hardening plastic hinges is presented for the first time in the literature.

14.1 Advantages of the Proposed Method

The method is simple to implement, mainly due to the fact that the force-based approach is intuitively understandable; the symbolic form of the constitutive equations is characterized by its' mathematical elegance plus it is easily linked to the physical problem which they represent.

A number of different and complex yield functions are included in the formulation. As it was demonstrated, bi-axial bending moment alone or combined with axial force interaction or torsion, as well as the effect of shear, are all natively and efficiently accommodated by the proposed mathematical formalism; only properly linearized yield functions that suit the expected failure types of the respective parts of the structure need be selected.

Non-holonomic plasticity is taken into account by following a stepwise holonomic approach that is contained into the proposed numerical strategy via a simple remedy; the proposed method is formulated on the basis of satisfying Drucker's postulate, thus it is closer to the physical problem where plastic deformations are irreversible.

Another advantage that arises from the usage of optimization algorithms is that the bounds of the yield function of each critical section are always satisfied; no return to the yield surface is required, as it would be the case when working with the direct stiffness method.

The proposed numerical method requires only a few parameters for tuning; it has good convergence properties which are independent of the mesh density of the structural system, and yields good results even for large scale problems. Implementation using an IPM solver suitable for sparse matrices [194] yielded approximately a 45% reduction of CPU time as compared to the SQP solver [70].

14.2 Disadvantages of the Proposed Method

It is known that the linear/super-linear convergence rate of optimization algorithms is not competitive to the quadratic rate of algorithms which are based on the Newton-Raphson method.

Furthermore, it was found that, for large scale examples, the cycling of the optimization algorithms through the active set, which is required in order to properly accommodate non-holonomic material behaviour, results in increased computational times; in the case of non-holonomic material hardening, a maximum of two calls to the solver may often be required within the same incremental step, meaning that a reformulation of the Hessian matrix of the problem is also required. In the latter case, a re-decomposition of the Hessian may also be necessary, depending on the solver being used.

When performing inelastic analysis with 2^{nd} order effects using an SQP algorithm, the Broyden-Fletcher-Goldfarb-Shanno (BFGS) formula for the quadratic approximation of the non-linear Hessian follows the descending direction of the locally convex problem. Moreover, all optimization algorithms that were used in this work determine a solution under the prerequisite for marginally fulfilling the problem's constraints. From a statics point of view, these solvers assume that sufficient structural stability exists so that the plastic hinges reach their plasticization phase prior to the occurrence of any instability phenomena (*e.g. buckling within the elastic region*); therefore, phenomena such as local buckling of beam/column members and the post-buckling behaviour of structures could not be determined.

It is known that load-controlled numerical strategies are unable to efficiently trace the post-buckling equilibrium path of structures.

The herein proposed automation techniques for the computation of the equilibrium matrices due to statical indeterminacy (*redundant components*) may not always yield a minimal, but a near-minimal cycle basis; this leads to a set of global flexibility matrices [$\mathbf{B}_i^T \cdot \mathbf{F} \cdot \mathbf{B}_j$] (*where {i,j}={0,1},{1,0}{1,1}*) with more elements than the minimum possible ones.

Furthermore, in the case of modelling statically indeterminate structures with internal discontinuities, the herein proposed Lagrange multiplier automation technique does not reduce the number of redundant components accordingly, meaning that a partially discontinuous structure is always assumed to have the same number of redundant components as its' geometrically equivalent fully continuous one.

15 Acknowledgements

If you managed to read this far without falling asleep on the way, then a true Jedi [195] of patience, you are· may the Force [196] be with you!

Good family and personal life environments, as well as good educators, are crucial for setting the foundations in order to grow and evolve; they can be of great help for the noble goal of continuously improving oneself through the journey of life.

Above all, I am thankful to my family: without their emotional and financial support, all educational efforts of mine would have never officially reached a mentionable milestone.

I am also thankful to my supervisor, for he encouraged me to start this doctoral work; this Ph.D. ended up proving itself to be a fortunate stroke of serendipity: by trying to devise and program an unconventional computational procedure from scratch, I got to develop –through hard personal work– some quite worthy skills regarding not only numerical analysis and the (*modern*) ForTran language, but also computer coding in general.

The first results of the herein presented research were for planar (2D) structural frames, and were partially funded from the Special Account for Research Grants (ΕΛΚΕ) of the NTUA; their support is kindly acknowledged.

Finally, I am also thankful for all the obstacles I met along the road I chose to walk; I got to learn valuable lessons by working on how to overcome them.

16 Appendix I – A short User Manual for the Programme

The programme that was authored for this work runs in a command prompt window; due to the excessive work load (*all coding was done from scratch*) the inclusion of a graphical user interface (GUI) was left out of the project.

16.1 Structure of the Input Files

The whole implementation of the input file's format was done with simplicity and easiness of typing in the data in mind; all programming efforts focused on achieving a rather self-explanatory type of syntax. The input file's structure is divided into 18 sections; each one of them is abstractly presented below:

1. Introductory line:
   a. Input Filename (Name) | Space (2D/3D) | Structure's Type (Frame)
2. Nodes' Definitions:
   a. Number of Nodes
   b. Node Number | Coordinates (x,y,z) | Condition (Boundary/Loaded/Free)
3. Beam Members' Definitions:
   a. Number of Members
   b. Member Number | Start/End Nodes | Eccentricities | Strong/Weak Axis Rotation Angle | Internal Boundary Conditions | Number/Length of Internal Finite Element(s) | Status (Loaded/Free)
4. Boundary Conditions' Definitions
   a. Number of Boundary Conditions
   b. Boundary Condition Name | Displacements & Rotations (u_x,u_y,u_z,φ_x,φ_y,φ_z)
5. Boundary Condition Assignments
   a. Number of Assignments
   b. Node Number(s) => Boundary Condition Name
6. Point Loads' Definitions
   a. Number of Point Loads
   b. Load Name | Load Type | Forces & Moments (F_x,F_y,F_z,M_x,M_y,M_z)
7. Point Load Assignments
   a. Number of Assignments
   b. Node Number(s) => Point Load Name
8. Distributed Loads' Definitions
   a. Number of Distributed Loads
   b. Load Name | Load Type | Distribution Type | Distribution Specifics
9. Distributed Load Assignments
   a. Number of Assignments
   b. Member Number(s) => Distributed Load Name
10. Materials' Definitions
    a. Number of Distributed Loads
    b. Type | Name | Mass per Unit Volume | Gravity Acceleration | Elasticity Modulus | Poisson's Ratio | Yield Stress Values | Ultimate Stress Values | Constitutive Law Type/Name | Plastic Hardening Rule
    c. Specifics (Linearized Stress vs. Strain Backbone Curve) – for Custom Constitutive Laws only
11. Material Assignments
    a. Number of Assignments
    b. Member Number(s) => Material Name

12. Cross-Section Definitions
    a. Number of Cross-Sections
    b. Type | Shape | Name | Shape Specifics (B,H,t_f,t_w,etc)
13. Cross-Section Assignments
    a. Number of Assignments
    b. Member Number(s) => Cross-Section Name
14. Yield Functions' Definitions
    a. Number of Yield Functions
    b. Yield Function's Name | List of Interacting Components
15. Yield Function Assignments
    a. Number of Assignments
    b. Member Number(s) => Yield Function's Name
16. Analysis Parameters
    a. P-Δ Effects (yes/no)
    b. Displacements (small/large)
    c. Solver Selection (QPROG/LCONG/MOSEK)
    d. Analysis Type (Limit/Pushover/Scenario/Cyclic)
    e. Load Combination
    f. Number of Steps
    g. Arc-Length
    h. Analysis Specifics
17. Plastic Hinge Parameters
    a. Plastic Barriers (on/off)
    b. Intermediate Hinges within Beam Members (yes/no)
    c. Compatibility Mode for Yield Rotations (None/SAP2000)
18. Printout Parameters for Local Components (Stresses vs. Deformations)
    a. Auto/Full/Custom
    b. Printout Specifics – for "Custom" defined parameters only

A detailed explanation of the respective input data format and internal functions/command declarations has been included in section 16.2 of this Appendix; comments above or next to each line are included in order to clarify assumptions of the defined syntax as well as features of the program itself. In section 16.3, an input file for a simple portal frame is provided as a practical example.

Note that, usage of capital letters in the input files is not a prerequisite; it was only left as a tribute to the old days of the very alpha version of the program that did not contain character string data reading and manipulation functions (lol).

16.2 Explanation of the Input Files' Syntax

```
*****************************************************************Beginning of Input File*****************************************************************

+-----------------------+-----------------+----------------+
|   STRUCTURE`S NAME    |  SPACE (2D/3D)  |STRUCTURE`S TYPE|
+-----------------------+-----------------+----------------+
 INPUT_FILE_v.2.8.0_3D          3D              FRAME
 ===================================================
+-----------------+
|NUMBER OF NODES:| 4
+-----------------+
  +------+------+------+------+-----------+
  |      |                    |NODE TYPE; |
  |      |                    |B=BOUNDARY,|
  |NODE'S| NODE'S COORDINATES |L=LOADED,  |
  |NUMBER|  X      Y      Z   |F=FREE     |
  +------+------+------+------+-----------+
      1     0.00   0.00   0.00  B
      2     0.00   0.00   3.00  L
      3     6.00   0.00   3.00  F
      4     6.00   0.00   0.00  B
+------------------+
|NUMBER OF MEMBERS:| 3
+------------------+
  +------+-----+-----+-----------------+------------------+------------------+--+--+--+--+--+--+--+--+--+--+--+--+-----------+-----------+
  |      |           |    GLOBAL NODAL ECCENTRICITIES    |SECTION`S ROTATION|  INTERNAL BOUNDARY CONDITIONS;    |NUMBER (N) | MEMBER`S  |
  |      |           |                                    |      AROUND      |                                    |OR LENGTH  |  STATUS   |
  |MEMBER|START END  | START OF MEMBER |  END OF MEMBER  |  LOCAL AXIS (1)  | START OF MEMBER |  END OF MEMBER  |(L) OF BEAM| L=LOADED  |
  |NUMBER|NODE  NODE | Ex1   Ey1   Ez1 | Ex2   Ey2   Ez2 | (degres/radians) |Q1 Q2 Q3 M1 M2 M3|Q1 Q2 Q3 M1 M2 M3|ELEMENTS   | F=FREE    |
  +------+-----+-----+-----+-----+-----+-----+-----+-----+------------------+--+--+--+--+--+--+--+--+--+--+--+--+-----------+-----------+
     1      1     2   +0.00 +0.00 +0.10 +0.00 +0.00 -0.10      0.00000 rad    1  1  1  1  1  0  1  1  1  1  1  1  N= 3/L=1.0     F
     2      2     3   +0.10 +0.00 +0.00 -0.10 +0.00 +0.00    -90.00000 deg    1  1  1  1  1  1  1  1  1  1  1  1  N=10/L=0.6     L
     3      3     4   +0.00 +0.00 -0.10 +0.00 +0.00 +0.10   +180.00000 deg    1  1  1  1  1  1  1  1  1  1  1  0  N= 3/L=1.0     F
+-----------------------------------------+
|NUMBER OF DIFFERENT BOUNDARY CONDITIONS:| 1
+-----------------------------------------+
  +---------+-+-----+-----+-----+-----+-----+-----+
  |BOUNDARY | | IMPOSED           | IMPOSED         |
  |CONDITION| | BOUNDARY          | BOUNDARY        |
  |NAME     | | DISPLACEMENTS;    | ROTATIONS;      |
  |         | | Ux    Uy    Uz    | Rx    Ry    Rz  |
  +---------+-+-----+-----+-----+-----+-----+-----+
    B_COND_1 :  0.0   0.0   0.0   0.0   0.0   0.0
+------------------------------------------------+
|TOTAL NUMBER OF BOUNDARY CONDITION ASSIGNMENTS:| 1
+------------------------------------------------+
  +-----------------------------------------------------------+
  | ASSIGNING BOUNDARY CONDITIONS TO THE BOUNDARY NODES... |
  +---------------+-----------------------------------------+
  |    NODE...    |BOUNDARY CONDITION ASSIGNMENTS (BY NAME)|
  | NUMBERS/RANGE |[NOTE: ONLY ONE (1) CONDITION PER NODE!]|
  +---------------+-----------------------------------------+
        1,4      =>              B_COND_1
```

|NUMBER OF DIFFERENT POINT LOAD TYPES:| 2

LOAD NAME	LOAD TYPE: E=EARTHQUAKE, G=GRAVITY, Q=MOBILE, S=SNOW, W=WIND	FORCES F(x)	F(y)	F(z)	MOMENTS M(x)	M(y)	M(z)
P_LOAD_1	E	+1.00	0.00	0.00	0.00	0.00	0.00
P_LOAD_2	Q	0.00	0.00	-5.00	0.00	0.00	0.00

|TOTAL NUMBER OF POINT LOAD ASSIGNMENTS:| 1

ASSIGNING LOADS TO THE LOADED NODES...

NODE... NUMBERS/RANGE	LOAD ASSIGNMENTS (BY LOAD NAME) [NOTE: MUST BE COMMA SEPARATED!]
2	=> P_LOAD_1 , P_LOAD_2

|NUMBER OF DIFFERENT DISTRIBUTED LOAD TYPES:| 4

LOAD NAME	KIND : E=EARTHQUAKE, G=GRAVITY, Q=MOBILE, S=SNOW, W=WIND	DISTRIBUTION: U=UNIFORM, T=TRAPEZOID, D=DISCRETE	NUMBER OF LOADS	LOAD DISTANCE FROM THE START OF THE MEMBER, AS A PERCENTAGE OF THE MEMBER`S LENGTH. [NODAL ECCENTRICITY INCLUDED]	FORCE & MOMENT VALUES PER UNIT LENGTH OF THE MEMBER (ONLY FOR "Q","S","W" LOADS; "G" AND "E" LOADS ARE AUTOMATICALLY COMPUTED!) (START) F(x)	F(y)	F(z)	M(x)	M(y)	M(z)	(END) F(x)	F(y)	F(z)	M(x)	M(y)	M(z)	
D_LOAD_1	G	U			0.00	0.00	-2.50	0.00	0.00	0.00							(for "U", end=start values, thus omitted)
D_LOAD_2	Q	T			0.00	0.00	-3.00	0.00	0.00	0.00	0.00	0.00	-6.00	0.00	0.00	0.00	
D_LOAD_3	Q	D	2														
				0.33	0.00	0.00	-0.70	0.00	0.00	0.00							(for "D", end=start values, thus omitted)
				0.66	0.00	0.00	-1.30	0.00	0.00	0.00							(for "D", end=start values, thus omitted)
D_LOAD_4	Q	U			0.00	0.00	-5.00	0.00	0.00	0.00							(for "U", end=start values, thus omitted)

|TOTAL NUMBER OF DISTRIBUTED LOAD ASSIGNMENTS:| 1

ASSIGNING LOADS TO THE LOADED MEMBERS...

MEMBER... NUMBERS/RANGE	LOAD ASSIGNMENTS (BY LOAD NAME) [NOTE: MUST BE COMMA SEPARATED!]
2	=> D_LOAD_1 , D_LOAD_4

+--------------------+
|NUMBER OF MATERIALS:| 4
+--------------------+

MATERIAL'S TYPE	MATERIAL'S NAME	MASS PER UNIT VOLUME	GRAVITATIONAL ACCELERATION	(E) YOUNG'S MODULUS	(v) POISSON`S RATIO	YIELD STRESS (fy) TENSION	YIELD STRESS (fy) COMPRESSION	ULTIMATE STRESS (fu) TENSION	ULTIMATE STRESS (fu) COMPRESSION	PIECE-WISE LINEAR MATERIAL LAW TYPE (SIMPLE / ATC-40 / KANEPE / CUSTOM)	ISOTROPIC/KINEMATIC HARDENING RULE (NONE/DRUCKER/PRAGER/ZIEGLER)
CONCRETE	C20/25	2.54842	9.810	29000000.0	0.25	+666.6	-8000.0	+1666.6	-20000.0	ATC-40	DRUCKER
STEEL	S235	8.05000	9.810	210000000.0	0.3	+235000.0	-235000.0	+235000.0	-235000.0	SIMPLE	NONE
STEEL	S220	8.05000	9.810	210000000.0	0.3	+220000.0	-220000.0	+231000.0	-231000.0	CUSTOM	PRAGER
STEEL	S400	8.05000	9.810	210000000.0	0.3	+400000.0	-400000.0	+420000.0	-420000.0	CUSTOM	ZIEGLER

Backbone curve`s type.....:
SYMMETRIC / ASYMMETRIC
In the first case, only the positive values need be defined.
In the second case, the negative values follow after the
positive ones; all values must be defined in ascending order
according to their coupled absolute strain values.

SYMMETRIC

NUMBER OF POINTS FOR THE CUSTOM PIECE-WISE LINEAR MATERIAL
CONSTITUTIVE LAW
Note: For all other constitutive law types, these lines must
---- be omitted!

6

NORMALIZED... STRESS	NORMALIZED... STRAIN
1.00	1.00
1.25	6.00
0.20	6.00
0.20	8.00
0.00	8.00
0.00	1E+99

+------------------------------+
|NUMBER OF MATERIAL ASSIGNMENTS:| 3
+------------------------------+

ASSIGNING MATERIALS TO MEMBERS...	
MEMBER... NUMBERS/RANGE	NAME OF MATERIAL
1,3	S220
2	S220
1:3 (=1,2,3)	S220

```
+-------------------+
|NUMBER OF SECTIONS:| 18
+-------------------+
  +----------+----------------+----------+------+------+
  |SECTION'S | SECTION`S SHAPE |SECTION`S |WIDTH |HEIGHT|
  |TYPE      |(BUILT IN SHAPES)|NAME      |  B   |  H   |
  +----------+----------------+----------+------+------+
   STEEL      RECTANGULAR       REC_1       0.25   0.50
  +----------+----------------+----------+------+------+------+------+
  |SECTION'S | SECTION`S SHAPE |SECTION`S |WIDTH |HEIGHT|FLANGE| WEB  |
  |TYPE      |(BUILT IN SHAPES)|NAME      |  B   |  H   |  tf  |  tw  |
  +----------+----------------+----------+------+------+------+------+
   STEEL      RECTANGULAR_TUBE  REC_TUB_1   0.25   0.50   0.10   0.10
  +----------+----------------+----------+----------+
  |SECTION'S | SECTION`S SHAPE |SECTION`S | Diameter |
  |TYPE      |(BUILT IN SHAPES)|NAME      |    D     |
  +----------+----------------+----------+----------+
   STEEL      CIRCULAR          CIR_1         0.60
  +----------+----------------+--------------+------------+------------+
  |SECTION'S | SECTION`S SHAPE |   SECTION`S   |  External   |  Internal   |
  |TYPE      |(BUILT IN SHAPES)|   NAME        | Radius (Re) | Radius (Ri) |
  +----------+----------------+--------------+------------+------------+
   STEEL      CIRCULAR_TUBE     CIR_TUB_1           0.5000         0.40
  +----------+----------------+----------+------+------+------+------+-------------+
  |SECTION'S | SECTION`S SHAPE |SECTION`S |WIDTH |HEIGHT|FLANGE| WEB  |FILLET RADIUS|
  |TYPE      |(BUILT IN SHAPES)|NAME      |  B   |  H   |  tf  |  tw  |     Ri      |
  +----------+----------------+----------+------+------+------+------+-------------+
   STEEL      T_SECTION         T_SEC_1     0.25   0.50   0.10   0.10       --
   STEEL      U_SECTION         U_SEC_1     0.25   0.50   0.10   0.10       --
   STEEL      L_SECTION         L_SEC_1     0.25   0.50   0.10   0.10       --
   STEEL      I_SECTION         I_SEC_1     0.25   0.50   0.10   0.10     0.025
  +----------+----------------+----------+
  |          |EUROPEAN SECTIONS|          |
  |SECTION'S | IPE 80-750X...& |SECTION`S |
  |TYPE      | HE-B/M 100-1000 |NAME      |
  +----------+----------------+----------+
    STEEL         EURO            IPE80
    STEEL         EURO          IPE750X196
    STEEL         EURO            HEB160
    STEEL         EURO            HEM160
    STEEL         EURO            HEM220
    STEEL         EURO            HEM260
  +----------+----------------+----------+
  |SECTION'S |  AISC SECTIONS  |SECTION`S |
  |TYPE      |  W6X25 , W8X21  |NAME      |
  +----------+----------------+----------+
    STEEL         AISC           W6X25
    STEEL         AISC           W8X21
  +----------+-----------------+
  |SECTION'S | SECTION`S SHAPE |
  |TYPE      |(NON-DEFORMABLE!)|
  +----------+-----------------+
    STEEL         RIGID
    CONCRETE      RIGID
+------------------------------+
|NUMBER OF SECTION ASSIGNMENTS:| 3
+------------------------------+
  +--------------------------------+
  | ASSIGNING SECTIONS TO MEMBERS...|
  +---------------+-----------------+
  |    MEMBER...  |                 |
  | NUMBERS/RANGE | NAME OF SECTION |
  +---------------+-----------------+
       1,3      =>     HEM160
        2       =>     HEM160
    1:3 (=1,2,3) =>     HEM160
```

```
+-----------------------+
|NUMBER OF YIELD FUNCTIONS:| 27
+-----------------------+

  +-------------------------------+
  | FAILURE CRITERION DEFINITIONS |
  | (all possible combos displayed) |
  +-------------------------------+
   (N/Np)=1                : {N}
   (M/Mp)=1                : {M2}
   (M/Mp)=1                : {M3}
   (M/Mp)=1                : {M2,M3}
   (M/Mp)^2=1              : {M2,M3}   [Approximates each quadrant of the circle with 4 linear segments]
   (M/Mp)+(N/Np)=1         : {N,M2}
   (M/Mp)+(N/Np)=1         : {N,M3}
   (M/Mp)+(N/Np)=1         : {N,M2,M3}
   (M/Mp)+(N/Np)^2=1       : {N,M2}    [Approximates each quadrant of the parabola with 5 linear segments]
   (M/Mp)+(N/Np)^2=1       : {N,M3}    [Approximates each quadrant of the parabola with 5 linear segments]
   (M/Mp)+(N/Np)^2=1       : {N,M2,M3} [Approximates each quadrant of the parabola with 5 planar segments]
   (M/Mp)^2+(N/Np)^2=1     : {N,M2,M3} [Approximates each quadrant of the sphere with 9 planar segments]
   AISC-LRFD               : {N,M2}
   AISC-LRFD               : {N,M3}
   AISC-LRFD               : {N,M2,M3}
   DIN-18800               : {N,M2,Q3}
   DIN-18800               : {N,M3,Q2}
   DIN-18800               : {N,M2,M3,Q2,Q3}
   (M/Mp)+(T/Tp)=1         : {T,M2}
   (M/Mp)+(T/Tp)=1         : {T,M3}
   (M/Mp)+(T/Tp)=1         : {T,M2,M3}
   (M/Mp)^2+(T/Tp)^2=1     : {T,M2}    [Approximates each quadrant of the circle with 4 linear segments]
   (M/Mp)^2+(T/Tp)^2=1     : {T,M3}    [Approximates each quadrant of the circle with 4 linear segments]
   (M/Mp)^2+(T/Tp)^2=1     : {T,M2,M3} [Approximates each quadrant of the sphere with 9 planar segments]
   POLYTOPON               : {N,Q2,Q3,T,M2,M3}
   CUSTOM                  : {CUSTOM}
   ELASTIC                 : {NONE}    [No plasticity implementation; provides pure elastic solutions]
  +-----------------------------------------------------------------------------+
                    NUMBER OF PLANES (EQUATIONS) OF THE CUSTOM MANIFOLD
      (FOR "CUSTOM" CRITERION ONLY! FOR ALL OTHER CRITERIA TYPES THESE LINES MUST BE OMMITED!)
  +-----------------------------------------------------------------------------+
                                        3
  +-----------------------------------------------------------------------------+
                    COEFFICIENTS FOR EACH LINE OF THE YIELD FUNCTION:

                                        k=N
                                        ---
                                  g(Q[k]) = >   S[k] * ----- - C = 0
                                        ---
                                        k=1

      (FOR "CUSTOM" CRITERION ONLY! FOR ALL OTHER CRITERIA TYPES THESE LINES MUST BE OMMITED!)
          S1 (N)          S2 (Q2)          S3 (Q3)          S4 (Mt)          S5 (M2)          S6 (M3)
  +---------------+---------------+---------------+---------------+---------------+---------------+
     1.000000000     0.000000000     0.000000000     1.000000000     1.000000000     1.000000000
     0.000000000     1.111111111     0.000000000     1.000000000     0.000000000     1.000000000
     0.000000000     0.000000000     1.111111111     1.000000000     1.000000000     0.000000000
  +-----------------------------------------------------------------------------+
  |NUMBER OF YIELD FUNCTION ASSIGNMENTS:| 3
  +-------------------------------------+

   +-----------------------------------------+
   | ASSIGNING YIELD FUNCTIONS TO MEMBERS... |
   +-----------------+-----------------------+
   |    MEMBER...    |          ...          |
   | NUMBERS/RANGE | NAME OF YIELD FUNCTION  |
   +-----------------+-----------------------+
         1,3       =>      AISC-LFRD
           2       =>      DIN-18800
       1:3 (=1,2,3) =>     POLYTOPON
```

```
+----------------+
|P-DELTA EFFECTS:| YES / NO
+----------------+
+--------------+
|DISPLACEMENTS:| SMALL / LARGE
+--------------+
+-------+
|SOLVER:| QPROG / LCONG / MOSEK
+-------+
+--------------+
|ANALYSIS TYPE:| ELASTIC / LIMIT / SCENARIO / PUSHOVER / CYCLIC
+--------------+

  +----------------------------------------+
   PARAMETERS FOR [ELASTIC_] ANALYSIS (ONLY!):
  +----------------------------------------+
   LOAD COMBINATION   : 1.00*G+0.30*Q+1.00*E
   MAX NUMBER OF STEPS: 1000
   ARC-LENGTH         : 0.001
   LOAD SCALE FACTOR  : 1.00

  +----------------------------------------+
   PARAMETERS FOR [LIMIT___] ANALYSIS (ONLY!):
  +----------------------------------------+
   LOAD COMBINATION   : 1.00*G+0.30*Q+1.00*E
   MAX NUMBER OF STEPS: 1000
   ARC-LENGTH         : 0.001

  +----------------------------------------+
   PARAMETERS FOR [PUSHOVER] ANALYSIS (ONLY!):
  +----------------------------------------+
   LOAD COMBINATION   : 1.00*G+0.30*Q+1.00*E
   MAX NUMBER OF STEPS: 1000
   ARC-LENGTH         : 0.001
   REFERENCE NODE     : 2
   MAX. DISPLACEMENT  : 1.00

  +----------------------------------------+
   PARAMETERS FOR [SCENARIO] ANALYSIS (ONLY!):
  +----------------------------------------+
   LOAD COMBINATION    : 1.00*G+0.30*Q+1.00*E
   MAX NUMBER OF STEPS : 1000
   ARC-LENGTH          : 0.001
    +--------------------+                              --.
     NUMBER OF PATH PEAKS:                                |
    +--------------------+                                |
              1                                           |
    +---------+----------+----------+ .... +----------+    > Put these lines at the end of the input file.
     EXTERNAL LOADPATH VALUES:                            |
    [   Q1    ,    Q2    ,    Q3    , .... ,    QN    ]   |
    +---------+----------+----------+ .... +----------+   |
      155.412   155.412    ........   ....   ........    --'

  +----------------------------------------+
   PARAMETERS FOR [CYCLIC__] ANALYSIS (ONLY!):
  +----------------------------------------+
   LOAD COMBINATION    : 1.00*G+0.30*Q+1.00*E
   MAX NUMBER OF STEPS : 1000
   ARC-LENGTH          : 0.001
   REFERENCE NODE      : 2
   NUMBER OF LOAD PEAKS: 5
   PEAK SCALE FACTORS  : +1.0,-0.8,+0.8,-0.8,+0.8
```

```
+-------------------------+
|PLASTIC HINGE PARAMETERS:|
+-------------------------+
   PLASTIC BARRIERS   : ON / OFF
   INTERMEDIATE HINGES: ON / OFF
   COMPATIBILITY MODE : NONE / SAP2000

   NOTE #1: For "Elastic" analysis, no plastic hinge parameters
   -------  are allowed to be defined.

   NOTE #2: For "Limit" analysis, no plastic barriers and no
   -------  compatibility mode are allowed to be defined; only
            the intermediate hinges may be defined.

+--------------+
| Q=f(q) PRINT:| AUTO / CUSTOM / FULL
+--------------+
  +-------------------------------------------------------------------------+
   ADDITIONAL PARAMETERS (APPLIES TO [CUSTOM] Q=f(q) PRINT OPTION ONLY !) :
  +-------------------------------------------------------------------------+
  +-------------------------+
  |NUMBER OF PRINT REQUESTS:|    4
  +-------------------------+
                           +------+---------+---------+-----------------+-------------+
                           |Member|Element  |Section  |Stress component | q-function  |
                           |      /         /         :      name(s)    =             |
                           |Number|Number(s)|Number(s)|{N,Q2,Q3,T,M2,M3}|    type     |
                           +------+---------+---------+-----------------+-------------+
                               1  /     1   /   1,2   :      N,M3       = f(q-elastic)
                               2  /     1   /     1   :        M3       = f(q-plastic)
                               2  /    10   /     2   :        M3       = f(q-plastic)
                               3  /     1   /   1,2   :      N,M3       = f(q-total)

 ********************************************************************************End of Input File*********************************************************************************
```

16.3 An Example Input File

A simple portal frame that is pictured below (*Figure 71*) is used to create an indicative input file for the program that was authored within the context of this work.

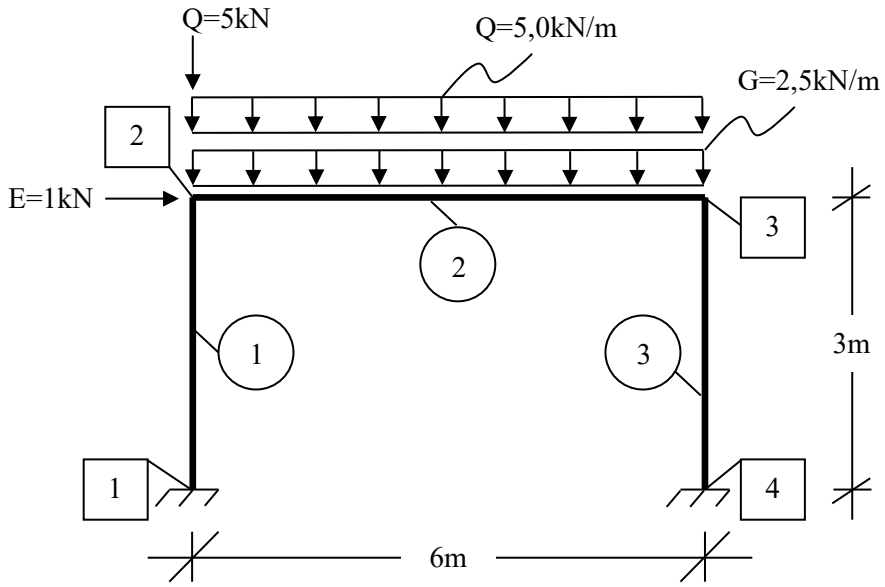

Figure 71: Structure's geometry, boundary conditions, and loading considerations for the sample input file.

The frame is defined using four nodes (1,2,3,4) and three beam/column Euler-Bernoulli finite elements (1,2,3); all elements have been aligned so that they bend around their strong axis (#3), and the beam member is subdivided into ten finite elements. The boundary nodes are completely fixed. Two nodal load types are defined; an earthquake load (E) and a mobile load (Q); they are both applied to node #2. Two uniformly distributed load types are also defined; a dead load (G) and a mobile load (Q), which are applied on member #2. The material of the structure is structural steel S220; a piece-wise linear, custom-defined constitutive law is assumed for the backbone curve of the material, while plastic hardening is assumed kinematic according to Ziegler's rule. The section for the columns is HEB180 and for the beam is HEB160. Bending moment and axial force interaction according to the AISC-LRFD bilinear yield function is assumed for the columns, and pure bending behaviour is assumed for the beam of the frame. P-Δ effects and large displacements are not taken into account (*1st order analysis*). The frame is subjected to a pushover analysis under a load combination that considers a 100% participation of the dead loads (G) and a 30% participation of the mobile loads (Q). The maximum allowed number of analysis steps is defined to be equal to 100. The "arc-length" (ρ) parameter is set equal to 0.001. Node #2 is selected as the reference (*roof*) node for the pushover analysis curve, while the maximum tolerated horizontal displacement is set equal to 0.50 length units. The plastic hinge parameters do not impose a perfectly plastic behaviour on the axial force components, while all subdivided elements may also contain plastic hinges within their span. Plastic hardening flexibility coefficients are defined so as to maintain compatibility with widely accepted commercial software. Printout of the local stress components vs. their respective elastic/plastic deformations is automatically generated and only for those plastic hinges that are activated (*i.e. that develop plastic deformations*) during the incremental analysis procedure.

The input file that corresponds to the portal frame pictured and described above follows in the next page.

```
****************************************Beginning of Input File*****************************************

INPUT_FILE_v.2.8.0_3D   3D   Frame
==================================
4
  1   0.00   0.00   0.00  B
  2   0.00   0.00   3.00  L
  3   6.00   0.00   3.00  F
  4   6.00   0.00   0.00  B
3
  1   1   2   +0.00 +0.00 +0.00 +0.00 +0.00 -0.08   +180.00000 deg    1 1 1 1 1 1  1 1 1 1 1 1    N=3   F
  2   2   3   +0.10 +0.00 +0.00 -0.10 +0.00 +0.00    +90.00000 deg    1 1 1 1 1 1  1 1 1 1 1 1    N=10  L
  3   4   3   +0.00 +0.00 +0.00 +0.00 +0.00 -0.08   +180.00000 deg    1 1 1 1 1 1  1 1 1 1 1 1    N=3   F
1
  B_COND_1:  0.0   0.0   0.0   0.0   0.0   0.0
1
  1,4  =>  B_COND_1
2
  P_LOAD_1:  E   +1.00   0.00   0.00   0.00   0.00   0.00
  P_LOAD_2:  Q    0.00   0.00  -5.00   0.00   0.00   0.00
1
  2  =>  P_LOAD_1 , P_LOAD_2
2
  D_LOAD_1:  G  U        0.00   0.00  -2.50   0.00   0.00   0.00
  D_LOAD_2:  Q  U        0.00   0.00  -5.00   0.00   0.00   0.00
1
  2  =>  D_LOAD_1 , D_LOAD_2
1
  STEEL  S220  8.05000  9.810  2.1E+8  0.3   +220000.0 -220000.0 +231000.0 -231000.0  CUSTOM  PRAGER
    SYMMETRIC
    3
    1.00 1.00
    1.25 6.00
    1.25 1E+99
1
  1:3  =>  S220
2
  STEEL   EURO   HEB160
  STEEL   EURO   HEM180
2
  1,3  =>  HEM180
  2    =>  HEB160
2
   (M/Mp)=1  : {M3}
   AISC-LRFD : {N,M3}
2
  1,3  =>  AISC-LRFD
  2    =>  (M/Mp)=1

P-D EFFECTS  : NO
DISPLACEMENTS: SMALL
SOLVER       : QPROG
ANALYSIS TYPE: PUSHOVER
               LOAD COMBINATION   : 1.00*G+0.30*Q+1.00*E
               MAX NUMBER OF STEPS: 100
               ARC-LENGTH         : 0.01
               REFERENCE NODE     : 2
               MAX. DISPLACEMENT  : 0.50

PLASTIC HINGE PARAMETERS:
               PLASTIC BARRIERS   : OFF
               INTERMEDIATE HINGES: ON
               COMPATIBILITY MODE : SAP2000

Q=f(q) PRINT : AUTO

 ****************************************End of Input File*****************************************
```

16.4 An Example Output File

In this section, a selection from the respective output generated by the program for the input file corresponding to the simple portal frame pictured in Figure 71 may be seen:

```
+----------------------------------------------------------------------------------------+
| Program SBS - v._2.8.0_3D - Force_Method - Theodoros N. Patsios, Dr.Eng. Candidate |
+----------------------------------------------------------------------------------------+
|Input File:                               EXAMPLE_INPUT.TXT|12/Mar/2019|22:07:12|
+----------------------------------------------------------------------------------------+

+-----------------------------+
|Analysis Category:   PUSHOVER|
|P-Delta Effects..:         NO|
|Displacements....:      SMALL|
+-----------------------------+

+------+---------------------------+----------------------------------------------------------+
|Node #|   Coordinates  {x,y,z}    |   Boundary Conditions    { Ux , Uy , Uz , Rx , Ry , Rz }  |
+------+---------------------------+----------------------------------------------------------+
|     1|   0.00     0.00     0.00|     0.000     0.000     0.000     0.000     0.000     0.000|
|     2|   0.00     0.00     3.00|                                                            |
|     3|   6.00     0.00     3.00|                                                            |
|     4|   6.00     0.00     0.00|     0.000     0.000     0.000     0.000     0.000     0.000|
+------+---------------------------+----------------------------------------------------------+

+----------+---------------------+----------+-----------+----------------+------------------------+------------+------------+------------+------------+------------+------------+------------+------------+
| Member # | Node: Start --> End | Material |  Section  | Yield Function | Interacting Components |     E      |     v      |   A (1)    |   A (2)    |   A (3)    |   I (1)    |   I (2)    |   I (3)    |
+----------+---------------------+----------+-----------+----------------+------------------------+------------+------------+------------+------------+------------+------------+------------+------------+
|        1 |       1 -->       2 |     S220 |    HEM180 |      AISC-LRFD |                {N,M3}  | 0.210E+09 | 0.300E+00 | 0.113E-01 | 0.556E-01 | 0.186E-01 | 0.206E-05 | 0.258E-04 | 0.748E-04 |
|        2 |       2 -->       3 |     S220 |    HEB160 |       (M/Mp)=1 |                  {M3}  | 0.210E+09 | 0.300E+00 | 0.543E-02 | 0.270E-01 | 0.881E-02 | 0.318E-06 | 0.889E-05 | 0.249E-04 |
|        3 |       4 -->       3 |     S220 |    HEM180 |      AISC-LRFD |                {N,M3}  | 0.210E+09 | 0.300E+00 | 0.113E-01 | 0.556E-01 | 0.186E-01 | 0.206E-05 | 0.258E-04 | 0.748E-04 |
+----------+---------------------+----------+-----------+----------------+------------------------+------------+------------+------------+------------+------------+------------+------------+------------+

+--------+-----------+------------+------------+------------+------------+------------+------------+
| Node # | Load Kind | Force -> X | Force -> Y | Force -> Z | Moment @ X | Moment @ Y | Moment @ Z |
+--------+-----------+------------+------------+------------+------------+------------+------------+
|      2 |     E     |      1.000 |      0.000 |      0.000 |      0.000 |      0.000 |      0.000 |
|      2 |     Q     |      0.000 |      0.000 |     -5.000 |      0.000 |      0.000 |      0.000 |
+--------+-----------+------------+------------+------------+------------+------------+------------+

+---------------------------------------------------------------------------------------------------+
|     Table of Uniformly Distributed Loads applied to the Beam/Column Members of the Structure:      |
+----------+-----------+------------+------------+------------+------------+------------+------------+
| Member # | Load Kind |   (Fx/L)   |   (Fz/L)   |   (Fz/L)   |   (Mx/L)   |   (My/L)   |   (Mz/L)   |
+----------+-----------+------------+------------+------------+------------+------------+------------+
|        2 |     G     |      0.000 |      0.000 |     -2.500 |      0.000 |      0.000 |      0.000 |
|        2 |     Q     |      0.000 |      0.000 |     -5.000 |      0.000 |      0.000 |      0.000 |
+----------+-----------+------------+------------+------------+------------+------------+------------+
```

Member #	Section #	Xcrit.	Ycrit.	Zcrit.	Releases	Np (+)	Np (-)	Qp [2] (+)	Qp [2] (-)	Qp [3] (+)	Qp [3] (-)	Mp [1] (+)	Mp [1] (-)	Mp [2] (+)	Mp [2] (-)	Mp [3] (+)	Mp [3] (-)
1	1	0.00	0.00	0.00	1 1 1 1 1 1	0.249E+04	-0.249E+04	0.706E+04	-0.706E+04	0.237E+04	-0.237E+04	0.782E+01	-0.782E+01	0.935E+02	-0.935E+02	0.194E+03	-0.194E+03
	2	0.00	0.00	0.97		0.249E+04	-0.249E+04	0.706E+04	-0.706E+04	0.237E+04	-0.237E+04	0.782E+01	-0.782E+01	0.935E+02	-0.935E+02	0.194E+03	-0.194E+03
	3	0.00	0.00	0.97		0.249E+04	-0.249E+04	0.706E+04	-0.706E+04	0.237E+04	-0.237E+04	0.782E+01	-0.782E+01	0.935E+02	-0.935E+02	0.194E+03	-0.194E+03
	4	0.00	0.00	1.95		0.249E+04	-0.249E+04	0.706E+04	-0.706E+04	0.237E+04	-0.237E+04	0.782E+01	-0.782E+01	0.935E+02	-0.935E+02	0.194E+03	-0.194E+03
	5	0.00	0.00	1.95		0.249E+04	-0.249E+04	0.706E+04	-0.706E+04	0.237E+04	-0.237E+04	0.782E+01	-0.782E+01	0.935E+02	-0.935E+02	0.194E+03	-0.194E+03
	6	0.00	0.00	2.92	1 1 1 1 1 1	0.249E+04	-0.249E+04	0.706E+04	-0.706E+04	0.237E+04	-0.237E+04	0.782E+01	-0.782E+01	0.935E+02	-0.935E+02	0.194E+03	-0.194E+03
2	7	0.10	0.00	3.00	1 1 1 1 1 1	0.119E+04	-0.119E+04	0.343E+04	-0.343E+04	0.112E+04	-0.112E+04	0.199E+01	-0.199E+01	0.374E+02	-0.374E+02	0.779E+02	-0.779E+02
	8	0.68	0.00	3.00		0.119E+04	-0.119E+04	0.343E+04	-0.343E+04	0.112E+04	-0.112E+04	0.199E+01	-0.199E+01	0.374E+02	-0.374E+02	0.779E+02	-0.779E+02
	9	0.68	0.00	3.00		0.119E+04	-0.119E+04	0.343E+04	-0.343E+04	0.112E+04	-0.112E+04	0.199E+01	-0.199E+01	0.374E+02	-0.374E+02	0.779E+02	-0.779E+02
	10	1.26	0.00	3.00		0.119E+04	-0.119E+04	0.343E+04	-0.343E+04	0.112E+04	-0.112E+04	0.199E+01	-0.199E+01	0.374E+02	-0.374E+02	0.779E+02	-0.779E+02
	11	1.84	0.00	3.00		0.119E+04	-0.119E+04	0.343E+04	-0.343E+04	0.112E+04	-0.112E+04	0.199E+01	-0.199E+01	0.374E+02	-0.374E+02	0.779E+02	-0.779E+02
	12	1.84	0.00	3.00		0.119E+04	-0.119E+04	0.343E+04	-0.343E+04	0.112E+04	-0.112E+04	0.199E+01	-0.199E+01	0.374E+02	-0.374E+02	0.779E+02	-0.779E+02
	13	1.84	0.00	3.00		0.119E+04	-0.119E+04	0.343E+04	-0.343E+04	0.112E+04	-0.112E+04	0.199E+01	-0.199E+01	0.374E+02	-0.374E+02	0.779E+02	-0.779E+02
	14	2.42	0.00	3.00		0.119E+04	-0.119E+04	0.343E+04	-0.343E+04	0.112E+04	-0.112E+04	0.199E+01	-0.199E+01	0.374E+02	-0.374E+02	0.779E+02	-0.779E+02
	15	2.42	0.00	3.00		0.119E+04	-0.119E+04	0.343E+04	-0.343E+04	0.112E+04	-0.112E+04	0.199E+01	-0.199E+01	0.374E+02	-0.374E+02	0.779E+02	-0.779E+02
	16	3.00	0.00	3.00		0.119E+04	-0.119E+04	0.343E+04	-0.343E+04	0.112E+04	-0.112E+04	0.199E+01	-0.199E+01	0.374E+02	-0.374E+02	0.779E+02	-0.779E+02
	17	3.00	0.00	3.00		0.119E+04	-0.119E+04	0.343E+04	-0.343E+04	0.112E+04	-0.112E+04	0.199E+01	-0.199E+01	0.374E+02	-0.374E+02	0.779E+02	-0.779E+02
	18	3.58	0.00	3.00		0.119E+04	-0.119E+04	0.343E+04	-0.343E+04	0.112E+04	-0.112E+04	0.199E+01	-0.199E+01	0.374E+02	-0.374E+02	0.779E+02	-0.779E+02
	19	3.58	0.00	3.00		0.119E+04	-0.119E+04	0.343E+04	-0.343E+04	0.112E+04	-0.112E+04	0.199E+01	-0.199E+01	0.374E+02	-0.374E+02	0.779E+02	-0.779E+02
	20	4.16	0.00	3.00		0.119E+04	-0.119E+04	0.343E+04	-0.343E+04	0.112E+04	-0.112E+04	0.199E+01	-0.199E+01	0.374E+02	-0.374E+02	0.779E+02	-0.779E+02
	21	4.16	0.00	3.00		0.119E+04	-0.119E+04	0.343E+04	-0.343E+04	0.112E+04	-0.112E+04	0.199E+01	-0.199E+01	0.374E+02	-0.374E+02	0.779E+02	-0.779E+02
	22	4.74	0.00	3.00		0.119E+04	-0.119E+04	0.343E+04	-0.343E+04	0.112E+04	-0.112E+04	0.199E+01	-0.199E+01	0.374E+02	-0.374E+02	0.779E+02	-0.779E+02
	23	4.74	0.00	3.00		0.119E+04	-0.119E+04	0.343E+04	-0.343E+04	0.112E+04	-0.112E+04	0.199E+01	-0.199E+01	0.374E+02	-0.374E+02	0.779E+02	-0.779E+02
	24	5.32	0.00	3.00		0.119E+04	-0.119E+04	0.343E+04	-0.343E+04	0.112E+04	-0.112E+04	0.199E+01	-0.199E+01	0.374E+02	-0.374E+02	0.779E+02	-0.779E+02
	25	5.32	0.00	3.00		0.119E+04	-0.119E+04	0.343E+04	-0.343E+04	0.112E+04	-0.112E+04	0.199E+01	-0.199E+01	0.374E+02	-0.374E+02	0.779E+02	-0.779E+02
	26	5.90	0.00	3.00	1 1 1 1 1 1	0.119E+04	-0.119E+04	0.343E+04	-0.343E+04	0.112E+04	-0.112E+04	0.199E+01	-0.199E+01	0.374E+02	-0.374E+02	0.779E+02	-0.779E+02
3	27	6.00	0.00	0.00	1 1 1 1 1 1	0.249E+04	-0.249E+04	0.706E+04	-0.706E+04	0.237E+04	-0.237E+04	0.782E+01	-0.782E+01	0.935E+02	-0.935E+02	0.194E+03	-0.194E+03
	28	6.00	0.00	0.97		0.249E+04	-0.249E+04	0.706E+04	-0.706E+04	0.237E+04	-0.237E+04	0.782E+01	-0.782E+01	0.935E+02	-0.935E+02	0.194E+03	-0.194E+03
	29	6.00	0.00	0.97		0.249E+04	-0.249E+04	0.706E+04	-0.706E+04	0.237E+04	-0.237E+04	0.782E+01	-0.782E+01	0.935E+02	-0.935E+02	0.194E+03	-0.194E+03
	30	6.00	0.00	1.95		0.249E+04	-0.249E+04	0.706E+04	-0.706E+04	0.237E+04	-0.237E+04	0.782E+01	-0.782E+01	0.935E+02	-0.935E+02	0.194E+03	-0.194E+03
	31	6.00	0.00	1.95		0.249E+04	-0.249E+04	0.706E+04	-0.706E+04	0.237E+04	-0.237E+04	0.782E+01	-0.782E+01	0.935E+02	-0.935E+02	0.194E+03	-0.194E+03
	32	6.00	0.00	2.92	1 1 1 1 1 1	0.249E+04	-0.249E+04	0.706E+04	-0.706E+04	0.237E+04	-0.237E+04	0.782E+01	-0.782E+01	0.935E+02	-0.935E+02	0.194E+03	-0.194E+03

<STEP: 1> |dGmin= 0.705E+01|		Local Strain Components						Local Stress Components					
|Member |Section|Criterion Values|		q(1)	q(2)	q(3)	q(4)	q(5)	q(6)	Q(1)	Q(2)	Q(3)	Q(4)	Q(5)	Q(6)
1	1	0.201E-01	-0.502E-05 | 0.000E+00	| 0.000E+00	-0.261E-05 |	0.279E-03 |	0.717E-04	-0.123E+02 |	0.311E+01	-0.417E+01 |	-0.447E-03 |	0.445E+01 |	0.333E+01 |
	2	0.627E-02	-0.502E-05 | 0.000E+00	| 0.000E+00	-0.261E-05 |	0.157E-03 |	0.404E-04	-0.123E+02 |	0.311E+01	-0.417E+01 |	-0.447E-03 |	0.396E+00 |	0.296E+00 |
	3	0.627E-02	-0.502E-05 | 0.000E+00	| 0.000E+00	-0.261E-05 |	-0.859E-04 |	-0.221E-04	-0.123E+02 |	0.311E+01	-0.417E+01 |	-0.447E-03 |	0.396E+00 |	0.296E+00 |
	4	0.174E-01	-0.502E-05 | 0.000E+00	| 0.000E+00	-0.261E-05 |	-0.207E-03 |	-0.534E-04	-0.123E+02 |	0.311E+01	-0.417E+01 |	-0.447E-03 |	-0.366E+01 |	-0.274E+01 |
	5	0.174E-01	-0.502E-05 | 0.000E+00	| 0.000E+00	-0.261E-05 |	-0.450E-03 |	-0.116D-03	-0.123E+02 |	0.311E+01	-0.417E+01 |	-0.447E-03 |	-0.366E+01 |	-0.274E+01 |
	6	0.321E-01	-0.502E-05 | 0.000E+00	| 0.000E+00	-0.261E-05 |	-0.572E-03 |	-0.147E-03	-0.123E+02 |	0.311E+01	-0.417E+01 |	-0.447E-03 |	-0.772E+01 |	-0.577E+01 |
2	7	0.115E+00	-0.265E-05 | 0.000E+00	| 0.000E+00	-0.172E-04 |	-0.626E-07 |	-0.392E-03	-0.520E+01 |	-0.981E+01	0.149E-03 |	-0.764E-03 |	-0.432E-03 |	-0.898E+01 |
	8	0.422E-01	-0.265E-05 | 0.000E+00	| 0.000E+00	-0.172E-04 |	-0.581E-07 |	-0.287D-03	-0.520E+01 |	-0.981E+01	0.149E-03 |	-0.764E-03 |	-0.345E-03 |	-0.329E+01 |
	9	0.422E-01	-0.265E-05 | 0.000E+00	| 0.000E+00	-0.172E-04 |	-0.492E-07 |	-0.971E-04	-0.520E+01 |	-0.793E+01	0.149E-03 |	-0.764E-03 |	-0.345E-03 |	-0.329E+01 |
	10	0.169E-01	-0.265E-05 | 0.000E+00	| 0.000E+00	-0.172E-04 |	-0.447E-07 |	-0.122E-04	-0.520E+01 |	-0.793E+01	0.149E-03 |	-0.764E-03 |	-0.259E-03 |	0.131E+01 |
	11	0.169E-01	-0.265E-05 | 0.000E+00	| 0.000E+00	-0.172E-04 |	-0.358E-07 |	0.133D-03	-0.520E+01 |	-0.561E+01	0.149E-03 |	-0.764E-03 |	-0.259E-03 |	0.131E+01 |
	12	0.586E-01	-0.265E-05 | 0.000E+00	| 0.000E+00	-0.172E-04 |	-0.313E-07 |	0.193E-03 |	-0.520E+01 |	-0.561E+01	0.149E-03 |	-0.764E-03 |	-0.173E-03 |	0.457E+01 |
	13	0.586E-01	-0.265E-05 | 0.000E+00	| 0.000E+00	-0.172E-04 |	-0.223E-07 |	0.288E-03 |	-0.520E+01 |	-0.329E+01	0.149E-03 |	-0.764E-03 |	-0.173E-03 |	0.457E+01 |
	14	0.831E-01	-0.265E-05 | 0.000E+00	| 0.000E+00	-0.172E-04 |	-0.179E-07 |	0.323E-03 |	-0.520E+01 |	-0.329E+01	0.149E-03 |	-0.764E-03 |	-0.863E-04 |	0.647E+01 |
	15	0.831E-01	-0.265E-05 | 0.000E+00	| 0.000E+00	-0.172E-04 |	-0.894E-08 |	0.369E-03 |	-0.520E+01 |	-0.968E+00	0.149E-03 |	-0.764E-03 |	-0.863E-04 |	0.647E+01 |
	16	0.903E-01	-0.265E-05 | 0.000E+00	| 0.000E+00	-0.172E-04 |	-0.447E-08 |	0.379E-03 |	-0.520E+01 |	-0.968E+00	0.149E-03 |	-0.764E-03 |	0.000E+00 |	0.703E+01 |
	17	0.903E-01	-0.265E-05 | 0.000E+00	| 0.000E+00	-0.172E-04 |	0.447E-08 |	0.375E-03 |	-0.520E+01 |	0.135E+01	0.149E-03 |	-0.764E-03 |	0.000E+00 |	0.703E+01 |
	18	0.802E-01	-0.265E-05 | 0.000E+00	| 0.000E+00	-0.172E-04 |	0.894E-08 |	0.361E-03 |	-0.520E+01 |	0.135E+01	0.149E-03 |	-0.764E-03 |	0.863E-04 |	0.625E+01 |
	19	0.802E-01	-0.265E-05 | 0.000E+00	| 0.000E+00	-0.172E-04 |	0.179E-07 |	0.307D-03	-0.520E+01 |	0.367E+01	0.149E-03 |	-0.764E-03 |	0.863E-04 |	0.625E+01 |
	20	0.529E-01	-0.265E-05 | 0.000E+00	| 0.000E+00	-0.172E-04 |	0.223E-07 |	0.268E-03 |	-0.520E+01 |	0.367E+01	0.149E-03 |	-0.764E-03 |	0.173E-03 |	0.412E+01 |
	21	0.529E-01	-0.265E-05 | 0.000E+00	| 0.000E+00	-0.172E-04 |	0.313E-07 |	0.164E-03 |	-0.520E+01 |	0.599E+01	0.149E-03 |	-0.764E-03 |	0.173E-03 |	0.412E+01 |
	22	0.827E-02	-0.265E-05 | 0.000E+00	| 0.000E+00	-0.172E-04 |	0.358E-07 |	0.999E-04	-0.520E+01 |	0.599E+01	0.149E-03 |	-0.764E-03 |	0.259E-03 |	0.644E+00 |
	23	0.827E-02	-0.265E-05 | 0.000E+00	| 0.000E+00	-0.172E-04 |	0.447E-07 |	-0.534E-04	-0.520E+01 |	0.831E+01	0.149E-03 |	-0.764E-03 |	0.259E-03 |	0.644E+00 |
	24	0.536E-01	-0.265E-05 | 0.000E+00	| 0.000E+00	-0.172E-04 |	0.492E-07 |	-0.142E-03	-0.520E+01 |	0.831E+01	0.149E-03 |	-0.764E-03 |	0.345E-03 |	-0.418E+01 |
	25	0.536E-01	-0.265E-05 | 0.000E+00	| 0.000E+00	-0.172E-04 |	0.581E-07 |	-0.345E-03	-0.520E+01 |	0.106E+02	0.149E-03 |	-0.764E-03 |	0.345E-03 |	-0.418E+01 |
	26	0.133E+00	-0.265E-05 | 0.000E+00	| 0.000E+00	-0.172E-04 |	0.626E-07 |	-0.459E-03	-0.520E+01 |	0.106E+02	0.149E-03 |	-0.764E-03 |	0.432E-03 |	-0.103E+02 |
3	27	0.238E-01	-0.435E-05 | 0.000E+00	| 0.000E+00	-0.261E-05 |	-0.329E-07 |	-0.780E-04	-0.106E+02 |	-0.520E+01	-0.149E-03 |	-0.447E-03 |	-0.318E-03 |	-0.421E+01 |
	28	0.820E-02	-0.435E-05 | 0.000E+00	| 0.000E+00	-0.261E-05 |	-0.372E-07 |	-0.257E-04	-0.106E+02 |	-0.520E+01	-0.149E-03 |	-0.447E-03 |	-0.462E-03 |	0.860E+00 |
	29	0.820E-02	-0.435E-05 | 0.000E+00	| 0.000E+00	-0.261E-05 |	-0.459E-07 |	0.789E-04	-0.106E+02 |	-0.520E+01	-0.149E-03 |	-0.447E-03 |	-0.462E-03 |	0.860E+00 |
	30	0.326E-01	-0.435E-05 | 0.000E+00	| 0.000E+00	-0.261E-05 |	-0.502E-07 |	0.131D-03	-0.106E+02 |	-0.520E+01	-0.149E-03 |	-0.447E-03 |	-0.607E-03 |	0.593E+01 |
	31	0.326E-01	-0.435E-05 | 0.000E+00	| 0.000E+00	-0.261E-05 |	-0.589E-07 |	0.236E-03 |	-0.106E+02 |	-0.520E+01	-0.149E-03 |	-0.447E-03 |	-0.607E-03 |	0.593E+01 |
	32	0.587E-01	-0.435E-05 | 0.000E+00	| 0.000E+00	-0.261E-05 |	-0.632E-07 |	0.288E-03 |	-0.106E+02 |	-0.520E+01	-0.149E-03 |	-0.447E-03 |	-0.752E-03 |	0.110E+02 |

<STEP: 2>		dGmin= 0.139E+03	Local Strain Components						Local Stress Components					
Member	Section	Criterion Values	q(1)	q(2)	q(3)	q(4)	q(5)	q(6)	Q(1)	Q(2)	Q(3)	Q(4)	Q(5)	Q(6)
1	1	0.301E+00	0.356E-05	0.000E+00	0.000E+00	0.341E-03	-0.584E-02	-0.151E-02	0.869E+01	-0.295E+02	0.394E+02	0.584E-01	-0.778E+02	-0.582E+02
	2	0.154E+00	0.356E-05	0.000E+00	0.000E+00	0.341E-03	-0.469E-02	-0.121E-02	0.869E+01	-0.295E+02	0.394E+02	0.584E-01	-0.394E+02	-0.295E+02
	3	0.154E+00	0.356E-05	0.000E+00	0.000E+00	0.341E-03	-0.239E-02	-0.618E-03	0.869E+01	-0.295E+02	0.394E+02	0.584E-01	-0.394E+02	-0.295E+02
	4	0.732E-02	0.356E-05	0.000E+00	0.000E+00	0.341E-03	-0.125E-02	-0.322E-03	0.869E+01	-0.295E+02	0.394E+02	0.584E-01	-0.107E+01	-0.838E+00
	5	0.732E-02	0.356E-05	0.000E+00	0.000E+00	0.341E-03	0.105E-02	0.270E-03	0.869E+01	-0.295E+02	0.394E+02	0.584E-01	-0.107E+01	-0.838E+00
	6	0.145E+00	0.356E-05	0.000E+00	0.000E+00	0.341E-03	0.220E-02	0.566E-03	0.869E+01	-0.295E+02	0.394E+02	0.584E-01	0.373E+02	0.279E+02
2	7	0.635E+00	-0.458E-04	0.000E+00	0.000E+00	-0.213E-03	0.819E-05	0.262E-02	-0.899E+02	0.111E+02	-0.195E-01	-0.943E-02	0.565E-01	0.495E+02
	8	0.552E+00	-0.458E-04	0.000E+00	0.000E+00	-0.213E-03	0.760E-05	0.250E-02	-0.899E+02	0.111E+02	-0.195E-01	-0.943E-02	0.452E-01	0.430E+02
	9	0.552E+00	-0.458E-04	0.000E+00	0.000E+00	-0.213E-03	0.643E-05	0.224E-02	-0.899E+02	0.130E+02	-0.195E-01	-0.943E-02	0.452E-01	0.430E+02
	10	0.455E+00	-0.458E-04	0.000E+00	0.000E+00	-0.213E-03	0.585E-05	0.210E-02	-0.899E+02	0.130E+02	-0.195E-01	-0.943E-02	0.339E-01	0.355E+02
	11	0.455E+00	-0.458E-04	0.000E+00	0.000E+00	-0.213E-03	0.468E-05	0.180E-02	-0.899E+02	0.153E+02	-0.195E-01	-0.943E-02	0.339E-01	0.355E+02
	12	0.341E+00	-0.458E-04	0.000E+00	0.000E+00	-0.213E-03	0.409E-05	0.164E-02	-0.899E+02	0.153E+02	-0.195E-01	-0.943E-02	0.226E-01	0.266E+02
	13	0.341E+00	-0.458E-04	0.000E+00	0.000E+00	-0.213E-03	0.292E-05	0.128E-02	-0.899E+02	0.177E+02	-0.195E-01	-0.943E-02	0.226E-01	0.266E+02
	14	0.210E+00	-0.458E-04	0.000E+00	0.000E+00	-0.213E-03	0.234E-05	0.109E-02	-0.899E+02	0.177E+02	-0.195E-01	-0.943E-02	0.113E-01	0.163E+02
	15	0.210E+00	-0.458E-04	0.000E+00	0.000E+00	-0.213E-03	0.117E-05	0.691E-03	-0.899E+02	0.200E+02	-0.195E-01	-0.943E-02	0.113E-01	0.163E+02
	16	0.609E-01	-0.458E-04	0.000E+00	0.000E+00	-0.213E-03	0.585E-06	0.477E-03	-0.899E+02	0.200E+02	-0.195E-01	-0.943E-02	0.754E-17	0.474E+01
	17	0.609E-01	-0.458E-04	0.000E+00	0.000E+00	-0.213E-03	-0.585E-06	0.240E-04	-0.899E+02	0.223E+02	-0.195E-01	-0.943E-02	0.754E-17	0.474E+01
	18	0.105E+00	-0.458E-04	0.000E+00	0.000E+00	-0.213E-03	-0.117E-05	-0.215E-03	-0.899E+02	0.223E+02	-0.195E-01	-0.943E-02	-0.113E-01	-0.819E+01
	19	0.105E+00	-0.458E-04	0.000E+00	0.000E+00	-0.213E-03	-0.234E-05	-0.717E-03	-0.899E+02	0.246E+02	-0.195E-01	-0.943E-02	-0.113E-01	-0.819E+01
	20	0.288E+00	-0.458E-04	0.000E+00	0.000E+00	-0.213E-03	-0.292E-05	-0.981E-03	-0.899E+02	0.246E+02	-0.195E-01	-0.943E-02	-0.226E-01	-0.225E+02
	21	0.288E+00	-0.458E-04	0.000E+00	0.000E+00	-0.213E-03	-0.409E-05	-0.153E-02	-0.899E+02	0.269E+02	-0.195E-01	-0.943E-02	-0.226E-01	-0.225E+02
	22	0.489E+00	-0.458E-04	0.000E+00	0.000E+00	-0.213E-03	-0.468E-05	-0.182E-02	-0.899E+02	0.269E+02	-0.195E-01	-0.943E-02	-0.339E-01	-0.381E+02
	23	0.489E+00	-0.458E-04	0.000E+00	0.000E+00	-0.213E-03	-0.585E-05	-0.242E-02	-0.899E+02	0.293E+02	-0.195E-01	-0.943E-02	-0.339E-01	-0.381E+02
	24	0.707E+00	-0.458E-04	0.000E+00	0.000E+00	-0.213E-03	-0.643E-05	-0.274E-02	-0.899E+02	0.293E+02	-0.195E-01	-0.943E-02	-0.452E-01	-0.551E+02
	25	0.707E+00	-0.458E-04	0.000E+00	0.000E+00	-0.213E-03	-0.760E-05	-0.339E-02	-0.899E+02	0.316E+02	-0.195E-01	-0.943E-02	-0.452E-01	-0.551E+02
	26	0.942E+00	-0.458E-04	0.000E+00	0.000E+00	-0.213E-03	-0.819E-05	-0.373E-02	-0.899E+02	0.316E+02	-0.195E-01	-0.943E-02	-0.565E-01	-0.734E+02
3	27	0.100E+01	-0.129E-04	0.000E+00	0.000E+00	0.341E-03	-0.553E-05	-0.508E-02	-0.316E+02	-0.899E+02	0.195E-01	0.584E-01	-0.679E-01	-0.193E+03
	28	0.550E+00	-0.129E-04	0.000E+00	0.000E+00	0.341E-03	-0.496E-05	-0.417E-02	-0.316E+02	-0.899E+02	0.195E-01	0.584E-01	-0.489E-01	-0.106E+03
	29	0.550E+00	-0.129E-04	0.000E+00	0.000E+00	0.341E-03	-0.382E-05	-0.237E-02	-0.316E+02	-0.899E+02	0.195E-01	0.584E-01	-0.489E-01	-0.106E+03
	30	0.997E-01	-0.129E-04	0.000E+00	0.000E+00	0.341E-03	-0.326E-05	-0.147E-02	-0.316E+02	-0.899E+02	0.195E-01	0.584E-01	-0.299E-01	-0.181E+02
	31	0.997E-01	-0.129E-04	0.000E+00	0.000E+00	0.341E-03	-0.212E-05	0.341E-03	-0.316E+02	-0.899E+02	0.195E-01	0.584E-01	-0.299E-01	-0.181E+02
	32	0.363E+00	-0.129E-04	0.000E+00	0.000E+00	0.341E-03	-0.155E-05	0.124E-02	-0.316E+02	-0.899E+02	0.195E-01	0.584E-01	-0.110E-01	0.693E+02

<STEP: 3> |dGmin= 0.692E+01|									Local Strain Components										Local Stress Components					
|Member |Section|Criterion Values|			q(1)	|	q(2)	|	q(3)	|	q(4)	|	q(5)	|	q(6)	|	Q(1)	|	Q(2)	|	Q(3)	|	Q(4)	|	Q(5)	|	Q(6) |
|	1 |	0.330E+00	|	0.422E-05|	0.000E+00|	0.000E+00|	0.374E-03|	-0.640E-02|	-0.165E-02|	0.103E+02|	-0.324E+02|	0.433E+02|	0.640E-01|	-0.853E+02|	-0.638E+02|
|	2 |	0.168E+00	|	0.422E-05|	0.000E+00|	0.000E+00|	0.374E-03|	-0.514E-02|	-0.133E-02|	0.103E+02|	-0.324E+02|	0.433E+02|	0.640E-01|	-0.432E+02|	-0.323E+02|
|	3 |	0.168E+00	|	0.422E-05|	0.000E+00|	0.000E+00|	0.374E-03|	-0.262E-02|	-0.676E-03|	0.103E+02|	-0.324E+02|	0.433E+02|	0.640E-01|	-0.432E+02|	-0.323E+02|
|	4 |	0.796E-02	|	0.422E-05|	0.000E+00|	0.000E+00|	0.374E-03|	-0.136E-02|	-0.351E-03|	0.103E+02|	-0.324E+02|	0.433E+02|	0.640E-01|	-0.106E+01|	-0.835E+00|
|	5 |	0.796E-02	|	0.422E-05|	0.000E+00|	0.000E+00|	0.374E-03|	0.117E-02|	0.299E-03|	0.103E+02|	-0.324E+02|	0.433E+02|	0.640E-01|	-0.106E+01|	-0.835E+00|
|	6 |	0.160E+00	|	0.422E-05|	0.000E+00|	0.000E+00|	0.374E-03|	0.243E-02|	0.624E-03|	0.103E+02|	-0.324E+02|	0.433E+02|	0.640E-01|	0.411E+02|	0.307E+02|
| 2 |	7 |	0.698E+00	|	-0.468E-04|	0.000E+00|	0.000E+00|	-0.232E-03|	0.896E-05|	0.288E-02|	-0.920E+02|	0.128E+02|	-0.213E-01|	-0.103E-01|	0.618E-01|	0.544E+02|
|	8 |	0.603E+00	|	-0.468E-04|	0.000E+00|	0.000E+00|	-0.232E-03|	0.832E-05|	0.274E-02|	-0.920E+02|	0.128E+02|	-0.213E-01|	-0.103E-01|	0.495E-01|	0.470E+02|
|	9 |	0.603E+00	|	-0.468E-04|	0.000E+00|	0.000E+00|	-0.232E-03|	0.704E-05|	0.245E-02|	-0.920E+02|	0.146E+02|	-0.213E-01|	-0.103E-01|	0.495E-01|	0.470E+02|
|	10 |	0.494E+00	|	-0.468E-04|	0.000E+00|	0.000E+00|	-0.232E-03|	0.640E-05|	0.229E-02|	-0.920E+02|	0.146E+02|	-0.213E-01|	-0.103E-01|	0.371E-01|	0.385E+02|
|	11 |	0.494E+00	|	-0.468E-04|	0.000E+00|	0.000E+00|	-0.232E-03|	0.512E-05|	0.195E-02|	-0.920E+02|	0.170E+02|	-0.213E-01|	-0.103E-01|	0.371E-01|	0.385E+02|
|	12 |	0.368E+00	|	-0.468E-04|	0.000E+00|	0.000E+00|	-0.232E-03|	0.448E-05|	0.177E-02|	-0.920E+02|	0.170E+02|	-0.213E-01|	-0.103E-01|	0.247E-01|	0.287E+02|
|	13 |	0.368E+00	|	-0.468E-04|	0.000E+00|	0.000E+00|	-0.232E-03|	0.320E-05|	0.138E-02|	-0.920E+02|	0.193E+02|	-0.213E-01|	-0.103E-01|	0.247E-01|	0.287E+02|
|	14 |	0.224E+00	|	-0.468E-04|	0.000E+00|	0.000E+00|	-0.232E-03|	0.256E-05|	0.117E-02|	-0.920E+02|	0.193E+02|	-0.213E-01|	-0.103E-01|	0.124E-01|	0.175E+02|
|	15 |	0.224E+00	|	-0.468E-04|	0.000E+00|	0.000E+00|	-0.232E-03|	0.128E-05|	0.737E-03|	-0.920E+02|	0.216E+02|	-0.213E-01|	-0.103E-01|	0.124E-01|	0.175E+02|
|	16 |	0.635E-01	|	-0.468E-04|	0.000E+00|	0.000E+00|	-0.232E-03|	0.640E-06|	0.506E-03|	-0.920E+02|	0.216E+02|	-0.213E-01|	-0.103E-01|	0.904E-17|	0.495E+01|
|	17 |	0.635E-01	|	-0.468E-04|	0.000E+00|	0.000E+00|	-0.232E-03|	-0.640E-06|	0.179E-04|	-0.920E+02|	0.239E+02|	-0.213E-01|	-0.103E-01|	0.904E-17|	0.495E+01|
|	18 |	0.115E+00	|	-0.468E-04|	0.000E+00|	0.000E+00|	-0.232E-03|	-0.128E-05|	-0.238E-03|	-0.920E+02|	0.239E+02|	-0.213E-01|	-0.103E-01|	-0.124E-01|	-0.893E+01|
|	19 |	0.115E+00	|	-0.468E-04|	0.000E+00|	0.000E+00|	-0.232E-03|	-0.256E-05|	-0.776E-03|	-0.920E+02|	0.262E+02|	-0.213E-01|	-0.103E-01|	-0.124E-01|	-0.893E+01|
|	20 |	0.310E+00	|	-0.468E-04|	0.000E+00|	0.000E+00|	-0.232E-03|	-0.320E-05|	-0.106E-02|	-0.920E+02|	0.262E+02|	-0.213E-01|	-0.103E-01|	-0.247E-01|	-0.241E+02|
|	21 |	0.310E+00	|	-0.468E-04|	0.000E+00|	0.000E+00|	-0.232E-03|	-0.448E-05|	-0.164E-02|	-0.920E+02|	0.286E+02|	-0.213E-01|	-0.103E-01|	-0.247E-01|	-0.241E+02|
|	22 |	0.523E+00	|	-0.468E-04|	0.000E+00|	0.000E+00|	-0.232E-03|	-0.512E-05|	-0.195E-02|	-0.920E+02|	0.286E+02|	-0.213E-01|	-0.103E-01|	-0.371E-01|	-0.407E+02|
|	23 |	0.523E+00	|	-0.468E-04|	0.000E+00|	0.000E+00|	-0.232E-03|	-0.640E-05|	-0.259E-02|	-0.920E+02|	0.309E+02|	-0.213E-01|	-0.103E-01|	-0.371E-01|	-0.407E+02|
|	24 |	0.753E+00	|	-0.468E-04|	0.000E+00|	0.000E+00|	-0.232E-03|	-0.704E-05|	-0.292E-02|	-0.920E+02|	0.309E+02|	-0.213E-01|	-0.103E-01|	-0.495E-01|	-0.586E+02|
|	25 |	0.753E+00	|	-0.468E-04|	0.000E+00|	0.000E+00|	-0.232E-03|	-0.832E-05|	-0.360E-02|	-0.920E+02|	0.332E+02|	-0.213E-01|	-0.103E-01|	-0.495E-01|	-0.586E+02|
|	26 |	0.100E+01	|	-0.468E-04|	0.000E+00|	0.000E+00|	-0.232E-03|	-0.896E-05|	-0.396E-02|	-0.920E+02|	0.332E+02|	-0.213E-01|	-0.103E-01|	-0.618E-01|	-0.779E+02|
| 3 |	27 |	0.101E+01	|	-0.514E-04|	0.000E+00|	0.000E+00|	0.374E-03|	-0.605E-05|	-0.610E-02|	-0.332E+02|	-0.920E+02|	0.213E-01|	0.640E-01|	-0.743E-01|	-0.195E+03|
|	28 |	0.548E+00	|	-0.136E-04|	0.000E+00|	0.000E+00|	0.374E-03|	-0.543E-05|	-0.418E-02|	-0.332E+02|	-0.920E+02|	0.213E-01|	0.640E-01|	-0.535E-01|	-0.105E+03|
|	29 |	0.548E+00	|	-0.136E-04|	0.000E+00|	0.000E+00|	0.374E-03|	-0.418E-05|	-0.234E-02|	-0.332E+02|	-0.920E+02|	0.213E-01|	0.640E-01|	-0.535E-01|	-0.105E+03|
|	30 |	0.875E-01	|	-0.136E-04|	0.000E+00|	0.000E+00|	0.374E-03|	-0.356E-05|	-0.141E-02|	-0.332E+02|	-0.920E+02|	0.213E-01|	0.640E-01|	-0.328E-01|	-0.157E+02|
|	31 |	0.875E-01	|	-0.136E-04|	0.000E+00|	0.000E+00|	0.374E-03|	-0.232E-05|	0.438E-03|	-0.332E+02|	-0.920E+02|	0.213E-01|	0.640E-01|	-0.328E-01|	-0.157E+02|
|	32 |	0.387E+00	|	-0.136E-04|	0.000E+00|	0.000E+00|	0.374E-03|	-0.170E-05|	0.136E-02|	-0.332E+02|	-0.920E+02|	0.213E-01|	0.640E-01|	-0.120E-01|	0.738E+02|

<STEP: 4>		dGmin= 0.327E+02	Local Strain Components						Local Stress Components					
Member	Section	Criterion Values	q(1)	q(2)	q(3)	q(4)	q(5)	q(6)	Q(1)	Q(2)	Q(3)	Q(4)	Q(5)	Q(6)
1	1	0.516E+00	0.609E-05	0.000E+00	0.000E+00	0.602E-03	-0.101E-01	-0.260E-02	0.149E+02	-0.491E+02	0.657E+02	0.103E+00	-0.133E+03	-0.998E+02
	2	0.270E+00	0.609E-05	0.000E+00	0.000E+00	0.602E-03	-0.815E-02	-0.210E-02	0.149E+02	-0.491E+02	0.657E+02	0.103E+00	-0.694E+02	-0.520E+02
	3	0.270E+00	0.609E-05	0.000E+00	0.000E+00	0.602E-03	-0.432E-02	-0.112E-02	0.149E+02	-0.491E+02	0.657E+02	0.103E+00	-0.694E+02	-0.520E+02
	4	0.250E-01	0.609E-05	0.000E+00	0.000E+00	0.602E-03	-0.241E-02	-0.623E-03	0.149E+02	-0.491E+02	0.657E+02	0.103E+00	-0.549E+01	-0.417E+01
	5	0.250E-01	0.609E-05	0.000E+00	0.000E+00	0.602E-03	0.142E-02	0.364E-03	0.149E+02	-0.491E+02	0.657E+02	0.103E+00	-0.549E+01	-0.417E+01
	6	0.228E+00	0.609E-05	0.000E+00	0.000E+00	0.602E-03	0.334E-02	0.858E-03	0.149E+02	-0.491E+02	0.657E+02	0.103E+00	0.585E+02	0.436E+02
2	7	0.100E+01	-0.492E-04	0.000E+00	0.000E+00	-0.393E-03	0.144E-04	0.413E-02	-0.967E+02	0.173E+02	-0.343E-01	-0.174E-01	0.995E-01	0.779E+02
	8	0.871E+00	-0.492E-04	0.000E+00	0.000E+00	-0.393E-03	0.134E-04	0.394E-02	-0.967E+02	0.173E+02	-0.343E-01	-0.174E-01	0.796E-01	0.678E+02
	9	0.871E+00	-0.492E-04	0.000E+00	0.000E+00	-0.393E-03	0.113E-04	0.355E-02	-0.967E+02	0.192E+02	-0.343E-01	-0.174E-01	0.796E-01	0.678E+02
	10	0.728E+00	-0.492E-04	0.000E+00	0.000E+00	-0.393E-03	0.103E-04	0.335E-02	-0.967E+02	0.192E+02	-0.343E-01	-0.174E-01	0.597E-01	0.567E+02
	11	0.728E+00	-0.492E-04	0.000E+00	0.000E+00	-0.393E-03	0.824E-05	0.291E-02	-0.967E+02	0.215E+02	-0.343E-01	-0.174E-01	0.597E-01	0.567E+02
	12	0.568E+00	-0.492E-04	0.000E+00	0.000E+00	-0.393E-03	0.721E-05	0.268E-02	-0.967E+02	0.215E+02	-0.343E-01	-0.174E-01	0.398E-01	0.442E+02
	13	0.568E+00	-0.492E-04	0.000E+00	0.000E+00	-0.393E-03	0.515E-05	0.219E-02	-0.967E+02	0.238E+02	-0.343E-01	-0.174E-01	0.398E-01	0.442E+02
	14	0.390E+00	-0.492E-04	0.000E+00	0.000E+00	-0.393E-03	0.412E-05	0.194E-02	-0.967E+02	0.238E+02	-0.343E-01	-0.174E-01	0.199E-01	0.304E+02
	15	0.390E+00	-0.492E-04	0.000E+00	0.000E+00	-0.393E-03	0.206E-05	0.140E-02	-0.967E+02	0.262E+02	-0.343E-01	-0.174E-01	0.199E-01	0.304E+02
	16	0.195E+00	-0.492E-04	0.000E+00	0.000E+00	-0.393E-03	0.103E-05	0.112E-02	-0.967E+02	0.262E+02	-0.343E-01	-0.174E-01	0.904E-17	0.152E+02
	17	0.195E+00	-0.492E-04	0.000E+00	0.000E+00	-0.393E-03	-0.103E-05	0.538E-03	-0.967E+02	0.285E+02	-0.343E-01	-0.174E-01	0.904E-17	0.152E+02
	18	0.167E-01	-0.492E-04	0.000E+00	0.000E+00	-0.393E-03	-0.206E-05	0.233E-03	-0.967E+02	0.285E+02	-0.343E-01	-0.174E-01	-0.199E-01	-0.130E+01
	19	0.167E-01	-0.492E-04	0.000E+00	0.000E+00	-0.393E-03	-0.412E-05	-0.402E-03	-0.967E+02	0.308E+02	-0.343E-01	-0.174E-01	-0.199E-01	-0.130E+01
	20	0.246E+00	-0.492E-04	0.000E+00	0.000E+00	-0.393E-03	-0.515E-05	-0.732E-03	-0.967E+02	0.308E+02	-0.343E-01	-0.174E-01	-0.398E-01	-0.192E+02
	21	0.246E+00	-0.492E-04	0.000E+00	0.000E+00	-0.393E-03	-0.721E-05	-0.142E-02	-0.967E+02	0.331E+02	-0.343E-01	-0.174E-01	-0.398E-01	-0.192E+02
	22	0.493E+00	-0.492E-04	0.000E+00	0.000E+00	-0.393E-03	-0.824E-05	-0.177E-02	-0.967E+02	0.331E+02	-0.343E-01	-0.174E-01	-0.597E-01	-0.384E+02
	23	0.493E+00	-0.492E-04	0.000E+00	0.000E+00	-0.393E-03	-0.103E-04	-0.251E-02	-0.967E+02	0.354E+02	-0.343E-01	-0.174E-01	-0.597E-01	-0.384E+02
	24	0.757E+00	-0.492E-04	0.000E+00	0.000E+00	-0.393E-03	-0.113E-04	-0.289E-02	-0.967E+02	0.354E+02	-0.343E-01	-0.174E-01	-0.796E-01	-0.589E+02
	25	0.757E+00	-0.492E-04	0.000E+00	0.000E+00	-0.393E-03	-0.134E-04	-0.367E-02	-0.967E+02	0.378E+02	-0.343E-01	-0.174E-01	-0.796E-01	-0.589E+02
	26	0.104E+01	-0.492E-04	0.000E+00	0.000E+00	-0.393E-03	-0.144E-04	-0.145E-01	-0.967E+02	0.378E+02	-0.343E-01	-0.174E-01	-0.995E-01	-0.808E+02
3	27	0.106E+01	-0.160E-03	0.000E+00	0.000E+00	0.602E-03	-0.982E-05	-0.126E-01	-0.378E+02	-0.967E+02	0.343E-01	0.103E+00	-0.120E+00	-0.205E+03
	28	0.580E+00	-0.155E-04	0.000E+00	0.000E+00	0.602E-03	-0.882E-05	-0.442E-02	-0.378E+02	-0.967E+02	0.343E-01	0.103E+00	-0.870E-01	-0.111E+03
	29	0.580E+00	-0.155E-04	0.000E+00	0.000E+00	0.602E-03	-0.681E-05	-0.248E-02	-0.378E+02	-0.967E+02	0.343E-01	0.103E+00	-0.870E-01	-0.111E+03
	30	0.961E-01	-0.155E-04	0.000E+00	0.000E+00	0.602E-03	-0.581E-05	-0.150E-02	-0.378E+02	-0.967E+02	0.343E-01	0.103E+00	-0.536E-01	-0.172E+02
	31	0.961E-01	-0.155E-04	0.000E+00	0.000E+00	0.602E-03	-0.381E-05	0.438E-03	-0.378E+02	-0.967E+02	0.343E-01	0.103E+00	-0.536E-01	-0.172E+02
	32	0.403E+00	-0.155E-04	0.000E+00	0.000E+00	0.602E-03	-0.281E-05	0.141E-02	-0.378E+02	-0.967E+02	0.343E-01	0.103E+00	-0.202E-01	0.769E+02

```
+---------------+---------------+-----------------------------------------------------------------+-----------------------------------------------------------------+
| <STEP:     5> |dGmin= 0.685E+02|                   Local Strain Components                       |                   Local Stress Components                       |
+-------+-------+---------------+----------+----------+----------+----------+----------+----------+----------+----------+----------+----------+----------+----------+
|Member |Section|Criterion Values|   q(1)   |   q(2)   |   q(3)   |   q(4)   |   q(5)   |   q(6)   |   Q(1)   |   Q(2)   |   Q(3)   |   Q(4)   |   Q(5)   |   Q(6)   |
+-------+-------+---------------+----------+----------+----------+----------+----------+----------+----------+----------+----------+----------+----------+----------+
|     1 |     1 |    0.100E+01   | 0.714E-05| 0.000E+00| 0.000E+00| 0.132E-02|-0.200E-01|-0.517E-02| 0.175E+02|-0.822E+02| 0.110E+03| 0.227E+00|-0.259E+03|-0.194E+03|
|       |     2 |    0.588E+00   | 0.714E-05| 0.000E+00| 0.000E+00| 0.132E-02|-0.168E-01|-0.435E-02| 0.175E+02|-0.822E+02| 0.110E+03| 0.227E+00|-0.152E+03|-0.114E+03|
|       |     3 |    0.588E+00   | 0.714E-05| 0.000E+00| 0.000E+00| 0.132E-02|-0.104E-01|-0.270E-02| 0.175E+02|-0.822E+02| 0.110E+03| 0.227E+00|-0.152E+03|-0.114E+03|
|       |     4 |    0.177E+00   | 0.714E-05| 0.000E+00| 0.000E+00| 0.132E-02|-0.724E-02|-0.187E-02| 0.175E+02|-0.822E+02| 0.110E+03| 0.227E+00|-0.449E+02|-0.337E+02|
|       |     5 |    0.177E+00   | 0.714E-05| 0.000E+00| 0.000E+00| 0.132E-02|-0.831E-03|-0.218E-03| 0.175E+02|-0.822E+02| 0.110E+03| 0.227E+00|-0.449E+02|-0.337E+02|
|       |     6 |    0.242E+00   | 0.714E-05| 0.000E+00| 0.000E+00| 0.132E-02| 0.237E-02| 0.608E-03| 0.175E+02|-0.822E+02| 0.110E+03| 0.227E+00| 0.621E+02| 0.463E+02|
+-------+-------+---------------+----------+----------+----------+----------+----------+----------+----------+----------+----------+----------+----------+----------+
|     2 |     7 |    0.111E+01   |-0.560E-04| 0.000E+00| 0.000E+00|-0.103E-02| 0.317E-04| 0.349E-01|-0.110E+03| 0.199E+02|-0.755E-01|-0.458E-01| 0.219E+00| 0.865E+02|
|       |     8 |    0.963E+00   |-0.560E-04| 0.000E+00| 0.000E+00|-0.103E-02| 0.295E-04| 0.437E-02|-0.110E+03| 0.199E+02|-0.755E-01|-0.458E-01| 0.175E+00| 0.750E+02|
|       |     9 |    0.963E+00   |-0.560E-04| 0.000E+00| 0.000E+00|-0.103E-02| 0.249E-04| 0.392E-02|-0.110E+03| 0.218E+02|-0.755E-01|-0.458E-01| 0.175E+00| 0.750E+02|
|       |    10 |    0.800E+00   |-0.560E-04| 0.000E+00| 0.000E+00|-0.103E-02| 0.227E-04| 0.369E-02|-0.110E+03| 0.218E+02|-0.755E-01|-0.458E-01| 0.131E+00| 0.623E+02|
|       |    11 |    0.800E+00   |-0.560E-04| 0.000E+00| 0.000E+00|-0.103E-02| 0.181E-04| 0.320E-02|-0.110E+03| 0.241E+02|-0.755E-01|-0.458E-01| 0.131E+00| 0.623E+02|
|       |    12 |    0.621E+00   |-0.560E-04| 0.000E+00| 0.000E+00|-0.103E-02| 0.159E-04| 0.294E-02|-0.110E+03| 0.241E+02|-0.755E-01|-0.458E-01| 0.876E-01| 0.483E+02|
|       |    13 |    0.621E+00   |-0.560E-04| 0.000E+00| 0.000E+00|-0.103E-02| 0.113E-04| 0.240E-02|-0.110E+03| 0.264E+02|-0.755E-01|-0.458E-01| 0.876E-01| 0.483E+02|
|       |    14 |    0.424E+00   |-0.560E-04| 0.000E+00| 0.000E+00|-0.103E-02| 0.907E-05| 0.211E-02|-0.110E+03| 0.264E+02|-0.755E-01|-0.458E-01| 0.438E-01| 0.330E+02|
|       |    15 |    0.424E+00   |-0.560E-04| 0.000E+00| 0.000E+00|-0.103E-02| 0.453E-05| 0.152E-02|-0.110E+03| 0.287E+02|-0.755E-01|-0.458E-01| 0.438E-01| 0.330E+02|
|       |    16 |    0.210E+00   |-0.560E-04| 0.000E+00| 0.000E+00|-0.103E-02| 0.227E-05| 0.121E-02|-0.110E+03| 0.287E+02|-0.755E-01|-0.458E-01| 0.239E-16| 0.164E+02|
|       |    17 |    0.210E+00   |-0.560E-04| 0.000E+00| 0.000E+00|-0.103E-02|-0.227E-05| 0.573E-03|-0.110E+03| 0.311E+02|-0.755E-01|-0.458E-01| 0.239E-16| 0.164E+02|
|       |    18 |    0.213E-01   |-0.560E-04| 0.000E+00| 0.000E+00|-0.103E-02|-0.453E-05| 0.241E-03|-0.110E+03| 0.311E+02|-0.755E-01|-0.458E-01|-0.438E-01|-0.166E+01|
|       |    19 |    0.213E-01   |-0.560E-04| 0.000E+00| 0.000E+00|-0.103E-02|-0.907E-05|-0.450E-03|-0.110E+03| 0.334E+02|-0.755E-01|-0.458E-01|-0.438E-01|-0.166E+01|
|       |    20 |    0.270E+00   |-0.560E-04| 0.000E+00| 0.000E+00|-0.103E-02|-0.113E-04|-0.807E-03|-0.110E+03| 0.334E+02|-0.755E-01|-0.458E-01|-0.876E-01|-0.210E+02|
|       |    21 |    0.270E+00   |-0.560E-04| 0.000E+00| 0.000E+00|-0.103E-02|-0.159E-04|-0.155E-02|-0.110E+03| 0.357E+02|-0.755E-01|-0.458E-01|-0.876E-01|-0.210E+02|
|       |    22 |    0.536E+00   |-0.560E-04| 0.000E+00| 0.000E+00|-0.103E-02|-0.181E-04|-0.193E-02|-0.110E+03| 0.357E+02|-0.755E-01|-0.458E-01|-0.131E+00|-0.417E+02|
|       |    23 |    0.536E+00   |-0.560E-04| 0.000E+00| 0.000E+00|-0.103E-02|-0.227E-04|-0.272E-02|-0.110E+03| 0.380E+02|-0.755E-01|-0.458E-01|-0.131E+00|-0.417E+02|
|       |    24 |    0.819E+00   |-0.560E-04| 0.000E+00| 0.000E+00|-0.103E-02|-0.249E-04|-0.313E-02|-0.110E+03| 0.380E+02|-0.755E-01|-0.458E-01|-0.175E+00|-0.638E+02|
|       |    25 |    0.819E+00   |-0.560E-04| 0.000E+00| 0.000E+00|-0.103E-02|-0.295E-04|-0.397E-02|-0.110E+03| 0.403E+02|-0.755E-01|-0.458E-01|-0.175E+00|-0.638E+02|
|       |    26 |    0.112E+01   |-0.560E-04| 0.000E+00| 0.000E+00|-0.103E-02|-0.317E-04|-0.371E-01|-0.110E+03| 0.403E+02|-0.755E-01|-0.458E-01|-0.219E+00|-0.872E+02|
+-------+-------+---------------+----------+----------+----------+----------+----------+----------+----------+----------+----------+----------+----------+----------+
|     3 |    27 |    0.124E+01   |-0.221E-03| 0.000E+00| 0.000E+00| 0.132E-02|-0.223E-04|-0.330E-01|-0.403E+02|-0.110E+03| 0.755E-01| 0.227E+00|-0.272E+00|-0.239E+03|
|       |    28 |    0.685E+00   |-0.165E-04| 0.000E+00| 0.000E+00| 0.132E-02|-0.201E-04|-0.518E-02|-0.403E+02|-0.110E+03| 0.755E-01| 0.227E+00|-0.199E+00|-0.132E+03|
|       |    29 |    0.685E+00   |-0.165E-04| 0.000E+00| 0.000E+00| 0.132E-02|-0.157E-04|-0.297E-02|-0.403E+02|-0.110E+03| 0.755E-01| 0.227E+00|-0.199E+00|-0.132E+03|
|       |    30 |    0.135E+00   |-0.165E-04| 0.000E+00| 0.000E+00| 0.132E-02|-0.135E-04|-0.187E-02|-0.403E+02|-0.110E+03| 0.755E-01| 0.227E+00|-0.125E+00|-0.246E+02|
|       |    31 |    0.135E+00   |-0.165E-04| 0.000E+00| 0.000E+00| 0.132E-02|-0.906E-05| 0.343E-03|-0.403E+02|-0.110E+03| 0.755E-01| 0.227E+00|-0.125E+00|-0.246E+02|
|       |    32 |    0.432E+00   |-0.165E-04| 0.000E+00| 0.000E+00| 0.132E-02|-0.686E-05| 0.145E-02|-0.403E+02|-0.110E+03| 0.755E-01| 0.227E+00|-0.519E-01| 0.824E+02|
+-------+-------+---------------+----------+----------+----------+----------+----------+----------+----------+----------+----------+----------+----------+----------+
```

<STEP: 6>		dGmin= 0.305E+01	Local Strain Components						Local Stress Components					
Member	Section	Criterion Values	q(1)	q(2)	q(3)	q(4)	q(5)	q(6)	Q(1)	Q(2)	Q(3)	Q(4)	Q(5)	Q(6)
1	1	0.102E+01	0.116E-04	0.000E+00	0.000E+00	0.123E-02	-0.204E-01	-0.709E-02	0.176E+02	-0.833E+02	0.111E+03	0.210E+00	-0.263E+03	-0.197E+03
	2	0.599E+00	0.722E-05	0.000E+00	0.000E+00	0.123E-02	-0.171E-01	-0.442E-02	0.176E+02	-0.833E+02	0.111E+03	0.210E+00	-0.155E+03	-0.116E+03
	3	0.599E+00	0.722E-05	0.000E+00	0.000E+00	0.123E-02	-0.106E-01	-0.275E-02	0.176E+02	-0.833E+02	0.111E+03	0.210E+00	-0.155E+03	-0.116E+03
	4	0.181E+00	0.722E-05	0.000E+00	0.000E+00	0.123E-02	-0.739E-02	-0.191E-02	0.176E+02	-0.833E+02	0.111E+03	0.210E+00	-0.461E+02	-0.346E+02
	5	0.181E+00	0.722E-05	0.000E+00	0.000E+00	0.123E-02	-0.890E-03	-0.233E-03	0.176E+02	-0.833E+02	0.111E+03	0.210E+00	-0.461E+02	-0.346E+02
	6	0.243E+00	0.722E-05	0.000E+00	0.000E+00	0.123E-02	0.236E-02	0.604E-03	0.176E+02	-0.833E+02	0.111E+03	0.210E+00	0.624E+02	0.466E+02
2	7	0.112E+01	-0.565E-04	0.000E+00	0.000E+00	-0.981E-03	0.294E-04	0.369E-01	-0.111E+03	0.201E+02	-0.700E-01	-0.435E-01	0.203E+00	0.871E+02
	8	0.969E+00	-0.565E-04	0.000E+00	0.000E+00	-0.981E-03	0.273E-04	0.440E-02	-0.111E+03	0.201E+02	-0.700E-01	-0.435E-01	0.162E+00	0.754E+02
	9	0.969E+00	-0.565E-04	0.000E+00	0.000E+00	-0.981E-03	0.231E-04	0.394E-02	-0.111E+03	0.220E+02	-0.700E-01	-0.435E-01	0.162E+00	0.754E+02
	10	0.805E+00	-0.565E-04	0.000E+00	0.000E+00	-0.981E-03	0.210E-04	0.371E-02	-0.111E+03	0.220E+02	-0.700E-01	-0.435E-01	0.122E+00	0.627E+02
	11	0.805E+00	-0.565E-04	0.000E+00	0.000E+00	-0.981E-03	0.168E-04	0.321E-02	-0.111E+03	0.243E+02	-0.700E-01	-0.435E-01	0.122E+00	0.627E+02
	12	0.624E+00	-0.565E-04	0.000E+00	0.000E+00	-0.981E-03	0.147E-04	0.295E-02	-0.111E+03	0.243E+02	-0.700E-01	-0.435E-01	0.812E-01	0.486E+02
	13	0.624E+00	-0.565E-04	0.000E+00	0.000E+00	-0.981E-03	0.105E-04	0.241E-02	-0.111E+03	0.266E+02	-0.700E-01	-0.435E-01	0.812E-01	0.486E+02
	14	0.426E+00	-0.565E-04	0.000E+00	0.000E+00	-0.981E-03	0.840E-05	0.212E-02	-0.111E+03	0.266E+02	-0.700E-01	-0.435E-01	0.406E-01	0.332E+02
	15	0.426E+00	-0.565E-04	0.000E+00	0.000E+00	-0.981E-03	0.420E-05	0.153E-02	-0.111E+03	0.289E+02	-0.700E-01	-0.435E-01	0.406E-01	0.332E+02
	16	0.210E+00	-0.565E-04	0.000E+00	0.000E+00	-0.981E-03	0.210E-05	0.122E-02	-0.111E+03	0.289E+02	-0.700E-01	-0.435E-01	0.239E-16	0.164E+02
	17	0.210E+00	-0.565E-04	0.000E+00	0.000E+00	-0.981E-03	-0.210E-05	0.573E-03	-0.111E+03	0.313E+02	-0.700E-01	-0.435E-01	0.239E-16	0.164E+02
	18	0.224E-01	-0.565E-04	0.000E+00	0.000E+00	-0.981E-03	-0.420E-05	0.238E-03	-0.111E+03	0.313E+02	-0.700E-01	-0.435E-01	-0.406E-01	-0.174E+01
	19	0.224E-01	-0.565E-04	0.000E+00	0.000E+00	-0.981E-03	-0.840E-05	-0.456E-03	-0.111E+03	0.336E+02	-0.700E-01	-0.435E-01	-0.406E-01	-0.174E+01
	20	0.272E+00	-0.565E-04	0.000E+00	0.000E+00	-0.981E-03	-0.105E-04	-0.816E-03	-0.111E+03	0.336E+02	-0.700E-01	-0.435E-01	-0.812E-01	-0.212E+02
	21	0.272E+00	-0.565E-04	0.000E+00	0.000E+00	-0.981E-03	-0.147E-04	-0.156E-02	-0.111E+03	0.359E+02	-0.700E-01	-0.435E-01	-0.812E-01	-0.212E+02
	22	0.540E+00	-0.565E-04	0.000E+00	0.000E+00	-0.981E-03	-0.168E-04	-0.194E-02	-0.111E+03	0.359E+02	-0.700E-01	-0.435E-01	-0.122E+00	-0.420E+02
	23	0.540E+00	-0.565E-04	0.000E+00	0.000E+00	-0.981E-03	-0.210E-04	-0.274E-02	-0.111E+03	0.382E+02	-0.700E-01	-0.435E-01	-0.122E+00	-0.420E+02
	24	0.824E+00	-0.565E-04	0.000E+00	0.000E+00	-0.981E-03	-0.231E-04	-0.315E-02	-0.111E+03	0.382E+02	-0.700E-01	-0.435E-01	-0.162E+00	-0.642E+02
	25	0.824E+00	-0.565E-04	0.000E+00	0.000E+00	-0.981E-03	-0.273E-04	-0.399E-02	-0.111E+03	0.405E+02	-0.700E-01	-0.435E-01	-0.162E+00	-0.642E+02
	26	0.113E+01	-0.565E-04	0.000E+00	0.000E+00	-0.981E-03	-0.294E-04	-0.389E-01	-0.111E+03	0.405E+02	-0.700E-01	-0.435E-01	-0.203E+00	-0.877E+02
3	27	0.125E+01	-0.225E-03	0.000E+00	0.000E+00	0.123E-02	-0.207E-04	-0.347E-01	-0.405E+02	-0.111E+03	0.700E-01	0.210E+00	-0.253E+00	-0.241E+03
	28	0.694E+00	-0.166E-04	0.000E+00	0.000E+00	0.123E-02	-0.187E-04	-0.524E-02	-0.405E+02	-0.111E+03	0.700E-01	0.210E+00	-0.185E+00	-0.133E+03
	29	0.694E+00	-0.166E-04	0.000E+00	0.000E+00	0.123E-02	-0.146E-04	-0.301E-02	-0.405E+02	-0.111E+03	0.700E-01	0.210E+00	-0.185E+00	-0.133E+03
	30	0.138E+00	-0.166E-04	0.000E+00	0.000E+00	0.123E-02	-0.126E-04	-0.190E-02	-0.405E+02	-0.111E+03	0.700E-01	0.210E+00	-0.117E+00	-0.252E+02
	31	0.138E+00	-0.166E-04	0.000E+00	0.000E+00	0.123E-02	-0.849E-05	0.335E-03	-0.405E+02	-0.111E+03	0.700E-01	0.210E+00	-0.117E+00	-0.252E+02
	32	0.435E+00	-0.166E-04	0.000E+00	0.000E+00	0.123E-02	-0.645E-05	0.145E-02	-0.405E+02	-0.111E+03	0.700E-01	0.210E+00	-0.491E-01	0.829E+02

<STEP: 7> |dGmin= 0.110E+02|							Local Strain Components						Local Stress Components					
|Member |Section|Criterion Values|			q(1)	q(2)	q(3)	q(4)	q(5)	q(6)	Q(1)	Q(2)	Q(3)	Q(4)	Q(5)	Q(6)
1	1	0.110E+01	0.345E-04	0.000E+00	0.000E+00	0.722E-03	-0.221E-01	-0.171E-01	0.186E+02	-0.894E+02	0.120E+03	0.124E+00	-0.285E+03	-0.213E+03
	2	0.652E+00	0.762E-05	0.000E+00	0.000E+00	0.722E-03	-0.186E-01	-0.480E-02	0.186E+02	-0.894E+02	0.120E+03	0.124E+00	-0.169E+03	-0.126E+03
	3	0.652E+00	0.762E-05	0.000E+00	0.000E+00	0.722E-03	-0.117E-01	-0.301E-02	0.186E+02	-0.894E+02	0.120E+03	0.124E+00	-0.169E+03	-0.126E+03
	4	0.205E+00	0.762E-05	0.000E+00	0.000E+00	0.722E-03	-0.817E-02	-0.211E-02	0.186E+02	-0.894E+02	0.120E+03	0.124E+00	-0.522E+02	-0.391E+02
	5	0.205E+00	0.762E-05	0.000E+00	0.000E+00	0.722E-03	-0.120E-02	-0.312E-03	0.186E+02	-0.894E+02	0.120E+03	0.124E+00	-0.522E+02	-0.391E+02
	6	0.250E+00	0.762E-05	0.000E+00	0.000E+00	0.722E-03	0.228E-02	0.587E-03	0.186E+02	-0.894E+02	0.120E+03	0.124E+00	0.642E+02	0.479E+02
2	7	0.116E+01	-0.570E-04	0.000E+00	0.000E+00	-0.706E-03	0.173E-04	0.476E-01	-0.112E+03	0.210E+02	-0.412E-01	-0.313E-01	0.119E+00	0.901E+02
	8	0.100E+01	-0.570E-04	0.000E+00	0.000E+00	-0.706E-03	0.161E-04	0.454E-02	-0.112E+03	0.210E+02	-0.412E-01	-0.313E-01	0.955E-01	0.779E+02
	9	0.100E+01	-0.570E-04	0.000E+00	0.000E+00	-0.706E-03	0.136E-04	0.407E-02	-0.112E+03	0.229E+02	-0.412E-01	-0.313E-01	0.955E-01	0.779E+02
	10	0.829E+00	-0.570E-04	0.000E+00	0.000E+00	-0.706E-03	0.124E-04	0.382E-02	-0.112E+03	0.229E+02	-0.412E-01	-0.313E-01	0.717E-01	0.646E+02
	11	0.829E+00	-0.570E-04	0.000E+00	0.000E+00	-0.706E-03	0.989E-05	0.331E-02	-0.112E+03	0.253E+02	-0.412E-01	-0.313E-01	0.717E-01	0.646E+02
	12	0.641E+00	-0.570E-04	0.000E+00	0.000E+00	-0.706E-03	0.865E-05	0.304E-02	-0.112E+03	0.253E+02	-0.412E-01	-0.313E-01	0.478E-01	0.499E+02
	13	0.641E+00	-0.570E-04	0.000E+00	0.000E+00	-0.706E-03	0.618E-05	0.247E-02	-0.112E+03	0.276E+02	-0.412E-01	-0.313E-01	0.478E-01	0.499E+02
	14	0.436E+00	-0.570E-04	0.000E+00	0.000E+00	-0.706E-03	0.495E-05	0.218E-02	-0.112E+03	0.276E+02	-0.412E-01	-0.313E-01	0.239E-01	0.339E+02
	15	0.436E+00	-0.570E-04	0.000E+00	0.000E+00	-0.706E-03	0.247E-05	0.156E-02	-0.112E+03	0.299E+02	-0.412E-01	-0.313E-01	0.239E-01	0.339E+02
	16	0.213E+00	-0.570E-04	0.000E+00	0.000E+00	-0.706E-03	0.124E-05	0.124E-02	-0.112E+03	0.299E+02	-0.412E-01	-0.313E-01	-0.143E-16	0.166E+02
	17	0.213E+00	-0.570E-04	0.000E+00	0.000E+00	-0.706E-03	-0.124E-05	0.574E-03	-0.112E+03	0.322E+02	-0.412E-01	-0.313E-01	-0.143E-16	0.166E+02
	18	0.269E-01	-0.570E-04	0.000E+00	0.000E+00	-0.706E-03	-0.247E-05	0.229E-03	-0.112E+03	0.322E+02	-0.412E-01	-0.313E-01	-0.239E-01	-0.209E+01
	19	0.269E-01	-0.570E-04	0.000E+00	0.000E+00	-0.706E-03	-0.495E-05	-0.486E-03	-0.112E+03	0.345E+02	-0.412E-01	-0.313E-01	-0.239E-01	-0.209E+01
	20	0.284E+00	-0.570E-04	0.000E+00	0.000E+00	-0.706E-03	-0.618E-05	-0.856E-03	-0.112E+03	0.345E+02	-0.412E-01	-0.313E-01	-0.478E-01	-0.221E+02
	21	0.284E+00	-0.570E-04	0.000E+00	0.000E+00	-0.706E-03	-0.865E-05	-0.162E-02	-0.112E+03	0.369E+02	-0.412E-01	-0.313E-01	-0.478E-01	-0.221E+02
	22	0.559E+00	-0.570E-04	0.000E+00	0.000E+00	-0.706E-03	-0.989E-05	-0.202E-02	-0.112E+03	0.369E+02	-0.412E-01	-0.313E-01	-0.717E-01	-0.435E+02
	23	0.559E+00	-0.570E-04	0.000E+00	0.000E+00	-0.706E-03	-0.124E-04	-0.283E-02	-0.112E+03	0.392E+02	-0.412E-01	-0.313E-01	-0.717E-01	-0.435E+02
	24	0.850E+00	-0.570E-04	0.000E+00	0.000E+00	-0.706E-03	-0.136E-04	-0.325E-02	-0.112E+03	0.392E+02	-0.412E-01	-0.313E-01	-0.955E-01	-0.662E+02
	25	0.850E+00	-0.570E-04	0.000E+00	0.000E+00	-0.706E-03	-0.161E-04	-0.411E-02	-0.112E+03	0.415E+02	-0.412E-01	-0.313E-01	-0.955E-01	-0.662E+02
	26	0.116E+01	-0.570E-04	0.000E+00	0.000E+00	-0.706E-03	-0.173E-04	-0.481E-01	-0.112E+03	0.415E+02	-0.412E-01	-0.313E-01	-0.119E+00	-0.903E+02
3	27	0.125E+01	-0.595E-03	0.000E+00	0.000E+00	0.722E-03	-0.127E-04	-0.442E-01	-0.415E+02	-0.112E+03	0.412E-01	0.124E+00	-0.155E+00	-0.241E+03
	28	0.689E+00	-0.170E-04	0.000E+00	0.000E+00	0.722E-03	-0.115E-04	-0.522E-02	-0.415E+02	-0.112E+03	0.412E-01	0.124E+00	-0.115E+00	-0.132E+03
	29	0.689E+00	-0.170E-04	0.000E+00	0.000E+00	0.722E-03	-0.911E-05	-0.298E-02	-0.415E+02	-0.112E+03	0.412E-01	0.124E+00	-0.115E+00	-0.132E+03
	30	0.129E+00	-0.170E-04	0.000E+00	0.000E+00	0.722E-03	-0.791E-05	-0.185E-02	-0.415E+02	-0.112E+03	0.412E-01	0.124E+00	-0.747E-01	-0.235E+02
	31	0.129E+00	-0.170E-04	0.000E+00	0.000E+00	0.722E-03	-0.551E-05	0.398E-03	-0.415E+02	-0.112E+03	0.412E-01	0.124E+00	-0.747E-01	-0.235E+02
	32	0.448E+00	-0.170E-04	0.000E+00	0.000E+00	0.722E-03	-0.431E-05	0.152E-02	-0.415E+02	-0.112E+03	0.412E-01	0.124E+00	-0.346E-01	0.855E+02

<STEP: 8>		dGmin= 0.189E+02	Local Strain Components						Local Stress Components					
Member	Section	Criterion Values	q(1)	q(2)	q(3)	q(4)	q(5)	q(6)	Q(1)	Q(2)	Q(3)	Q(4)	Q(5)	Q(6)
1	1	0.125E+01	0.650E-04	0.000E+00	0.000E+00	-0.176E-03	-0.252E-01	-0.350E-01	0.199E+02	-0.996E+02	0.133E+03	-0.300E-01	-0.324E+03	-0.242E+03
	2	0.751E+00	0.814E-05	0.000E+00	0.000E+00	-0.176E-03	-0.213E-01	-0.550E-02	0.199E+02	-0.996E+02	0.133E+03	-0.300E-01	-0.194E+03	-0.145E+03
	3	0.751E+00	0.814E-05	0.000E+00	0.000E+00	-0.176E-03	-0.136E-01	-0.350E-02	0.199E+02	-0.996E+02	0.133E+03	-0.300E-01	-0.194E+03	-0.145E+03
	4	0.252E+00	0.814E-05	0.000E+00	0.000E+00	-0.176E-03	-0.969E-02	-0.249E-02	0.199E+02	-0.996E+02	0.133E+03	-0.300E-01	-0.646E+02	-0.482E+02
	5	0.252E+00	0.814E-05	0.000E+00	0.000E+00	-0.176E-03	-0.191E-02	-0.492E-03	0.199E+02	-0.996E+02	0.133E+03	-0.300E-01	-0.646E+02	-0.482E+02
	6	0.255E+00	0.814E-05	0.000E+00	0.000E+00	-0.176E-03	0.198E-02	0.509E-03	0.199E+02	-0.996E+02	0.133E+03	-0.300E-01	0.653E+02	0.487E+02
2	7	0.119E+01	-0.578E-04	0.000E+00	0.000E+00	-0.225E-03	-0.421E-05	0.568E-01	-0.114E+03	0.223E+02	0.100E-01	-0.999E-02	-0.290E-01	0.927E+02
	8	0.102E+01	-0.578E-04	0.000E+00	0.000E+00	-0.225E-03	-0.391E-05	0.111E-01	-0.114E+03	0.223E+02	0.100E-01	-0.999E-02	-0.232E-01	0.797E+02
	9	0.102E+01	-0.578E-04	0.000E+00	0.000E+00	-0.225E-03	-0.331E-05	0.106E-01	-0.114E+03	0.242E+02	0.100E-01	-0.999E-02	-0.232E-01	0.797E+02
	10	0.843E+00	-0.578E-04	0.000E+00	0.000E+00	-0.225E-03	-0.301E-05	0.390E-02	-0.114E+03	0.242E+02	0.100E-01	-0.999E-02	-0.174E-01	0.656E+02
	11	0.843E+00	-0.578E-04	0.000E+00	0.000E+00	-0.225E-03	-0.241E-05	0.335E-02	-0.114E+03	0.265E+02	0.100E-01	-0.999E-02	-0.174E-01	0.656E+02
	12	0.645E+00	-0.578E-04	0.000E+00	0.000E+00	-0.225E-03	-0.211E-05	0.307E-02	-0.114E+03	0.265E+02	0.100E-01	-0.999E-02	-0.116E-01	0.503E+02
	13	0.645E+00	-0.578E-04	0.000E+00	0.000E+00	-0.225E-03	-0.150E-05	0.248E-02	-0.114E+03	0.289E+02	0.100E-01	-0.999E-02	-0.116E-01	0.503E+02
	14	0.430E+00	-0.578E-04	0.000E+00	0.000E+00	-0.225E-03	-0.120E-05	0.217E-02	-0.114E+03	0.289E+02	0.100E-01	-0.999E-02	-0.581E-02	0.335E+02
	15	0.430E+00	-0.578E-04	0.000E+00	0.000E+00	-0.225E-03	-0.601E-06	0.152E-02	-0.114E+03	0.312E+02	0.100E-01	-0.999E-02	-0.581E-02	0.335E+02
	16	0.198E+00	-0.578E-04	0.000E+00	0.000E+00	-0.225E-03	-0.301E-06	0.119E-02	-0.114E+03	0.312E+02	0.100E-01	-0.999E-02	-0.143E-16	0.154E+02
	17	0.198E+00	-0.578E-04	0.000E+00	0.000E+00	-0.225E-03	0.301E-06	0.496E-03	-0.114E+03	0.335E+02	0.100E-01	-0.999E-02	-0.143E-16	0.154E+02
	18	0.513E-01	-0.578E-04	0.000E+00	0.000E+00	-0.225E-03	0.601E-06	0.137E-03	-0.114E+03	0.335E+02	0.100E-01	-0.999E-02	0.581E-02	-0.400E+01
	19	0.513E-01	-0.578E-04	0.000E+00	0.000E+00	-0.225E-03	0.120E-05	-0.605E-03	-0.114E+03	0.358E+02	0.100E-01	-0.999E-02	0.581E-02	-0.400E+01
	20	0.318E+00	-0.578E-04	0.000E+00	0.000E+00	-0.225E-03	0.150E-05	-0.989E-03	-0.114E+03	0.358E+02	0.100E-01	-0.999E-02	0.116E-01	-0.248E+02
	21	0.318E+00	-0.578E-04	0.000E+00	0.000E+00	-0.225E-03	0.211E-05	-0.178E-02	-0.114E+03	0.381E+02	0.100E-01	-0.999E-02	0.116E-01	-0.248E+02
	22	0.602E+00	-0.578E-04	0.000E+00	0.000E+00	-0.225E-03	0.241E-05	-0.219E-02	-0.114E+03	0.381E+02	0.100E-01	-0.999E-02	0.174E-01	-0.469E+02
	23	0.602E+00	-0.578E-04	0.000E+00	0.000E+00	-0.225E-03	0.301E-05	-0.303E-02	-0.114E+03	0.405E+02	0.100E-01	-0.999E-02	0.174E-01	-0.469E+02
	24	0.904E+00	-0.578E-04	0.000E+00	0.000E+00	-0.225E-03	0.331E-05	-0.347E-02	-0.114E+03	0.405E+02	0.100E-01	-0.999E-02	0.232E-01	-0.704E+02
	25	0.904E+00	-0.578E-04	0.000E+00	0.000E+00	-0.225E-03	0.391E-05	-0.436E-02	-0.114E+03	0.428E+02	0.100E-01	-0.999E-02	0.232E-01	-0.704E+02
	26	0.122E+01	-0.578E-04	0.000E+00	0.000E+00	-0.225E-03	0.421E-05	-0.655E-01	-0.114E+03	0.428E+02	0.100E-01	-0.999E-02	0.290E-01	-0.952E+02
3	27	0.125E+01	-0.126E-02	0.000E+00	0.000E+00	-0.176E-03	0.151E-05	-0.613E-01	-0.428E+02	-0.114E+03	-0.100E-01	-0.300E-01	0.201E-01	-0.241E+03
	28	0.681E+00	-0.175E-04	0.000E+00	0.000E+00	-0.176E-03	0.122E-05	-0.519E-02	-0.428E+02	-0.114E+03	-0.100E-01	-0.300E-01	0.103E-01	-0.131E+03
	29	0.681E+00	-0.175E-04	0.000E+00	0.000E+00	-0.176E-03	0.634E-06	-0.291E-02	-0.428E+02	-0.114E+03	-0.100E-01	-0.300E-01	0.103E-01	-0.131E+03
	30	0.112E+00	-0.175E-04	0.000E+00	0.000E+00	-0.176E-03	0.343E-06	-0.177E-02	-0.428E+02	-0.114E+03	-0.100E-01	-0.300E-01	0.564E-03	-0.202E+02
	31	0.112E+00	-0.175E-04	0.000E+00	0.000E+00	-0.176E-03	-0.241E-06	0.516E-03	-0.428E+02	-0.114E+03	-0.100E-01	-0.300E-01	0.564E-03	-0.202E+02
	32	0.474E+00	-0.175E-04	0.000E+00	0.000E+00	-0.176E-03	-0.533E-06	0.166E-02	-0.428E+02	-0.114E+03	-0.100E-01	-0.300E-01	-0.919E-02	0.904E+02

<STEP: 9>	dGmin= 0.100E-01		Local Strain Components						Local Stress Components					
Member	Section	Criterion Values	q(1)	q(2)	q(3)	q(4)	q(5)	q(6)	Q(1)	Q(2)	Q(3)	Q(4)	Q(5)	Q(6)
1	1	0.125E+01	0.696E-04	0.000E+00	0.000E+00	-0.183E-03	-0.252E-01	-0.351E-01	0.199E+02	-0.996E+02	0.133E+03	-0.313E-01	-0.324E+03	-0.242E+03
	2	0.751E+00	0.814E-05	0.000E+00	0.000E+00	-0.183E-03	-0.213E-01	-0.550E-02	0.199E+02	-0.996E+02	0.133E+03	-0.313E-01	-0.194E+03	-0.145E+03
	3	0.751E+00	0.814E-05	0.000E+00	0.000E+00	-0.183E-03	-0.136E-01	-0.350E-02	0.199E+02	-0.996E+02	0.133E+03	-0.313E-01	-0.194E+03	-0.145E+03
	4	0.252E+00	0.814E-05	0.000E+00	0.000E+00	-0.183E-03	-0.969E-02	-0.249E-02	0.199E+02	-0.996E+02	0.133E+03	-0.313E-01	-0.646E+02	-0.482E+02
	5	0.252E+00	0.814E-05	0.000E+00	0.000E+00	-0.183E-03	-0.191E-02	-0.492E-03	0.199E+02	-0.996E+02	0.133E+03	-0.313E-01	-0.646E+02	-0.482E+02
	6	0.255E+00	0.814E-05	0.000E+00	0.000E+00	-0.183E-03	0.198E-02	0.509E-03	0.199E+02	-0.996E+02	0.133E+03	-0.313E-01	0.653E+02	0.488E+02
2	7	0.119E+01	-0.578E-04	0.000E+00	0.000E+00	-0.221E-03	-0.439E-05	0.568E-01	-0.114E+03	0.223E+02	0.104E-01	-0.979E-02	-0.303E-01	0.927E+02
	8	0.102E+01	-0.578E-04	0.000E+00	0.000E+00	-0.221E-03	-0.408E-05	0.111E-01	-0.114E+03	0.223E+02	0.104E-01	-0.979E-02	-0.242E-01	0.797E+02
	9	0.102E+01	-0.578E-04	0.000E+00	0.000E+00	-0.221E-03	-0.345E-05	0.106E-01	-0.114E+03	0.242E+02	0.104E-01	-0.979E-02	-0.242E-01	0.797E+02
	10	0.843E+00	-0.578E-04	0.000E+00	0.000E+00	-0.221E-03	-0.313E-05	0.390E-02	-0.114E+03	0.242E+02	0.104E-01	-0.979E-02	-0.182E-01	0.657E+02
	11	0.843E+00	-0.578E-04	0.000E+00	0.000E+00	-0.221E-03	-0.251E-05	0.335E-02	-0.114E+03	0.265E+02	0.104E-01	-0.979E-02	-0.182E-01	0.657E+02
	12	0.645E+00	-0.578E-04	0.000E+00	0.000E+00	-0.221E-03	-0.219E-05	0.307E-02	-0.114E+03	0.265E+02	0.104E-01	-0.979E-02	-0.121E-01	0.503E+02
	13	0.645E+00	-0.578E-04	0.000E+00	0.000E+00	-0.221E-03	-0.157E-05	0.248E-02	-0.114E+03	0.289E+02	0.104E-01	-0.979E-02	-0.121E-01	0.503E+02
	14	0.430E+00	-0.578E-04	0.000E+00	0.000E+00	-0.221E-03	-0.125E-05	0.217E-02	-0.114E+03	0.289E+02	0.104E-01	-0.979E-02	-0.606E-02	0.335E+02
	15	0.430E+00	-0.578E-04	0.000E+00	0.000E+00	-0.221E-03	-0.627E-06	0.152E-02	-0.114E+03	0.312E+02	0.104E-01	-0.979E-02	-0.606E-02	0.335E+02
	16	0.198E+00	-0.578E-04	0.000E+00	0.000E+00	-0.221E-03	-0.313E-06	0.119E-02	-0.114E+03	0.312E+02	0.104E-01	-0.979E-02	-0.146E-16	0.154E+02
	17	0.198E+00	-0.578E-04	0.000E+00	0.000E+00	-0.221E-03	0.313E-06	0.496E-03	-0.114E+03	0.335E+02	0.104E-01	-0.979E-02	-0.146E-16	0.154E+02
	18	0.514E-01	-0.578E-04	0.000E+00	0.000E+00	-0.221E-03	0.627E-06	0.137E-03	-0.114E+03	0.335E+02	0.104E-01	-0.979E-02	0.606E-02	-0.401E+01
	19	0.514E-01	-0.578E-04	0.000E+00	0.000E+00	-0.221E-03	0.125E-05	-0.606E-03	-0.114E+03	0.358E+02	0.104E-01	-0.979E-02	0.606E-02	-0.401E+01
	20	0.318E+00	-0.578E-04	0.000E+00	0.000E+00	-0.221E-03	0.157E-05	-0.990E-03	-0.114E+03	0.358E+02	0.104E-01	-0.979E-02	0.121E-01	-0.248E+02
	21	0.318E+00	-0.578E-04	0.000E+00	0.000E+00	-0.221E-03	0.219E-05	-0.178E-02	-0.114E+03	0.381E+02	0.104E-01	-0.979E-02	0.121E-01	-0.248E+02
	22	0.602E+00	-0.578E-04	0.000E+00	0.000E+00	-0.221E-03	0.251E-05	-0.219E-02	-0.114E+03	0.381E+02	0.104E-01	-0.979E-02	0.182E-01	-0.469E+02
	23	0.602E+00	-0.578E-04	0.000E+00	0.000E+00	-0.221E-03	0.313E-05	-0.303E-02	-0.114E+03	0.405E+02	0.104E-01	-0.979E-02	0.182E-01	-0.469E+02
	24	0.904E+00	-0.578E-04	0.000E+00	0.000E+00	-0.221E-03	0.345E-05	-0.347E-02	-0.114E+03	0.405E+02	0.104E-01	-0.979E-02	0.242E-01	-0.704E+02
	25	0.904E+00	-0.578E-04	0.000E+00	0.000E+00	-0.221E-03	0.408E-05	-0.436E-02	-0.114E+03	0.428E+02	0.104E-01	-0.979E-02	0.242E-01	-0.704E+02
	26	0.122E+01	-0.578E-04	0.000E+00	0.000E+00	-0.221E-03	0.439E-05	-0.656E-01	-0.114E+03	0.428E+02	0.104E-01	-0.979E-02	0.303E-01	-0.952E+02
3	27	0.125E+01	-0.127E-02	0.000E+00	0.000E+00	-0.183E-03	0.163E-05	-0.614E-01	-0.428E+02	-0.114E+03	-0.104E-01	-0.313E-01	0.215E-01	-0.241E+03
	28	0.681E+00	-0.175E-04	0.000E+00	0.000E+00	-0.183E-03	0.133E-05	-0.519E-02	-0.428E+02	-0.114E+03	-0.104E-01	-0.313E-01	0.114E-01	-0.131E+03
	29	0.681E+00	-0.175E-04	0.000E+00	0.000E+00	-0.183E-03	0.718E-06	-0.291E-02	-0.428E+02	-0.114E+03	-0.104E-01	-0.313E-01	0.114E-01	-0.131E+03
	30	0.112E+00	-0.175E-04	0.000E+00	0.000E+00	-0.183E-03	0.413E-06	-0.177E-02	-0.428E+02	-0.114E+03	-0.104E-01	-0.313E-01	0.121E-02	-0.202E+02
	31	0.112E+00	-0.175E-04	0.000E+00	0.000E+00	-0.183E-03	-0.195E-06	0.517E-03	-0.428E+02	-0.114E+03	-0.104E-01	-0.313E-01	0.121E-02	-0.202E+02
	32	0.474E+00	-0.175E-04	0.000E+00	0.000E+00	-0.183E-03	-0.500E-06	0.166E-02	-0.428E+02	-0.114E+03	-0.104E-01	-0.313E-01	-0.895E-02	0.904E+02

<STEP: 10>		dGmin= 0.114E+01	Local Strain Components						Local Stress Components					
Member	Section	Criterion Values	q(1)	q(2)	q(3)	q(4)	q(5)	q(6)	Q(1)	Q(2)	Q(3)	Q(4)	Q(5)	Q(6)
1	1	0.125E+01	0.573E-03	0.000E+00	0.000E+00	-0.103E-02	-0.252E-01	-0.481E-01	0.204E+02	-0.998E+02	0.134E+03	-0.176E+00	-0.324E+03	-0.242E+03
	2	0.750E+00	0.836E-05	0.000E+00	0.000E+00	-0.103E-02	-0.213E-01	-0.549E-02	0.204E+02	-0.998E+02	0.134E+03	-0.176E+00	-0.194E+03	-0.145E+03
	3	0.750E+00	0.836E-05	0.000E+00	0.000E+00	-0.103E-02	-0.136E-01	-0.349E-02	0.204E+02	-0.998E+02	0.134E+03	-0.176E+00	-0.194E+03	-0.145E+03
	4	0.250E+00	0.836E-05	0.000E+00	0.000E+00	-0.103E-02	-0.966E-02	-0.248E-02	0.204E+02	-0.998E+02	0.134E+03	-0.176E+00	-0.641E+02	-0.478E+02
	5	0.250E+00	0.836E-05	0.000E+00	0.000E+00	-0.103E-02	-0.186E-02	-0.477E-03	0.204E+02	-0.998E+02	0.134E+03	-0.176E+00	-0.641E+02	-0.478E+02
	6	0.258E+00	0.836E-05	0.000E+00	0.000E+00	-0.103E-02	0.204E-02	0.526E-03	0.204E+02	-0.998E+02	0.134E+03	-0.176E+00	0.661E+02	0.494E+02
2	7	0.120E+01	-0.582E-04	0.000E+00	0.000E+00	0.296E-03	-0.247E-04	0.603E-01	-0.114E+03	0.229E+02	0.588E-01	0.131E-01	-0.170E+00	0.936E+02
	8	0.103E+01	-0.582E-04	0.000E+00	0.000E+00	0.296E-03	-0.229E-04	0.135E-01	-0.114E+03	0.229E+02	0.588E-01	0.131E-01	-0.136E+00	0.804E+02
	9	0.103E+01	-0.582E-04	0.000E+00	0.000E+00	0.296E-03	-0.194E-04	0.130E-01	-0.114E+03	0.248E+02	0.588E-01	0.131E-01	-0.136E+00	0.804E+02
	10	0.848E+00	-0.582E-04	0.000E+00	0.000E+00	0.296E-03	-0.176E-04	0.392E-02	-0.114E+03	0.248E+02	0.588E-01	0.131E-01	-0.102E+00	0.660E+02
	11	0.848E+00	-0.582E-04	0.000E+00	0.000E+00	0.296E-03	-0.141E-04	0.337E-02	-0.114E+03	0.271E+02	0.588E-01	0.131E-01	-0.102E+00	0.660E+02
	12	0.646E+00	-0.582E-04	0.000E+00	0.000E+00	0.296E-03	-0.124E-04	0.308E-02	-0.114E+03	0.271E+02	0.588E-01	0.131E-01	-0.682E-01	0.503E+02
	13	0.646E+00	-0.582E-04	0.000E+00	0.000E+00	0.296E-03	-0.882E-05	0.247E-02	-0.114E+03	0.294E+02	0.588E-01	0.131E-01	-0.682E-01	0.503E+02
	14	0.427E+00	-0.582E-04	0.000E+00	0.000E+00	0.296E-03	-0.706E-05	0.216E-02	-0.114E+03	0.294E+02	0.588E-01	0.131E-01	-0.341E-01	0.332E+02
	15	0.427E+00	-0.582E-04	0.000E+00	0.000E+00	0.296E-03	-0.353E-05	0.150E-02	-0.114E+03	0.317E+02	0.588E-01	0.131E-01	-0.341E-01	0.332E+02
	16	0.191E+00	-0.582E-04	0.000E+00	0.000E+00	0.296E-03	-0.176E-05	0.116E-02	-0.114E+03	0.317E+02	0.588E-01	0.131E-01	-0.146E-16	0.148E+02
	17	0.191E+00	-0.582E-04	0.000E+00	0.000E+00	0.296E-03	0.176E-05	0.458E-03	-0.114E+03	0.340E+02	0.588E-01	0.131E-01	-0.146E-16	0.148E+02
	18	0.629E-01	-0.582E-04	0.000E+00	0.000E+00	0.296E-03	0.353E-05	0.933E-04	-0.114E+03	0.340E+02	0.588E-01	0.131E-01	0.341E-01	-0.490E+01
	19	0.629E-01	-0.582E-04	0.000E+00	0.000E+00	0.296E-03	0.706E-05	-0.661E-03	-0.114E+03	0.364E+02	0.588E-01	0.131E-01	0.341E-01	-0.490E+01
	20	0.334E+00	-0.582E-04	0.000E+00	0.000E+00	0.296E-03	0.882E-05	-0.105E-02	-0.114E+03	0.364E+02	0.588E-01	0.131E-01	0.682E-01	-0.260E+02
	21	0.334E+00	-0.582E-04	0.000E+00	0.000E+00	0.296E-03	0.124E-04	-0.185E-02	-0.114E+03	0.387E+02	0.588E-01	0.131E-01	0.682E-01	-0.260E+02
	22	0.622E+00	-0.582E-04	0.000E+00	0.000E+00	0.296E-03	0.141E-04	-0.227E-02	-0.114E+03	0.387E+02	0.588E-01	0.131E-01	0.102E+00	-0.484E+02
	23	0.622E+00	-0.582E-04	0.000E+00	0.000E+00	0.296E-03	0.176E-04	-0.312E-02	-0.114E+03	0.410E+02	0.588E-01	0.131E-01	0.102E+00	-0.484E+02
	24	0.927E+00	-0.582E-04	0.000E+00	0.000E+00	0.296E-03	0.194E-04	-0.356E-02	-0.114E+03	0.410E+02	0.588E-01	0.131E-01	0.136E+00	-0.722E+02
	25	0.927E+00	-0.582E-04	0.000E+00	0.000E+00	0.296E-03	0.229E-04	-0.447E-02	-0.114E+03	0.433E+02	0.588E-01	0.131E-01	0.136E+00	-0.722E+02
	26	0.125E+01	-0.582E-04	0.000E+00	0.000E+00	0.296E-03	0.247E-04	-0.733E-01	-0.114E+03	0.433E+02	0.588E-01	0.131E-01	0.170E+00	-0.973E+02
3	27	0.125E+01	-0.157E-02	0.000E+00	0.000E+00	-0.103E-02	0.153E-04	-0.691E-01	-0.433E+02	-0.114E+03	-0.588E-01	-0.176E+00	0.189E+00	-0.241E+03
	28	0.678E+00	-0.177E-04	0.000E+00	0.000E+00	-0.103E-02	0.136E-04	-0.517E-02	-0.433E+02	-0.114E+03	-0.588E-01	-0.176E+00	0.132E+00	-0.130E+03
	29	0.678E+00	-0.177E-04	0.000E+00	0.000E+00	-0.103E-02	0.102E-04	-0.288E-02	-0.433E+02	-0.114E+03	-0.588E-01	-0.176E+00	0.132E+00	-0.130E+03
	30	0.105E+00	-0.177E-04	0.000E+00	0.000E+00	-0.103E-02	0.845E-05	-0.173E-02	-0.433E+02	-0.114E+03	-0.588E-01	-0.176E+00	0.750E-01	-0.187E+02
	31	0.105E+00	-0.177E-04	0.000E+00	0.000E+00	-0.103E-02	0.503E-05	0.568E-03	-0.433E+02	-0.114E+03	-0.588E-01	-0.176E+00	0.750E-01	-0.187E+02
	32	0.485E+00	-0.177E-04	0.000E+00	0.000E+00	-0.103E-02	0.331E-05	0.172E-02	-0.433E+02	-0.114E+03	-0.588E-01	-0.176E+00	0.178E-01	0.925E+02

<STEP: 11>		dGmin= 0.159E+01	Local Strain Components						Local Stress Components					
Member	Section	Criterion Values	q(1)	q(2)	q(3)	q(4)	q(5)	q(6)	Q(1)	Q(2)	Q(3)	Q(4)	Q(5)	Q(6)
1	1	0.125E+01	0.287E-02	0.000E+00	0.000E+00	-0.489E-02	-0.253E-01	-0.107E+00	0.211E+02	-0.101E+03	0.135E+03	-0.837E+00	-0.326E+03	-0.242E+03
	2	0.746E+00	0.863E-05	0.000E+00	0.000E+00	-0.489E-02	-0.214E-01	-0.548E-02	0.211E+02	-0.101E+03	0.135E+03	-0.837E+00	-0.194E+03	-0.144E+03
	3	0.746E+00	0.863E-05	0.000E+00	0.000E+00	-0.489E-02	-0.135E-01	-0.345E-02	0.211E+02	-0.101E+03	0.135E+03	-0.837E+00	-0.194E+03	-0.144E+03
	4	0.242E+00	0.863E-05	0.000E+00	0.000E+00	-0.489E-02	-0.956E-02	-0.244E-02	0.211E+02	-0.101E+03	0.135E+03	-0.837E+00	-0.626E+02	-0.463E+02
	5	0.242E+00	0.863E-05	0.000E+00	0.000E+00	-0.489E-02	-0.169E-02	-0.422E-03	0.211E+02	-0.101E+03	0.135E+03	-0.837E+00	-0.626E+02	-0.463E+02
	6	0.270E+00	0.863E-05	0.000E+00	0.000E+00	-0.489E-02	0.225E-02	0.589E-03	0.211E+02	-0.101E+03	0.135E+03	-0.837E+00	0.689E+02	0.517E+02
2	7	0.125E+01	-0.582E-04	0.000E+00	0.000E+00	0.265E-02	-0.117E-03	0.735E-01	-0.114E+03	0.235E+02	0.279E+00	0.117E+00	-0.809E+00	0.973E+02
	8	0.107E+01	-0.582E-04	0.000E+00	0.000E+00	0.265E-02	-0.109E-03	0.253E-01	-0.114E+03	0.235E+02	0.279E+00	0.117E+00	-0.647E+00	0.837E+02
	9	0.107E+01	-0.582E-04	0.000E+00	0.000E+00	0.265E-02	-0.922E-04	0.248E-01	-0.114E+03	0.254E+02	0.279E+00	0.117E+00	-0.647E+00	0.837E+02
	10	0.886E+00	-0.582E-04	0.000E+00	0.000E+00	0.265E-02	-0.838E-04	0.409E-02	-0.114E+03	0.254E+02	0.279E+00	0.117E+00	-0.486E+00	0.690E+02
	11	0.886E+00	-0.582E-04	0.000E+00	0.000E+00	0.265E-02	-0.670E-04	0.352E-02	-0.114E+03	0.277E+02	0.279E+00	0.117E+00	-0.486E+00	0.690E+02
	12	0.679E+00	-0.582E-04	0.000E+00	0.000E+00	0.265E-02	-0.586E-04	0.323E-02	-0.114E+03	0.277E+02	0.279E+00	0.117E+00	-0.324E+00	0.529E+02
	13	0.679E+00	-0.582E-04	0.000E+00	0.000E+00	0.265E-02	-0.419E-04	0.261E-02	-0.114E+03	0.300E+02	0.279E+00	0.117E+00	-0.324E+00	0.529E+02
	14	0.455E+00	-0.582E-04	0.000E+00	0.000E+00	0.265E-02	-0.335E-04	0.229E-02	-0.114E+03	0.300E+02	0.279E+00	0.117E+00	-0.162E+00	0.355E+02
	15	0.455E+00	-0.582E-04	0.000E+00	0.000E+00	0.265E-02	-0.168E-04	0.162E-02	-0.114E+03	0.324E+02	0.279E+00	0.117E+00	-0.162E+00	0.355E+02
	16	0.214E+00	-0.582E-04	0.000E+00	0.000E+00	0.265E-02	-0.838E-05	0.127E-02	-0.114E+03	0.324E+02	0.279E+00	0.117E+00	-0.146E-16	0.167E+02
	17	0.214E+00	-0.582E-04	0.000E+00	0.000E+00	0.265E-02	0.838E-05	0.554E-03	-0.114E+03	0.347E+02	0.279E+00	0.117E+00	-0.146E-16	0.167E+02
	18	0.439E-01	-0.582E-04	0.000E+00	0.000E+00	0.265E-02	0.168E-04	0.182E-03	-0.114E+03	0.347E+02	0.279E+00	0.117E+00	0.162E+00	-0.342E+01
	19	0.439E-01	-0.582E-04	0.000E+00	0.000E+00	0.265E-02	0.335E-04	-0.586E-03	-0.114E+03	0.370E+02	0.279E+00	0.117E+00	0.162E+00	-0.342E+01
	20	0.320E+00	-0.582E-04	0.000E+00	0.000E+00	0.265E-02	0.419E-04	-0.982E-03	-0.114E+03	0.370E+02	0.279E+00	0.117E+00	0.324E+00	-0.249E+02
	21	0.320E+00	-0.582E-04	0.000E+00	0.000E+00	0.265E-02	0.586E-04	-0.180E-02	-0.114E+03	0.393E+02	0.279E+00	0.117E+00	0.324E+00	-0.249E+02
	22	0.612E+00	-0.582E-04	0.000E+00	0.000E+00	0.265E-02	0.670E-04	-0.222E-02	-0.114E+03	0.393E+02	0.279E+00	0.117E+00	0.486E+00	-0.477E+02
	23	0.612E+00	-0.582E-04	0.000E+00	0.000E+00	0.265E-02	0.838E-04	-0.309E-02	-0.114E+03	0.416E+02	0.279E+00	0.117E+00	0.486E+00	-0.477E+02
	24	0.923E+00	-0.582E-04	0.000E+00	0.000E+00	0.265E-02	0.922E-04	-0.354E-02	-0.114E+03	0.416E+02	0.279E+00	0.117E+00	0.647E+00	-0.718E+02
	25	0.923E+00	-0.582E-04	0.000E+00	0.000E+00	0.265E-02	0.109E-03	-0.445E-02	-0.114E+03	0.440E+02	0.279E+00	0.117E+00	0.647E+00	-0.718E+02
	26	0.125E+01	-0.582E-04	0.000E+00	0.000E+00	0.265E-02	0.117E-03	-0.112E+00	-0.114E+03	0.440E+02	0.279E+00	0.117E+00	0.809E+00	-0.973E+02
3	27	0.125E+01	-0.294E-02	0.000E+00	0.000E+00	-0.489E-02	0.776E-04	-0.104E+00	-0.440E+02	-0.114E+03	-0.279E+00	-0.837E+00	0.954E+00	-0.241E+03
	28	0.677E+00	-0.180E-04	0.000E+00	0.000E+00	-0.489E-02	0.695E-04	-0.517E-02	-0.440E+02	-0.114E+03	-0.279E+00	-0.837E+00	0.683E+00	-0.130E+03
	29	0.677E+00	-0.180E-04	0.000E+00	0.000E+00	-0.489E-02	0.532E-04	-0.288E-02	-0.440E+02	-0.114E+03	-0.279E+00	-0.837E+00	0.683E+00	-0.130E+03
	30	0.105E+00	-0.180E-04	0.000E+00	0.000E+00	-0.489E-02	0.451E-04	-0.173E-02	-0.440E+02	-0.114E+03	-0.279E+00	-0.837E+00	0.411E+00	-0.187E+02
	31	0.105E+00	-0.180E-04	0.000E+00	0.000E+00	-0.489E-02	0.288E-04	0.570E-03	-0.440E+02	-0.114E+03	-0.279E+00	-0.837E+00	0.411E+00	-0.187E+02
	32	0.485E+00	-0.180E-04	0.000E+00	0.000E+00	-0.489E-02	0.207E-04	0.172E-02	-0.440E+02	-0.114E+03	-0.279E+00	-0.837E+00	0.140E+00	0.926E+02

<STEP: 12> |dGmin= 0.100E-01|									Local Strain Components										Local Stress Components						
|Member |Section|Criterion Values|			q(1)		q(2)		q(3)		q(4)		q(5)		q(6)		Q(1)		Q(2)		Q(3)		Q(4)		Q(5)		Q(6)
1	1	0.125E+01	0.294E-02	0.000E+00	-0.500E-02	-0.253E-01	-0.109E+00	0.211E+02	-0.101E+03	0.135E+03	-0.856E+00	-0.326E+03	-0.242E+03
	2	0.746E+00	0.863E-05	0.000E+00	-0.500E-02	-0.214E-01	-0.548E-02	0.211E+02	-0.101E+03	0.135E+03	-0.856E+00	-0.194E+03	-0.144E+03
	3	0.746E+00	0.863E-05	0.000E+00	-0.500E-02	-0.135E-01	-0.345E-02	0.211E+02	-0.101E+03	0.135E+03	-0.856E+00	-0.194E+03	-0.144E+03
	4	0.242E+00	0.863E-05	0.000E+00	-0.500E-02	-0.957E-02	-0.244E-02	0.211E+02	-0.101E+03	0.135E+03	-0.856E+00	-0.626E+02	-0.463E+02
	5	0.242E+00	0.863E-05	0.000E+00	-0.500E-02	-0.169E-02	-0.422E-03	0.211E+02	-0.101E+03	0.135E+03	-0.856E+00	-0.626E+02	-0.463E+02
	6	0.270E+00	0.863E-05	0.000E+00	-0.500E-02	0.225E-02	0.589E-03	0.211E+02	-0.101E+03	0.135E+03	-0.856E+00	0.689E+02	0.517E+02
2	7	0.125E+01	-0.582E-04	0.000E+00	0.271E-02	-0.120E-03	0.745E-01	-0.114E+03	0.235E+02	0.285E+00	0.120E+00	-0.828E+00	0.973E+02
	8	0.107E+01	-0.582E-04	0.000E+00	0.271E-02	-0.111E-03	0.253E-01	-0.114E+03	0.235E+02	0.285E+00	0.120E+00	-0.662E+00	0.837E+02
	9	0.107E+01	-0.582E-04	0.000E+00	0.271E-02	-0.943E-04	0.248E-01	-0.114E+03	0.254E+02	0.285E+00	0.120E+00	-0.662E+00	0.837E+02
	10	0.886E+00	-0.582E-04	0.000E+00	0.271E-02	-0.857E-04	0.409E-02	-0.114E+03	0.254E+02	0.285E+00	0.120E+00	-0.497E+00	0.690E+02
	11	0.886E+00	-0.582E-04	0.000E+00	0.271E-02	-0.686E-04	0.352E-02	-0.114E+03	0.277E+02	0.285E+00	0.120E+00	-0.497E+00	0.690E+02
	12	0.679E+00	-0.582E-04	0.000E+00	0.271E-02	-0.600E-04	0.323E-02	-0.114E+03	0.277E+02	0.285E+00	0.120E+00	-0.331E+00	0.529E+02
	13	0.679E+00	-0.582E-04	0.000E+00	0.271E-02	-0.429E-04	0.261E-02	-0.114E+03	0.300E+02	0.285E+00	0.120E+00	-0.331E+00	0.529E+02
	14	0.455E+00	-0.582E-04	0.000E+00	0.271E-02	-0.343E-04	0.229E-02	-0.114E+03	0.300E+02	0.285E+00	0.120E+00	-0.166E+00	0.355E+02
	15	0.455E+00	-0.582E-04	0.000E+00	0.271E-02	-0.171E-04	0.162E-02	-0.114E+03	0.324E+02	0.285E+00	0.120E+00	-0.166E+00	0.355E+02
	16	0.214E+00	-0.582E-04	0.000E+00	0.271E-02	-0.857E-05	0.127E-02	-0.114E+03	0.324E+02	0.285E+00	0.120E+00	-0.102E-16	0.167E+02
	17	0.214E+00	-0.582E-04	0.000E+00	0.271E-02	0.857E-05	0.554E-03	-0.114E+03	0.347E+02	0.285E+00	0.120E+00	-0.102E-16	0.167E+02
	18	0.439E-01	-0.582E-04	0.000E+00	0.271E-02	0.171E-04	0.182E-03	-0.114E+03	0.347E+02	0.285E+00	0.120E+00	0.166E+00	-0.342E+01
	19	0.439E-01	-0.582E-04	0.000E+00	0.271E-02	0.343E-04	-0.586E-03	-0.114E+03	0.370E+02	0.285E+00	0.120E+00	0.166E+00	-0.342E+01
	20	0.320E+00	-0.582E-04	0.000E+00	0.271E-02	0.429E-04	-0.982E-03	-0.114E+03	0.370E+02	0.285E+00	0.120E+00	0.331E+00	-0.249E+02
	21	0.320E+00	-0.582E-04	0.000E+00	0.271E-02	0.600E-04	-0.180E-02	-0.114E+03	0.393E+02	0.285E+00	0.120E+00	0.331E+00	-0.249E+02
	22	0.612E+00	-0.582E-04	0.000E+00	0.271E-02	0.686E-04	-0.222E-02	-0.114E+03	0.393E+02	0.285E+00	0.120E+00	0.497E+00	-0.477E+02
	23	0.612E+00	-0.582E-04	0.000E+00	0.271E-02	0.857E-04	-0.309E-02	-0.114E+03	0.416E+02	0.285E+00	0.120E+00	0.497E+00	-0.477E+02
	24	0.923E+00	-0.582E-04	0.000E+00	0.271E-02	0.943E-04	-0.354E-02	-0.114E+03	0.416E+02	0.285E+00	0.120E+00	0.662E+00	-0.718E+02
	25	0.923E+00	-0.582E-04	0.000E+00	0.271E-02	0.111E-03	-0.445E-02	-0.114E+03	0.440E+02	0.285E+00	0.120E+00	0.662E+00	-0.718E+02
	26	0.125E+01	-0.582E-04	0.000E+00	0.271E-02	0.120E-03	-0.113E+00	-0.114E+03	0.440E+02	0.285E+00	0.120E+00	0.828E+00	-0.973E+02
3	27	0.125E+01	-0.298E-02	0.000E+00	-0.500E-02	0.794E-04	-0.105E+00	-0.440E+02	-0.114E+03	-0.285E+00	-0.856E+00	0.977E+00	-0.241E+03
	28	0.677E+00	-0.180E-04	0.000E+00	-0.500E-02	0.711E-04	-0.517E-02	-0.440E+02	-0.114E+03	-0.285E+00	-0.856E+00	0.699E+00	-0.130E+03
	29	0.677E+00	-0.180E-04	0.000E+00	-0.500E-02	0.545E-04	-0.288E-02	-0.440E+02	-0.114E+03	-0.285E+00	-0.856E+00	0.699E+00	-0.130E+03
	30	0.105E+00	-0.180E-04	0.000E+00	-0.500E-02	0.461E-04	-0.173E-02	-0.440E+02	-0.114E+03	-0.285E+00	-0.856E+00	0.421E+00	-0.187E+02
	31	0.105E+00	-0.180E-04	0.000E+00	-0.500E-02	0.295E-04	0.570E-03	-0.440E+02	-0.114E+03	-0.285E+00	-0.856E+00	0.421E+00	-0.187E+02
	32	0.485E+00	-0.180E-04	0.000E+00	-0.500E-02	0.212E-04	0.172E-02	-0.440E+02	-0.114E+03	-0.285E+00	-0.856E+00	0.143E+00	0.926E+02

Base Shear vs. Roof Displacement		
Step #	Displacement	Base Shear
0	0.000E+00	0.000E+00
1	0.231E-03	0.000E+00
2	0.305E-01	0.139E+03
3	0.334E-01	0.146E+03
4	0.537E-01	0.179E+03
5	0.118E+00	0.247E+03
6	0.124E+00	0.250E+03
7	0.152E+00	0.261E+03
8	0.203E+00	0.280E+03
9	0.203E+00	0.280E+03
10	0.226E+00	0.281E+03
11	0.331E+00	0.283E+03
12	0.334E+00	0.283E+03

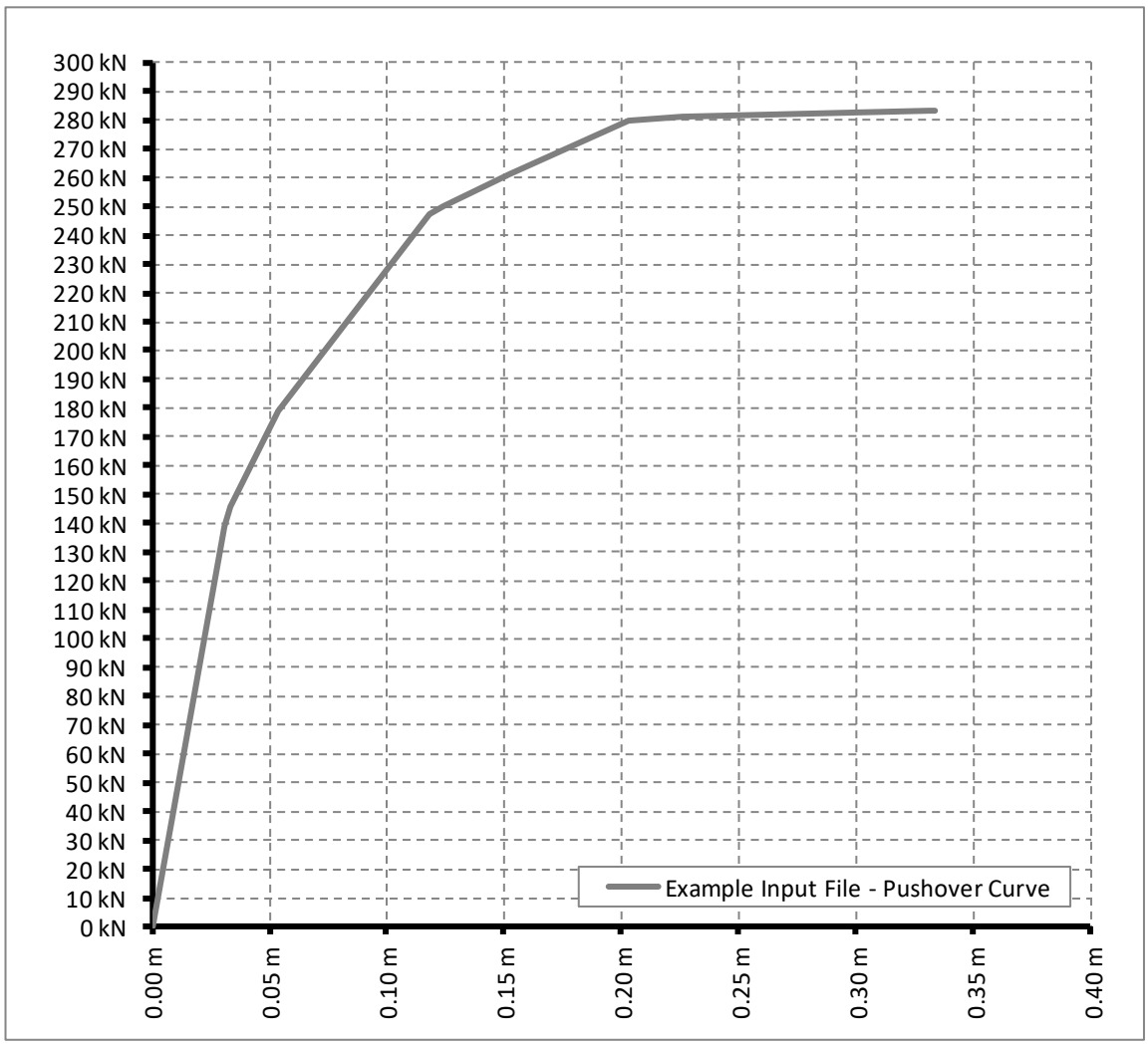

Figure 72: Pushover curve of the example input file.

Member # 1	Element # 1
Q(1)=f[q(1)] @ Section(1):	1

Plastic Hinge - Backbone Curve		
[q]plastic	[q]total	[Q]
-0.189E-01	-0.239E-01	-0.311E+04
-0.145E-01	-0.184E-01	-0.311E+04
-0.000E+00	-0.306E-02	-0.249E+04
0.000E+00	0.000E+00	0.000E+00
0.000E+00	0.306E-02	0.249E+04
0.145E-01	0.184E-01	0.311E+04
0.189E-01	0.239E-01	0.311E+04

Member # 1	Element # 1
Q(1)=f[q(1)] @ Section #	1

[q]plastic	[q]total	[Q]
0.000E+00	0.000E+00	0.000E+00
0.000E+00	-0.502E-05	-0.123E+02
0.000E+00	0.356E-05	0.869E+01
0.000E+00	0.422E-05	0.103E+02
0.000E+00	0.609E-05	0.149E+02
0.000E+00	0.714E-05	0.175E+02
0.443E-05	0.116E-04	0.176E+02
0.269E-04	0.345E-04	0.186E+02
0.569E-04	0.650E-04	0.199E+02
0.614E-04	0.696E-04	0.199E+02
0.565E-03	0.573E-03	0.204E+02
0.286E-02	0.287E-02	0.211E+02
0.293E-02	0.294E-02	0.211E+02

Member # 1	Element # 1

Q(6)=f[q(6)] @ Section(1): 1		
Plastic Hinge - Backbone Curve		
[q]plastic	[q]total	[Q]
-0.372E-01	-0.469E-01	-0.243E+03
-0.286E-01	-0.361E-01	-0.243E+03
-0.000E+00	-0.602E-02	-0.194E+03
0.000E+00	0.000E+00	0.000E+00
0.000E+00	0.602E-02	0.194E+03
0.286E-01	0.361E-01	0.243E+03
0.372E-01	0.469E-01	0.243E+03

Member # 1	Element # 1

Q(6)=f[q(6)] @ Section # 1		
[q]plastic	[q]total	[Q]
0.000E+00	0.000E+00	0.000E+00
0.000E+00	0.717E-04	0.333E+01
0.000E+00	-0.151E-02	-0.582E+02
0.000E+00	-0.165E-02	-0.638E+02
0.000E+00	-0.260E-02	-0.998E+02
0.000E+00	-0.517E-02	-0.194E+03
-0.183E-02	-0.709E-02	-0.197E+03
-0.114E-01	-0.171E-01	-0.213E+03
-0.285E-01	-0.350E-01	-0.242E+03
-0.286E-01	-0.351E-01	-0.242E+03
-0.416E-01	-0.481E-01	-0.242E+03
-0.100E+00	-0.107E+00	-0.242E+03
-0.102E+00	-0.109E+00	-0.242E+03

Member # 2 | Element # 1		
Q(6)=f[q(6)] @ Section(1): 7		
Plastic Hinge - Backbone Curve		
[q]plastic	[q]total	[Q]
-0.888E-01	-0.112E+00	-0.973E+02
-0.683E-01	-0.863E-01	-0.973E+02
-0.000E+00	-0.144E-01	-0.779E+02
0.000E+00	0.000E+00	0.000E+00
0.000E+00	0.144E-01	0.779E+02
0.683E-01	0.863E-01	0.973E+02
0.888E-01	0.112E+00	0.973E+02

Member # 2 | Element # 1		
Q(6)=f[q(6)] @ Section # 7		
[q]plastic	[q]total	[Q]
0.000E+00	0.000E+00	0.000E+00
0.000E+00	-0.392E-03	-0.898E+01
0.000E+00	0.262E-02	0.495E+02
0.000E+00	0.288E-02	0.544E+02
0.000E+00	0.413E-02	0.779E+02
0.303E-01	0.349E-01	0.865E+02
0.323E-01	0.369E-01	0.871E+02
0.428E-01	0.476E-01	0.901E+02
0.519E-01	0.568E-01	0.927E+02
0.519E-01	0.568E-01	0.927E+02
0.554E-01	0.603E-01	0.936E+02
0.683E-01	0.735E-01	0.973E+02
0.694E-01	0.745E-01	0.973E+02

Member # 2 | Element # 1		
Q(6)=f[q(6)] @ Section(2): 8		
Plastic Hinge - Backbone Curve		
[q]plastic	[q]total	[Q]
-0.888E-01	-0.112E+00	-0.973E+02
-0.683E-01	-0.863E-01	-0.973E+02
-0.000E+00	-0.144E-01	-0.779E+02
0.000E+00	0.000E+00	0.000E+00
0.000E+00	0.144E-01	0.779E+02
0.683E-01	0.863E-01	0.973E+02
0.888E-01	0.112E+00	0.973E+02

Member # 2 | Element # 1		
Q(6)=f[q(6)] @ Section # 8		
[q]plastic	[q]total	[Q]
0.000E+00	0.000E+00	0.000E+00
0.000E+00	-0.287E-03	-0.329E+01
0.000E+00	0.250E-02	0.430E+02
0.000E+00	0.274E-02	0.470E+02
0.000E+00	0.394E-02	0.678E+02
0.000E+00	0.437E-02	0.750E+02
0.000E+00	0.440E-02	0.754E+02
0.000E+00	0.454E-02	0.779E+02
0.640E-02	0.111E-01	0.797E+02
0.642E-02	0.111E-01	0.797E+02
0.879E-02	0.135E-01	0.804E+02
0.205E-01	0.253E-01	0.837E+02
0.205E-01	0.253E-01	0.837E+02

Member # 2 | Element # 2		
Q(6)=f[q(6)] @ Section(1): 9		
Plastic Hinge - Backbone Curve		
[q]plastic	[q]total	[Q]
-0.888E-01	-0.112E+00	-0.973E+02
-0.683E-01	-0.863E-01	-0.973E+02
-0.000E+00	-0.144E-01	-0.779E+02
0.000E+00	0.000E+00	0.000E+00
0.000E+00	0.144E-01	0.779E+02
0.683E-01	0.863E-01	0.973E+02
0.888E-01	0.112E+00	0.973E+02

Member # 2 | Element # 2		
Q(6)=f[q(6)] @ Section # 9		
[q]plastic	[q]total	[Q]
0.000E+00	0.000E+00	0.000E+00
0.000E+00	-0.971E-04	-0.329E+01
0.000E+00	0.224E-02	0.430E+02
0.000E+00	0.245E-02	0.470E+02
0.000E+00	0.355E-02	0.678E+02
0.000E+00	0.392E-02	0.750E+02
0.000E+00	0.394E-02	0.754E+02
0.000E+00	0.407E-02	0.779E+02
0.640E-02	0.106E-01	0.797E+02
0.642E-02	0.106E-01	0.797E+02
0.879E-02	0.130E-01	0.804E+02
0.205E-01	0.248E-01	0.837E+02
0.205E-01	0.248E-01	0.837E+02

Member # 2 | Element # 10
Q(6)=f[q(6)] @ Section(2): 26

Plastic Hinge - Backbone Curve		
[q]plastic	[q]total	[Q]
-0.888E-01	-0.112E+00	-0.973E+02
-0.683E-01	-0.863E-01	-0.973E+02
-0.000E+00	-0.144E-01	-0.779E+02
0.000E+00	0.000E+00	0.000E+00
0.000E+00	0.144E-01	0.779E+02
0.683E-01	0.863E-01	0.973E+02
0.888E-01	0.112E+00	0.973E+02

Member # 2 | Element # 10
Q(6)=f[q(6)] @ Section # 26

[q]plastic	[q]total	[Q]
0.000E+00	0.000E+00	0.000E+00
0.000E+00	-0.459E-03	-0.103E+02
0.000E+00	-0.373E-02	-0.734E+02
0.000E+00	-0.396E-02	-0.779E+02
-0.104E-01	-0.145E-01	-0.808E+02
-0.327E-01	-0.371E-01	-0.872E+02
-0.345E-01	-0.389E-01	-0.877E+02
-0.436E-01	-0.481E-01	-0.903E+02
-0.607E-01	-0.655E-01	-0.952E+02
-0.608E-01	-0.656E-01	-0.952E+02
-0.683E-01	-0.733E-01	-0.973E+02
-0.107E+00	-0.112E+00	-0.973E+02
-0.108E+00	-0.113E+00	-0.973E+02

Member # 3	Element # 1
Q(1)=f[q(1)] @ Section(1):	27

Plastic Hinge - Backbone Curve		
[q]plastic	[q]total	[Q]
-0.189E-01	-0.239E-01	-0.311E+04
-0.145E-01	-0.184E-01	-0.311E+04
-0.000E+00	-0.306E-02	-0.249E+04
0.000E+00	0.000E+00	0.000E+00
0.000E+00	0.306E-02	0.249E+04
0.145E-01	0.184E-01	0.311E+04
0.189E-01	0.239E-01	0.311E+04

Member # 3	Element # 1
Q(1)=f[q(1)] @ Section #	27

[q]plastic	[q]total	[Q]
0.000E+00	0.000E+00	0.000E+00
0.000E+00	-0.435E-05	-0.106E+02
0.000E+00	-0.129E-04	-0.316E+02
-0.378E-04	-0.514E-04	-0.332E+02
-0.144E-03	-0.160E-03	-0.378E+02
-0.204E-03	-0.221E-03	-0.403E+02
-0.209E-03	-0.225E-03	-0.405E+02
-0.578E-03	-0.595E-03	-0.415E+02
-0.125E-02	-0.126E-02	-0.428E+02
-0.125E-02	-0.127E-02	-0.428E+02
-0.155E-02	-0.157E-02	-0.433E+02
-0.292E-02	-0.294E-02	-0.440E+02
-0.296E-02	-0.298E-02	-0.440E+02

Member # 3	Element # 1
Q(6)=f[q(6)] @ Section(1):	27

Plastic Hinge - Backbone Curve		
[q]plastic	[q]total	[Q]
-0.372E-01	-0.469E-01	-0.243E+03
-0.286E-01	-0.361E-01	-0.243E+03
-0.000E+00	-0.602E-02	-0.194E+03
0.000E+00	0.000E+00	0.000E+00
0.000E+00	0.602E-02	0.194E+03
0.286E-01	0.361E-01	0.243E+03
0.372E-01	0.469E-01	0.243E+03

Member # 3	Element # 1
Q(6)=f[q(6)] @ Section #	27

[q]plastic	[q]total	[Q]
0.000E+00	0.000E+00	0.000E+00
0.000E+00	-0.780E-04	-0.421E+01
0.000E+00	-0.508E-02	-0.193E+03
-0.995E-03	-0.610E-02	-0.195E+03
-0.721E-02	-0.126E-01	-0.205E+03
-0.268E-01	-0.330E-01	-0.239E+03
-0.284E-01	-0.347E-01	-0.241E+03
-0.378E-01	-0.442E-01	-0.241E+03
-0.550E-01	-0.613E-01	-0.241E+03
-0.550E-01	-0.614E-01	-0.241E+03
-0.628E-01	-0.691E-01	-0.241E+03
-0.979E-01	-0.104E+00	-0.241E+03
-0.990E-01	-0.105E+00	-0.241E+03

17 Appendix II – Index of Figures

18 Appendix III – Index of Tables

19 Appendix IV – Bibliographic References

[1] J. Perry, Struts and Tie Rods with Lateral Loads, *Philosophical Magazine and Journal of Science*, *Taylor and Francis*, **33** (5), 269–284, 1892.

[2] A. Berry, Calculations of Stresses in Aerospace Wing Spars, *Transactions of the Royal Aeronautical Society,* **1**, 1919.

[3] A.J.S. Pippard, Sir J. Baker, *Analysis of Engineering Structures, E. Arnold & Co.*, London, 1936.

[4] R. Courant, Variational methods for the solution of problems of equilibrium and vibration, *Bulletin of the American Mathematical Society*, **49**, 1–43, 1943.

[5] K.J. Dallison, Stress analysis of circular frames in a non–tapering fuselage, *Journal of the Royal Aeronautical Society*, **57**, 151–176, 1953.

[6] J.H. Argyris, S.Kelsey, Enery Theorems and Structural Analysis, *Aircraft Engineering*, 1954 (*re-printed by Butterworth's Scientific Publications, London, 1960*).

[7] J.H. Argyris, S.Kelsey, Structural Analysis by the Force Method, with Application to Aircraft Wings, *Jahrbuch von Wissenschaftlicher Gesselschaft für Luftfahrt*, 1956.

[8] J.H. Argyris, S.Kelsey, The Matrix Force Method of Structural Analysis and some new applications, *British Aeronautical Research Council*, *R.&M. 3034*, February 1956.

[9] W.R. Spillers, Application of topology in structural analysis, *Journal of the Structural Division*, *ASCE*, **13**, 89–301, 1963.

[10] A.I. Roussopoulos, *Theory of Elastic Complexes*, Elsevier, 1965.

[11] J.T. Oden, A. Neighbors, Network-Topological Formulation of Analyses of Geometrically and Materially Non-linear Space Frames, *Proc. International Conference on Space Structures, Blackwell Scientific Publications*, 1966.

[12] J. C. de C. Henderson and E. A. W. Maunder., A problem in applied topology; on the selection of cycles for the flexibility analysis of skeletal structures, *J. Inst. Maths Applics*, **5**, 254−269, 1969.

[13] S.J. Fenvez, A. Gonzalez-Caro, Network Topological Formulation of Analysis and Design of Rigid-Plastic Framed Structures, *International Journal for Numerical Methods in Engineering*, **3**, 425–441, 1971.

[14] S.N. Patnaik, An Integrated Force Method for Discrete Analysis, *Int. J. for Numerical Methods in Engineering*, **6**, 237-251, 1973.

[15] A. Kaveh, *Application of topology and matroid theory to the analysis of structures, Ph.D. Thesis*, Imperial College, London, 1974.

[16] A. C. Cassell, J. C. de C. Henderson, A. Kaveh, Cycle Bases for the Flexibility Analysis of Structures, *International Journal for Numerical Methods In Engineering*, **8**, 521−528, 1974.

[17] A. Kaveh, Improved Cycle Bases for the Flexibility Analysis of Structures, *Computer Methods in Applied Mechanics & Engineering*, **9**, 267–272, 1976.

[18] C. Polizzotto, A Formulation of The Force Method in The Context of Large Displacements, *Comp. Methods in Applied Mechanics and Engineering*, **16**, 121–134, 1978.

[19] S.N. Patnaik, S. Yadagiri, Design for Frequency by the Integrated Force Method, *Computer Methods in Applied Mechanics and Engineering*, **16**, 213–230, 1978.

[20] A. Kaveh, A Combinatorial Optimization Problem; Optimal Generalized Cycle Bases, *Comp. Methods in Applied Mechanics and Engineering*, **20**, 39–51, 1979.

[21] I. Kaneko, M. Lawo, G. Thierauf, On Computational Procedures for the Force Method, *International Journal for Numerical Methods in Engineering*, **18**, 1469–1495, 1982.

[22] A. Kaveh, Statical Bases for an Efficient Flexibility Analysis of Planar Trusses, Journal of Structural Mechanics, 14 (4), 475-488, 1986.

[23] A. Kaveh, An Efficient Flexibility Analysis of Structures, *Computers & Structures*, **22** (6), 973–977, 1986.

[24] A. Kaveh, An Efficient Program for Generating Subminimal Cycle Bases for The Flexibility Analysis of Structures, *Communications in Applied Numerical Methods*, **2**, 339–344, 1986.

[25] A. Jennings, T.K.H. Tam, Automatic Plastic Design of Frames, *Engineering Structures*, **8**, 139–147, 1986.
[26] S.N. Patnaik, K.T. Joseph, Generation of the Compatibility Matrix in the Integrated Force Method, *Computer Methods in Applied Mechanics and Engineering*, **55**, 239–257, 1986.
[27] N.Z. Pereira, L.A. Borges, M.B. Hecke, A Force Method for Elastic-Plastic Analysis of Frames by Quadratic Optimization, *Int. J. of Solids and Structures*, **24** (2), 211–230, 1988.
[28] A. Kaveh, Topologial Properties of Skeletal Structures, *Computers & Structures*, **29** (3), 403–411, 1988.
[29] A. Kaveh, Optimizing the Conditioning of Structural Flexibility Matrices, *Computers & Structures*, **41** (3), 489–494, 1991.
[30] C.A. Felippa, K.C. Park, A Direct Flexibility Method, *Comp. Methods in Applied Mechanics and Engineering*, **149**, 319–337, 1997.
[31] K.V. Spiliopoulos, On the automation of the force method in the optimal plastic design of frames. *Computer Methods in Applied Mechanics and Engineering,* **141** (1–2), 141–156, 1997.
[32] K.V. Spiliopoulos, P.G. Souliotis, Automatic Collapse Load Analysis of Regular Plane Frames using The Force Method, Computers & Structures, **64** (1–4), 531–540, 1997.
[33] V.K. Koumousis, Recursive Formulation of Force Method Programmed in Logic, *Journal of Computing in Civil Engineering*, **12** (1), 19–29, 1998.
[34] S.N. Patnaik, R.M. Coroneos, D.A.Hopkins, Recent Advances in the Method of Forces: Integrated Force Method of Structural Analysis, *Advances in Engineering Software*, **29** (3–6), 463–474, 1998.
[35] N.R.B. Krishnam Raju, J. Nagabhushanam, Nonlinear Structural Analysis using Integrated Force Method, Sadhana, **25** (4), 353–365, 2000.
[36] A. Kaveh, V. Kalatjari, Genetic Algorithm for Discrete-Sizing Optimal Design of Trusses using the Force Method, *International Journal for Numerical Methods in Engineering*, **55**, 55–72, 2002.
[37] A. Kaveh, V. Kalatjari, Size/Geometry Optimization of Trusses by the Force Method and Genetic Algorithm, Zeitschrift für Angewandte Mathematik & Mechanik (ZAMM), **84** (5), 347–357, 2004.
[38] A. Kaveh, A. Abdietehrani, Design of Frames using Genetic Algorithm, Force Method, and Graph Theory, *International Journal for Numerical Methods in Engineering*, **61**, 2555–2565, 2004.
[39] R. Sedaghati, Benchmark Case Studies in Structural Design Optimization using The Force Method, *Int. J. of Solids and Structures*, **42**, 5848−5871, 2005.
[40] Y. Luo, J. Lu, Geometrically Non-Linear Force Method for Assemblies with Infinitesimal Mechanisms, *Computers & Structures*, **84**, 2194–2199, 2006.
[41] A. Kaveh, H. Moez, Analysis of frames with semi-rigid joints: A graph-theoretical approach, *Engineering Structures*, **28**, 829–836, 2006.
[42] A. Kaveh, H. Rahami, Analysis, Design and Optimization of Structures using Force Method and Genetic Algorithm, *International Journal for Numerical Methods in Engineering*, **65**, 1570–1584, 2006.
[43] A. Kaveh, H. Rahami, Nonlinear Analysis and Optimal Design of Structures via Force Method and Genetic Algorithm, *Computers & Structures*, **84**, 770-778, 2006.
[44] H. Rahami, A. Kaveh, Y. Gholipour, Sizing, Geometry and Topology Optimization of Trusses via Force Method and Genetic Algorithm, *Engineering Structures*, **30**, 2360–2369, 2008.
[45] A. Kaveh, M. Jahanshani, Plastic limit analysis of frames using ant colony systems, *Computers & Structures*, **86**, 1152–1163, 2008.
[46] A. Kaveh, H. Moez, Minimal Cycle Bases for Analysis of Frames with Semi-Rigid Joints, *Computers & Structures*, **86**, 503–510, 2008.
[47] K.V. Spiliopoulos, T.N. Patsios, A Quick Estimate of the Strength of Uniaxially Tied Framed Structures, *Journal of Constructional Steel Research*, **65** (8–9), 1763–1775, 2009.
[48] A. Kaveh, S. Malakouti Rad, Hybrid Genetic Algorithm and Particle Swarm Optimization for the Force Method-based Simultaneous Analysis and Design, *Iranian Journal of Science and Technology, Transaction B: Civil Engineering*, **34** (B1), 15-34, 2010.

[49] K.V. Spiliopoulos, T.N. Patsios, An Efficient Mathematical Programming Method for The Elastoplastic Analysis of Frames, *Engineering Structures*, **32**, 1199−1214, 2010.
[50] A. Kaveh, S. Talatahari, An enhanced charged system search for configuration optimization using the concept of fields of forces, Structural Multidisciplinary Optimization, **43**, 339−351, 2011
[51] A. Kaveh, H. Rahami, S.R. Mirghaderi, M.A. Asl, Analysis of Near-Regular Structures using The Force Method, *Engineering Computations*, **30** (1), 21−48, 2012.
[52] K.V. Spiliopoulos, T.N. Patsios, Numerical analysis of nonholonomic elastoplastic frames by mathematical programming, In: *G. de Saxcé, A. Oueslati, E. Charkaluk, J.B. Trisch (Editors), Limit States of Materials and Structures*, *Springer*, *Dodrecht*, 124−144, 2013.
[53] K.V. Spiliopoulos, N.G. Dais, A powerful force-based approach for the limit analysis of three-dimensional frames, *Archive of Applied Mechanics*, **83** (5), 723−742, 2013.
[54] T.N. Patsios, K.V. Spiliopoulos, A Force-Based Formulation for The 2nd Order Elastoplastic Analysis of Frames, *Proc. 2nd ECCOMAS Young Investigators Conference*, 104−107, 2013.
[55] T.N. Patsios, K.V. Spiliopoulos, A Force-Based Formulation for the Analysis of Frames with Non-Holonomic Hardening Plastic Hinges, *WCCM XI – ECCM V – ECFD VI Conference*, 2014.
[56] T.N. Patsios, K.V. Spiliopoulos, A Force-Based Formulation for The Analysis of 3-Dimensional Inelastic Structural Frames, *Proc. ECCOMAS VII Conference*, **2**, 3091−3106, ISBN: 978-618828440-1, National Technical University of Athens, 2016.
[57] T.N. Patsios, K.V. Spiliopoulos, A Force-Based Mathematical Programming Method for the Incremental Analysis of 3D Frames with Non-Holonomic Hardening Plastic Hinges, *Computers & Structures*, **208**, 51−74, 2018.
[58] J.L. Lagrange, Mécanique Analytique, *Seconde Partie de la Mechanique*, Section IV, 504−522, Paris, 1811.
[59] J.-B. J. Fourier, *Mémoires de l'Académie des Sciences de l' Institut de France*, Tome VI, Partie Mathématique (Analyse), xxix−xlj, Paris, 1823.
[60] L.V. Kantorovich, Mathematical Methods in the Organization and Planning of Production, 1939.
[61] W. Karush, Minima of functions of several variables with inequalities as side constraints, *M.Sc. Dissertation*, *Department of Mathematics*, *University of Chicago*, Chicago, Illinois, 1939.
[62] G.B. Dantzig, Maximization of a linear function of variables subject to linear inequalities, Chapter XXI of "Activity analysis of production and allocation", *Cowles Commission Monograph* **13**, T.C. Koopmans (editor), John Wiley, 1951.
[63] C.E. Lemke, The dual method of solving the linear programming problem, *Naval Research Logistics Quarterly*, **1** (1), 36−47, 1954.
[64] G.B. Dantzig, Linear programming and extensions, *Princeton University Press*, 1963.
[65] D.G. Luenberger, Linear and nonlinear programming (2nd Edition), *Addison-Wesley Publishing Company*, 1984.
[66] R.J. Vanderbei, Linear and nonlinear programming: Foundations and extensions, *Kluwer Academic Publishers*, 1998.
[67] R. Fletcher, Practical Methods of Optimization (2nd Edition), *Wiley*, 2001.
[68] D. Goldfarb, A. Idnani, A numerically stable dual method for solving strictly convex quadratic programs, *Mathematical Programming*, **27**, 1–33, 1983.
[69] N. Karmakar, A new polynomial-time algorithm for linear programming, *Combinatorica*, **4**, 373–397, 1984.
[70] M.J.D. Powell, TOLMIN: A Fortran Package for Linearly Constrained Optimization Calculation, *DAMTP*, *1989/NA2*, *University of Cambridge*, 1989.
[71] E.D. Andersen and Y. Ye, A computational study of the homogeneous algorithm for large-scale convex optimization, *Computational Optimization and Applications*, **10**, 243–269, 1998.
[72] E.D. Andersen and K.D. Andersen, The MOSEK interior point optimizer for linear programming: an implementation of the homogeneous algorithm, *High Performance Optimization*, 197–232, Kluwer Academic Publishers, 2000.

[73] E. D. Andersen, C. Roos, T. Terlaky, On implementing a primal-dual interior point method for conic quadratic optimization, *Mathematical Programming*, **95** (2), 249-277, 2003.
[74] Charnes A., Greenberg H.J., Plastic collapse and linear programming, Preliminary Report ("*The summer meeting in Mineapolis", Abstract Nr. 506, p.480*), *Bulletin of the American Mathematical Society*, **51** (6), 449–494, 1951.
[75] Dorn W.S., Greenberg H.J., Linear programming and plastic limit analysis of structures, *Quarterly of Applied Mathematics*, **15** (2), 155–167, 1957.
[76] Charnes A., Lemke C.E., Zienkewicz O.C., Virtual work, linear programming and plastic limit analysis, *Proceedings of the Royal Society of London, Series A, Mathematical and Physical Sciences*, **251** (1264), 110–116, 1959.
[77] Prager W., Mathematical programming and theory of structures, *Journal of the Society for Industrial and Applied Mathematics*, **13** (1), 312–332, 1965.
[78] Maier G., Drucker D.C., Elastic-plastic continua containing unstable elements obeying normality and convexity relations, *Schweizerische Bauzeitung*, **84** (23), 447–450, 1966.
[79] Maier G., On Elastic-Plastic Structures with Associated Stress-Strain Relations Allowing for Work Softening, *Meccanica*, **2** (1), 55–64, 1967.
[80] Maier G., A quadratic-programming approach for certain nonlinear structural problems, *Meccanica*, **3** (2), 121–130, 1968.
[81] Maier G., Quadratic programming and theory of elastic-perfectly plastic structures, *Meccanica*, **3** (4), 265–273, 1968.
[82] Maier G., Capurso M., Incremental Elastoplastic Analysis and Quadratic Optimization, *Meccanica*, **5** (2), 107–116, 1970.
[83] Maier G., A matrix structural theory of piecewise linear elastoplasticity with interacting yield planes, *Meccanica*, **5** (1), 54–66, 1970.
[84] Maier G., Incremental plastic analysis in the presence of large displacements and physical instabilizing effects. *International Journal of Solids and Structures*, **7** (4), 345–372, 1971.
[85] De Donato O., Maier G., Mathematical programming methods for the inelastic analysis of reinforced concrete frames allowing for limited rotation capacity, *International Journal of Numerical Methods in Engineering*, **4** (3), 307–329, 1972.
[86] Corradi L., Maier G., Inadaptation theorems in the dynamics of elastic-work hardening structures. *Ingenieur Archiv*, **43** (1), 44–57, 1973.
[87] Maier G., Zavelani Rossi A., Dotreppe J.C., Equilibrium branching due to flexural softening. *ASCE Journal of the Structural Division*, **99** (4), 897–901, 1973.
[88] Abdel-Baset S.B., Grierson D.E., Lind N.C., Second-order collapse load analysis: LP approach, *ASCE Journal of the Structural Division*, **99** (11), 2215–2228, 1973.
[89] De Donato O., Maier G., Historical deformation analysis of elastoplastic structures as a parametric linear complementarity problem, *Meccanica*, **11** (3), 166–171, 1976.
[90] Maier G., Piecewise linearization of yield criteria in structural plasticity, *Solid Mechanics Archive*, **2** (3), 239–281, 1976.
[91] Kaneko I., A mathematical programming method for the inelastic analysis of reinforced concrete frames, *International Journal for Numerical Methods in Engineering*, **11** (7), 1137–1154, 1977.
[92] Maier G., Grierson D.E., Best M.J., Mathematical programming methods for deformation analysis at plastic collapse, *Computers and Structures*, **7** (5), 599–612, 1977.
[93] Smith D.L., The Wolfe-Markowitz algorithm for non-holonomic elastoplastic analysis, *Engineering Structures*, **1** (1), 8–16, 1978.
[94] Maier G., Andreuzzi F., Elastic and elasto-plastic analysis of submarine pipelines as unilateral contact problems, *Computers and Structures*, **8** (3–4), 421–431, 1978.
[95] Maier G., Andreuzzi F., Giannessi F., Jurina L., Taddei F., Unilateral contact, elastoplasticity and complementarity with reference to offshore pipeline design, *Computer Methods in Applied Mechanics and Engineering*, **17**–**18**, 469–495, 1978.

[96] Kaneko I., Piecewise linear elastic-plastic analysis, *International Journal for Numerical Methods in Engineering*, **14** (5), 757–767, 1979.
[97] G. Maier, S. Giacomini, F. Paterlini, Combined elastoplastic and limit analysis via restricted basis linear programming, *Computer Methods in Applied Mechanics and Engineering*, **19** (1), 21–48, 1979.
[98] Maier G., Hueckel T., Nonassociated and coupled flow rules of elastoplasticity for rock-like materials, *International Journal of Rock Mechanics and Mining Sciences and Geomechanics Abstracts*, **16** (2), 77–92, 1979.
[99] Cohn M.Z., Maier G., Grierson D.E. (Editors), Engineering plasticity by mathematical programming, *Pergamon Press*, New York, 1979.
[100] Kaneko I., Complete solutions for a class of elastic-plastic structures, *Computer Methods in Applied Mechanics and Engineering*, **21** (2), 193–209, 1980.
[101] Franchi A. Cohn M.Z., Computer analysis of elastic-plastic structures, *Computer Methods in Applied Mechanics and Engineering*, **21** (3), 271–294, 1980.
[102] Faravelli L., Zanon P., Limit Analysis of Steel Structures Allowing for Shear Force, *Journal of Structural Mechanics*, **9** (3), 325–337, 1981.
[103] Maier G., Giannessi F., Nappi A., Indirect identification of yield limits by mathematical programming, *Engineering Structures*, **4** (2), 86–98, 1982.
[104] Giannessi F., Jurina L., Maier G., A quadratic complementarity problem related to the optimal design of a pipeline freely resting on a rough sea bottom, *Engineering Structures*, **4** (2), 186–196, 1982.
[105] Maier G., Munro J., Mathematical programming applications to engineering plastic analysis, *Applied Mechanics Reviews*, ASME, **35** (12), 1631–1643, 1982.
[106] Maier G., Novati G., Elastic plastic boundary element analysis as a linear complementarity problem. *Applied Mathematical Models*, **7** (2), 74–82, 1983.
[107] De Freltas J.A.T., Smith D.L., Elastoplastic Analysis of Planar Structures for Large Displacements, *Journal of Structural Mechanics*, **12** (4), 419–445, 1984.
[108] De Freitas J.A.T., Smith, D.L., A general methodology for nonlinear structural analysis by mathematical programming, *Engineering Structures*, **6** (1), 52–60, 1984.
[109] Maier G., Nappi A., On the unified framework provided by mathematical programming to plasticity, *Studies in Applied Mechanics*, **6** *(The D.C.Drucker Anniversary Volume)*, 253–273, 1984.
[110] Panagiotopoulos P.D., Baniotopoulos C.C., Avdelas A.V., Certain propositions on the activation of yield modes in elastoplasticity and their applications to deterministic and stochastic problems, *ZAMM*, **64** (11), 491–501, 1984.
[111] Panagiotopoulos P.D., *Inequality Problems in Mechanics and Applications – Convex and Nonconvex Energy Functions*, Birkhäüser, 1985.
[112] Maier G., Smith D.L., Update to "mathematical programming applications to engineering plastic analysis", *Applied Mechanics Update*, ASME, New York, 377–383, 1986.
[113] Zhong W.X., Zhang R.L., Parametric variational principles and their quadratic programming solutions in plasticity, *Computers and Structures*, **30** (4), 887-896, 1988.
[114] Maier G., Nappi A., Backward difference time integration, nonlinear programming and extremum theorems in elastoplastic analysis, *Solid Mechanics Archives*, **14** (1), 37–64, 1989.
[115] Tin-Loi F. Wong M.B., Nonholonomic computer analysis of elastoplastic frames, *Computer Methods in Applied Mechanics and Engineering*, **72** (3), 351–364, 1989.
[116] Maier G., Novati G., Extremum theorems for finite-step backward-difference analysis of elastic-plastic nonlinearly hardening solids, *International Journal of Plasticity*, **6** (1), 1–10, 1990.
[117] Tin-Loi F., On the optimal plastic synthesis of frames, *Engineering Optimization*, **16** (2), 91–108, 1990.
[118] Tin-Loi F., A yield surface linearization procedure in limit analysis, *Journal of Structural Mechanics*, **18** (1), 135–149, 1990.

[119] Wakefield R.R., Tin-Loi F., Mathematical programming and uniqueness in nonholonomic plasticity, *Computers and Structures*, **34**, 477–483, 1990.
[120] Wakefield R.R., Tin-Loi F., Large scale nonholonomic elastoplastic analysis using a linear complementarity formulation, *Computer Methods in Applied Mechanics and Engineering*, **84** (3), 229–242, 1990.
[121] Giannessi F., Maier G., Complementarity systems and optimization problems in structural engineering, *Engineering Optimization*, **18** (1), 43–66, 1991.
[122] Nappi A., Application of convex analysis concepts to the numerical solution of elastic-plastic problems by using an internal variable approach, *Engineering Optimization*, **18** (1–3), 79–92, 1991.
[123] Cen Z., Maier G., Bifurcations and instabilities in fracture of cohesive-softening structures: a boundary element analysis, *Fatigue and Fracture of Engineering Materials and Structures*, **15** (9), 911–928, 1992.
[124] Maier G., Perego U., Effects of softening in elastic-plastic structural dynamics, *International Journal for Numerical Methods in Engineering*, **34** (1), 319–347, 1992.
[125] Tin-Loi F., Optimal plastic design of arches, *Computers and Structures*, **43** (4), 675–679, 1992.
[126] Tin-Loi F., Pang J.S., Elastoplastic analysis of structures with nonlinear hardening: a nonlinear complementarity approach, Computer Methods in Applied Mechanics and Engineering, **107** (3), 299–312, 1993.
[127] Corigliano A., Numerical Analysis of discretized elastoplastic systems using the generalized mid-point time integration, *Engineering Computations*, **11** (5), 389–411, 1994.
[128] Bolzon G., Maier G., Novati G., Some aspects of quasibrittle fracture analysis as a linear complementarity problem, *Bažant Z.P., Bittnar Z., Jirasek M., Mazars J. (Editors): Fracture and damage in quasi-brittle structures: Experiment, modeling, and computer analysis*, *E&FN Spon*, 159–174, 1994.
[129] Shen W.Q., Limit analyses of plane frames with a penalty linear programming method, *Computers and Structures*, **56** (4), 687–695, 1995.
[130] Bolzon G., Maier G., Tin-Loi F., Holonomic and nonholonomic simulations of quasi-brittle fracture: a comparative study of mathematical programming approaches. In: *Wittmann FH (ed) Fracture mechanics of concrete structures, Proceedings FRAMCOS-2, Aedificatio Publishers, Freiburg*, 885–898, 1995.
[131] Mróz Z., Giambanco G., An interface model for analysis of deformation behaviour of discontinuities, *International Journal for Numerical and Analytical Methods in Geomechanics*, **20** (1), 1–33, 1996.
[132] Tin-Loi F., Vimonsatit V., Nonlinear analysis of semirigid frames: a parametric complementarity approach. *Engineering Structures*, **18** (2), 115–124, 1996.
[133] Tin-Loi F., Misa J.S., Large displacement elastoplastic analysis of semirigid frames, *International Journal for Numerical Methods in Engineering*, **39** (5), 741–762, 1996.
[134] Comi C., Corrigano A., On uniqueness of the dynamic finite-step problem in gradient–dependent softening plasticity, *International Journal of Solids and Structures*, **33** (26), 3881–3902, 1996.
[135] Bolzon G., Ghilotti D., Maier G., Parameter identification of the cohesive crack model. In: *Sol H., Oomens C.W.J. (Editors), Material identification using mixed numerical experimental methods. Kluwer Academic Publisher, Dordrecht*, 213–222, 1997.
[136] Bolzon G., Maier G., Tin-Loi F., On multiplicity of solutions in quasi-brittle fracture computations. Computational Mechanics, **19** (6), 511–516, 1997.
[137] Liu Y.H., Carvelli V., Maier G., Integrity assessment of defective pressurized pipelines by direct simplified methods, *International Journal for Pressure Vessels and Piping*, **74** (1), 49–57, 1997
[138] Bolzon G., Cocchetti G., On a case of crack path bifurcation in cohesive materials, *Archive of Applied Mechanics*, **68** (7), 513–523, 1998.
[139] Bolzon G., Tin-Loi F., Physical instability and geometric effects in frames, Engineering Structures, **21** (7), 557–567, 1999.

[140] Giambanco F., Elastic plastic analysis by the asymptotic pivoting method, *Computers and Structures*, **71** (2), 215–238, 1999.
[141] Maier G., Carvelli V., Cocchetti G., On direct methods for shakedown and limit analysis, *European Journal of Mechanics A / Solids*, **19** (Special Issue), S79–S100, 2000.
[142] Karakostas S.M., Mystakidis E.S., Evaluation of the ductility features in steel structures with softening moment-rotation behavior based on a non-convex optimization formulation, *Engineering Computations*, **17** (5), 573–592, 2000.
[143] Maier G., Bolzon G., Tin-Loi F., Mathematical programming in engineering mechanics: some current problems. In: *Ferris M.C., Mangasarian O.L., Pang J.-S (Editors), Complementarity: Applications, Algorithms and Extensions, Kluwer Academic Publishers*, 201–231, 2001.
[144] Tin-Loi F., Xia S.H., Holonomic softening: Models and analysis, *Mechanics of Structures and Machines*, **29** (1), 65-84, 2001.
[145] Papadrakakis M., Lagaros N.D., Tsompanakis Y., Plevris V., Large scale structural optimization: computational methods and optimization algorithms, *Archives of Computational Methods in Engineering*, **8** (3), 239–301, 2001.
[146] Tin-Loi F., Que N.S., Parameter identification of quasibrittle materials as a mathematical program with equilibrium constraints, *Computer Methods in Applied Mechanics and Engineering*, **190** (43–44), 5819–5836, 2001.
[147] Tin-Loi F., Que N.S., Nonlinear programming approaches for an inverse problem in quasibrittle fracture, *International Journal of Mechanical Sciences*, **44** (5), 843–858, 2002.
[148] Cocchetti G., Maier G., Shen X.P., Piecewise linear models for interfaces and mixed mode cohesive cracks. *Computer Modeling in Engineering and Sciences*, **3** (3), 279–298, 2002.
[149] Zhang H., Zhang X., A combined parametric quadratic programming and precise integration method based dynamic analysis of elastic-plastic hardening/softening problems, *Acta Meccanica Sinica, (English Series)*, **18** (6), 638–647, 2002.
[150] Cocchetti G, Maier G., Elastic-plastic and limit-state analyses of frames with softening plastic hinge models by mathematical programming, *International Journal of Solids and Structures*, **40** (25), 7219–7244, 2003.
[151] Zhang H., Zhang X., Chen J.S., A new algorithm for numerical solution of dynamic elastic–plastic hardening and softening problems, *Computers and Structures*, **81** (17), 1739–1749, 2003.
[152] Zhang H.W., Zhong W.X., Wu C.H., Liao A.H., Some advances and applications in quadratic programming method for numerical modeling of elastoplastic contact problems, *International Journal of Mechanical Sciences*, **48** (2), 176–189, 2006.
[153] Tangarmvong S., Tin-Loi F., Limit analysis of strain softening steel frames under pure bending, *Journal of Constructional Steel Research*, **63** (9), 1151–1159, 2007.
[154] Tangarmvong S., Tin-Loi F., A complementarity approach for elastoplastic analysis of strain softening frames under combined bending and axial force, *Engineering Structures*, **29** (5), 742–753, 2007.
[155] Krabbenhøft K., Lyamin A.V., Sloan S.W., Formulation and solution of some plasticity problems as conic programs, *International Journal of Solids and Structures*, **44** (5), 1533–1549, 2007.
[156] Tangaramvong S., Tin-Loi F., Simultaneous ultimate load and deformation analysis of strain softening frames under combined stresses, *Engineering Structures*, **30** (3), 664–674, 2008.
[157] Ardito R., Cocchetti G., Maier G., On structural safety assessment by load factor maximization in piecewise linear plasticity, *European Journal of Mechanics A / Solids*, **27** (5), 859–881, 2008.
[158] Pastor F., Loute E., Pastor J., Limit analysis and convex programming: a decomposition approach of the kinematic mixed method, *International Journal for Numerical Methods in Engineering*, **78** (3), 254–274, 2009.
[159] Tangaramvong S., Tin-Loi F., Limit analysis of elastoplastic frames considering 2nd-order geometric nonlinearity and displacement constraints. *International Journal of Mechanical Sciences*, **51** (3), 179–191, 2009.

[160] Tin-Loi F., Limit analysis by linear programming, In: Wong M.B. (Editor), *Plastic analysis and design of steel structures*, *Elsevier*, *Amsterdam*, 163–193, 2009.
[161] Tangaramvong S., Tin-Loi F., A constrained non-linear system approach for the solution of an extended limit analysis problem, *International Journal for Numerical Methods in Engineering*, **82** (8), 995–1021, 2009.
[162] Tangaramvong S., Tin-Loi F., The influence of geometric effects on the behavior of strain softening frames, *Computational Mechanics*, **46** (5), 661–678, 2010.
[163] Skordeli M.A.A., Bisbos C.D., Limit and shakedown analysis of 3D steel frames via approximate ellipsoidal yield surfaces, *Engineering Structures*, **32** (6), 1556–1567, 2010.
[164] Mahini M.R., Moharrami H., Cocchetti G., A dissipated energy maximization approach to elastic-perfectly plastic analysis of planar frames, *Archives of Mechanics*, **65** (3), 171–194, 2013.
[165] Wu D., Gao W., Tangaramvong S., Tin-Loi F., Robust stability analysis of structures with uncertain parameters using mathematical programming approach, *International Journal for Numerical Methods in Engineering*, **100** (10), 720–745, 2014.
[166] Tangaramvong S., Tin-Loi F., Topology optimization of softening structures under displacement constraints as an MPEC, *Structural and Multidisciplinary Optimization*, **49** (2), 299–314, 2014.
[167] Manola M.M.S., Koumousis V., Ultimate state of plane frame structures with piecewise linear yield conditions and multi-linear behavior: A reduced complementarity approach, *Computers and Structures*, **130**, 22–33, 2014.
[168] Moharrami H., Mahini M.R., Cocchetti G., Elastoplastic analysis of plane stress/strain structures via restricted basis linear programming, *Computers and Structures*, **146**, 1–11, 2015.
[169] Kanno Y., A fast first-order optimization approach to elastoplastic analysis of skeletal structures, *Optimization and Engineering*, **17** (4), 861–896, 2016.
[170] Cacho-Pérez M., 2D frames optimization. Criterion: maximum stability, *Applied Mathematical Modelling*, **46**, 591-601, 2017.
[171] Bolzon G., Complementarity Problems in Structural Engineering: An Overview, *Archive of Computational Methods in Engineering*, **24** (1), 23–36, 2017.
[172] Royer-Carfangi G., Buratti G., Plastic hinges as phase transitions in strain softening beams, *Journal of Mechanics of Materials and Structures*, **2** (9), 1677–1699, 2007.
[173] Martin Artieda C.C., Dargush G.F., Approximate limit load evaluation of structural frames using linear elastic analysis, *Engineering Structures*, **29**, 296–304, 2007.
[174] Barrera O., Cocks A.C.F., Ponter A.R.S., Evaluation of the convergent properties of the linear matching method for computing the collapse of structural components, *European Journal of Mechanics A / Solids*, **28** (4), 665–667, 2009.
[175] *Load and resistance factor design specification for structural steel buildings*, *2nd Edition*. Chicago: American Institute of Steel Construction; 1993.
[176] N. Gebbeken, *Eine Fliessgelenktheorie Höherer Ordnung für Raümliche Stabtragwerke*, Mitteilungen des Institus für Statik der Universität Hannover, Hannover, 1988.
[177] C.D. Comartin, R.W. Niewarowski, C. Rojahn, *ATC-40 - Seismic Evaluation and Retrofit of Concrete Buildings*, Volume 1, Applied Technology Council, Seismic Safety Commission, Report Nº SSC 96-01, 1996.
[178] SAP2000, v19.2.1, User's manual, CSI Inc., 2017.
[179] D.C. Drucker, The significance of the criterion for additional plastic deformation of metals, *Journal of Colloid Science*, **4** (3), 299–311, 1949.
[180] E. Melan, Zur Plastizität des räumlichen Kontinuums, *Ingenieur Archiv*, **9** (2), 116–126, 1938.
[181] W. Prager, Recent developments in the mathematical theory of plasticity, *Journal of Applied Physics*, **20** (3), 235–241, 1949.
[182] H. Ziegler, A modification of Prager's hardening rule, *Quarterly of Applied Mathematics*, *Brown University*, **17** (1), 55–65, 1959.

[183] D.C. Drucker, Some implications of work hardening and ideal plasticity, *Quarterly of Applied Mathematics*, *Brown University*, **7** (4), 411–418, 1950.
[184] D.C. Drucker, On uniqueness in the theory of plasticity, *Technical Report Nº. 116 (A11-116)*, *Division of Applied Mathematics*, *Brown University*, 1955.
[185] D.C. Drucker, A definition of stable inelastic material, *Technical Report No. 2 (Nonr-562(20)/2))*, *Division of Engineering*, *Brown University*, 1957.
[186] D. Capecchi, *History of Virtual Work Laws: A History of Mechanics Prospective*, Springer-Verlag, Italy, 2012.
[187] G.A. Wempner, Discrete approximations related to nonlinear theories of solids, *International Journal of Solids & Structures*, 7, 1581–1599, 1971.
[188] E. Riks, An incremental approach to the solution of snapping and buckling problems, *International Journal of Solids & Structures*, **15**, 529–551, 1979.
[189] M.A. Crisfield, An arc–length method including line searches and accelerations, *International Journal for Numerical Methods in Engineering*, **19**, 1269–1289, 1983.
[190] J. Heyman, *Elements of the Theory of Structures*, Cambridge University Press, 1996.
[191] S. Krenk, S. Vissing, C. Vissing-Jørgensen, A finite step updating method for the elastoplastic analysis of frames, *Journal of Engineering Mechanics*, *ASCE*, **119** (12), 2478–2495, 1993.
[192] E. Yarimci, *Incremental inelastic analysis of framed structures and some experimental verifications*, Technical Report Nº 273.45, Fritz Engineering Laboratory, Dept. Civil Engineering, Lehigh University, Pennsylvania, 1966.
[193] Toma, S., Chen, W.-F., White, D.W., A selection of calibration frames in North America for second-order inelastic analysis, *Engineering Structures*, **17** (2), 104–112, 1995.
[194] The MOSEK C Optimizer API Manual, Version 7.1 (Revision 49), MOSEK ApS, Copenhagen, Denmark.
[195] https://en.wikipedia.org/wiki/Jedi
[196] https://en.wikipedia.org/wiki/The_Force

(This page was intentionally left blank)


ΕΘΝΙΚΟΝ ΜΕΤΣΟΒΙΟ ΠΟΛΥΤΕΧΝΕΙΟΝ
ΣΧΟΛΗ ΕΦΑΡΜΟΣΜΕΝΩΝ ΜΑΘΗΜΑΤΙΚΩΝ ΚΑΙ ΦΥΣΙΚΩΝ ΕΠΙΣΤΗΜΩΝ